Targeting a key protein-protein interaction surface on mitogen-activated protein kinases by a precision-guided warhead scaffold with cyclic and chiral structure

Ádám Levente Póti[1,2,#], Dániel Bálint[3,4,#], Anita Alexa[1], Péter Sok[1], Kristóf Ozsváth[3], Krisztián Albert[1], Gábor Turczel[5], Sarolt Magyari[1], Orsolya Ember[1], Kinga Papp[1], Sándor Balázs Király[6], Tímea Imre[7], Krisztina Németh[7], Tibor Kurtán[6], Gergő Gógl[1], Szilárd Varga[3], Tibor Soós[3,&], Attila Reményi[1,&]

[1] Biomolecular Interaction Research Group, Institute of Organic Chemistry, Research Centre for Natural Sciences, 1117 Budapest, Hungary

[2]Doctoral School of Biology, Eötvös Loránd University, 1117 Budapest, Hungary

[3] Organocatalysis Research Group, Institute of Organic Chemistry, Research Centre for Natural Sciences, 1117 Budapest, Hungary

[4]Hevesy György PhD School of Chemistry, Eötvös Loránd University, 1117 Budapest, Hungary

[5] NMR Research Laboratory, Centre for Structural Science, Research Centre for Natural Sciences, 1117 Budapest, Hungary

[6] Department of Organic Chemistry, University of Debrecen, 4002 Debrecen, Hungary

[7] MS Metabolomic Research Laboratory, Centre for Structural Science, Research Centre for Natural Sciences, 1117 Budapest, Hungary

[#] Equal contribution

[&] Corresponding authors: soos.tibor@ttk.hu & remenyi.attila@ttk.hu

Supplementary Information

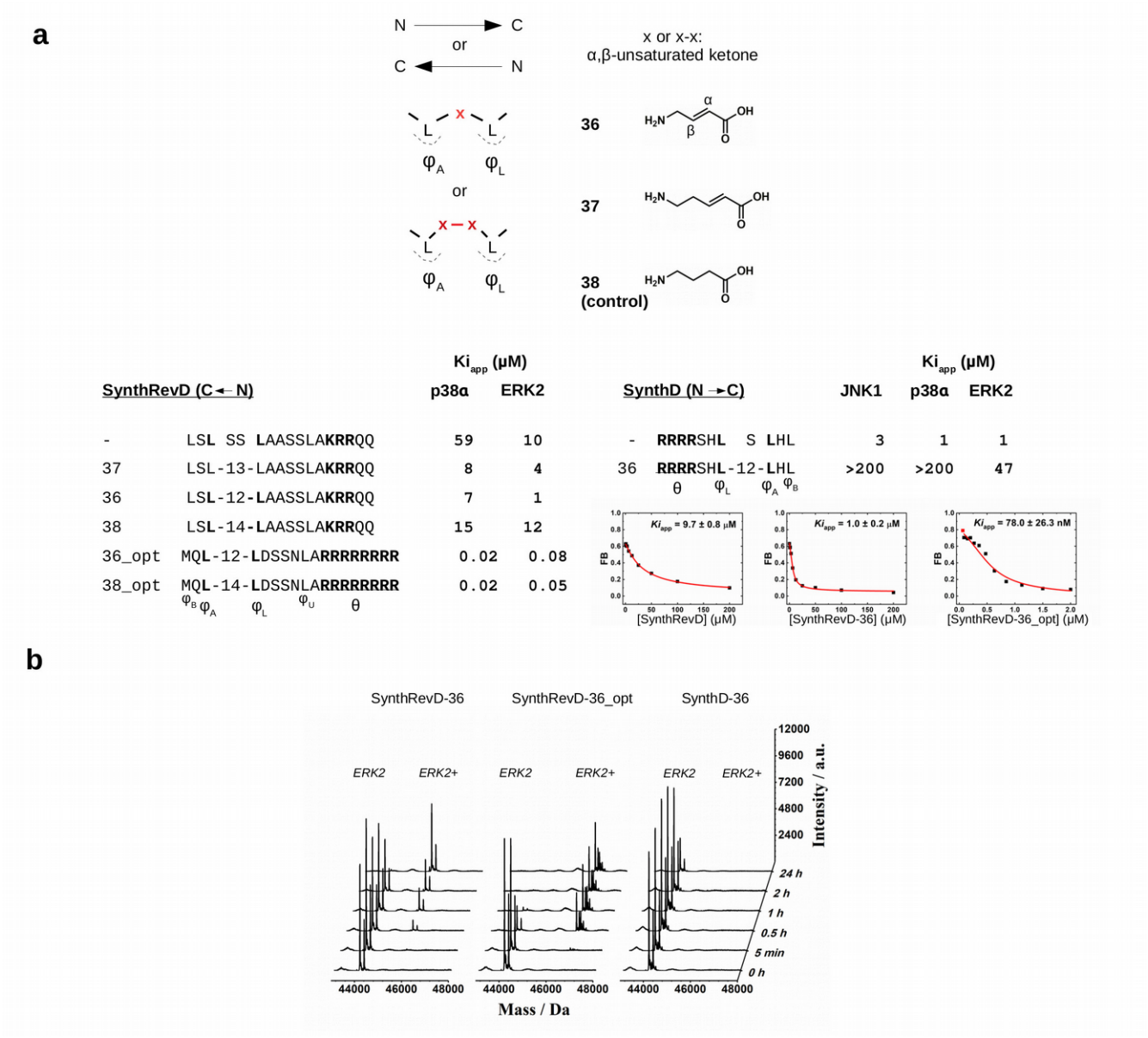

Supplementary Fig. 1. Characterization of D-peptides containing an intrachain acrylamide Michael acceptor

(**a**) Different binding modes of peptides binding in the D-groove: classical (D) or reverse (revD) directions; with a spacing of one or two amino acids between φ_L and φ_A (see Fig. 1a). N and C designate N- and C-terminus, and X denotes any amino acid. **36**, **37** and **38** were used as unnatural amino acids that were coupled into peptides by chemical peptide synthesis. The distance between φL and φA in the new peptides corresponds to approximately 1.5 or 2 amino acid residues in molecules **36** and **37**, respectively. The warhead of **36** or **37**, when used as unnatural amino acid residues synthesized into artificial peptides, could align with the sulfhydryl group of Cys161. Peptides with the intrachain acrylamide warhead bound weaker to all three tested MAPKs compared to the original SynthD peptide (see Supplementary Fig. 2). In contrast, modified peptides based on the SynthRevD pattern bound about 10-fold stronger than the original. To further enhance binding affinity, SynthRevD-36 was extended with a polyarginine stretch and modified at the intervening region (SynthRevD-36_opt;

referred to as SynthRevD^{COV} in the main text), resulting in an ~80 nM affinity to ERK2. Interestingly, a peptide containing an analogue of **36** without the warhead (**38**) also exhibited better binding, indicating that the geometry between φL and φA is more optimal in the artificial peptides. (Data points show the mean of three independent experiments. Ki_{app} values indicate the parameter error estimate from weighted least square method; n=3.)
(**b**) MS analysis of trypsin-digested ERK2–SynthRevD-36 indicated irreversible covalent modification of the Cys161-containing peptide as expected and intact mass measurements were used to follow protein-peptide adduct formation in time (n=1). These measurements revealed faster covalent bond formation to ERK2 with the stronger binding SynthRevD-36_opt compared to the weaker SynthRevD-36. Modified peptides with the SynthD pattern were found not linked to any of the kinases (see Supplementary Fig. 3). In conclusion, replacing the natural peptide backbone between φ_L and φ_A with an artificial spacer was well-tolerated, but the intrachain acrylamide warhead targeted the D-groove cysteine only in the SynthRevD context, presumably because of a better placement of the warhead next to the thiol group.

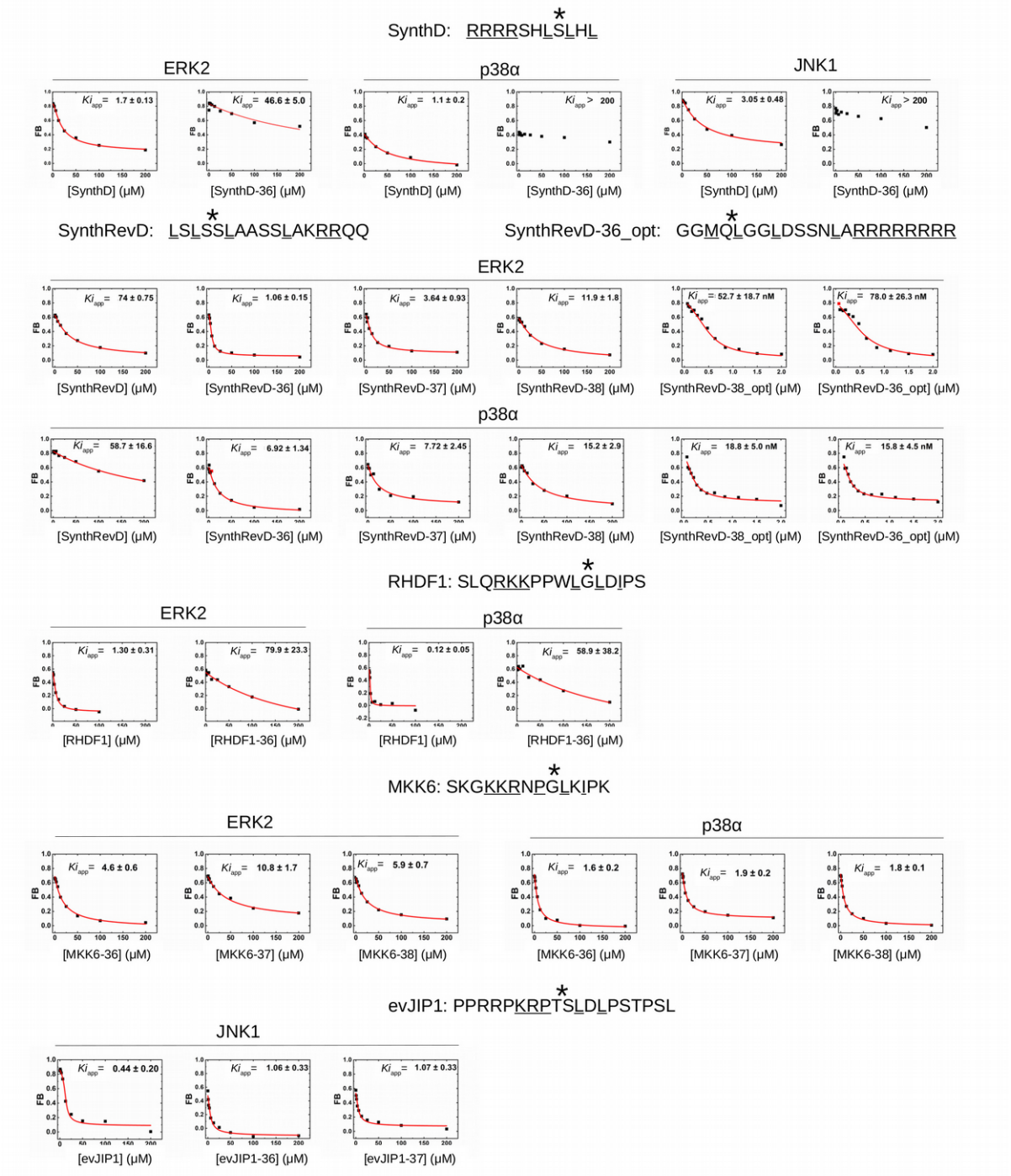

Supplementary Fig. 2. Results and details of fluorescence polarization based protein-peptide binding assays

FP binding assay results with peptides containing an intrachain acrylamide warhead (ERK2, p38α and JNK1). Amino acid sequence of SynthD, SynthRevD, RHDF1, MKK6 and evJIP1 peptides are shown where * shows the residue(s) between φ_L and φ_A that were replaced by **36**, **37** or **38**. Underlined amino acids indicate key contact residues (θ, φ_U, φ_L, φ_A, φ_B). FB: fraction bound. (Ki_{app} values indicate the parameter error estimate from weighted least square method; n=3.)

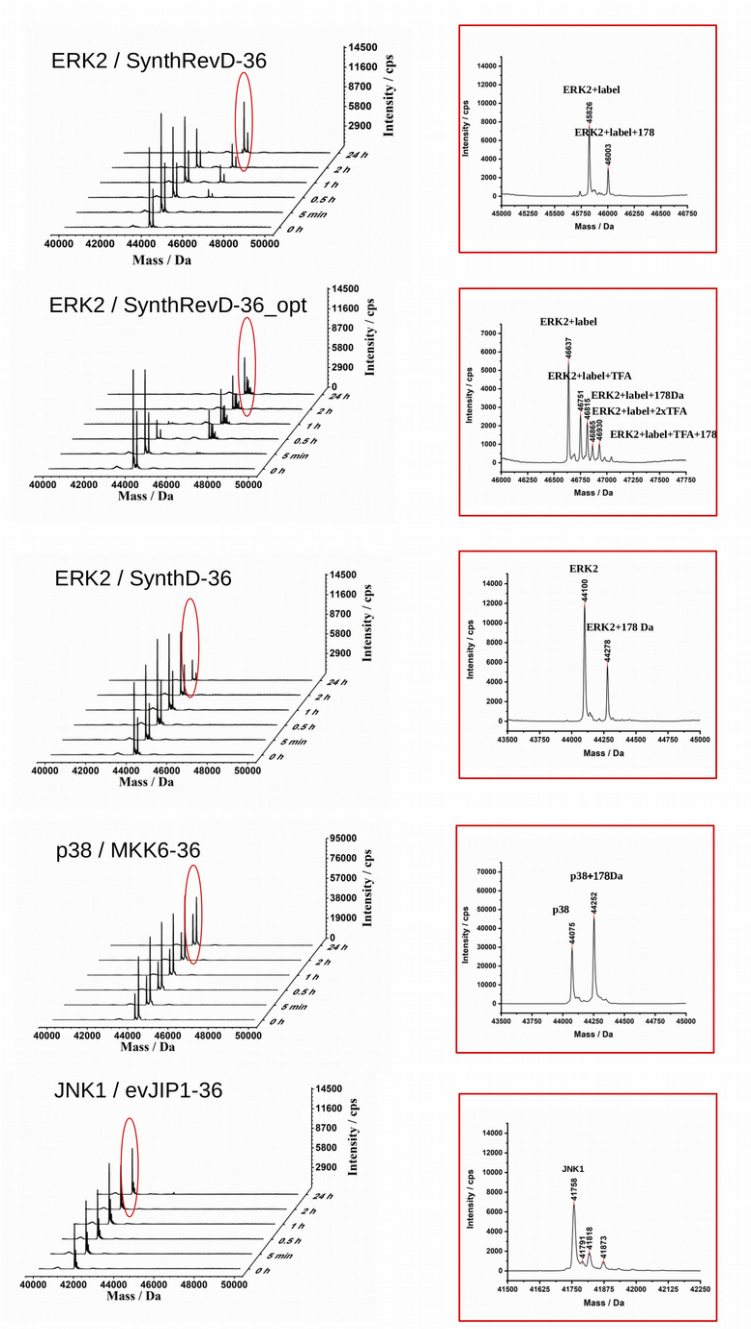

Supplementary Fig. 3. Results and details of mass spectrometry analysis with an intrachain acrylamide warhead

Results of intact mass measurements with D-peptides containing an intrachain acrylamide warhead (ERK2, p38 and JNK1; n=1). Panels on the right show the zoomed in-view of the area circled red on the left for the sample that was incubated with the peptide for 24 hours. Peptide concentration was 50 µM and protein concentration was 5 µM. (A mass difference of 178Da corresponds to clipped versions of the 6xHis tagged proteins, and the mass of different ion adducts is also indicated.) “Label” indicates the covalently bound mass of the peptide and “+TFA” denotes the adduct with TFA.

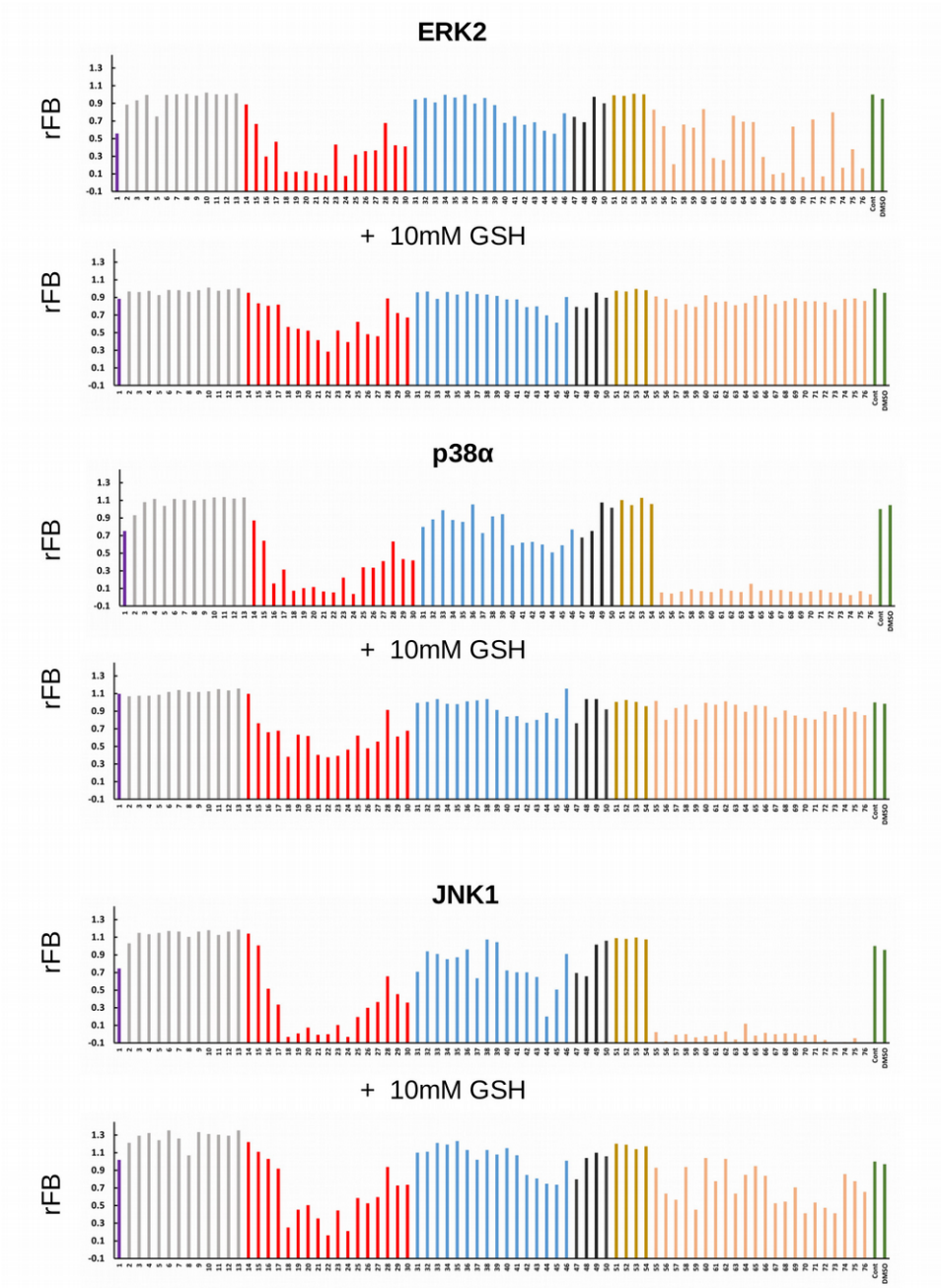

Supplementary Fig. 4. Fluorescence polarization based protein-peptide binding primary screen in the presence of 10 mM GSH

Results of the primary MAPK D-motif peptide displacement screen with 75 compounds (100 µM) from Group 1-7 (colored as in Fig. 1c) in the absence (upper panels) or in the presence of 10 mM GSH (lower panels) with ERK2, p38α, and JNK1. Cont: Control, where no compound or DMSO was added; DMSO: the binding mix contained the same amount of DMSO as for the compound set. Data represent the mean for three technical replicates. rFB: relative Fraction Bound compared to Control ($FP - FP_{min}$ / $FP_{control} - FP_{min}$). Lilac: Group 1 (intrachain acrylamide); gray: Group 2 (cyclohexenone); red: Group 3 ("frustrated" cyclohexenone); light blue: Group 4 (chalcone); black: Group 5 (cyanoacryl); gold: Group 6 ("frustrated" cyanoacryl); orange: Group 7 (nitroalkene); green: controls (cont: no compound added; DMSO: 1% DMSO added). Source data are provided as a Source Data file.

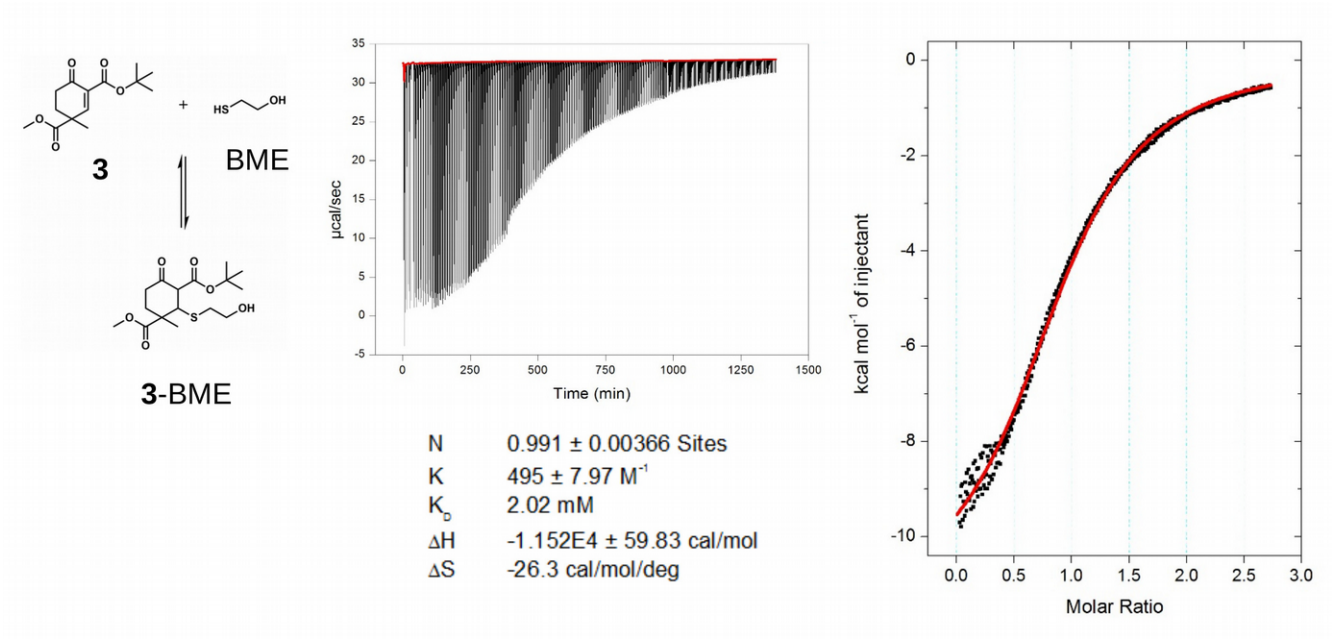

Supplementary Fig. 5. Binding of 3 with beta-mercaptoethanol (BME) characterized by ITC
3 was in 10 mM concentration (in 1x PBS with 10 % DMSO) and titration from the syringe containing 125 mM BME in the same buffer was done in small aliquots to stay within the dynamic range of the VP-ITC instrument (and delay time between injections was set to allow the system to return to the reference value; n=1).

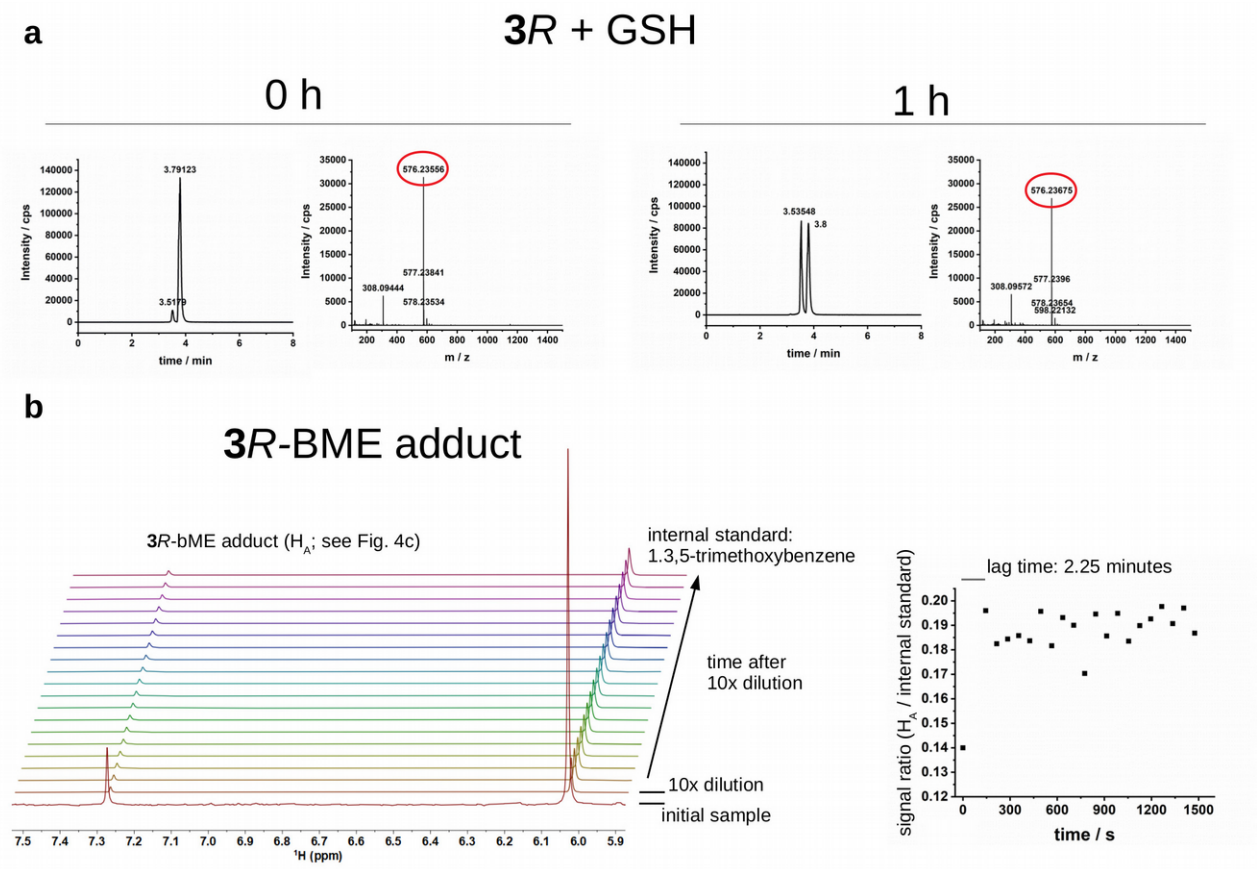

Supplementary Fig. 6. Characterization of the 3*R*-GSH covalent adduct (a) by mass spectometry and (b) the dissociation of the 3*R*-BME adduct by ^{1}H NMR (jump dilution)

(**a**) 10 mM GSH was mixed with 50 µM **3***R* in PBS (pH 7.4) and subjected to LC-MS analysis immediately (0 h, practically 5 minutes) and after 1 hour incubation (1 h). The left panel shows the total ion chromatograms while the right shows the mass spectum corresponding to the highest peak on the ion chromatogram (n=1). Note that the formation of the adduct generates new asymetric centers and the two peaks on the total ion chromatogram correspond to two diastereomers of the adduct, since their mass spectra were identical. The ion chromatogram at 0 h is shown for the bigger peak (right; elution time: ~3.8 minutes), while at the 1 h panel it is shown for the increased peak on the left (elution time: ~ 3.5 minutes). The indicated peaks (red circle) in the mass spectra correspond to the exact mass of the **3***R*-GSH adduct (576 Da). It appears that the adduct forms rapidly under these conditions since there was no significant difference in the combined peak area between 0 or 1 hour incubation, however one of the diastereomers forms faster than the other (possibly due to less activation energy), but the ~50-50% ratio observed after 1 hour incubation did not change even after longer incubation times (~ 4 hours), suggesting that the two diastereomer adducts may energetically be equal.

(**b**) The **3***R*-BME adduct was formed by mixing 81.6 mM **3***R* with 97.9 mM BME and this initial sample (also containing 23.9 mM 1,3,5-trimethoxibenzene) was diluted by 10-fold with a solution of DMSO:PBS (3:1) mixture (n=1). The 6.02 ppm proton signal from 1,3,5-trimethoxybenzene was used as an internal standard. The plot on the right shows the ratio of H_A proton (see Fig. 4c) and the internal standard signal from spectra recorded at different time points after the jump dilution. The lag time for recording the first spectrum after the jump dilution was 2.25 minutes. This data suggest that the dissociation of the **3***R*-BME adduct is fast.

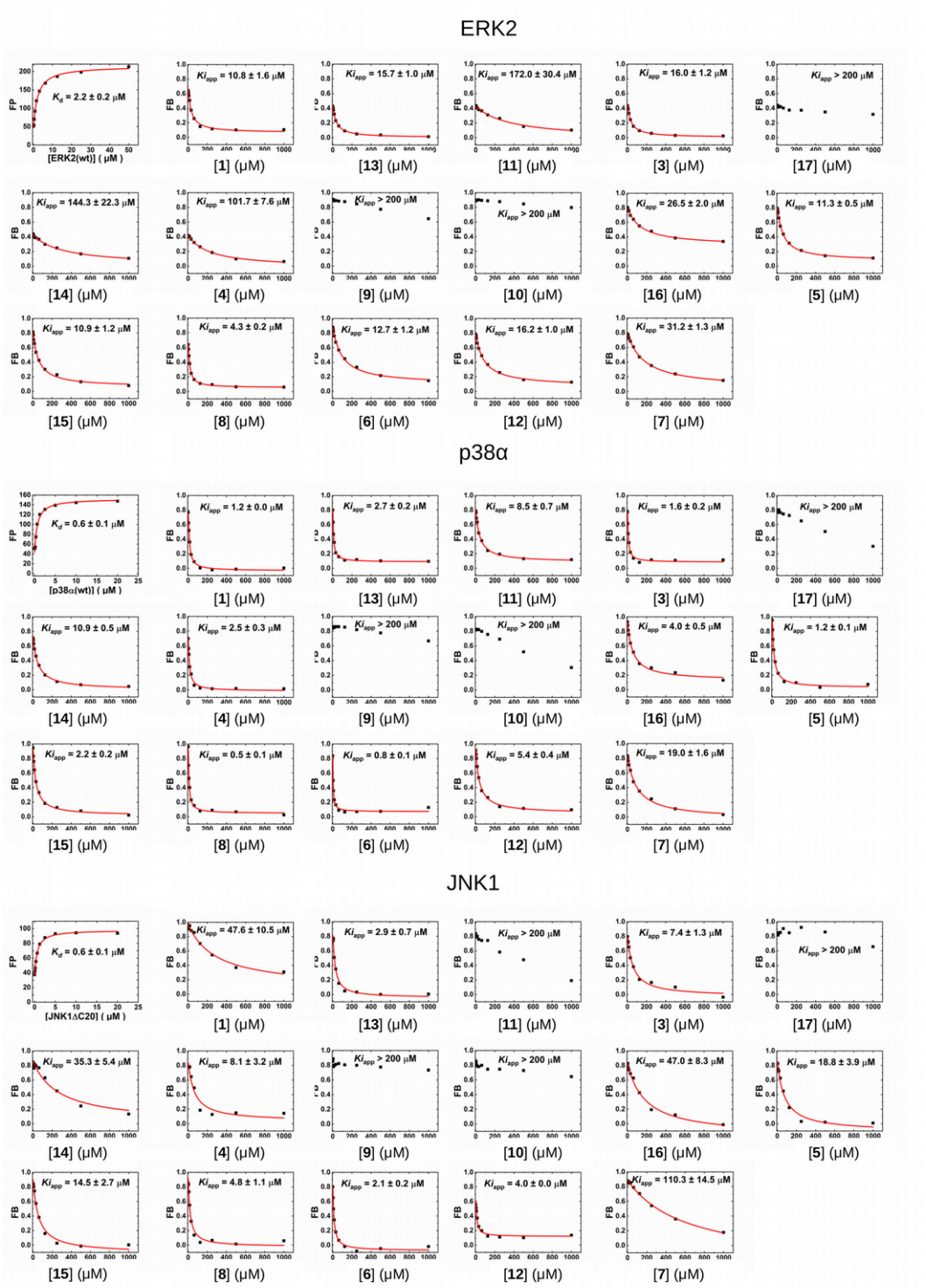

Supplementary Fig. 7. FP binding results with ERK2, p38α and JNK1
The first panels on the left for each series show the direct binding titration curve while the rest of the panels show competitive binding curves (see Table 1 for the summary) (FP: fluorescence polarization in arbitrary units; FB: fraction bound). (Ki_{app} values indicate the parameter error estimate from weighted least square method; n=3.)

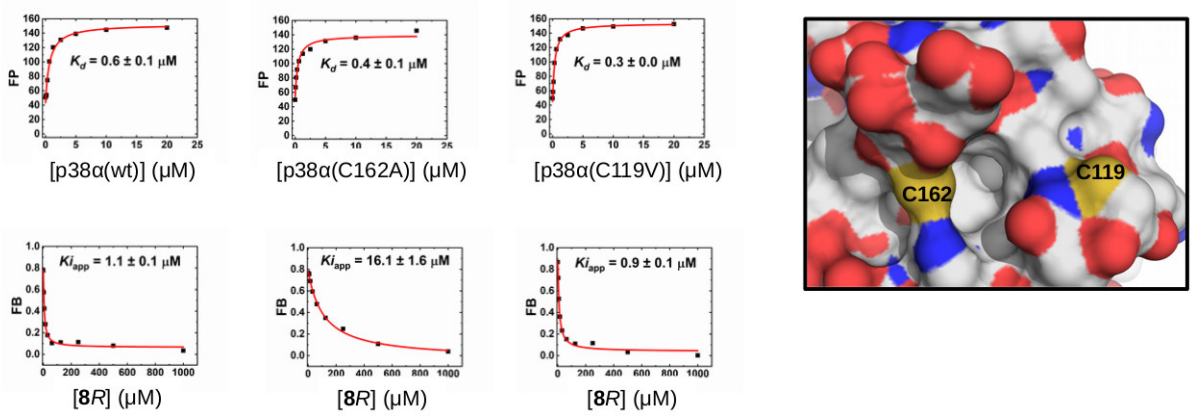

Supplementary Fig. 8. FP binding results with the p38α C162A or C119V mutants and 8*R*
The structural panel on the right shows the surface of p38α where surface cysteines – C162 corresponding to C161 in ERK2 and C119 located close but outside of the D-groove – are colored in yellow. (C, O, N, and S atoms are colored in gray, red, blue and yellow, respectively.) Note that C162A mutation greatly reduces **8***R* binding while mutating C119 does not have such an adverse affect. Upper panels show direct binding titration experiments which demonstrate that C162A or C119V mutations do not interfere with reporter peptide binding. FB: fraction bound. (Ki_{app} values indicate the parameter error estimate from weighted least square method; n=3.) Source data are provided as a Source Data file.

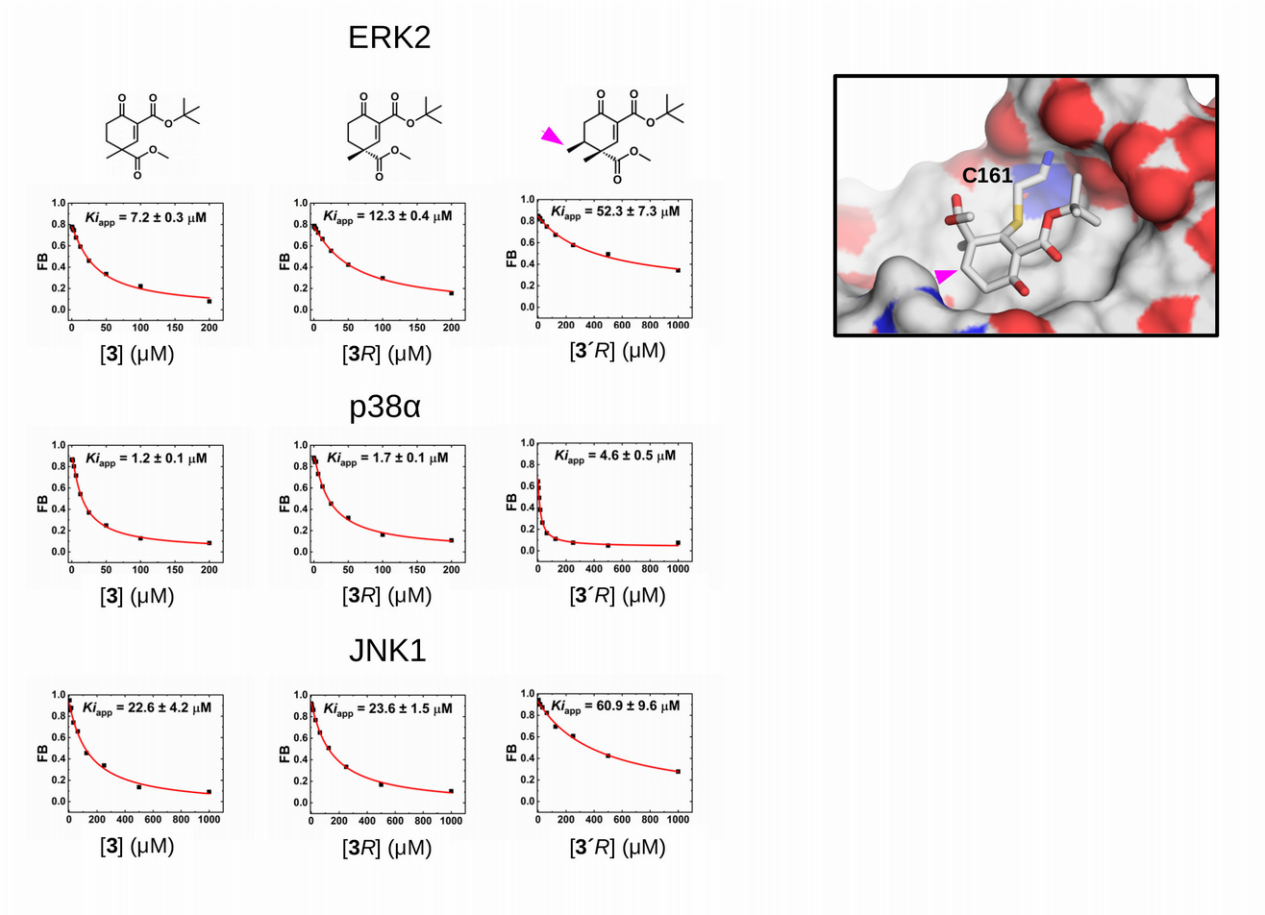

Supplementary Fig. 9. FP binding results with the 5-methyl derivative of 3*R*
Panels show competitive FP binding assay results with ERK2, p38α, or JNK1 and **3** (racemic), **3***R*, and **3'***R* (5-methyl derivative of **3***R*). The structural panel on the right shows the crystal structure of the ERK2-**3***R* complex. The magenta arrowhead indicates the position of the 5-methyl group which would clash with the rim of the hydrophobic pocket. (C, O, N, and S atoms are colored in gray, red, blue and yellow, respectively. FB: fraction bound.) (Ki_{app} values indicate the parameter error estimate from weighted least square method; n=3.) Source data are provided as a Source Data file.

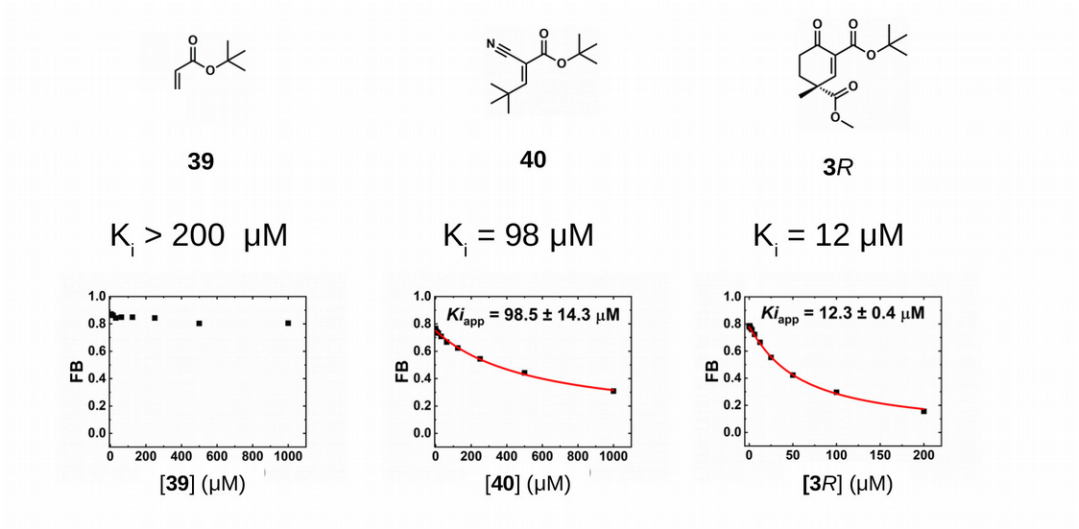

Supplementary Fig. 10. The cyclic cyclohexenone warhead (3*R*) is more efficient in targeting the MAPK D-groove cysteine compared to open-chain acryl- or cyanoacrylester
Panels show the results of FP competitive binding experiments with ERK2. FB: fraction bound. (Ki_{app} values indicate the parameter error estimate from weighted least square method; n=3.) Source data are provided as a Source Data file.

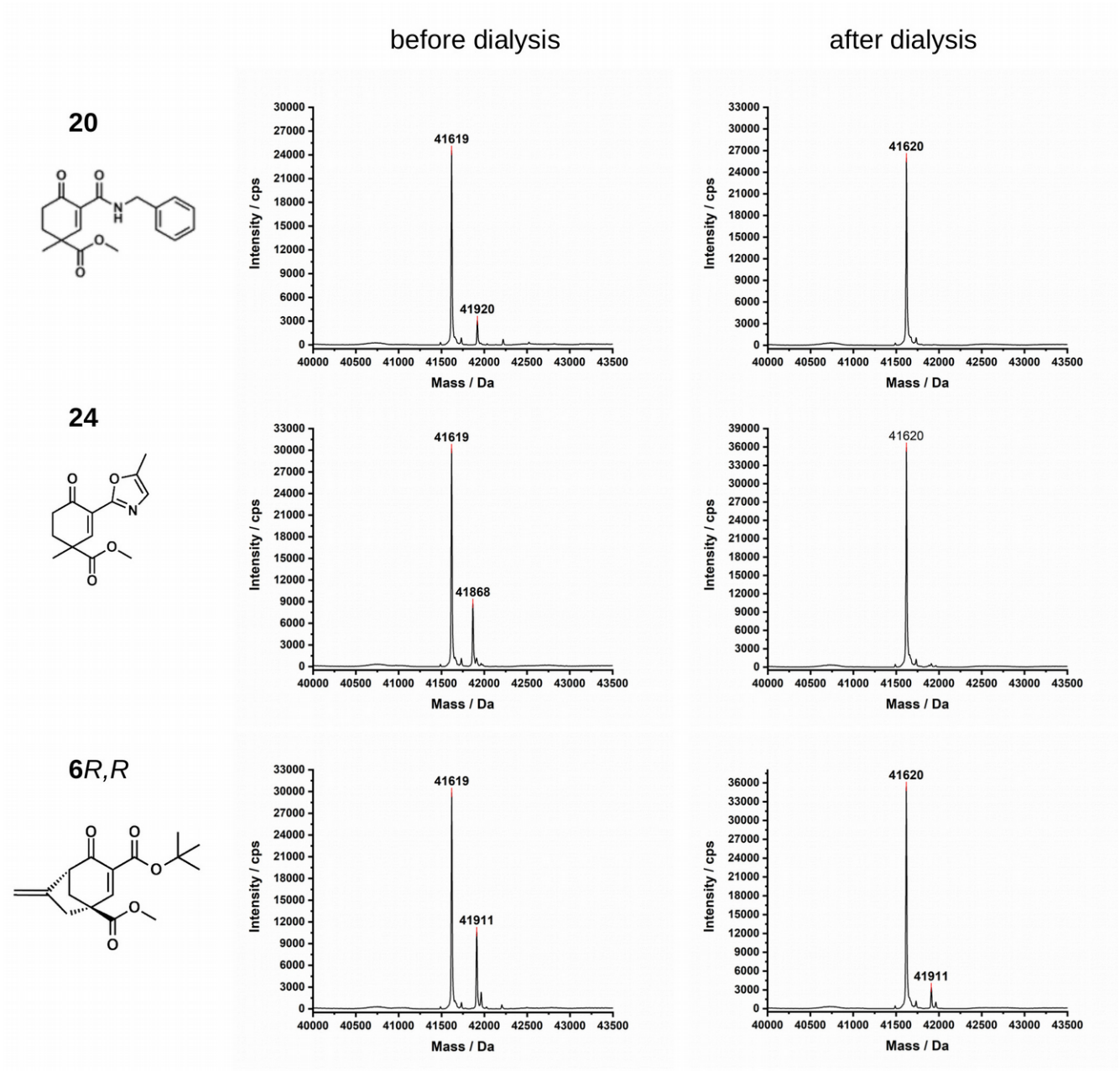

Supplementary Fig. 11. Reversibility of ERK2-cyclohexenone adduct formation
Panels show the intact mass before (left) and after dialysis (right) for ERK2-**20**, -**24** and -**6***R*,*R* complexes (n=1). 5 µM ERK2 was mixed with 50 µM compounds and analyzed by LC-MS, then the sample was dialyzed in buffer (20 mM Tris pH=8, 200 mM NaCl, 2 mM TCEP) overnight and analyzed by LC-MS again. Notice that the ratio of the ERK2 intact mass after the dialysis increases, and the ratio of the adduct decreases in the deconvoluted mass spectrum, indicating that protein-adduct formation is reversible.

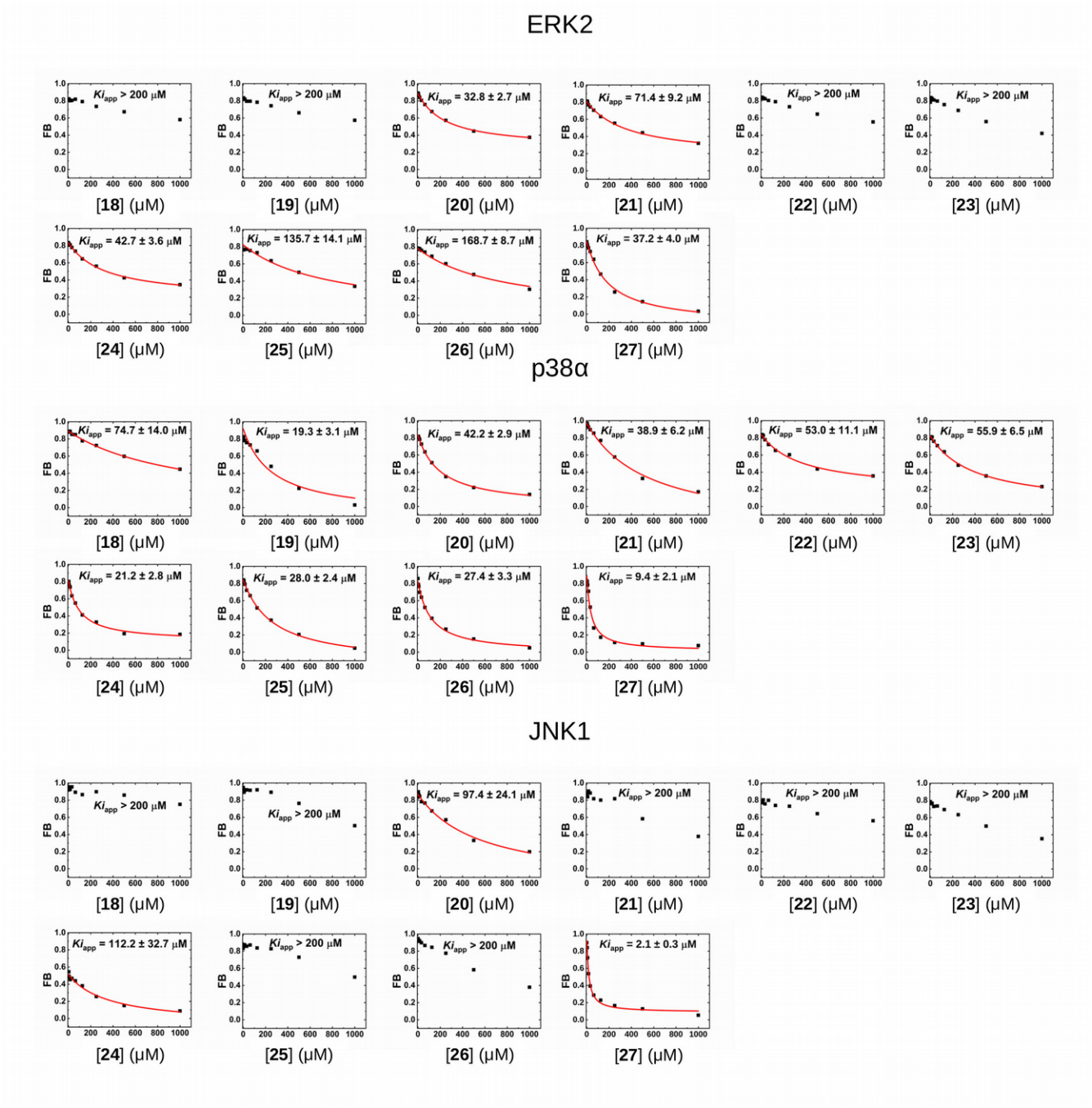

Supplementary Fig. 12. FP binding results with compounds containing different electron withdrawing groups at C2 or with the cyclopentenone scaffold

Panels show the competitive binding curves for all the measurements summarized in Table 2. FB: fraction bound. (Ki_{app} values indicate the parameter error estimate from weighted least square method; n=3.) Source data are provided as a Source Data file.

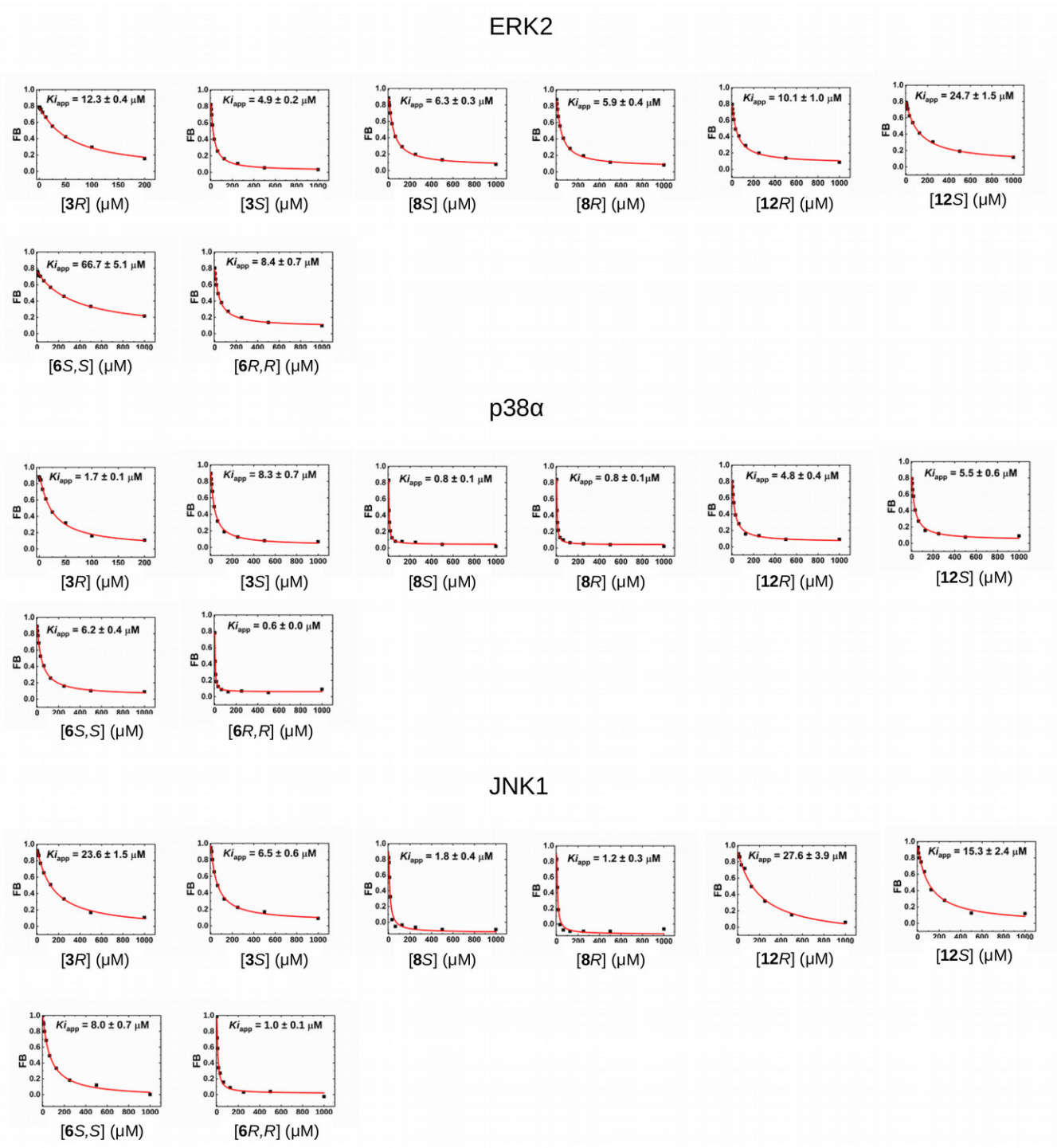

Supplementary Fig. 13. FP binding assay results with cyclohexenone enantiomers (3*R/S*, 8*R/S*, 12*R/S*, 6*S,S/R,R*)

Panels show the competitive binding curves for the measurements with ERK2, p38α, JNK1 and stereoisomers shown in Table 3. FB: fraction bound. (Ki_{app} values indicate the parameter error estimate from weighted least square method; n=3.) Source data are provided as a Source Data file.

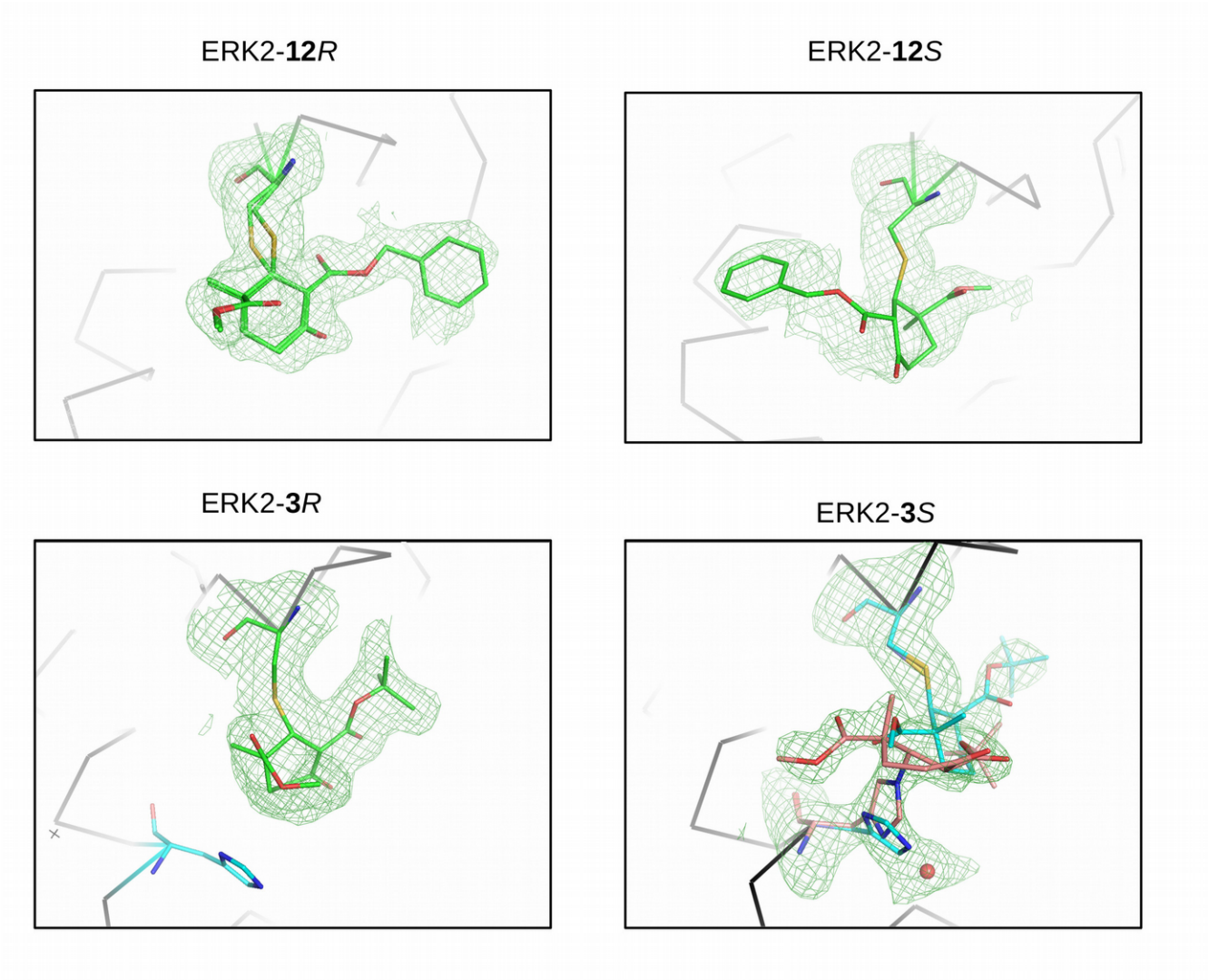

Supplementary Fig. 14. Simulated annealed omit maps for the ERK2-12*R/S* and ERK2-3*R/S* complexes

Maps are contoured at 2σ around the amino acid covalent adducts (Cys161 or His125). In the final crystallographic model for the ERK2-**3***S* complex the molecule forms an adduct with Cys161 (cyan) or with His125 (salmon). The red sphere in the ERK2-**3**S complex shows a water molecule H-bonded with the **3***S*-His125 adduct and with the protein backbone (Ser122). The occupancy of these two alternate conformations of the amino acid adducts are roughly equal; set to 0.42-0.58 occupancy by Phenix atomic occupancy refinement.

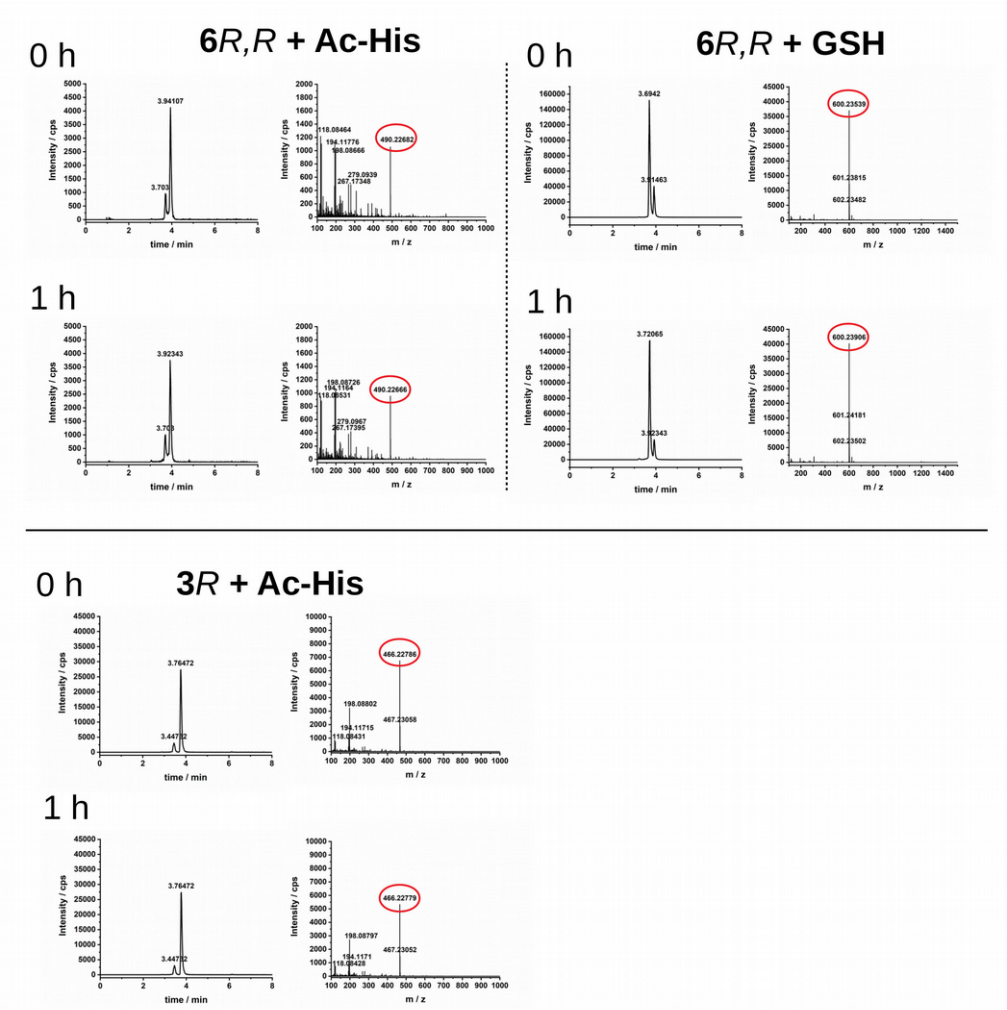

Supplementary Fig. 15. Covalent adduct formation of 6*R*,*R* and 3*R* with free histidine (*N*-acetyl-L-histidine, Ac-His) analyzed by mass spectrometry

10 mM Ac-His (left) was mixed with 50 µM **6***R*,*R* in PBS (pH 7.4) and subjected to LC-MS analysis immediately (0 h, practically 5 minutes) and after 1 hour incubation (1 h). The left panels show the total ion chromatogram while the mass spectra corresponding to the highest peak is shown on the right (n=1). Note that the two peaks on the total ion chromatogram correspond to two diastereomers of the adduct, since their mass spectra were identical. The indicated peaks (red circle) in the mass spectra correspond to the exact mass of the ***6****R*,*R*–Ac-His adduct (490 Da). It appears that the adduct forms rapidly under these conditions since there was no significant difference in the combined peak area between 0 or 1 hour incubation (and the spectra did not change after an even longer (~ 4 hours) incubation time). Note that the enantiomeric excess (ee) of **3***R* or **6***R*,*R* was >99% (see Supplementary Note 3) but adduct formation generates new asymetric centers. The experiment on the right panels (n=1; shown right of the vertical dashed line) shows the same analysis for the **6***R*,*R*-GSH adduct (600 Da). Here 10 mM GSH was mixed with 50 µM **3***R* in PBS (pH 7.4) and subjected to LC-MS analysis the same way as above (n=1). The experiment shown on the lower panels (n=1) below the solid line demonstrates that the **3***R*–Ac-His adduct (466 Da) can also form and was detected by LC-MS analysis similarly as shown for the ***3***R-GSH adduct (see Supplementary Fig. 6). Here 10 mM GSH was mixed with 50 µM **3***R* in PBS (pH 7.4) and subjected to LC-MS analysis the same way as above.

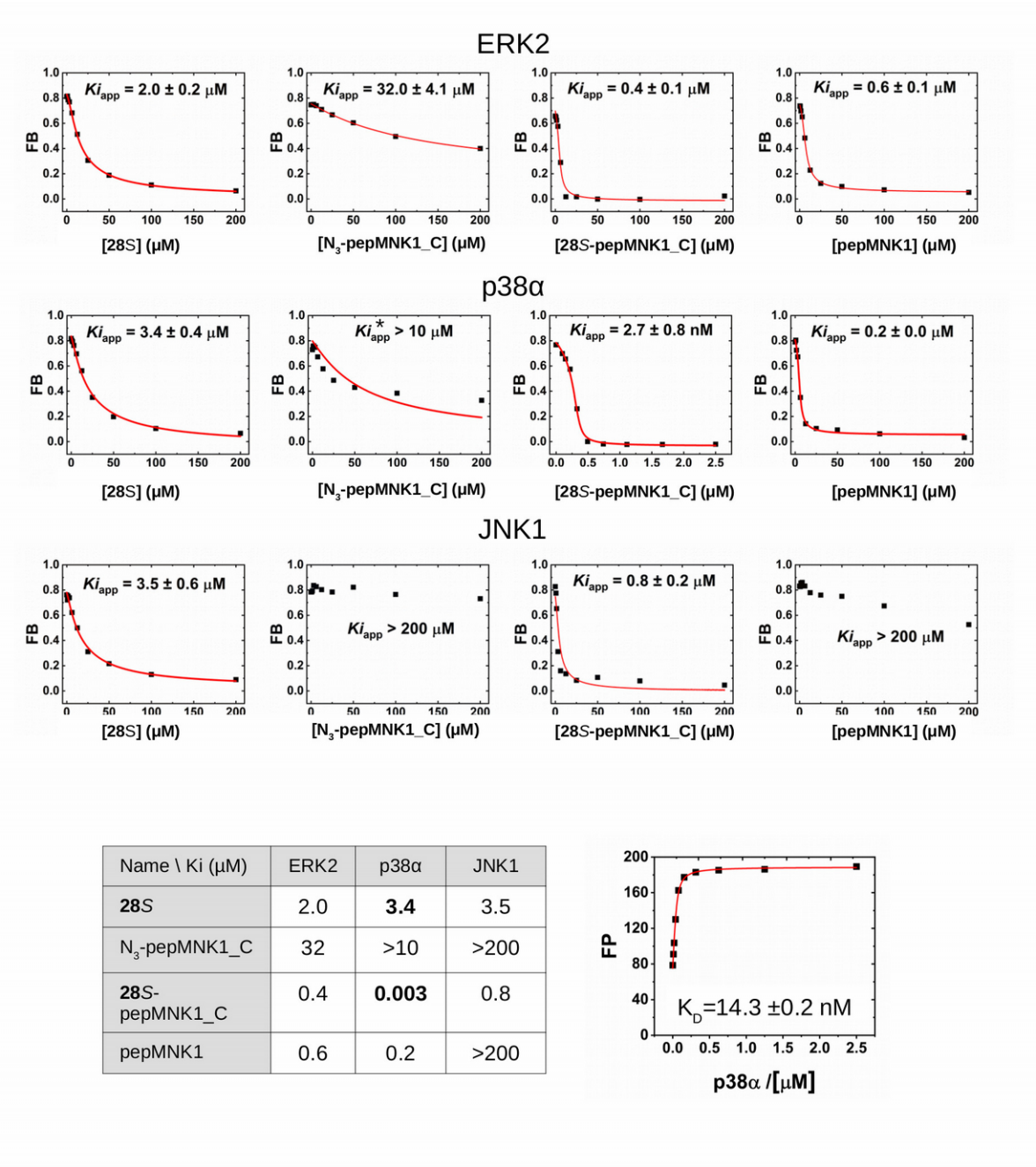

Name \ Ki (µM)	ERK2	p38α	JNK1
28*S*	2.0	**3.4**	3.5
N_3-pepMNK1_C	32	>10	>200
28*S*-pepMNK1_C	0.4	**0.003**	0.8
pepMNK1	0.6	0.2	>200

Supplementary Fig. 16. FP binding results with 28*S*, peptides and 28*S*-peptide chimeras
Panels show the competitive binding curves for the measurements with ERK2, p38α, and JNK1 summarized in the table below. FB: fraction bound. *: competition is incomplete, Ki_{app} is only estimated. The panel on the right to the table shows the results of a direct binding experiment with p38α and carboxyfluorescein labeled **28***S*-pepMNK1_C peptide. This confirms the low nanomolar binding affinity of the **28***S*-peptide chimera in a direct binding experiment (FP: fluorescence polarization in arbitrary units; K_D = 14 nM; n=3). (Ki_{app} values indicate the parameter error estimate from weighted least square method; n=3.) Source data are provided as a Source Data file.

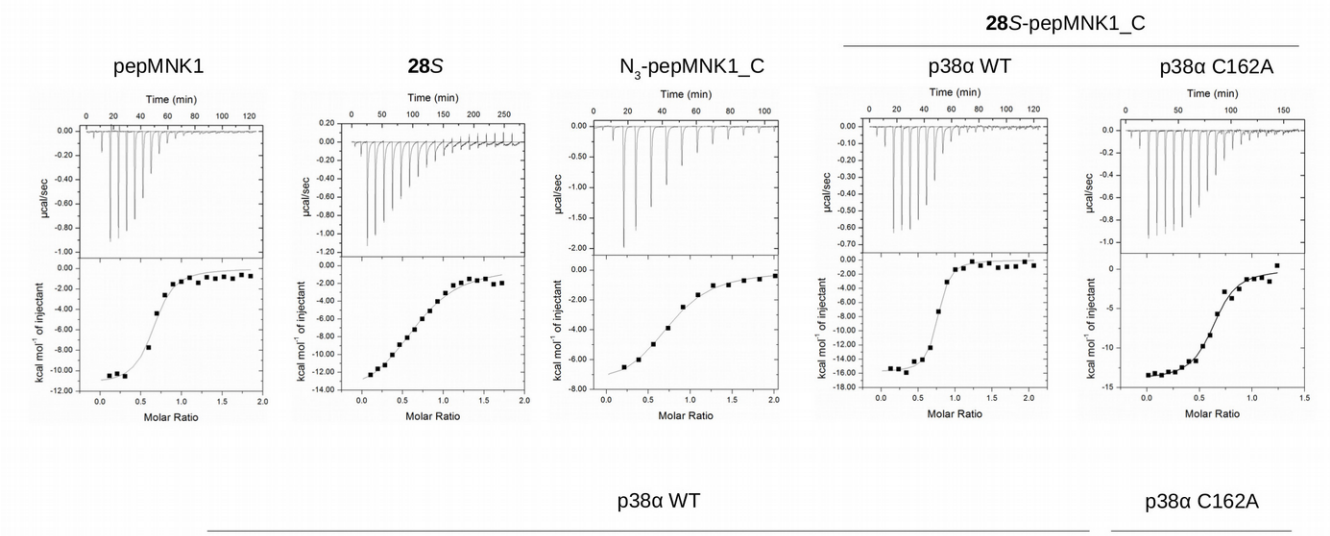

	pepMNK1	**28***S*	N_3-pepMNK1_C	**28***S*-pepMNK1_C	**28***S*-pepMNK1_C
N	0.64 ± 0.02	0.71 ± 0.03	0.73 ± 0.02	0.73 ± 0.01	0.63 ± 0.01
K_a (M^{-1})	$2.11*10^6 \pm 7.54*10^5$	$1.13*10^5 \pm 2.04*10^4$	$1.72*10^5 \pm 2.31*10^4$	$1.18*10^7 \pm 2.90*10^6$	$1.68*10^6 \pm 3.37*10^5$
K_d (µM)	0.47	8.85	5.81	0.085	0.596
ΔH (kcal/mol)	-11.34 ± 0.50	-15.42 ± 0.88	-8.12 ± 0.32	-15.83 ± 0.33	-14.00 ± 0.33
-TΔS (kcal/mol)	2.48	7.81	0.90	5.65	5.42

Supplementary Fig. 17. Results of ITC measurements with p38α.
Isothermal calorimetry (ITC) can be used to measure the contribution of enthalpy (ΔH) and the entropic cost (TΔS) of binding free energy (ΔG). N: stoichiometry of binding (~1), K_a and K_d: equilibrium association and dissociation constants, respectively (n=1).

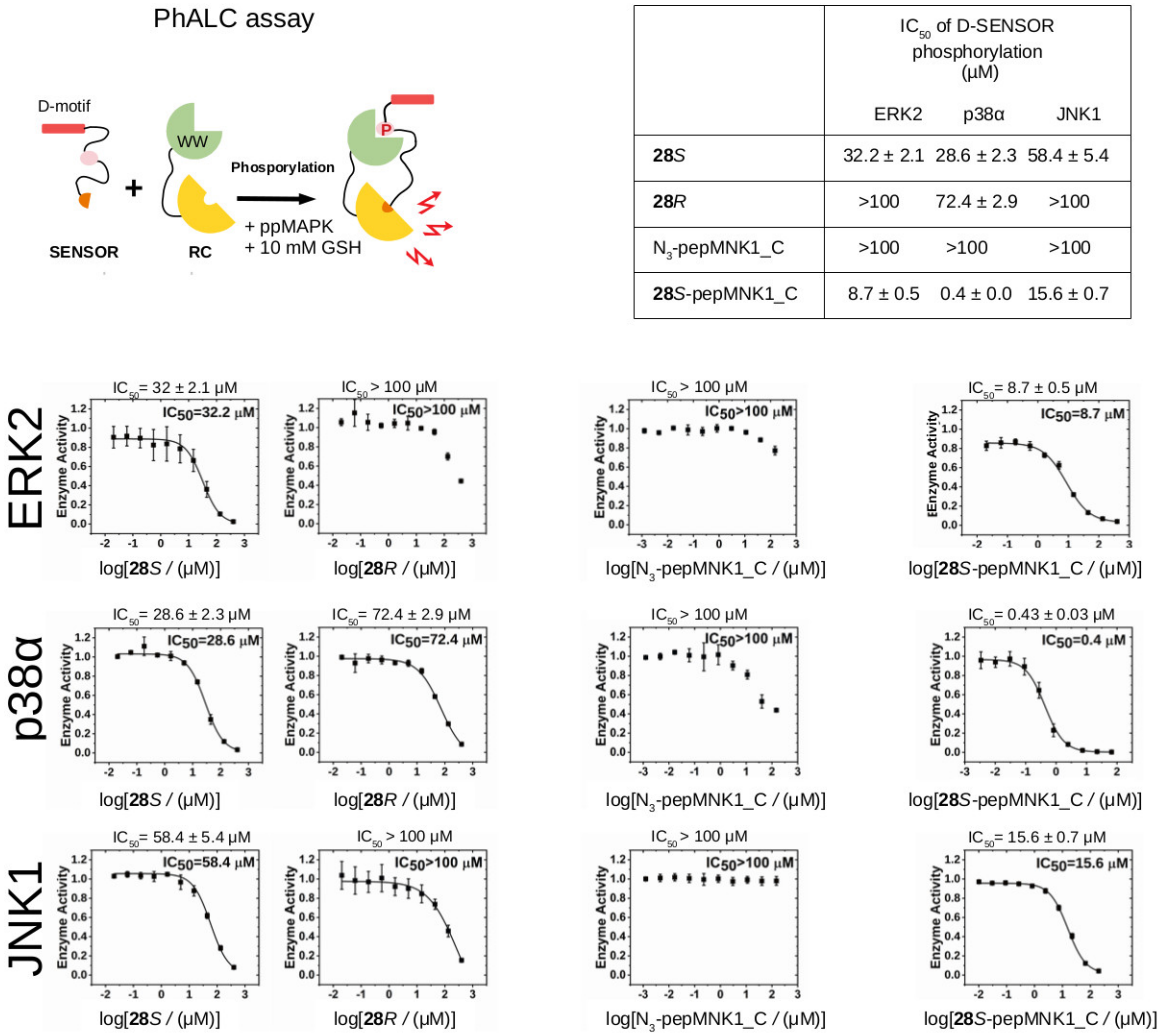

	IC_{50} of D-SENSOR phosphorylation (μM)		
	ERK2	p38α	JNK1
28*S*	32.2 ± 2.1	28.6 ± 2.3	58.4 ± 5.4
28*R*	>100	72.4 ± 2.9	>100
N_3-pepMNK1_C	>100	>100	>100
28*S*-pepMNK1_C	8.7 ± 0.5	0.4 ± 0.0	15.6 ± 0.7

Supplementary Fig. 18. Results of MAPK IC_{50} measurements carried out using the PhALC assay. The scheme shows the concept of the luciferase complementation based PhALC assay and the table on the right shows the summary of the IC50 values; while the panels below show the IC_{50} curves determined with this kinase activity assay. The assay was carried out using the D-SENSOR (MEF2A) in the presence of 10 mM GSH with pepMNK1, **28***S*, N_3-pepMNK1_C, **28***S*-pepMNK1_C and MAPKs (see Fig. 5c). (Data points show the mean and error bars show the SD based on three independent experiments. IC_{50} values above the panels indicate the parameter error estimate from weighted least square method; n=3) Source data are provided as a Source Data file.

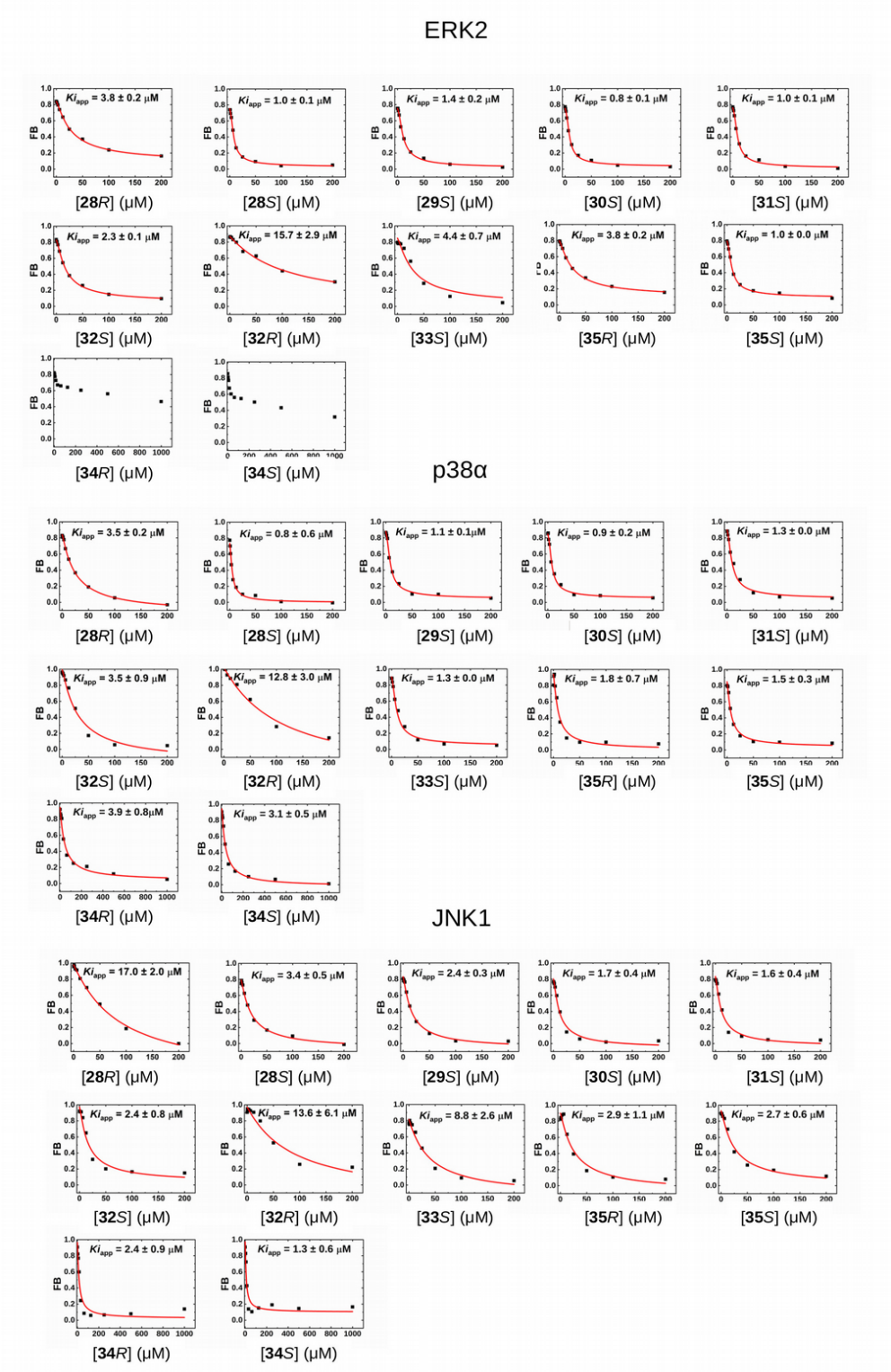

Supplementary Fig. 19. FP binding results with extended cyclohexenone scaffold containing compounds

Panels show the competitive binding curves for the measurements with ERK2, p38α, and JNK1 summarized in Table 4. FB: fraction bound. (Ki_{app} values indicate the parameter error estimate from weighted least square method; n=3.) Source data are provided as a Source Data file.

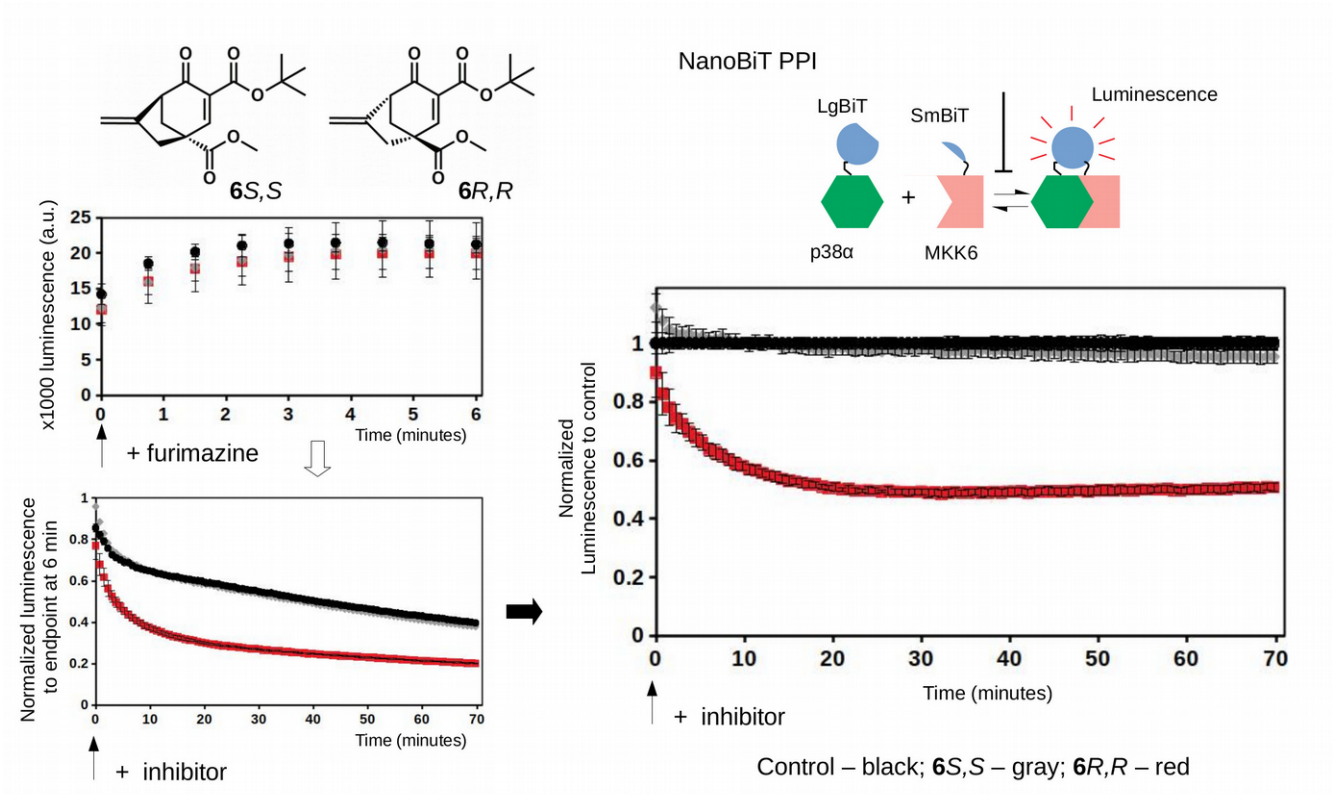

Supplementary Fig. 20. NanoBiT protein-protein interaction (PPI) assay in live HEK293T cells to monitor inhibitor uptake (6*R,R*) and target engagement in time

Cells were transfected with p38α-LgBit and MKK6-SmBiT construct and furimazine (a stable luciferase substrate) was added to cells after 24 hours (upper left panel; up to this point all wells were treated the same, albeit colored differently in triplicates to indicate wells destined for different later treatments: control, +**6***S,S* or +**6***R,R*). After the luminescence signal reached a steady level (~ 6 minutes), 10 μM inhibitor (or DMSO, 0.05%; Control) was added to cells and the signal was normalized to the luminescence value obtained at 6 minutes (left panel below). The panel on the right shows the luminescence signal normalized to Control. **6***R,R* efficiently blocks MKK6-p38 binding already after 15 minutes, while its enantiomer (**6***S,S*) does not affect this interaction. (Note that the fast drop at the second panel is because of dilution of the media with the inhibitor, and the shallow decrease of the signal later is due to constant time-dependent degradation of furimazine, which are all corrected for in the last panel.) Data represents the mean and error bars indicate SD (n=3; luminescence is measured in arbitrary units). Source data are provided as a Source Data file.

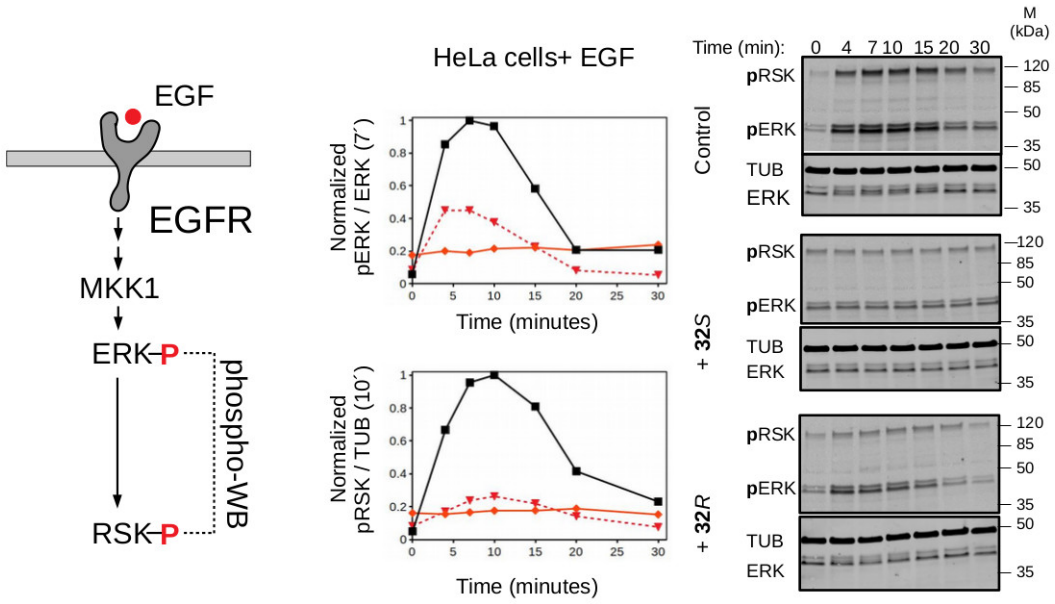

Supplementary Fig. 21. EGF stimulation of HeLa cells and the effect of 32*S* or 32*R* on ERK and RSK phosphorylation

HeLa cells were incubated with inhibitors (10 µM) for 1.5 hours before stimulation with 100 ng/mL EGF. The plots show the western blot (WB) signal of pERK/ERK normalized to control (Cont) at 7 minutes or the pRSK/tubulin signal normalized to the control at 10 minutes. Panels at the right show one set of western blot results. (pRSK: phosphoRSK antibody, pERK: phosphoERK antibody, ERK: anti-ERK antibody, TUB: anti-tubulin antibody as load control). Experiments were done in duplicates (n=2), data represents the mean. Source data are provided as a Source Data file.

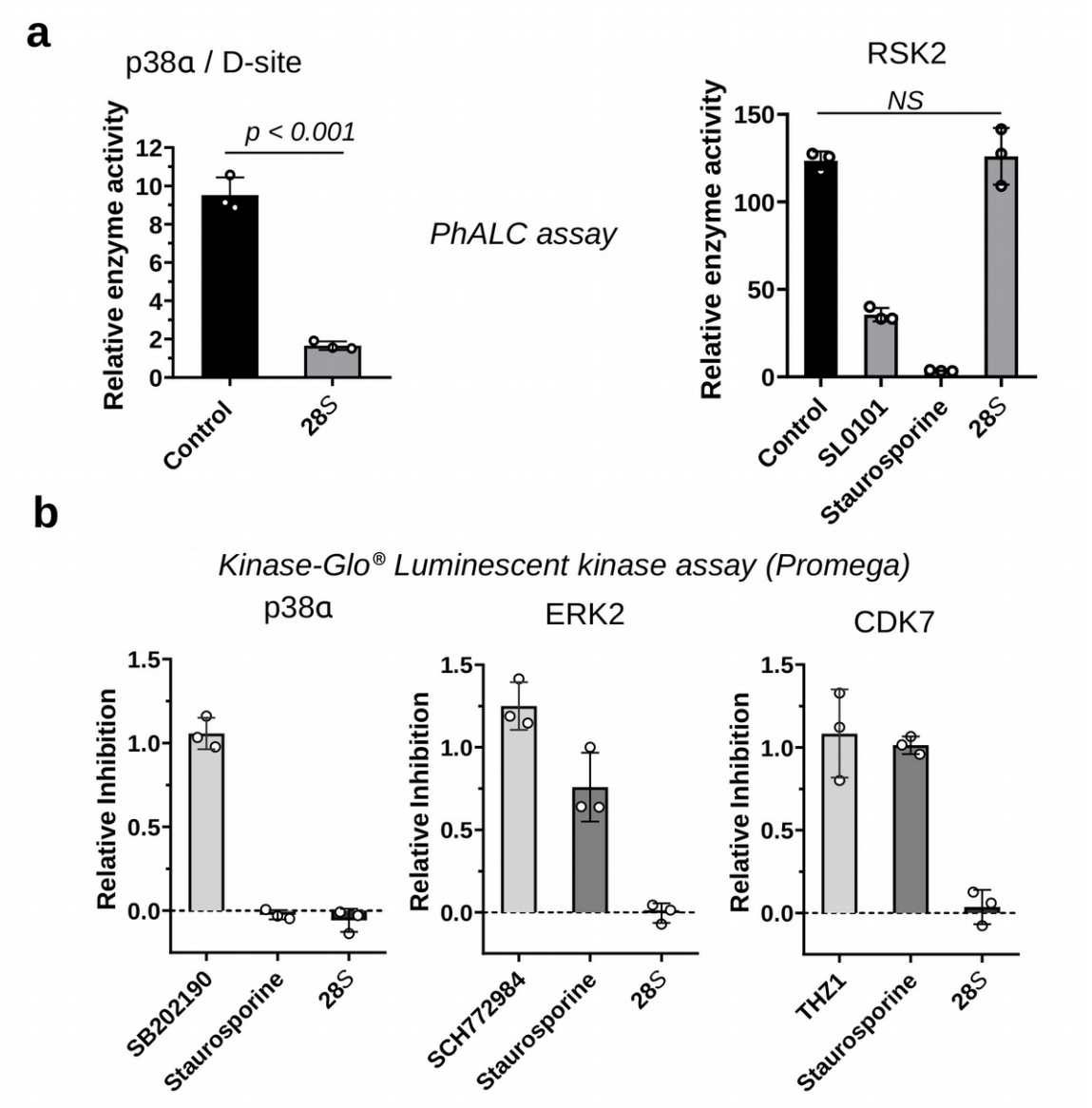

Supplementary Fig. 22. Results of selectivity tests with 28*S*.
(**a**) The left panel shows the results of in vitro PhALC assay experiments with a D-SENSOR construct whose phosphorylation is dependent on intact p38 docking[1]. (Control shows the relative activity for the reaction with active kinase normalized to the signal of the test without kinase added; **28**S: 10 μM inhibitor was added that efficiently blocked docking and thus inhibited phosphorylation assisted luciferase complementation (PhALC); Relative enzyme activity: the luminescence kinetic slope was normalized to that of the reaction which did not have active enzyme added.) The right panel shows a PhALC experiment with RSK-SENSOR (capable of detecting RSK2-mediated phosphorylation[1]. (Control shows the relative activity for the uninhibited reaction; this was normalized to the reaction which did not have any active kinase added; SL0101, staurosporine, and **28**S show the results with an RSK-specific or nonselective ATP-competitive inhibitor, or with the MAPK docking inhibitor respectively, all used in 10 μM concentration). Data represents the mean and error bars show SD (n=3). Notice, that the ATP-competitive inhibitors both inhibit RSK2 activity, while **28**S does not have this effect, as expected. (p-value: two-sided, unpaired t-test; NS: not significant).

(**b**) Results of Kinase-Glo Luminescent kinase assay with p38α, ERK2 and CDK7. Note that this assay monitors kinase activity by monitoring ATP co-factor decrease and the graphs show relative inhibition compared to the test containing no kinase. The experiments were carried out using specific inhibitors (e.g., SB202190, SCH772984, or THZ1 for p38α, ERK2 and CDK7, respectively), the non-specific ATP-competitive staurosporine as well as the MAPK D-groove binding **28**S compound. All compounds were used in 10 μM concentration. Note that **28**S did not inhibit the intrinsic kinase activity of the kinases, while the specific inhibitors or staurosporine, depending on its specificity profile, were effective. Data represents the mean and error bars show SD (n=3).
The more detailed description of the Kinase-Glo experiments is the following: The Kinase-Glo Max assay kit (Promega, Madison, WI; catalog no. V6071) was used to screen compounds for inhibition of CDK7/cyclin H/MNAT1, p38α, and ERK2. The enzymes CDK7/cyclin H/MNAT1 (catalog no. VA7402) were purchased from Promega, and the active MAPKs (p38α and ERK2) were produced in-house as previously described[1]. The kinase reaction system contained 25 ng/μL CDK7/cyclin H kinase, 10 μM of compounds, and 167 μg/μL kinase substrate (Native Swine Myelin Basic Protein) with 20 μM ATP in the case of CDK7 and 50 μM in the case of MAPKs. The reaction in each well was started immediately by adding ATP, followed by incubation for one hour at 25 °C. Then, 6 μL of Kinase-Glo Max reagent was added to each well, followed by 10 minutes of incubation. The luminescence signal was measured using a BioTek Cytation 3 microplate reader. After the signal was stable, the data were collected for five minutes. Data averages were normalized against control measurements both with and without kinase. Subsequently, the normalized data were plotted using the GraphPad Prism 8.0.1. software. Source data are provided as a Source Data file.

Supplementary Table 1. Details of crystallization, crystallographic data collection and structure refinement

	ERK2-SynthRev D^{COV}	ERK2-**8***S*	ERK2-**8***R*	ERK2-**12***R*	ERK2-**12***S*	ERK2-**3***R*	ERK2-**3***S*	ERK2-**6***R*,*R*
Data collection								
Space group	$P6_5$	$P2_12_12_1$	$P2_12_12_1$	$P2_12_12_1$	$P2_12_12_1$	$P2_12_12_1$	$P2_12_12_1$	$P2_12_12_1$
Cell dimensions								
a, *b*, *c* (Å)	62.13, 62.13, 214.98	41.47, 77.39, 127.22	41.90, 78.33, 127.14	41.49, 77.05, 123.39	41.58, 77.15, 123.68	41.65, 76.86, 124.92	41.44 76.84 123.32	41.94 78.47 122.74
α, β, γ (°)	90, 90, 120	90, 90, 90	90, 90, 90	90, 90, 90	90, 90, 90	90, 90, 90	90, 90, 90	90, 90, 90
Resolution range (Å)	43.03-1.85	49.14-2.0	49.36-2.55	38.52 - 1.65	48.25 - 1.8	48.47 - 1.9	61.66-1.95	48.34 - 1.80
$CC_{1/2}$*	0.998 (0.783)	0.998 (0.871)	0.998 (0.636)	0.999 (0.718)	0.999 (0.780)	0.999 (0.693)	0.999 (0.567)	1.000 (0.560)
R_{merge}†	0.19 (1.75)	0.16 (1.68)	0.16 (1.52)	0.097 (1.42)	0.12 (1.32)	0.06 (0.81)	0.13 (3.42)	0.063 (2.041)
$I/\sigma I$	12.0 (1.6)	10.5 (1.6)	11.8 (1.5)	14.0 (1.4)	13.4 (1.6)	12.8 (1.7)	12.3 (0.9)	20.3 (1.4)
Completeness (%)	99.7 (99.3)	100 (100)	99.9 (100)	100 (100)	100 (100)	91.7 (90.8)	100 (100)	100 (100)
Redundancy	20.0 (19.9)	11.8 (11.4)	11.6 (12.1)	12.5 (12.6)	12.7 (12.4)	4.6 (3.9)	13.4 (13.7)	13.3 (13.2)
No. reflections	39751	28489	14259	48499	37729	29741	29520	38411
Refinement								
R_{work}/ R_{free}	0.1795 / 0.2056	0.1892 / 0.2147	0.1897 / 0.2318	0.1768 / 0.2069	0.1791 / 0.2064	0.1904 / 0.2240	0.2039 / 0.2354	0.1867/ 0.2222
No. atoms	3346	2912	2832	3340	3206	2921	2917	3032
Protein	3025	2755	2761	2962	2939	2738	2756	2810
Ligand/ion	37	52	52	81	53	46	86	70
Water	284	105	19	297	214	137	75	152
B-factors (Å^2)	41.66	53.46	70.57	38.27	44.87	52.45	48.93	44.14
Protein	41.72	53.56	70.77	37.82	44.64	52.47	49.15	43.74
Ligand/ion	25.48	57.93	63.05	39.67	58.67	58.36	46.37	59.24
Water	43.18	48.43	62.40	42.42	44.73	50.10	44.08	44.43
Ramachandran								
Favored (%)	96.97 %	96.41 %	97.32 %	97.98 %	97.69 %	96.94 %	98.18 %	97.35 %
Allowed (%)	3.03 %	3.59 %	2.68 %	2.02 %	2.31 %	3.06 %	1.82 %	2.65 %
Outliers (%)	0.00 %	0.00 %	0.00 %	0.00 %	0.00 %	0.00 %	0.00 %	0.00 %
R.m.s deviations								
Bond lengths (Å)	0.008	0.004	0.008	0.012	0.009	0.006	0.006	0.011
Bond angles (°)	0.995	0.617	1.021	1.163	1.049	0.769	0.931	1.061
PDB ID	8PSR	8PSW	8PSY	8PT0	8PT1	8PST	8PT5	8PT3

*Values for the highest resolution bin is shown in parentheses

†$R_{merge} = \Sigma_{hkl}\Sigma_i |I_i(hkl)-<I(hkl)>|/\Sigma_{hkl}\Sigma_i I_i(hkl)$

Supplementary Table 2. Structures of Group1-7 compounds

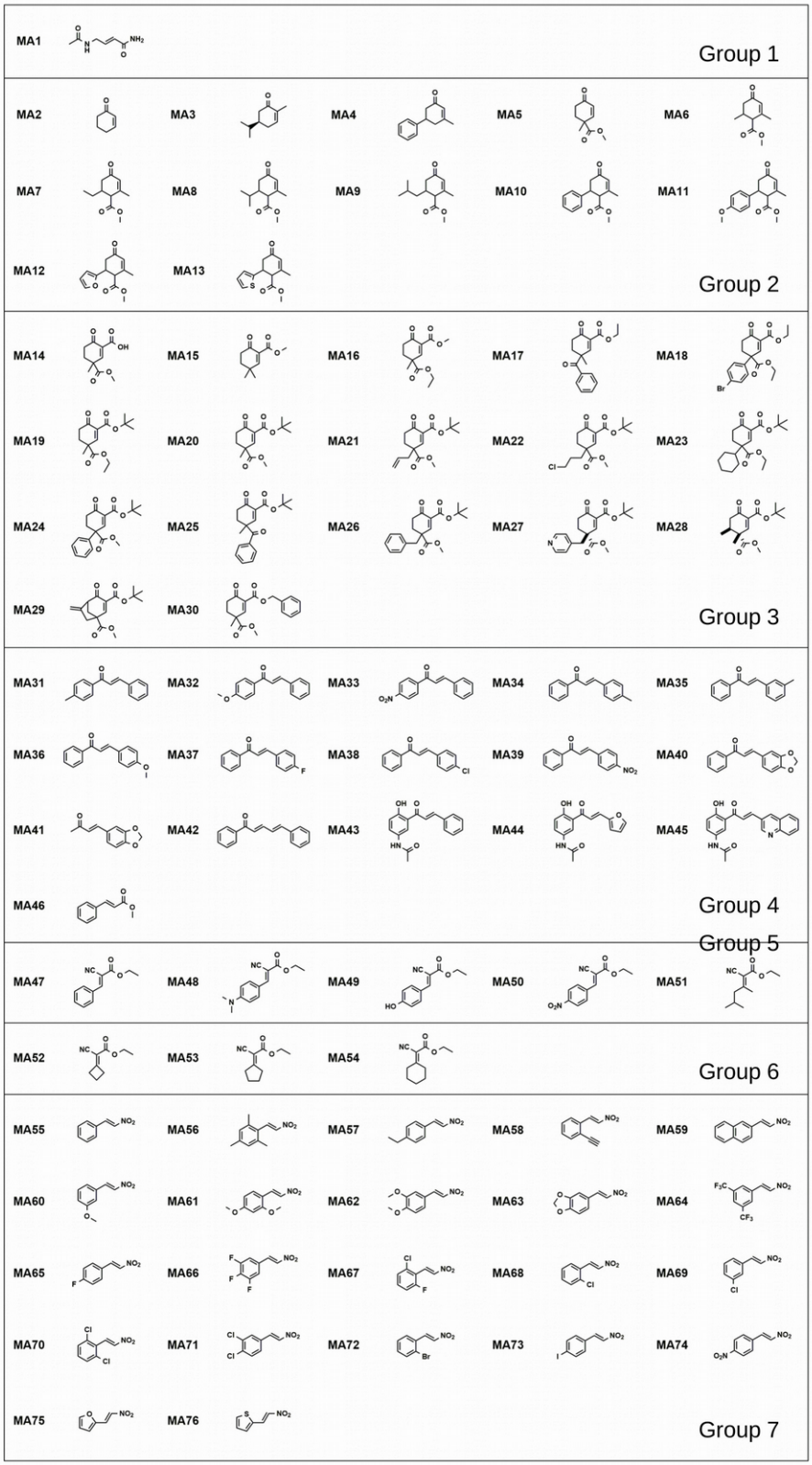

Supplementary Table 3. List of oligonucleotides used for cloning

Mutagenesis oligos	On wild-type bacterial expression plasmids
ERK2_H125R_Forw	ACA CAA CAC CTC AGC AAT GAC AGG ATC TGC TAT TTT CTC TAC CAG
ERK2_H125R_Rev	CTG GTA GAG AAA ATA GCA GAT CCT GTC ATT GCT GAG GTG TTG TGT
ERK2_H1254R_Forw	CACCTCAGCAATGACCGTATCTGCTATTTTCTCTACC
ERK2_H1254R_Rev	GGTAGAGAAAATAGCAGATACGGTCATTGCTGAGGTG
p38a_H126L_Forw	CAGAAGCTTACAGATGACCTTGTTCAGTTCCTTATCTAC
p38a_H126L_Rev	GTAGATAAGGAACTGAACAAGGTCATCTGTAAGCTTCTG
p38a_C162A_Forw	CTAGCTGTGAATGAAGACAGTGAGCTGAAGATTCTGG
p38a_C162A_Rev	CCAGAATCTTCAGCTCACTGTCTTCATTCACAGCTAG
p38a_C119V_Forw	CTGAACAACATTGTGAAAGTTCAGAAGCTTACAGATGACC
p38a_C119V_Rev	GGTCATCTGTAAGCTTCTGAACTTTCACAATGTTGTTCAG
For Nanobit constructs	Promega NanoBiT® MCS Starter System (N2014); Cloned into the following plasmids: pBiT1.1-N[TK/LgBiT] for p38a and JNK pBiT1.1-C[TK/LgBiT] for ERK2 pBiT2.1-N[TK/SmBiT] for partners (MKK1, MKK6, MKK7, RSK1 and MKP3)
ERK2_LC_NheI_Forw	TAT ATA GCT AGC CAC CAT GGC GGC GGC GGC G
ERK2_LC_Xho_R_Forw	TTA ATT CTC GAG CCA GAT CTG TAT CCT GGC TGG AAT C
JNK1_LN_XhoI_Forw	TTA ATT CTC GAG CGG TAT GAG CAG AAG CAA GCG TGA C
JNK1_LN_NheI_Rev	TAT ATA GCT AGC TCA CTG CTG CAC CTG TGC TAA AG
p38a_LN_XhoI_Forw	TTATCTCTCGAGCGGTA TGTCTCAGGA GAGGCCCACG
p38a_LN_NheI_Rev	AGATAAGCTAGCTCAGGACTCCATCTCTTCTTGGTC
MKK1_SN_XhoI_Forw	TTATCTCTCGAG**C**ATGCCCAAGAAGAAGCCGACG
MKK1_noStop_SN_NheI_Rev	AGATAAGCTAGCGACGCCAGCAGCATGGGTTG
MKK6_SN_XhoI_Forw	TTATCTCTCGAGCATGTCTCAGTCGAAAGGCAAG
MKK6_noStop_SN_NheI_Rev	AGATAAGCTAGCGTCTCCAAGAATCAGTTTTACAAAAGATGC
MKK7_SN_XhoI_Forw	TTATCTCTCGAGCATGGCGGCGTCCTCCCTGG
MKK7_nostop_SN_NheI_Rev	AGATAAGCTAGCCCTGAAGAAGGGCAGGTGGG
RSK1_SN_XhoI_Forw	TTATCTCTCGAGCATGCCGCTCGCCCAGCTCAAGG
RSK1_SN_NheI_Rev	AGATAAGCTAGCTCACAGGGTGGTGGATGGCAACTTC
MKP3_SN_XhoI_Forw	TTATCTCTCGAG**C**ATGATAGATACGCTCAGACCCGTGC
MKP3_noStop_SN_NheI_Rev	AGATAAGCTAGCCGTAGATTGCAGAGAGTCCACCTG

SUPPLEMENTARY NOTE 1 (on the adduct formation NMR experiments)

The adduct formation NMR experiments were conducted on Varian NMR System spectrometers with inverse detection probes, operating at 400 MHz and 600 MHz. ^{1}H and ^{13}C assignment assignments were established using a combination of two-dimensional ^{1}H-^{1}H COSY, ^{1}H-^{1}H TOCSY, ^{1}H-^{1}H ROESY, ^{1}H-^{13}C HSQC and ^{1}H-^{13}C HMBC measurements.

Titration of **3*R*** with **BME**:

2.28 mg (8.5 mmol) **3*R*** was dissolved in 3:1 mixture of DMSO-d_6–PBS (D_2O) buffer (575 µL). The mixture was transferred to an NMR tube. After the initial ^{1}H NMR measurement, **BME** (0.84 mmol, 0.1 equiv., 12 µl of 70.4 mM in DMSO-d_6–PBS (D_2O) buffer) was added to the sample and ^{1}H NMR spectra was acquired after 5 minutes of equilibration time. This step was repeated until the sample contained 1.4 equiv. of **BME**.

Summary of NMR data for diastereomeric adducts of **3*R*** and **BME**:

The (*S*,*S*)-diastereomeric adduct of **3*R*** and **BME** (seen in green in **Supplementary Fig. 23.**):

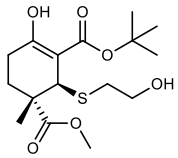

^{1}H NMR (400 MHz, DMSO-d_6–PBS): δ 3.87 (d, *J* = 2.1 Hz, 1H), 3.52 (s, 3H), 3.55 – 3.48 (m, 2H), 2.70 – 2.66 (m, 2H), 2.21 – 2.09 (m, 2H), 1.89 – 1.81 (m, 1H), 1.79 – 1.74 (m, 1H), 1.43 (s, 9H), 1.22 (s, 3H).

^{13}C NMR (101 MHz, DMSO-d_6–PBS): δ 176.3, 171.1, 170.62, 102.8, 83.0, 60.98, 52.6, 48.1, 47.2, 37.6, 28.18, 26.3, 25.9, 24.9;

The (*S*,*R*)-diastereomeric adduct of **3*R*** and **BME** (seen in blue in **Supplementary Fig. 23.**):

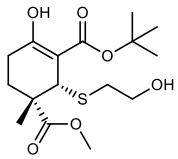

^{1}H NMR (400 MHz, DMSO-d_6–PBS): δ 3.60 (d, *J* = 2.0 Hz, 1H), 3.59 (s, 3H), 3.41 – 3.37 (m, 2H), 2.65 – 2.56 (m, 2H), 2.27 – 2.20 (m, 2H), 2.01 – 1.90 (m, 1H), 1.72 – 1.64 (m, 1H), 1.43 (s, 9H), 1.06 (s, 3H).

^{13}C NMR (101 MHz, DMSO-d_6–PBS): δ 176.0, 171.4, 170.57, 100.4, 82.7, 60.98, 52.2, 48.4, 46.8, 36.8, 28.18, 25.2, 24.0, 21.3;

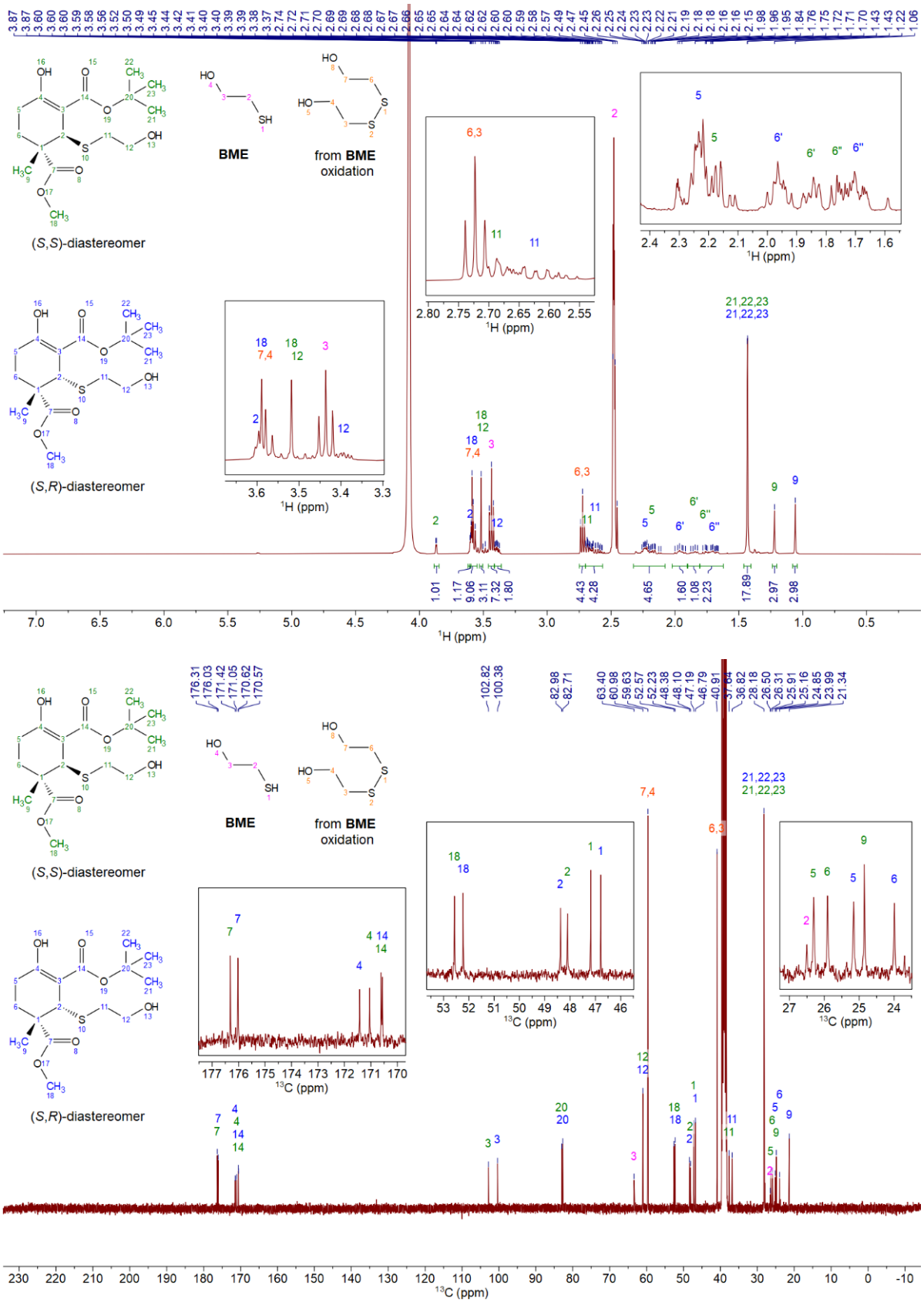

Supplementary Fig. 23. The ^{1}H-NMR (400 MHz) and ^{13}C-NMR (101 MHz) spectra and assignation of the diastereomeric **BME** adducts of **3*R*** in DMSO-d_6 –PBS (D_2O) buffer

Jump dilution measurement of **3*R*** with **BME**:

13.36 mg (49.8 mmol) **3*R*** was dissolved in 3:1 mixture of DMSO-d_6–PBS (D_2O) buffer (546 µL). A solution of **BME** (27 µL, 3.5 M in DMSO-d_6–PBS (D_2O) buffer, 1.2 equiv.) and an internal standard solution (37 µL, 394.2 mM, 1,3,5-trimethoxybenzene in DMSO-d_6–PBS (D_2O) buffer) were added to the substrate, and the mixture was transferred to an NMR tube. The sample was allowed to equilibrate for one hour while monitoring the isomerization of the formed diastereomers. The final diastereomer ratio of 1:1 was reached after 30 minutes. 60 µL of the sample was diluted to 600 µL with DMSO-d_6–PBS (D_2O) buffer, and the first measurement point was taken after 145 seconds, followed by scans every 35 seconds.

Titration of **6*R,R*** with **BME**:

2.59 mg (8.8 mmol) 6***R***,***R*** was dissolved in 3:1 mixture of DMSO-d_6–PBS (D_2O) buffer (573 µL). A solution of internal standard (27 µL, 354.1 mM, 1,3,5-trimethoxybenzene in DMSO-d_6–PBS (D_2O) buffer) was added to the sample and the mixture was transferred to an NMR tube. After the initial ^{1}H NMR measurement, **BME** (0.84 mmol, 0.1 equiv., 12 µl of 70.4 mM in DMSO-d_6–PBS (D_2O) buffer) was added to the sample and ^{1}H NMR spectra was acquired after 5 minutes of equilibration time. This step was repeated until the sample contained 2.4 equiv. of **BME**.

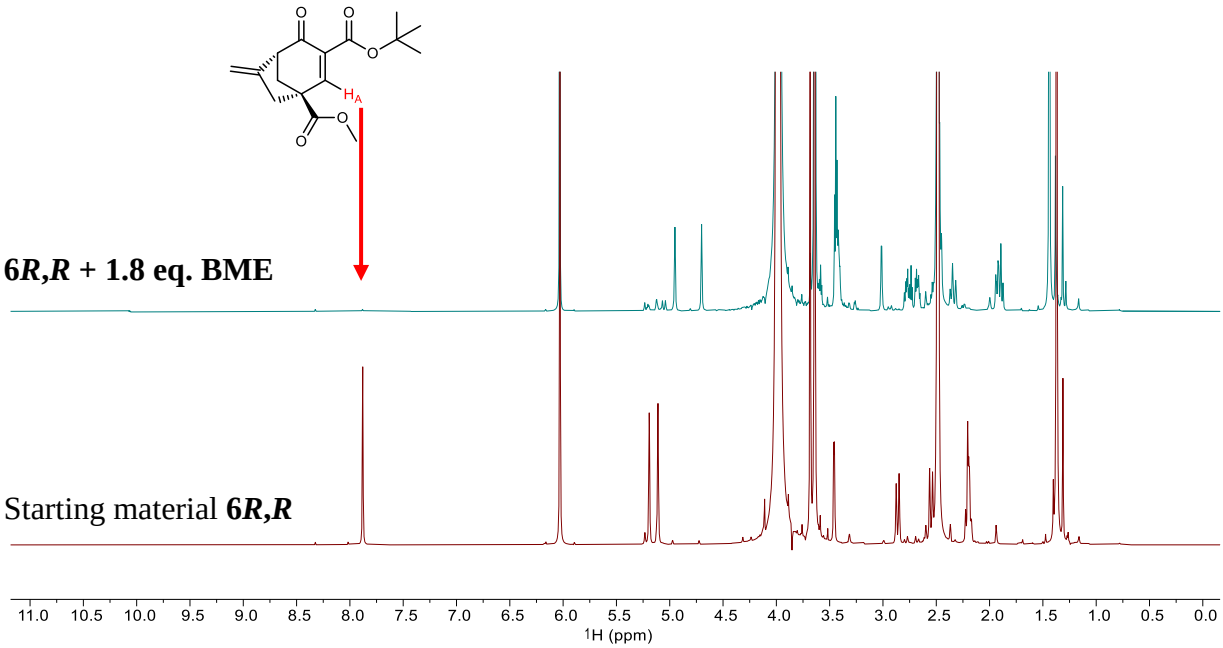

Supplementary Fig. 24. The ^{1}H NMR (600 MHz) spectra of **6*R*,*R*** before (lower spectrum) and after (upper spectrum) the addition of 1.8 eq. **BME** in DMSO-d_6 –PBS (D_2O) buffer. The disappearance of the H_A alkene hydrogen and the emergence of a new signal set indicating the Michael adduct formation

Summary of NMR data for diastereomeric adducts of **6*R,R*** and **BME**:

The (*S*,*S*,*R*)-diastereomeric adduct of **6*R,R*** and **BME** (seen in green in **Supplementary Fig. 25.**):

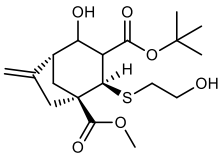

^{1}H NMR (600 MHz, DMSO-d_6–PBS) δ 4.96 (s, 1H), 4.71 (s, 1H), 3.66 – 3.65 (m, 1H), 3.64 (s, 3H), 3.44 – 3.42 (m, 2H), 3.02 (d, *J* = 3.9 Hz, 1H), 2.79 (dd, *J* = 12.4, 6.5 Hz, 1H), 2.72 – 2.65 (m, 1H), 2.48 – 2.44 (m, 1H), 2.33 (d, *J* = 17.9 Hz, 1H), 1.94 – 1.93 (m, 1H), 1.89 (d, *J* = 12.1 Hz, 1H), 1.44 (s, 9H).

^{13}C NMR (151 MHz, dmso) δ 174.80, 172.87, 171.95, 149.43, 107.97, 98.13, 83.49, 61.33, 55.01, 53.01, 51.46, 49.05, 39.90, 37.99, 33.15, 28.73.

The (*S*,*R*,*R*)-diastereomeric adduct of **6*R,R*** and **BME** (seen in blue in **Supplementary Fig. 25.**):

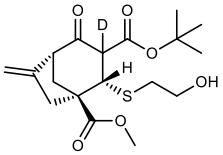

^{1}H NMR (600 MHz, DMSO-d_6–PBS) δ 5.07 (s, 1H), 5.05 (s, 1H), 3.66 (s, 3H), 3.62 – 3.61 (m, 1H), 3.42 – 3.37 (m, 2H), 3.27 (d, *J* = 5.4 Hz, 1H), 2.95 (d, *J* = 18.3 Hz, 1H), 2.72 – 2.65 (m, 1H), 2.55 (t, *J* = 7.2 Hz, 2H), 2.25 (dd, *J* = 12.8, 5.5 Hz, 1H), 1.95 – 1.94 (m, 1H), 1.39 (s, 9H).

^{13}C NMR (151 MHz, DMSO-d_6–PBS) δ 202.01, 173.81, 168.66, 145.66, 112.14, 83.32, 61.24, 60.78, 57.88, 55.90, 53.30, 52.84, 40.91, 35.93, 35.25, 28.44.

The deuterated α-carbon is only discernible in the ^{1}H-^{13}C HMBC measurement.

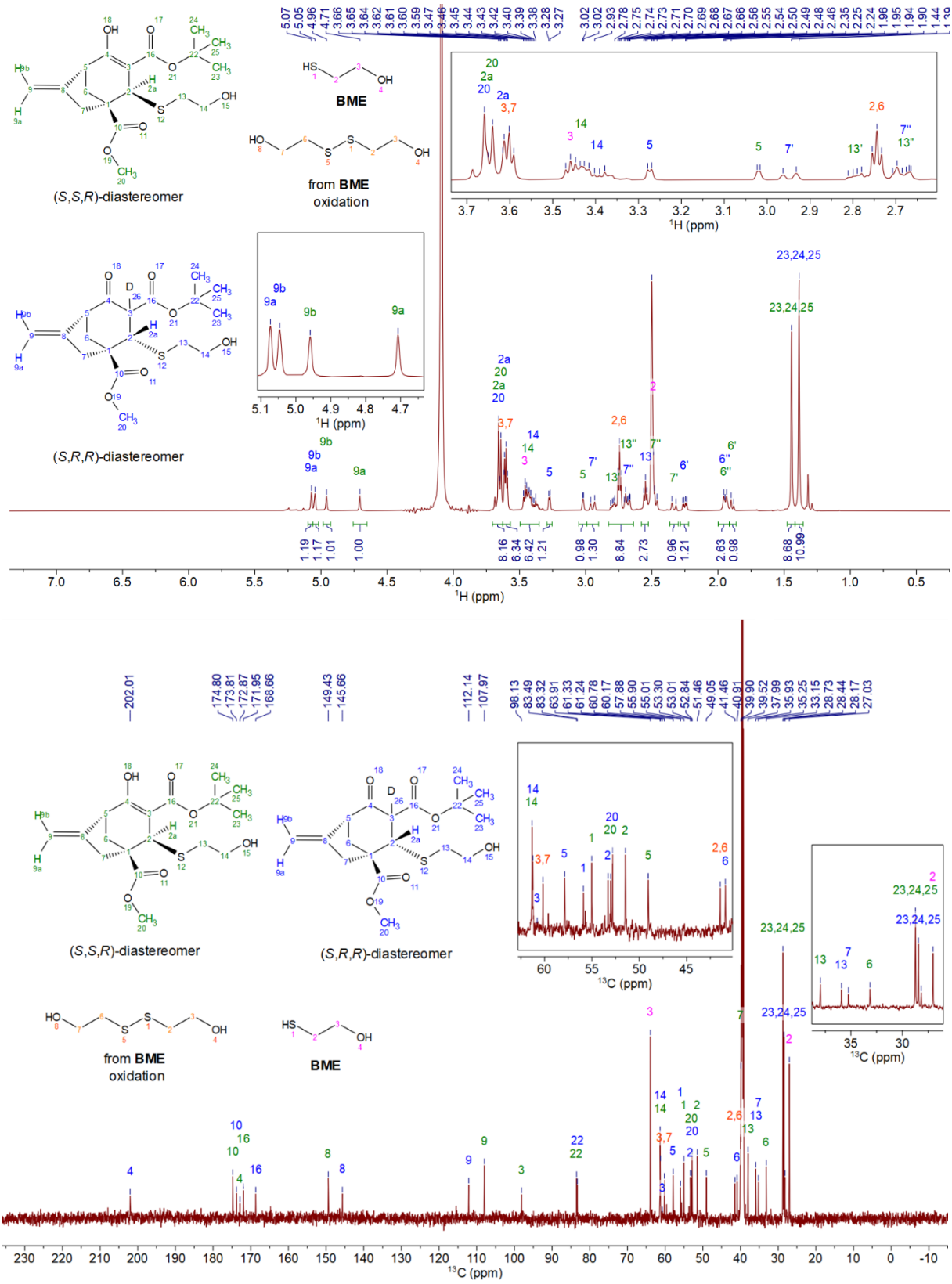

Supplementary Fig. 25. The ^{1}H-NMR (600 MHz) and ^{13}C-NMR (151 MHz) spectra and assignation of the isomeric **BME** adducts of ***6R,R*** in DMSO-d_6 –PBS (D_2O) buffer

Titration of **6*R,R*** with **His-Test**:

2.65 mg (9.1 mmol) **6*R,R*** was dissolved in 3:1 mixture of DMSO-d_6–PBS (D_2O) buffer (578 µL). A solution of internal standard (22 µL, 154.9 mM, 1,3,5-trimethoxybenzene in DMSO-d_6–PBS (D_2O) buffer) was added to the sample and the mixture was transferred to an NMR tube. After the initial ^{1}H NMR measurement, **His-Test** (1.1 mmol, 0.1 equiv., 10 µl of 109.3 mM in DMSO-d_6–PBS (D_2O) buffer) was added to the sample and ^{1}H NMR spectra was acquired after 5 minutes of equilibration time. This step was repeated until the sample contained 2.6 equiv. of **His-Test**.

The *N*-acetyl-L-histidine methyl ester (**His-Test**) was added at different concentrations into the solution of the compound **6*R*,*R*** during the NMR titration experiment. The concentrations of the reactants (compound **6*R*,*R*** and *N*-acetyl-L-histidine methyl ester) and the adduct were determined relative to the internal standard. The Kchem_off was determined for the various concentrations of *N*-acetyl-L-histidine methyl ester (using the following equation: Kchem_off = [reactant1] × [reactant2] / [product]). The average and standard deviation of the Kchem values, determined in the presence of histidine derivatives greater than 5 mM, have been calculated, assuming that equilibrium is established at those concentrations.

Supplementary Note 2 (on the ECD measurements)

The ECD spectrum of **3*R*** had an intense positive Cotton effect (CE) at 236 nm and a negative one at 209 nm, which were governed by the (*R*) absolute configuration of its quaternary chirality center. Upon addition of the 2-sulfanylethanol (BME) reagent, both of these two ECD transitions began diminishing and a new positive weaker CE appeared at 225 nm (**Supplementary Fig. 26a**). The change of the 236 nm positive CE was monitored in the function of the equivalent of 2-sulfanylethanol, which produced a smoothly decreasing curve. The curve fitting of the titration points gave the equilibrium constant with the value of 643±41 (M^{-1}) (**Supplementary Fig. 26b**).

The substrate **6*R*,*R*** had two chirality centers and a bridged skeleton, which were expected to induce remarkable diastereoselectivity during the conjugate addition. **6*R*,*R*** had an intense positive CEs at 341 nm and a negative one at 233 nm, the magnitude of which was decreasing continuously with the increasing amount of the reagent (**Supplementary Fig. 26c**). Simultaneously, a new negative ECD band at 265 nm and a positive one at 295 nm appeared, which could be attributed to the addition product. With an excess of the 2-sulfanylethanol reagent, the initial 341 nm CE of **6*R*,*R*** was converted to the baseline and monitoring the change of Δε at 341 nm allowed determining the equilibrium constant as 409±68 (M^{-1}) (**Supplementary Fig. 26d**).

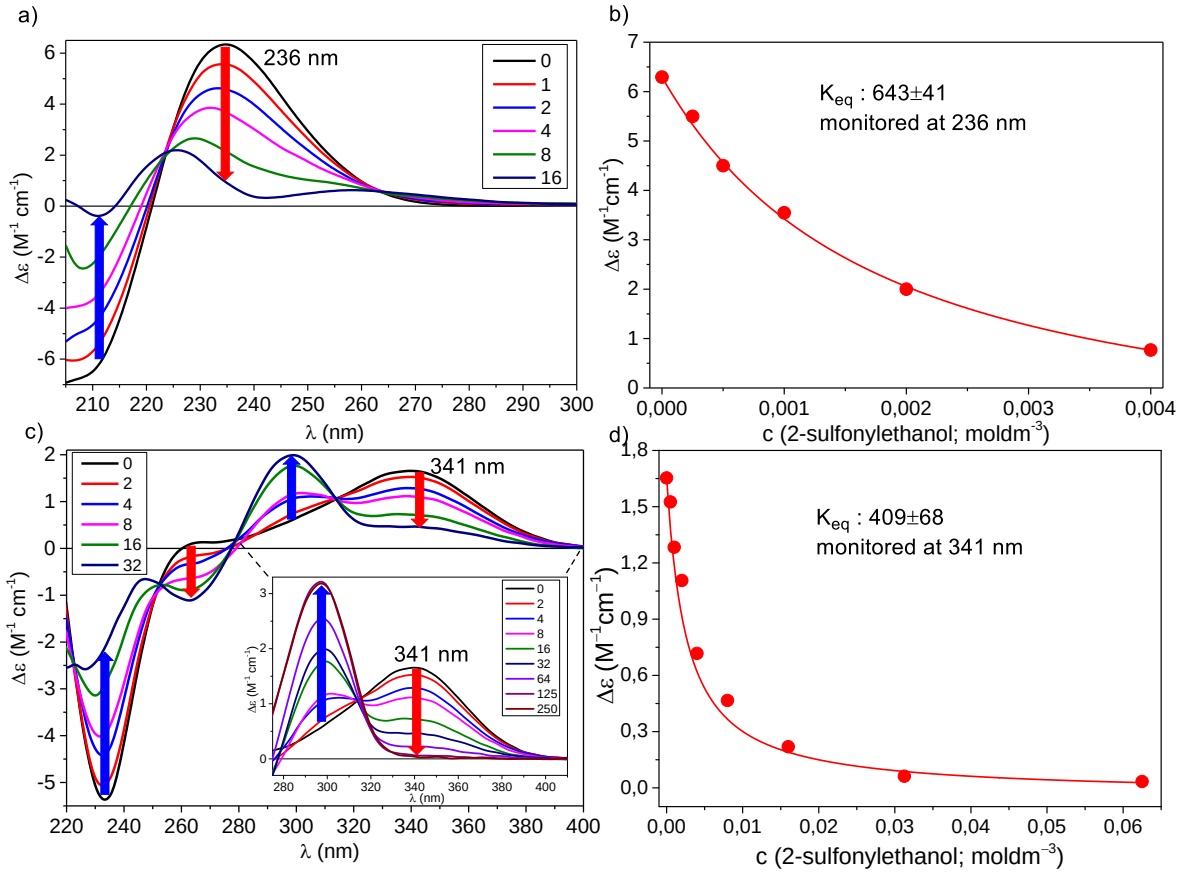

Supplementary Fig. 26. a) ECD spectrum of **3*R*** (black) in phosphate buffer saline compared (PBS) with those produced by addition of different equavalents of 2-sulfonylethanol (from 1 to 16 equivalents). b) Change of the ECD signal (Δε) of **3*R*** in the function of the increasing concentration of 2-sulfanylethanol monitored at 236 nm. Curve fitting produced the value of 643±41 (M^{-1}) for the equilibrium constant. c) ECD spectrum of **6*R*,*R*** (black) in PBS compared with those produced by addition of different equivalents of 2-sulfonylethanol (from 2 to 32

equivalents). Inset figure shows the enlarged 275-410 nm wavelength range with 0-250 equivalents of 2-sulfonylethanol. d) Change of the ECD signal of **6*R*,*R*** (Δε) in the function of the increasing concentration of 2-sulfanylethanol monitored at 341 nm. Curve fitting produced the value of 409±68 (M^{-1}) for the equilibrium constant.

Experimental data

3*R*: ECD [nm (Δε), PBS] (67 μg/1 ml): 329 (0.14), 236 (6.34), 209 (-6.57).

6*R*,*R*: ECD [nm (Δε), PBS] (73 μg/1 ml): 341 (1.66), 233 (-5.37), 209 (2.07).

19'*S*: ECD [nm (Δε), PBS] (89.5 μg/1 ml): 236 (3.78), 212sh (-4.11), 206 (-4.57).

18*R*: ECD [nm (Δε), PBS] (67 μg/1 ml): 331 (0.20), 236 (5.74), 208 (-6.36).

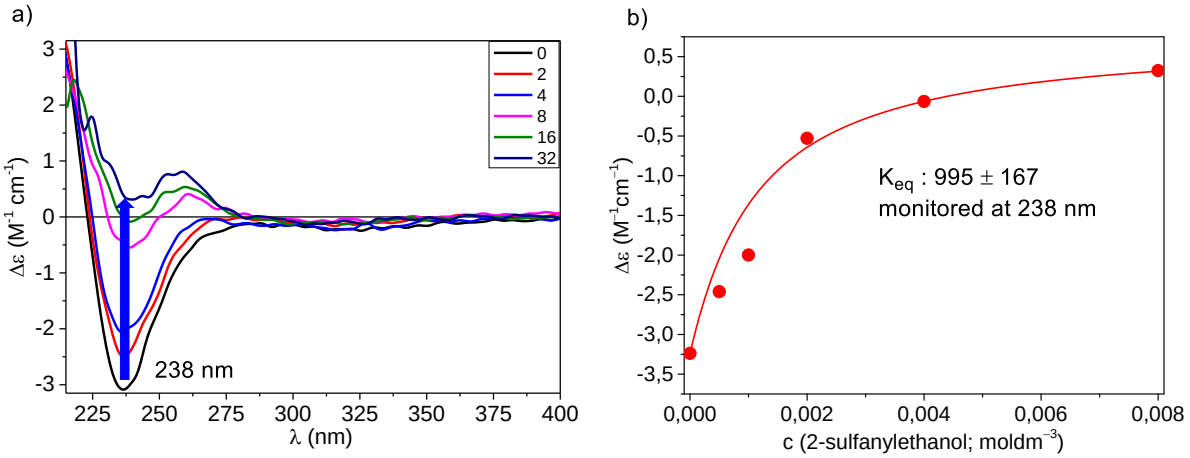

Supplementary Fig. 27. a) ECD spectrum of **19'*S*** (black) in phosphate buffer saline compared (PBS) with those produced by addition of different equavalents of 2-sulfonylethanol (from 2 to 32 equivalents). b) Change of the ECD signal (Δε) of **19'*S*** in the function of the increasing concentration of 2-sulfanylethanol monitored at 238 nm. Curve fitting produced the value of 995±167 (M^{-1}) for the equilibrium constant.

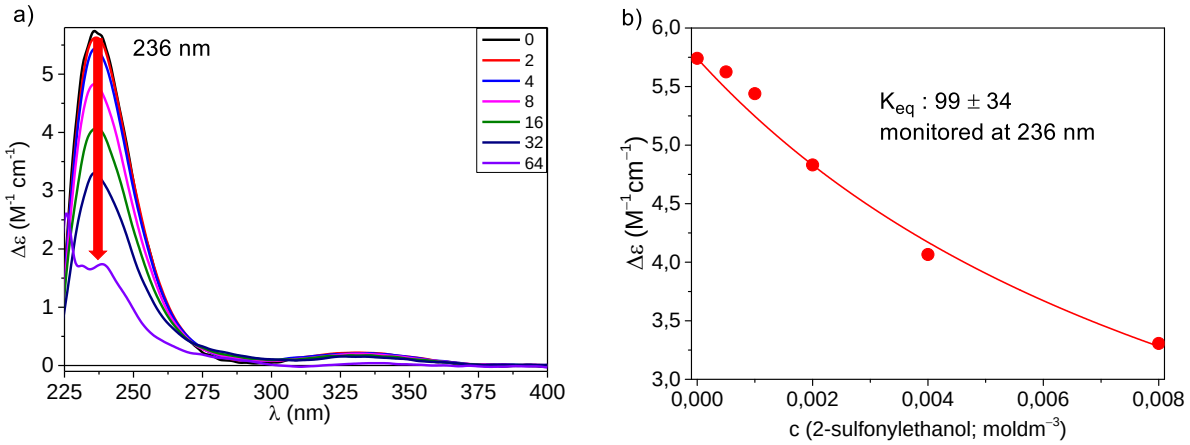

Supplementary Fig. 28. a) ECD spectrum of **18*R*** (black) in phosphate buffer saline compared (PBS) with those produced by addition of different equivalents of 2-sulfonylethanol (from 2 to 32 equivalents). b) Change of the ECD signal (Δε) of **18*R*** in the function of the increasing concentration of 2-sulfanylethanol monitored at 238 nm. Curve fitting produced the value of 99±34 (M^{-1}) for the equilibrium constant.

SUPPLEMENTARY NOTE 3 (on the synthesis of the compounds)

General procedure A for synthesizing cyclohexenone warhead compounds:

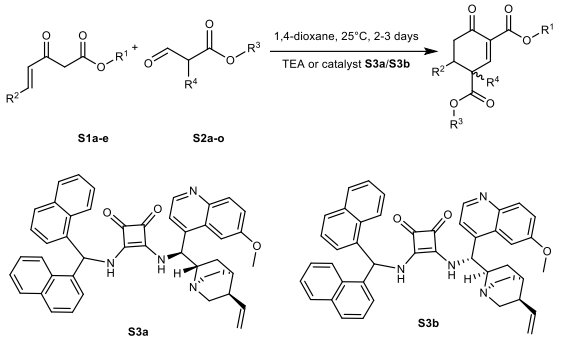

Compound **S1a-e** (1.0 eq.), compound **S2a-o** (1.1 eq.) and the catalyst (triethylamine (0.10 eq.) for racemic mixtures or catalyst **S3a** or **S3b** (0.02 eq.) for the enantiomerically enriched compounds respectively) was dissolved in 1,4-dioxane (1.0 M) and the reaction mixture was stirred at room temperature for 2-3 days. When the reaction was completed removal of the volatile compounds under reduced pressure was followed by purification by flash chromatography on silica gel (hexanes 0-25% ethyl acetate) giving the products as a yellow oil.

Compounds **S1a-e**, **S2a-j**, **S3a**, **S3b** were synthesized according to the literature procedures. [1,2]

Compound **1** was synthesized according to the literature procedure.[2]

Compounds **4**, **11** were synthesized according to the literature procedure.[1]

Compound **39** was purchased from Sigma.

N-(2-(2-(2-(2-azidoethoxy)ethoxy)ethoxy)ethyl)-5-((3a*S*,4*S*,6a*R*)-2-oxohexahydro-1*H*-thieno[3,4-*d*]imidazol-4-yl)pentanamide (S4):

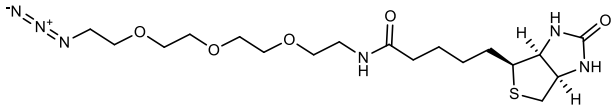

Compound **S4** was purchased from TCI.

Preparation of 1-(*tert*-butyl) 3-(4-(1-(13-oxo-17-((3a*S*,4*S*,6a*R*)-2-oxohexahydro-1*H*-thieno[3,4-d]imidazol-4-yl)-3,6,9-trioxa-12-azaheptadecyl)-1*H*-1,2,3-triazol-4-yl)butyl) (*S*)-3-methyl-6-oxocyclohex-1-ene-1,3-dicarboxylate (2-biotin):

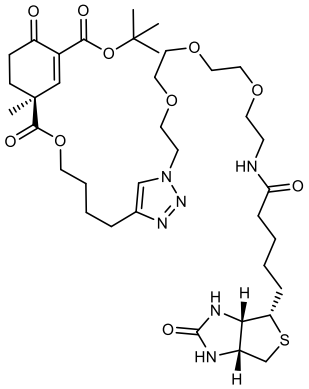

To the solution of **31*S*** (18.0 mg, 0.040 mmol, 1 eq.) in methylene chloride (162 µL) was added compound **S4** (20.3 mg, 0.061 mmol, 1.5 eq.). To this mixture was added the solution of copper(II) sulfate pentahydrate (5.1 mg, 0.020 mmol, 0.5 eq.) and sodium ascorbate (0.8 mg, 0.004 mmol, 0.1 eq.) in water (162 µL) and methanol (81 µL). The reaction mixture was vigorously stirred at 25°C. After 3 hours the mixture was diluted with methylene chloride and water then the aqueous phase was washed with methylene chloride two times. The combined organic phases were washed with brine then dried over anhydrous Na_2SO_4, filtered, and evaporated under reduced pressure. The crude product was purified by preparative RP-HPLC using a gradient method on a Gemini® 5µm C18 110 Å column (H_2O:MeCN = 95:5 (0.1 % HCOOH) to 100% MeCN (0.1 % HCOOH)). Compound **2-biotin** was obtained as a colorless oil (11.2 mg, 36%).

HRMS (ESI-TTOF) m/z $[M+H]^+$ calculated for $C_{37}H_{59}N_6O_{10}S$ 779.4007 found 779.3990

^{1}H NMR (600 MHz, $CDCl_3$): δ 7.49 (s, 1H), 7.34 (s, 1H), 6.76 (s, 1H), 4.52 (t, *J* = 5.2 Hz, 2H), 4.49 (dd, *J* = 7.8, 4.9 Hz, 1H), 4.31 (dd, *J* = 7.8, 4.6 Hz, 1H), 4.21 – 4.14 (m, 2H), 3.88 (t, *J* = 5.2 Hz, 2H), 3.60 – 3.60 (m, 2H), 3.60 – 3.59 (m, 2H), 3.59 – 3.57 (m, 4H), 3.54 (t, *J* = 5.1 Hz, 2H), 3.44 – 3.38 (m, 2H), 3.13 (td, *J* = 7.3, 4.4 Hz, 1H), 2.89 (dd, *J* = 12.8, 4.9 Hz, 1H), 2.74 – 2.73 (m, 2H), 2.73 – 2.72 (m, 1H), 2.56 – 2.45 (m, 2H), 2.43 (dt, *J* = 12.8, 6.2 Hz, 1H), 2.21 (t, *J* = 7.4 Hz, 2H), 1.97 (ddd, *J* = 14.0, 9.1, 5.4 Hz, 1H), 1.73 (s, 2H), 1.73 (s, 2H), 1.73 – 1.72 (m, 1H), 1.67 – 1.66 (m, 2H), 1.64 – 1.63 (m, 1H), 1.50 (s, 9H), 1.47 (s, 3H), 1.45 – 1.37 (m, 2H).

^{13}C NMR (151 MHz, $CDCl_3$): δ 193.7, 173.4, 173.3, 163.8, 163.7, 154.2, 147.2, 133.2, 122.1, 82.2, 70.5, 70.39, 70.35, 70.0, 69.9, 69.5, 65.4, 61.8, 60.2, 55.5, 50.2, 44.2, 40.5, 39.1, 35.8, 35.3, 31.9, 28.1, 28.04, 28.02, 25.7, 25.6, 25.1, 24.6;

Preparation of 1-(*tert*-butyl) 3-methyl 3-methyl-6-oxocyclohex-1-ene-1,3-dicarboxylate (3, 3*R*/3*S*):

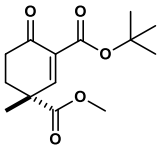

Following the **General Procedure A** using: **S1a** (2.50 g, 14.7 mmol), **S2b** (1.88 g, 16.2 mmol) and TEA (206 µL, 1.47 mmol) or **S3a**/**S3b** (201.0 mg, 0.29 mmol) in 1,4-dioxane (15 mL, 1.0 M) at room temperature for 2 days. After removal of the volatile compounds under reduced pressure, purification by flash chromatography on silica gel (hexanes 0-25% ethyl acetate) gave the product as a yellow oil (2.25 g, 57% for **3**, 2.81 g, 71% for **3*R***, 2.78 g, 71% for **3*S***).

ee: 99% with catalyst **S3a** (**3*R***)

ee: -89% with catalyst **S3b** (***3S***)

HRMS (ESI-TTOF) m/z $[M+H]^+$ calculated for $C_{14}H_{21}O_5$ 269.1379 found 269.1383

^{1}H NMR (500 MHz, $CDCl_3$): δ 7,31 (s, 1H); 3,73 (s, 3H); 2,53-2,45 (m, 2H); 2,44–2,37

(m, 1H); 2,00–1,90 (m, 1H); 1,48 (s, 9H); 1,45 (s, 3H).

^{13}C NMR (125 MHz, $CDCl_3$): δ 193,6; 173,9; 163,7; 153,9; 133,3; 82,2; 52,9; 44,2; 35,4;

32,1; 28,1; 24,7;

Preparation of 1-(tert-butyl) 3-methyl (3*R*,4*S*)-3,4-dimethyl-6-oxocyclohex-1-ene-1,3-dicarboxylate (3'*R*):

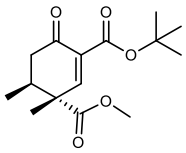

Following the **General Procedure A** using: **S1b** (184 mg, 1.0 mmol), **S2b** (174 mg, 1.5 mmol), and **S3a** (27,4 mg, 0.04 mmol) in 1,4-dioxane: hexanes 9:1 (1.0 mL, 1.0 M) at room temperature for 6 days. After removal of the volatile compounds under reduced pressure, purification by flash chromatography on silica gel (hexanes 0-25% ethyl acetate) gave the product as a yellow oil (52 mg, 18%).

dr: >20:1

ee: 89% with catalyst **S3a**

HRMS (ESI-TTOF) m/z $[M+H]^+$ calculated for $C_{15}H_{23}O_5$ 283.1545 found 283.1551

^{1}H NMR (500 MHz, $CDCl_3$): δ 7.27 (s, 1H), 3.75 (s, 3H), 2.70 (dqd, *J* = 11.3, 6.9, 4.4 Hz, 1H), 2.47 (dd, *J* = 16.8, 4.4 Hz, 1H), 2.30 (dd, *J* = 16.8, 11.7 Hz, 1H), 1.50 (s, 9H), 1.33 (s, 3H), 0.99 (d, *J* = 6.9 Hz, 3H).

^{13}C NMR (125 MHz, $CDCl_3$): δ 193.6, 174.2, 163.6, 154.8, 132.7, 82.3, 52.9, 48.5, 42.8, 34.7, 28.2, 16.7, 16.2;

Preparation of 3-(*tert*-butyl) 1-methyl 4-oxo-5,6-dihydro-[1,1'-biphenyl]-1,3(4*H*)-dicarboxylate (5):

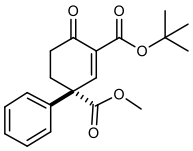

Following the **General Procedure A** using: **S1a** (85 mg, 0.5 mmol), **S2d** (98 mg, 0.55 mmol), and TEA (14 µL, 0.1 mmol) in 1,4-dioxane (0.5 mL, 1.0 M) at room temperature for 2 days. After removal of the volatile compounds under reduced pressure, purification by flash chromatography on silica gel (hexanes 0-25% ethyl acetate) gave the product as a yellow oil (62 mg, 38%).

HRMS (ESI-TTOF) m/z $[M+H]^+$ calculated for $C_{19}H_{23}O_5$ 331.1540 found 331.1544

^{1}H NMR (500 MHz, $CDCl_3$): δ 7.70 (s, 1H), 7.37 – 7.34 (m, 2H), 7.31 – 7.29 (m,1H), 7.26 – 7.24 (m, 2H), 3.74 (s, 3H), 2.75 – 2.69 (m, 1H), 2.56 – 2.50 (m, 1H), 2.39 – 2.29 (m, 2H), 1.53 (s, 9H).

^{13}C NMR (125 MHz, $CDCl_3$): δ 193.5, 172.0, 163.8, 152.0, 139.9, 135.2, 129.2, 128.1, 126.3, 82.5, 53.2, 52.7, 35.4, 33.4, 28.2;

Preparation of 3-(*tert*-butyl) 1-methyl 6-methylene-4-oxobicyclo[3.2.1]oct-2-ene-1,3-dicarboxylate (6, 6*S*,*S*/6*R*,*R*):

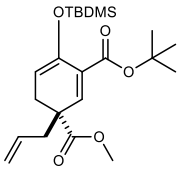

A flame-dried vial was charged with an anhydrous toluene solution (3.5 mL) of **13**/**13*R***/**13*S*** (1.00 g, 3.40 mmol, 1 eq.) and TEA (940 µL, 6.79 mmol, 2 eq.) under a nitrogen atmosphere. The reaction mixture was cooled to 0°C then TBDMSOTf (936 µL, 4.08 mmol, 1.2 eq.) was added dropwise, and it was stirred at 0°C for 2 hours. When the reaction was completed, the mixture was diluted with water and extracted with n-Hexane three times. The combined organic phases were washed two times with saturated $NaHCO_3$ solution and once with brine, dried over anhydrous Na_2SO_4, filtered and the solvent was removed under reduced pressure. The silyl-enol ether intermediate was obtained as a colorless oil (1.307 g, 94%) and was used without further purification in the next step.

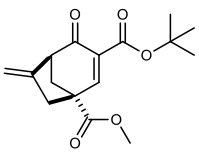

To an anhydrous dimethyl sulfoxide (18 mL) solution of the intermediate were added 4Å molecular sieves, and $Pd(OAc)_2$ (71.8mg, 320.0 mg, 0.1 eq.), and the atmosphere was charged with 3 bars of O_2. The reaction mixture was stirred at 60°C for 18 hours. After completion, the reaction mixture was cooled to 25°C and 50 mL of diethyl-ether was added and it was stirred for a further 1 hour. The reaction mixture was filtered through a pad of Celite then it was

washed with water twice. The aqueous phase was extracted with 30 mL of diethyl-ether three times, then the combined organics were washed three times with brine. The organic phase was dried over anhydrous Na_2SO_4, filtered and the solvent was removed under reduced pressure. Purification by flash chromatography on silica gel (hexanes, 0-25% ethyl acetate) to give the product as white solid (268.5 mg, 57% for **6**, 214,8 mg, 46% for **6*S,S***, 179.0 mg, 38% for **6*R,R***).

ee: 99+% with catalyst **S3a** (**6*S,S***)
ee: -99+% with catalyst **S3b** (**6*R,R***)

HRMS (ESI-TTOF) m/z $[M+H]^+$ calculated for $C_{16}H_{21}O_5$ 293.1383 found 293.1377

^{1}H NMR (500 MHz, $CDCl_3$): δ 8.02 (d, *J* = 1.9 Hz, 1H), 5.36 (s, 1H), 5.13 (s, 1H), 3.81 (s, 3H), 3.59 (d, *J* = 4.6, 1H), 2.96 (dt, *J* = 15.9, 2.7 Hz, 1H), 2.64 (d, *J* = 18.1 Hz, 1H), 2.37 – 2.29 (m, 2H), 1.50 (s, 9H).

^{13}C NMR (125 MHz, CDCl3): δ 192.0, 163.0, 155.7, 142.0, 131.0, 114.0, 82.2, 58.5, 52.9, 51.8, 42.2, 41.1, 28.2;

Preparation of *tert*-butyl 3,3-dimethyl-6-oxocyclohex-1-ene-1-carboxylate (7):

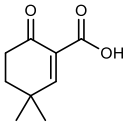

Compound **S5** was prepared according to the literature procedures.[3,4]

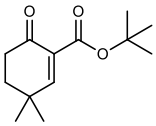

Compound **S5** (100.0 mg, 0.595 mmol, 1 eq.) was dissolved in anhydrous dimethylformamide (5.5 mL) in a flame-dried vial under a nitrogen atmosphere, HBTU (225.5 mg, 0.595 mmol, 1.5 eq.) and *N*-methylmorpholine (131 µL, 0.825 mmol, 2.0 eq.) were added and the mixture was stirred at 25°C. After 30 minutes *tert*-butyl alcohol (114 µL, 0.275 mmol, 2 eq.) was added and the reaction mixture was stirred at 25°C for 3 days. The reaction was monitored by HPLC-MS and when the starting material was consumed the reaction mixture was diluted with ethyl acetate, washed two times with a 5% citric acid solution, two times with a saturated aqueous Na_2CO_3 solution, and two times with brine. The organic phase was dried over anhydrous Na_2SO_4, filtered, then evaporated under reduced pressure. The resulting crude product was purified by preparative RP-HPLC using a gradient method on a Gemini® 5µm C18 110 Å column (H_2O:MeCN = 95:5 (0.1 % HCOOH) to 100% MeCN (0.1 % HCOOH)). Compound **7** was obtained as a yellow solid (19.4 mg, 14.5%).

HRMS (ESI-TTOF) m/z $[M+H]^+$ calculated for $C_{13}H_{20}O_3Na$ 247.1304 found 247.1297

^{1}H NMR (500 MHz, $CDCl_3$): δ 7.17 (t, *J* = 0.9 Hz, 1H), 2.51 (t, *J* = 6.8 Hz, 2H), 1.88 (dt, *J* = 6.8, 1.0 Hz, 2H), 1.52 (s, 9H), 1.22 (s, 6H).

^{13}C NMR (125 MHz, $CDCl_3$): δ 194.7, 164.3, 162.4, 131.8, 81.8, 35.7, 35.4, 33.4, 28.2, 27.6;

Preparation of 1-(*tert*-butyl) 3-methyl-3-benzyl-6-oxocyclohex-1-ene-1,3-dicarboxylate (8, 8*R*/8*S*):

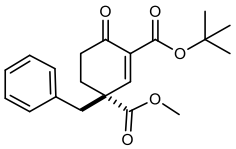

Following the **General Procedure A** using: **S1a** (85 mg, 0.5 mmol), **S2f** (106 mg, 0.55 mmol), and TEA (7 µl, 0.05 mmol) or **S3a**/**S3b** (6.9 mg, 0.01 mmol) in 1,4-dioxane (0.5 mL, 1.0 M) at room temperature for 2 days. After removal of the volatile compounds under reduced pressure, purification by flash chromatography on silica gel (hexanes 0-25% ethyl acetate) gave the product as a yellow oil (110.0 mg, 64% for **8**, 91.0 mg, 56% for **8*R***, 98.7 mg, 61% for **8*S***).

ee: -76% with catalyst **S3b** (**8*R***)

ee: 92% with catalyst **S3a (8*S***)

HRMS (ESI-TTOF) m/z $[M+H]^+$ calculated for $C_{20}H_{25}O_5$ 345.1696 found 345.1694

^{1}H NMR (500 MHz, $CDCl_3$): δ 7.42 (s, 1H), 7.26 (m, 3H), 7.10 – 7.05 (m, 2H), 3.68 (s, *J* = 4.8 Hz, 3H), 3.10 (s, 2H), 2.51 – 2.47 (m, 2H), 2.42 – 2.33 (m, 1H), 2.08 – 2.00 (m, 1H), 1.51 (s, *J* = 4.6 Hz, 9H).

^{13}C NMR (125 MHz, $CDCl_3$): δ 193.5, 172.5, 163.5, 153.0, 135.0, 133.6, 129.8, 128.5, 127.49, 82.1, 52,5, 49.4, 44.5, 35.3, 30.0, 28.1;

Preparation of methyl 1-methyl-4-oxocyclohex-2-ene carboxylate (9):

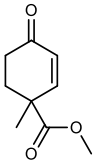

To methyl vinyl ketone (500 µL, 6.00 mmol, 1 eq.), dissolved in 6 mL of 1,4-dioxane, was added **S2b** (770.0 mg, 6.60 mmol, 1.1 eq.) and triethylamine (170 µL, 1.5 mmol, 0.25 eq.). The reaction mixture was stirred at room temperature and monitored by TLC. Upon completion, p-toluenesulfonic acid (630 mg, 3.3 mmol, 0.55 eq.) along with 3 mL of 1,4-dioxane was added, and the reaction was stirred at 100°C until complete conversion of the intermediate product. After removal of the solvent under reduced pressure, the residue was purified by flash column chromatography on silica gel (hexanes 0-25% ethyl acetate) to afford compound **9** as a yellow oil (131 mg, 51%).

HRMS (ESI-TTOF) m/z $[M+H]^+$ calculated for $C_9H_{13}O_3$ 169.0859 found 169.0865

^{1}H NMR (500 MHz, $CDCl_3$): δ 6.87 (d, *J* = 10.2 Hz, 1H), 5.98 (d, *J* = 10.2 Hz, 1H), 3.74 (s, 3H), 2.56 – 2.43 (m, 3H), 2.00 – 1.95 (m, 1H), 1.44 (s, 3H).

^{13}C NMR (125 MHz, $CDCl_3$): δ 198.2, 174.5, 151.5, 128.6, 52.5, 43.8, 34.5, 32.5, 24.8;

3-(methoxycarbonyl)-3-methyl-6-oxocyclohex-1-ene-1-carboxylic acid (10, 10*R*/10*S*):

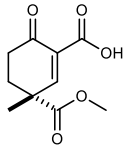

Trifluoroacetic acid (811 µL, 10.53 mmol, 3 eq.) was added to a solution of compound **3**/**3*R***/**3*S*** (942 mg, 3.51 mmol, 1 eq.) in methylene chloride (20 mL) and then the mixture was stirred at 25°C for 3 hours. The reaction was monitored by TLC and when it was completed the reaction mixture was evaporated. The remaining trifluoroacetic acid was removed by redissolving the mixture in toluene and evaporating to dryness at 50°C three times. Compound **10**, **10*R***/**10*S*** was obtained as a yellow oil in quantitative yield (745.0 mg) and was used in the next step without further purification.

HRMS (ESI-TTOF) m/z $[M+H]^+$ calculated for $C_{10}H_{13}O_5$ 213.0757 found 213.0759

^{1}H NMR (500 MHz, $CDCl_3$): δ 8.30 (s, 1H), 3.79 (s, 3H), 2.78 – 2.65 (m, 2H), 2.58 – 2.53 (m, 1H), 2.08 – 2.02 (m, 1H), 1.56 (s, 1H).

^{13}C NMR (125 MHz, $CDCl_3$): δ 202.1, 172.6, 165.2, 163.4, 126.0, 53.2, 45.4, 34.6, 31.8, 24.5;

Preparation of 1-benzyl 3-methyl-3-methyl-6-oxocyclohex-1-ene-1,3-dicarboxylate (12, 12*R*/12*S*):

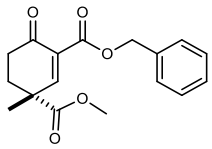

Following the **General Procedure A** using: **S1c** (300 mg, 1.5 mmol), **S2b** (190 mg, 1.6 mmol), and TEA (41 µl, 0.3 mmol) or **S3a**/**S3b** (20.8 mg, 0.03 mmol) in 1,4-dioxane (1.5 mL, 1.0 M) at room temperature for 2 days. After removal of the volatile compounds under reduced pressure, purification by flash chromatography on silica gel (hexanes 0-25% ethyl acetate) gave the product as a yellow oil (99.0 mg, 22% for **12**, 155.8 mg, 35% for **12*R***, 180.4 mg, 41% for **12*S***).

ee: 92% with catalyst **S3a** (**12*R***)

ee: -80% with catalyst **S3b** (**12*S***)

HRMS (ESI-TTOF) m/z $[M+H]^+$ calculated for $C_{17}H_{19}O_5$ 303.1227 found 303.1224

^{1}H NMR (500 MHz, CDCl3): δ 7.51 (s, 1H), 7.43 – 7.39 (m, 2H), 7.36 (ddd, *J* = 5.9, 3.5, 1.2 Hz, 2H), 7.32 (dt, *J* = 5.4, 2.1 Hz, 1H), 5.25 (d, *J* = 3.4 Hz, 2H), 3.74 (s, 3H), 2.61 – 2.51 (m, 2H), 2.51 – 2.43 (m, 1H), 1.98 (ddd, *J* = 14.0, 9.4, 5.0 Hz, 1H), 1.47 (s, 3H).

^{13}C NMR (125 MHz, CDCl3): δ 193.2, 173.5, 164.1, 155.9, 135.5, 131.7, 128.6, 128.6, 128.3, 128.2, 67.1, 52.9, 44.4, 35.3, 32.0, 24.6;

Preparation of 1-(*tert*-butyl) 3-methyl-3-allyl-6-oxocyclohex-1-ene-1,3-dicarboxylate (13, 13*R*/13*S*):

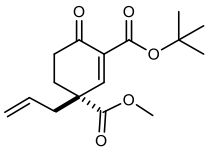

Following the **General Procedure A** using: **S1a** (14.3 g, 83.8 mmol), **S2e** (13.1 g, 92.2 mmol) and TEA (1.17 mL, 8.38 mmol) or catalyst **S3a**/**S3b** (1.15 g, 1.68 mmol) in 1,4-dioxane (84 mL, 1.0 M) at room temperature for 2 days. After removal of the volatile compounds under reduced pressure, purification by flash chromatography on silica gel (hexanes 0-25% ethyl acetate) gave the product as a yellow oil (12.17 g, 50% for **13**, 18.4 g, 75% for **13*R***, 12.1 g, 49% for **13*S***).

ee: 99+% with catalyst **S3a (13*S*)**
ee: -99+% with catalyst **S3b (13*R*)**

HRMS (ESI-TTOF) m/z $[M+H]^+$ calculated for $C_{16}H_{23}O_5$ 295.1540 found 295.1543

^{1}H NMR (500 MHz, $CDCl_3$): δ 7.30 (d, *J* = 1.27 Hz, 1H), 5.71 – 5.6 (m, 1H), 5.1 – 5.12 (m, 2H), 3.73 (s, 3H), 2.57-2.51 (m, 3H), 2.49 (t, *J* = 5.76 Hz, 1H), 2.45 – 2.38 (m, 1H), 2.03 – 1.97 (m, 1H), 1.50 (s, 9H).

^{13}C NMR (125 MHz, $CDCl_3$): δ 193.7, 172.6, 163.7, 152.8, 133.9, 131.5, 120.2, 82.3, 52.7, 48.2, 42.8, 35.4, 29.8, 28.1;

Preparation of ethyl 3-benzoyl-3-methyl-6-oxocyclohex-1-ene-1-carboxylate (14):

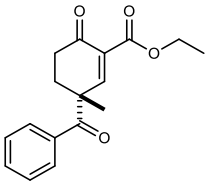

Following the **General Procedure A** using: **S1d** (426.5 mg, 3.0 mmol), **S2i** (535.3 mg, 3. mmol), and TEA (42 µl, 0.3 mmol) in 1,4-dioxane (3 mL, 1.0 M) at room temperature for 2 days. After removal of the volatile compounds under reduced pressure, purification by flash chromatography on silica gel (hexanes 0-25% ethyl acetate) gave the product as a yellow oil (409.0 mg, 48%).

HRMS (ESI-TTOF) m/z $[M+H]^+$ calculated for $C_{17}H_{19}O_4$ 287.1277 found 287.1289

^{1}H NMR (500 MHz, $CDCl_3$): δ 7.77 (d, *J* = 7.7 Hz, 1H), 7.72 (s, 1H), 7.54 (t, *J* = 7.5 Hz, 1H), 7.45 (t, *J* = 7.7 Hz, 1H), 4.28 (q, *J* = 7.2 Hz, 1H), 2.74 – 2.68 (m, 1H), 2.66 – 2.56(m, 2H), 2.12 – 2.07 (m, 1H), 1.62 (s, 3H), 1.32 (t, *J* = 7.1 Hz, 3H).

^{13}C NMR (125 MHz, $CDCl_3$): δ 201.3, 193.3, 164.2, 156.9, 136.6, 132.6, 131.3, 128.6, 128.5, 61.4, 49.8, 35.2, 32.9, 30.0, 14.1;

Preparation of *tert*-butyl 3-benzoyl-3-methyl-6-oxocyclohex-1-ene-1-carboxylate (15):

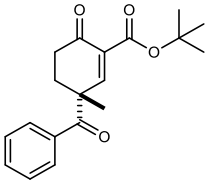

Following the **General Procedure A** using: **S1a** (85 mg, 0.5 mmol), **S2i** (89 mg, 0.55 mmol), and TEA (14 µl, 0.1 mmol) in 1,4-dioxane (0.5 mL, 1.0 M) at room temperature for 2 days. After removal of the volatile compounds under reduced pressure, purification by flash chromatography on silica gel (hexanes 0-25% ethyl acetate) gave the product as a yellow oil (72.0 mg, 46%).

HRMS (ESI-TTOF) m/z $[M+H]^+$ calculated for $C_{19}H_{23}O_4$ 315.1590 found 315.1596

^{1}H NMR (500 MHz, $CDCl_3$): δ 7.77 – 7.72 (m, 2H), 7.56 (s, 1H), 7.54 – 7.49 (m, 1H), 7.47 – 7.39 (m, 2H), 2.70 – 2.62 (m, 1H), 2.56 (tdt, *J* = 17.1, 8.3, 4.3 Hz, 2H), 2.08 – 2.00 (m, 1H), 1.57 (s, 3H), 1.49 (s, 9H).

^{13}C NMR (125 MHz, $CDCl_3$): δ 201.7, 193.5, 163.7, 155.4, 136.7, 132.6, 128.7 128.6, 82.3, 58.0, 49.7, 35.4, 33.1, 28.1, 24.1;

Preparation of 3-(*tert*-butyl) 1-ethyl (*S*)-4-oxo-[1,1'-bi(cyclohexan)]-2-ene-1,3-dicarboxylate (16):

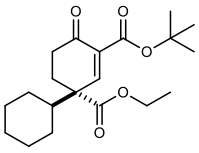

Following the **General Procedure A** using: **S1a** (85.1 mg, 0.50 mmol), **S2j** (109 mg, 0.55 mmol), and DBU (15 µL, 0.10 mmol) in 1,4-dioxane (0.50 mL, 1.0 M) at room temperature for 2 days. After removal of the volatile compounds under reduced pressure, purification by flash chromatography on silica gel (hexanes 0-25% ethyl acetate) gave the product as a yellow oil (39.0 mg, 22%).

HRMS (ESI-TTOF) m/z $[M+H]^+$ calculated for $C_{20}H_{31}O_5$ 351.2166 found 351.2172

^{1}H NMR (500 MHz, $CDCl_3$): δ 7.49 (d, J = 1.7 Hz, 1 H), 4.28 (q, *J* = 7.1 Hz, 2 H) 4.26 – 4.13 (m, 2 H), 2.59 – 2.48 (m, 2 H), 2.40 – 2.35 (m, 1 H), 2.04 (dt, *J* = 13.2, 5.3 Hz, 1 H), 1.90 (tt, *J* = 12.1, 2.9 Hz, 1 H), 1.83 – 1.77 (m, 2 H), 1.69 (d, *J* = 12.9 Hz, 1 H), 1.64 – 1.57 (m, 2 H), 1.33 (t, *J* = 7.1 Hz, 3 H), 1.28 (t, *J* = 7.1 Hz, 4 H), 1.24 – 1.01 (m, 4 H).

^{13}C NMR (125 MHz, $CDCl_3$): δ 194.4, 171.1, 163.9, 154.8, 133.9, 82.1, 61.4, 652.1, 46.1, 36.1, 28.2, 28.1, 27.9, 27.7, 26.7, 26.2, 26.0,14.3;

Preparation of 3-ethyl 1-methyl 3-methyl-6-oxocyclohexa-1,4-diene-1,3-dicarboxylate (17):

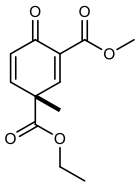

To a stirred solution of compound **11** (1.01 g, 4.2 mmol) in anhydrous 1,4-dioxane (40 mL) were added 4Å molecular sieves and camphorsulfonic acid (0.54 g, 2.3 mmol). DDQ (1.16 g, 5.1 mmol) was added portionwise with vigorous stirring. The reaction mixture was heated to reflux and stirred for 48 hours. Upon completion, the mixture was cooled to 0°C, filtered through a pad of Celite, washed with 1,4-dioxane, and the solvent was evaporated under reduced pressure. The residue was dissolved in toluene, distilled water was added, then the pH was adjusted to 7-8 with a saturated $NaHCO_3$ solution. The organic layer was washed with brine, dried over Na_2SO_4, the solvent was removed under reduced pressure to give the product as a yellow oil (0.65 g, 65%).

HRMS (ESI-TTOF) m/z $[M+H]^+$ calculated for $C_{12}H_{15}O_5$ 239.0914 found 239.0917

^{1}H NMR (500 MHz, $CDCl_3$): δ 7.67 (d, J = 3.0 Hz, 1H), 7.01 (dd, *J* = 10.1, 3.0 Hz, 1H), 6.31 (d, *J* = 10.1 Hz, 1H), 4.19 (q, *J* = 7.2 Hz, 2H), 3.84 (s, 3H), 1.59 (s, 3H), 1.26 (t, *J* = 7.1 Hz, 3H).

^{13}C NMR (125 MHz, $CDCl_3$): δ 180.6, 169.8, 164.8, 153.7, 147.6, 131.7, 129.6, 62.8, 52.5, 48.5, 24.9, 14.1;

Preparation of methyl 2-formyl-3-(pyridin-4-yl)propanoate (S2k):

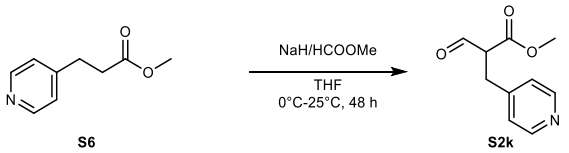

S6 **S2k**

Compound **S6** was synthesized according to literature procedures.[5]

A flame-dried vial under a nitrogen atmosphere was charged with NaH (73.0mg, 3.00mmol, 1 eq.) anhydrous THF (9 mL) and methyl-formate (1.90 mL, 30.0 mmol, 10 eq.). The reaction mixture was cooled to 0°C then a THF solution (3 mL) of compound **S6** was added dropwise and was stirred for 10 minutes at 0°C. The reaction mixture was warmed to 25°C where it was stirred for 2 days. When the reaction was completed, the reaction was quenched with 50 mL of water and extracted with diethyl ether three times. The pH of the aqueous phase was adjusted to 7 by the addition of 10% citric acid solution then it was extracted three times with ethyl acetate. The combined ethyl acetate phases were dried over anhydrous Na_2SO_4, filtered and the solvent was removed under reduced pressure. Compound **S2k** was obtained without further purification as a yellow solid (205 mg, 35%).

^{1}H NMR (500 MHz, $CDCl_3$): δ 8.46-8.44 (m, 2H), 8.03 (s, 1H), 7.31 (d, *J* = 5.1 Hz, 2H), 3.69 (s, 3H), 3.68 (s, 1H), 3.40 (s, 2H)

^{13}C NMR (125 MHz, $CDCl_3$) partial: δ 150.4, 149.3, 123.9, 51.8, 51.1, 32.9;

Preparation of 1-(*tert*-butyl) 3-methyl (*S*)-6-oxo-3-(pyridin-4-ylmethyl)cyclohex-1-ene-1,3-dicarboxylate (S7):

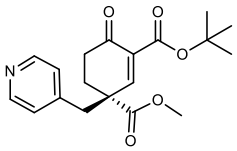

Following the **General Procedure A** using: **S1a** (201 mg, 1.18 mmol), **S2k** (209 mg, 1.08 mmol), and **3a** (14,7 mg, 0.02 mmol) in 1,4-dioxane (1.1 mL, 1.0 M) at room temperature for 6 days. After removal of the volatile compounds under reduced pressure, purification by flash chromatography on silica gel (hexanes 0-25% ethyl acetate) gave the product as a yellow oil (120.0 mg, 32%).

ee: 90% with catalyst **S3a** (**S7**)

HRMS (ESI-TTOF) m/z $[M+H]^+$ calculated for $C_{19}H_{24}NO_5$ 346.1648 found 346.1656

^{1}H NMR (500 MHz, CDCl3): δ 8.53 (d, *J* = 5.3 Hz, 2H), 7.32 (s, 1H), 7.03 (d, *J* = 6.0 Hz, 2H), 3.71 (d, *J* = 5.4 Hz, 3H), 3.08 (d, *J* = 13.1 Hz, 2H), 2.59 – 2.46 (m, 2H), 2.43 – 2.35 (m, 1H), 2.03 (dq, *J* = 9.3, 5.7 Hz, 1H), 1.50 (s, 9H).

^{13}C NMR (125 MHz, CDCl3): δ 193.0, 172.1, 163.4, 151.5, 150.1, 144.1, 134.2, 125.1, 82.5, 52.9, 48.9, 43.6, 35.2, 30.3, 28.1;

General procedure B for the amidation of compound 10:

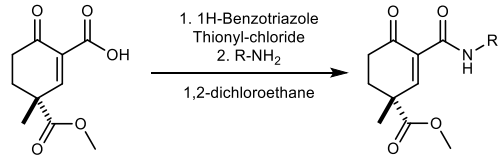

1*H*-benzotriazole (4 eq.) was dissolved in 1,2-dichloroethane (0.75 M) under a nitrogen atmosphere and was left to stir for 10 minutes at 25°C. To this solution thionyl chloride (1.1 eq.) was added dropwise and was stirred for 30 minutes at 25°C. The reaction mixture was cooled to 0°C and was stirred for 15 minutes. A 1,2-dichloroethane solution of compound **10** (0.88 M, 1 eq.) was added dropwise to the reaction mixture which was stirred at 0°C for 24 hours. When the carboxylic acid was completely consumed the reaction mixture was filtered, the filtrate was washed two times with 1,2-dichloroethane, and the organic phase was washed three times with a saturated $NaHCO_3$ solution. The organic phase was dried over anhydrous Na_2SO_4, filtered, then the corresponding amine (1.2 eq.) was added, and the reaction mixture was stirred for 1 hour. After the reaction was completed, the mixture was washed two times with a 10% HCl solution, two times with a saturated Na_2CO_3 solution, and once with brine. The organic phase was dried over anhydrous Na_2SO_4, filtered, the solvent was removed under reduced pressure. The product was purified with flash chromatography (hexanes 0-25% ethyl acetate) if necessary.

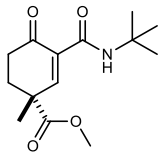

Compound **18**/**18*R*** was synthesized according to the **General procedure B** using: 1*H*-benzotriazole (560 mg, 4.72 mmol, 4 eq.), thionyl chloride (94.0 µL, 1.30 mmol, 1.1 eq.), compound **10**/**10*R*** (250.0 mg, 1.18 mmol, 1 eq.), *tert*-butylamine (149.0 µL, 1.41 mmol, 1.2 eq.) and was obtained as a yellow oil (177.0 mg, 56%).

HRMS (ESI-TTOF) m/z $[M+H]^+$ calculated for $C_{14}H_{22}NO_4$ 268.1543 found 268.1550

^{1}H NMR (500 MHz, $CDCl_3$): δ 8.60 (s, 1H), 8.09 (s, 1H), 3.74 (s, 3H), 2.65 – 2.53 (m, 2H), 2.52 – 2.45 (m, 1H), 1.98 – 1.92 (m, 1H), 1.50 (s, 3H), 1.40 (s, 9H).

^{13}C NMR (125 MHz, $CDCl_3$): δ 199.4, 173.7, 161.4, 159.6, 130.0, 52.9, 51.2, 44.9, 36.1, 32.2, 28.8, 24.8;

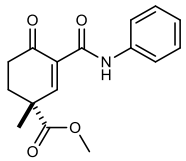

Compound **19** was synthesized according to the **General procedure B** using: 1*H*-benzotriazole (560 mg, 4.72 mmol, 4 eq.), thionyl chloride (94.0 µL, 1.30 mmol, 1.1 eq.), compound **10** (250.0 mg, 1.18 mmol, 1 eq.), aniline (129.0 µL, 1.41 mmol, 1.2 eq.) and was obtained as an orange oil (267.0 mg, 79%).

HRMS (ESI-TTOF) m/z $[M+H]^+$ calculated for $C_{16}H_{18}NO_4$ 288.1230 found 288.1234

^{1}H NMR (500 MHz, $CDCl_3$): δ 10.68 (s, 1H), 8.20 (s, 1H), 7.66 – 7.64 (m, 2H), 7.36 – 7.32 (m, 2H), 7.14 – 7.11 (m, 1H), 3.77 (s, 3H), 2.74 – 2.61 (m, 2H), 2.56 – 2.51 (m, 1H), 2.05 – 1.99 (m, 1H), 1.55 (s, 3H).

^{13}C NMR (125 MHz, $CDCl_3$): δ 199.6, 173.5, 161.5, 160.4, 138.0, 129.3, 129.1, 124.6, 120.6, 53.0, 45.2, 36.0, 32.2, 24.8;

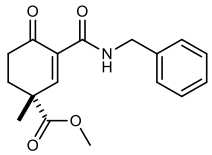

Compound **20** was synthesized according to the **General procedure B** using: 1*H*-benzotriazole (337 mg, 2.83 mmol, 4 eq.), thionyl chloride (56.5 µL, 0.78 mmol, 1.1 eq.), compound **10** (150.0 mg, 0.71 mmol, 1 eq.), benzylamine (92.0 µL, 0.85 mmol, 1.2 eq.) and was obtained as a yellow oil (168.0 mg, 79%).

HRMS (ESI-TTOF) m/z $[M+H]^+$ calculated for $C_{17}H_{20}NO_4$ 302.1386 found 302.1379

^{1}H NMR (500 MHz, $CDCl_3$): δ 8.99 (s, 1H), 8.17 (s, 1H), 7.35-7.30 (m, H), 4.56 (dd, J = 5.8, 2.5 Hz, 2H), 3.75 (s, 3H), 2.66 – 2.55 (m, 2H), 2.53 – 2.46 (m, 1H), 2.00 – 1.94 (m, 1H), 1.51 (s, 3H).

^{13}C NMR (125 MHz, $CDCl_3$): δ 199.2, 173.6, 162.6, 160.7, 138.3, 129.1, 128.7, 127.8, 127.4, 53.0, 45.0, 43.7, 36.0, 32.2, 24.8**;**

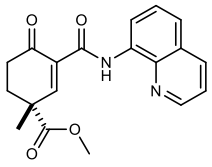

Compound **21** was synthesized according to the **General procedure B** using: 1*H*-benzotriazole (532 mg, 4.47 mmol, 4 eq.), thionyl chloride (89.0 µL, 0.15 mmol, 1.1 eq.), compound **10** (237.0 mg, 1.12 mmol, 1 eq.), quinoline-8-amine (193 mg, 1.34 mmol, 1.2 eq.) and was obtained as a brown oil (237.0 mg, 63%).

HRMS (ESI-TTOF) m/z $[M+H]^+$ calculated for $C_{19}H_{19}N_2O_4$ 339.1339 found 339.1333

^{1}H NMR (500 MHz, CDCl3): δ 12.50 (s, 1H), 8.94 (dd, *J* = 4.2, 1.7 Hz, 1H), 8.87 (dd, *J* = 6.5, 2.5 Hz, 1H), 8.26 (s, 1H), 8.11 (dd, *J* = 8.3, 1.7 Hz, 1H), 7.53 – 7.49 (m, 2H), 7.42 (dd, *J* = 8.2, 4.2 Hz, 1H), 3.74 (s, 3H), 2.77 – 2.65 (m, 2H), 2.55 – 2.50 (m, 1H), 2.06 – 1.99 (m, 1H), 1.54 (s, 3H).

^{13}C NMR (125 MHz, CDCl3): δ 198.8, 173.6, 160.9, 160.8, 148.9, 139.6, 136.2, 135.2, 130.2, 128.2, 127.2, 122.4, 121.6, 118.1, 52.9, 45.1, 36.0, 32.1, 24.8;

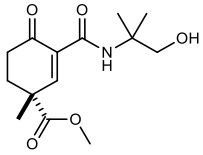

Compound **22** was synthesized according to the **General procedure B** using: 1*H*-benzotriazole (674 mg, 5.66 mmol, 4 eq.), thionyl chloride (113.0 µL, 1.56 mmol, 1.1 eq.), compound **10** (300.0 mg, 1.41 mmol, 1 eq.), 2-amino-2-methyl-1-propanol (168.0 mg, 1.70 mmol, 1.2 eq.) and was obtained as a yellow oil (220.0 mg, 55%).

HRMS (ESI-TTOF) m/z $[M+H]^+$ calculated for $C_{14}H_{22}NO_5$ 284.1492 found 284.1486

^{1}H NMR (300 MHz, $CDCl_3$): δ 8.96 (s, 1H), 8.13 (s, 1H), 3.76 (s, 3H), 3.62 (d, *J* = 4.1 Hz, 2H), 2.65 – 2.55 (m, 2H), 2.54 – 2.41 (m, 1H), 2.05 – 1.90 (m, 1H), 1.51 (s, 3H), 1.34 (s, 6H).

^{13}C NMR (75 MHz, $CDCl_3$): δ 199.3, 173.4, 162.9, 160.7, 129.1, 70.8, 56.4, 53.0, 45.0, 35.9, 32.1, 29.8, 24.8, 24.74, 24.71;

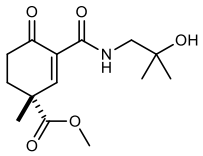

Compound **23** was synthesized according to the **General procedure B** using: 1*H*-benzotriazole (1.15g, 9.69 mmol, 4 eq.), thionyl chloride (194.5 µL, 2.66 mmol, 1.1 eq.), compound **10** (514.0 mg, 2.42 mmol, 1 eq.), 1-amino-2-methyl-propan-2-ol (259.1 mg, 2.91 mmol, 1.2 eq.) and was obtained as a yellow oil (386.0 mg, 56%).

HRMS (ESI-TTOF) m/z $[M+H]^+$ calculated for $C_{14}H_{22}NO_5$ 284.1492 found 284.1486

^{1}H NMR (300 MHz, $CDCl_3$): δ 9.00 (s, 1H), 8.15 (s, 1H), 3.75 (s, 3H), 3.39 (dd, *J* = 5.9, 2.6 Hz, 2H), 2.66-2.57 (m, 2H), 2.50 – 2.44 (m, 1H), 2.04 – 1.92 (m, 1H), 1.52 (s, 3H), 1.25 (s, 6H).

^{13}C NMR (75 MHz, $CDCl_3$): δ 199.1, 173.5, 163.9, 160.7, 128.9, 71.1, 52.9, 50.9, 45.0, 43.5, 35.9, 32.1, 27.5, 27.4, 24.7;

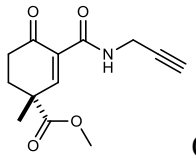

Compound **S8** was synthesized according to the **General procedure B** using: 1*H*-benzotriazole (1.12 g, 9.43 mmol, 4 eq.), thionyl chloride (189 µL, 2.60 mmol, 1.1 eq.), compound **10** (500.0 mg, 2.36 mmol, 1 eq.), propargylamine (181 µL, 1.34 mmol, 1.2 eq.) and was obtained as a red oil (182.0 mg, 30%).

HRMS (ESI-TTOF) m/z $[M+H]^+$ calculated for $C_{13}H_{16}NO_4$ 250.1073 found 250.1078

^{1}H NMR (500 MHz, $CDCl_3$): δ 8.89 (s, 1H), 8.16 (s, 1H), 4.17 – 4.14 (m, 2H), 3.75 (s, 3H), 2.88 (s, 1H), 2.64 – 2.57 (m, 2H), 2.53 – 2.47 (m, 1H), 2.24 – 2.22 (m, 1H), 1.51 (s, 3H).

^{13}C NMR (125 MHz, $CDCl_3$): δ 198.9, 173.4, 162.5, 161.1, 128.7, 71.4, 53.0, 45.0, 38.7, 35.9, 32.1, 29.2, 24.8;

Preparation of 3-amino-*N*,*N*-dimethylbenzamide (S9):

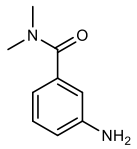

Compound **S9** was prepared according to the literature procedures.[6,7]

Preparation of methyl (*S*)-3-((3-(dimethylcarbamoyl)phenyl)carbamoyl)-1-methyl-4-oxocyclohex-2-ene-1-carboxylate (19'*S*):

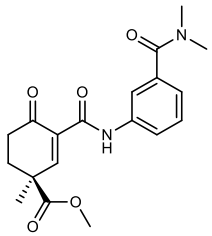

Compound **10*S*** (50.0 mg, 0.236 mmol, 1 eq.) was dissolved in anhydrous dimethylformamide (0.50 mL) in a flame-dried vial under a nitrogen atmosphere, HBTU (89.4 mg, 0.236 mmol, 1 eq.) and *N*-methylmorpholine (51.8 µL, 0.471 mmol, 2.0 eq.) were added and the mixture was stirred at 25°C. After 30 minutes an anhydrous DMF solution (0.50 mL) of compound **S9** (48.4 mg, 0.295 mmol, 1.25 eq.) was added and the reaction mixture was stirred at 25°C for 3 days. The reaction was monitored by HPLC-MS and when the starting material was consumed the reaction mixture was diluted with ethyl acetate, washed two times with a 5% citric acid solution, two times with a saturated aqueous Na_2CO_3 solution, and two times with brine. The organic phase was dried over anhydrous Na_2SO_4, filtered, then evaporated under reduced pressure. The resulting crude product was purified by preparative RP-HPLC using a gradient method on a Gemini® 5µm C18 110 Å column (H_2O:MeCN = 95:5 (0.1 % HCOOH) to 100% MeCN (0.1 % HCOOH)). Compound **19'*S*** was obtained as a yellow oil (62.7 mg, 74.2%).

HRMS (ESI-TTOF) m/z $[M+H]^+$ calculated for $C_{19}H_{23}N_2O_5$ 359.1601 found 359.1594

^{1}H NMR (500 MHz, $CDCl_3$): δ 10.77 (s, 1H), 8.25 (s, 1H), 7.76 (t, *J* = 1.9 Hz, 1H), 7.67 (dt, *J* = 8.2, 1.6 Hz, 1H), 7.37 (t, *J* = 7.9 Hz, 1H), 7.19 (dt, *J* = 7.6, 1.3 Hz, 1H), 3.77 (s, 3H), 3.11 (s, 3H), 3.00 (s, 3H), 2.74 – 2.61 (m, 2H), 2.56 – 2.51 (m, 1H), 2.05 – 2.00 (m, 1H), 1.55 (s, 3H).

^{13}C NMR (125 MHz, $CDCl_3$) partial: δ 199.5, 173.3, 171.1, 161.7, 160.5, 137.9, 137.2, 129.2, 129.1, 123.2, 121.5, 119.2, 53.0, 45.1, 35.9, 32.0, 24.7;

Preparation of methyl 1-methyl-3-(5-methyloxazol-2-yl)-4-oxocyclohex-2-ene-1-carboxylate (24):

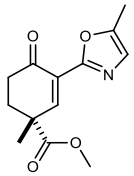

Compound **S7** (75.0 mg, 0.301mmol, 1 eq.) was dissolved in 1,4-dioxane (0.50 mL), TfOH was added (80 µL, 0.903 mmol, 1.1 eq.) and the reaction mixture was stirred at 90°C for 3 hours. After the reaction was completed, the mixture was diluted with ethyl acetate then washed two times with a saturated $NaHCO_3$ solution. The organic phase was washed with brine then dried over anhydrous Na_2SO_4, filtered, and evaporated under reduced pressure. The crude product was purified by column chromatography (hexane: ethyl acetate) and compound **24** was obtained as a yellow oil (26.0 mg, 35%).

HRMS (ESI-TTOF) m/z $[M+H]^+$ calculated for $C_{13}H_{16}NO_4$ 250.1073 found 250.1067

^{1}H NMR (500 MHz, $CDCl_3$): δ 7.53 (s, 1H), 6.79 (d, *J* = 1.1 Hz, 1H), 3.75 (s, 3H), 2.68 – 2.60 (m, 2H), 2.54 – 2.49 (m, 1H), 2.34 (d, *J* = 1.1 Hz, 3H), 2.05 – 2.00 (m, 1H), 1.51 (s, 3H).

^{13}C NMR (125 MHz, $CDCl_3$): δ 193.8, 174.0, 156.5, 152.1, 149.5, 127.3, 124.1, 52.9, 44.6, 35.6, 32.2, 25.1, 11.0;

Preparation of methyl 3,3-dimethyl-5-oxocyclopent-1-ene-1-carboxylate (25):

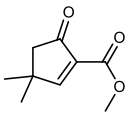

Compound **25** was prepared according to the literature procedures.[8–10]

Preparation of *tert*-butyl 3,3-dimethyl-5-oxocyclopent-1-ene-1-carboxylate (26):

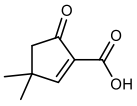

Compound **S10** was prepared according to the literature procedures.[8–10]

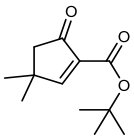

Compound **S10** (50.0 mg, 0.324 mmol, 1 eq.) was dissolved in anhydrous dimethylformamide (2.50 mL) in a flame-dried vial under a nitrogen atmosphere, HBTU (123.0 mg, 0.324 mmol, 1 eq.) and *N*-methylmorpholine (71.3 µL, 0.649 mmol, 2.0 eq.) were added and the mixture was stirred at 25°C. After 30 minutes *tert*-butyl alcohol (62.0 µL, 0.649 mmol, 2 eq.) was added and the reaction mixture was stirred at 25°C for 3 days. The reaction was monitored by HPLC-MS and when the starting material was consumed the reaction mixture was diluted with ethyl acetate, washed two times with a 5% citric acid solution, two times with a saturated aqueous Na_2CO_3 solution, and two times with brine. The organic phase was dried over anhydrous Na_2SO_4, filtered, then evaporated under reduced pressure. The resulting crude product was purified by preparative RP-HPLC using a gradient method on a Gemini® 5µm C18 110 Å column (H_2O:MeCN = 95:5 (0.1 % HCOOH) to 100% MeCN (0.1 % HCOOH)). Compound **26** was obtained as a yellow oil (40.0 mg, 58.7%).

HRMS (ESI-TTOF) m/z $[M+H]^+$ calculated for $C_{12}H_{19}O_3$ 211.1328 found 211.1324

^{1}H NMR (500 MHz, $CDCl_3$): δ 7.97 (s, 1H), 2.39 (s, 2H), 1.53 (s, 9H), 1.27 (s, 6H).

^{13}C NMR (125 MHz, $CDCl_3$): δ 202.9, 178.7, 161.2, 135.1, 81.9, 51.4, 38.6, 28.2, 27.6;

Preparation of dimethyl 3-methyl-5-oxocyclopent-1-ene-1,3-dicarboxylate (S16):

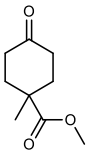

Compound **9** (517 mg, 3.07 mmol, 1 eq.) was dissolved in ethyl acetate (3.11 mL) in a vial under a nitrogen atmosphere. 20.0 mg of 10% palladium on carbon was added and the reaction mixture was purged with hydrogen with the use of a balloon. After purging the atmosphere, three hydrogen balloons were attached to the vial and the mixture was vigorously stirred for 16 hours at 25°C. The reaction was monitored by HPLC-MS and when the starting material was consumed the reaction mixture was diluted with ethyl acetate and filtered through a pad of Celite which was washed two times with ethyl acetate. The solvent was evaporated under reduced pressure affording compound **S11** as a colorless oil without further purification (463.0 mg, 88%).

HRMS (ESI-TTOF) m/z $[M+H]^+$ calculated for $C_9H_{15}O_3$ 171.1021 found 171.1023

^{1}H NMR (500 MHz, $CDCl_3$): δ 3.76 (s, 3H), 2.47 – 2.37 (m, 4H), 2.36 – 2.27 (m, 2H), 1.75 – 1.63 (m, 2H), 1.31 (s, 3H).

^{13}C NMR (125 MHz, $CDCl_3$): δ 210.9, 176.8, 52.2, 42.5, 38.5, 35.3, 25.7;

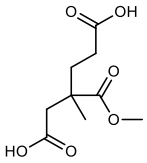

To a suspension of compound **S11** (400.0 mg, 2.35 mmol, 1 eq.) and $KMnO_4$ (742.8 mg, 4.70 mmol, 2 eq.) in water (14 mL) was added a solution of NaOH (35.0 mg, 0.869 mmol, 0.36 eq.) in water (2 mL). The reaction was stirred at 25°C for 16 h, over which time the solid dissolved. A saturated aqueous $NaHSO_3$ solution was added until the purple color disappeared. The reaction mixture was filtered through a pad of Celite which was washed two times with diethyl ether to remove the brown solid. The filtrate was acidified with conc. HCl until pH 1. The reaction was washed with diethyl ether three times, and the combined extracts were dried over anhydrous Na_2SO_4, the solvent was evaporated under reduced pressure, affording compound **S12** as a colorless oil without further purification (240.0 mg, 47%).

HRMS (ESI-TTOF) m/z $[M+H]^+$ calculated for $C_9H_{15}O_6$ 219.0868 found 219.0871

^{1}H NMR (500 MHz, $CDCl_3$): δ 3.70 (s, 3H), 2.77 (d, *J* = 16.5 Hz, 1H), 2.58 (d, *J* = 16.4, 1.4 Hz, 1H) 2.38 (t, *J* = 8.1 Hz, 2H), 2.03 (ddd, *J* = 14.1, 9.2, 6.8 Hz, 1H), 1.94 (ddd, *J* = 14.1, 9.4, 6.5 Hz, 1H), 1.30 (s, 3H).

^{13}C NMR (125 MHz, $CDCl_3$): δ 179.5, 177.4, 175.9, 52.4, 43.3, 42.5, 33.3, 29.4, 21.7;

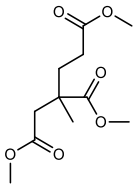

To compound **S12** (240.0 mg, 1.10 mmol, 1 eq.) in toluene (2.5 mL) was added MeOH (245µL, 6.05 mmol, 5.5 eq.) and cc. H_2SO_4 (91 µL, 1.70 mmol, 1.6 eq.). The reaction was stirred for 16 hours at 90°C and after cooling to room temperature the organic solvent was removed under reduced pressure. The residue was diluted with ethyl acetate and washed with a saturated $NaHCO_3$ solution and brine two times. The organic layer was dried over anhydrous Na_2SO_4, the solvent was evaporated under reduced pressure affording compound **S13** as a yellow oil without further purification (163.0 mg, 60%).

HRMS (ESI-TTOF) m/z $[M+H]^+$ calculated for $C_{11}H_{19}O_6$ 247.1181 found 247.1189

^{1}H NMR (500 MHz, $CDCl_3$): δ 3.70 (s, 3H), 3.67 (s, 3H), 3.66 (s, 3H), 2.76 (d, *J* = 15.9 Hz, 1H), 2.46 (d, *J* = 15.9 Hz, 1H), 2.38 – 2.23 (m, 2H), 2.01 (ddd, *J* = 14.0, 10.3, 6.0 Hz, 1H), 1.89 (ddd, *J* = 14.0, 10.2, 6.4 Hz, 1H), 1.27 (s, 3H).

^{13}C NMR (125 MHz, $CDCl_3$): δ 175.9, 173.5, 171.4, 52.2, 51.8, 51.7, 43.7, 42.7, 33.9, 29.5, 21.7;

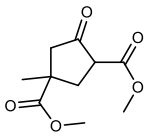

A solution of KO^{t}Bu (111.4 mg, 0.993 mmol, 1.5 eq.) in anhydrous THF (1 mL) was cooled to 0 ˚C and compound **S13** in anhydrous THF (1.5 mL) was added dropwise. The reaction was allowed to stir at 25°C for 1.5 hours, during which time it turned brown. Glacial acetic acid (0.20 mL) was added, resulting in a brownish solution containing a white precipitate. A solution of 0.40 g Na_2HPO_4 in 1.45 mL of water was added, causing the suspension to become homogeneous. The organic layer was separated, and the aqueous layer was washed with chloroform three times. The combined organic layers were washed with brine, dried over anhydrous Na_2SO_4, the solvent was evaporated under reduced pressure. The resulting crude product was purified by flash chromatography (hexanes: ethyl acetate) to give compound **S14** as inseparable diastereomers as a yellow oil (50.0 mg, 35%).

HRMS (ESI-TTOF) m/z $[M+H]^+$ calculated for $C_{10}H_{15}O_5$ 215.0919 found 215.0922

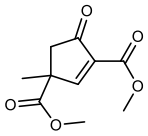

To a solution of compound **S14** (50.0 mg, 0.233 mmol, 1 eq.) in methylene chloride (0.1 mL) at 0°C was added pyridine (23 µL, 0.280 mmol, 1.2 eq.). After 5 min, a solution of phenylselenyl chloride (53.6 mg, 0.280 mmol, 1.2 eq.) in methylene chloride (0.1 mL) was added dropwise. After 16 hours the reaction mixture was quenched with a saturated aqueous solution of ammonium chloride and washed twice with ethyl acetate. The combined organic layers were washed with water two times and dried over anhydrous Na_2SO_4. The solvent was evaporated under reduced pressure affording **S15**.

To a solution of the above prepared **S15** in methylene chloride (1 mL) was added m-CPBA (138.1 mg, 0.560 mmol, 2.4 eq.) at 0°C in small amounts. After 16 hours, water was added and the mixture was washed three times with methylene chloride. The organic layers were washed with a 5% $NaHCO_3$ solution and brine two times, dried over anhydrous Na_2SO_4. The solvent was evaporated under reduced pressure. The resulting crude product was purified by flash chromatography (hexanes: ethyl acetate) to give compound **S16** as a yellow oil (26.3 mg, 53%).

HRMS (ESI-TTOF) m/z $[M+H]^+$ calculated for $C_{10}H_{13}O_5$ 213.0762 found 213.0763

^{1}H NMR (500 MHz, $CDCl_3$): δ 8.20 (s, 1H), 3.82 (s, 3H), 3.73 (s, 3H), 3.11 (d, *J* = 18.9 Hz, 1H), 2.41 (d, *J* = 18.9 Hz, 1H), 1.53 (s, 3H).

^{13}C NMR (125 MHz, $CDCl_3$): δ 200.2, 172.9, 171.9, 161.9, 135.6, 53.2, 52.3, 49.0, 47.2, 24.4;

Preparation of 1-benzyl 3-methyl 3-methyl-5-oxocyclopent-1-ene-1,3-dicarboxylate (27):

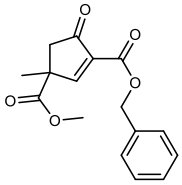

To a solution of compound **S16** (120.0 mg, 0.566 mmol, 1 eq.) in toluene (2.4 mL) was added benzyl-alcohol (588 µL, 5.66 mmol, 10 eq.) and the resulting mixture was stirred at 110 °C for 48 hours. After the starting material was fully consumed the volatiles were evaporated under reduced pressure. The crude product was purified by flash chromatography (hexanes: ethyl acetate) to give compound **27** as a yellow oil (72.0 mg, 44%).

HRMS (ESI-TTOF) m/z $[M+H]^+$ calculated for $C_{16}H_{17}O_5$ 289.1075 found 289.1079

^{1}H NMR (500 MHz, $CDCl_3$): δ 8.20 (s, 1H), 7.43 (m, 2H), 7.40 – 7.31 (m, 3H), 5.28 (d, *J* = 2.3 Hz, 2H), 3.74 (s, 3H), 3.14 (d, *J* = 18.9 Hz, 1H), 2.42 (d, *J* = 18.9 Hz, 1H), 1.54 (s, 3H).

^{13}C NMR (125 MHz, $CDCl_3$): δ 200.1, 172.8, 171.6, 161.1, 135.4, 135.3, 128.6, 128.43, 128.41, 66.8, 53.1, 48.9, 47.0, 24.3;

Preparation of 3-(methoxycarbonyl)-3-methyl-5-oxocyclopent-1-ene-1-carboxylic acid (S17):

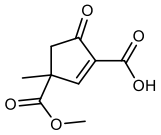

To a solution of compound **27** (450.0 mg, 1.56 mmol, 1 eq.) in methylene chloride (9 mL) was added TFA (1.19 mL, 15.6 mmol, 10 eq.) and 98% sulfuric acid (10 drops, 0.5 mL) and the resulting mixture was stirred at 25°C for 10 minutes. After the starting material was consumed, the reaction mixture was diluted with 150 mL of water and was washed with methylene chloride three times. The combined organic layers were washed two times with brine, dried over anhydrous Na_2SO_4. The solvent was evaporated under reduced pressure affording compound **S17** as an off-white solid (309.0 mg, 99 %).

HRMS (ESI-TTOF) m/z $[M+Na]^+$ calculated for $C_9H_{10}O_5Na$ 221.0425 found 221.0428

^{1}H NMR (500 MHz, $CDCl_3$): δ 8.48 (s, 1H), 3.78 (s, 3H), 3.32 (d, 1H), 2.57 (d, 1H), 1.61 (s, 3H).

^{13}C NMR (125 MHz, $CDCl_3$): δ 206.2, 175.0, 172.1, 161.1, 133.1, 53.3, 49.7, 46.4, 24.0;

General procedure C for the transesterification of compound S18:

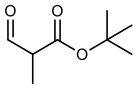

Compound **S18** was synthesized according to literature procedures.[11]

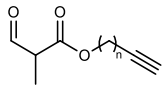

S2l-o

n: 1-4

Compound **S18** (1.00 g, 6.321 mmol, 1 eq.) was dissolved in toluene (30 mL) then the appropriate propargyl alcohol derivative (1.5 eq.) was added, and the mixture was heated to 110°C where it was kept for until full conversion was achieved (1-3 hours). The mixture was cooled to room temperature and then concentrated under reduced pressure at 30°C. Compounds **S2l-o** were obtained by vacuum distillation as colorless oils.

n: 1; Prop-2-yn-1-yl 2-methyl-3-oxopropanoate: (624.0 mg, 68%) **S2l**

^{1}H NMR (500 MHz, $CDCl_3$) enol-form: δ 11.04 (d, *J* = 12.8 Hz, 1H), 7.03 (dq, *J* = 12.8, 1.2 Hz, 1H), 4.79 (d, *J* = 2.5 Hz, 2H), 2.50 (t, *J* = 2.5 Hz, 1H), 1.72 (d, *J* = 1.2 Hz, 3H).

^{13}C NMR (125 MHz, $CDCl_3$) enol form: δ 196.6, 171.5, 99.6, 75.6, 75.1, 51.8, 12.1;

n: 2; But-3-yn-1-yl 2-methyl-3-oxopropanoate: (444.0 mg, 46%) **S2m**

^{1}H NMR (500 MHz, $CDCl_3$) enol form: δ 11.14 (d, *J* = 12.6 Hz, 1H), 7.01 (dq, *J* = 12.6, 1.2 Hz, 1H), 4.30 (t, *J* = 6.8 Hz, 2H), 2.58 (dtd, *J* = 7.3, 6.8, 2.6 Hz, 2H), 2.01 (td, *J* = 2.7, 1.5 Hz, 1H), 1.70 (d, *J* = 1.2 Hz, 3H).

^{13}C NMR (125 MHz, $CDCl_3$) enol form: δ 197.0, 160.6, 79.6, 70.3, 63.0, 52.6, 28.1, 12.4;

n: 3; Pent-4-yn-1-yl 2-methyl-3-oxopropanoate: (574.0 mg, 54%) **S2n**

^{1}H NMR (300 MHz, $CDCl_3$) enol form: δ 11.25 (d, *J* = 12.5 Hz, 1H), 7.00 (dd, *J* = 12.6, 1.2 Hz, 1H), 4.29 (t, *J* = 6.2 Hz, 2H), 2.34 – 2.29 (m, 2H), 1.97 (dt, *J* = 5.0, 2.7 Hz, 1H), 1.95 – 1.88 (m, 2H), 1.68 (d, *J* = 1.2 Hz, 3H).

^{13}C NMR (75 MHz, $CDCl_3$) enol form: δ 197.3, 162.9, 89.3, 69.6, 61.6, 52.7, 27.2, 21.5, 15.1;

n: 4; Hex-5-yn-1-yl 2-methyl-3-oxopropanoat): (641.0 mg, 56%) **S2o**

^{1}H NMR (300 MHz, $CDCl_3$) enol form: δ 11.28 (d, *J* = 12.5 Hz, 1H), 7.00 (dq, *J* = 12.5, 1.2 Hz, 1H), 4.22 (t, *J* = 6.41 Hz, 2H), 2.27 – 2.23 (m, 2H), 1.97 – 1.94 (m, 1H), 1.86 – 1.7 (m, 2H), 1.68 (d, *J* = 1.2 Hz, 3H), 1.66-1.59 (m, 2H).

^{13}C NMR (75 MHz, $CDCl_3$) enol form: δ 197.3, 169.9, 83.7, 69.0, 62.4, 52.7, 31.7l, 27.6, 24.9, 18.1;

Preparation of 1-(*tert*-butyl) 3-(prop-2-yn-1-yl) 3-methyl-6-oxocyclohex-1-ene-1,3-dicarboxylate (28*R*/28*S*):

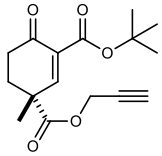

Following the **General Procedure A** using: **S1a** (300.0 mg, 1.76 mmol), **S2l** (271.7 mg, 1.94 mmol) and catalyst **S3a**/**S3b** (24.14 mg, 0.0353 mmol) in 1,4-dioxane (1.8 mL, 1.0 M) at room temperature for 3 days. After removal of the volatile compounds under reduced

pressure, purification by flash chromatography on silica gel (hexanes 0-25% ethyl acetate) gave the product as a colorless oil (442.7 mg, 86% for **28*R***, 433.0 mg, 84% for **28*S***).

ee: 92% with catalyst **S3a** (**28*R***)
ee: -87% with catalyst **S3b** (**28*S***)

HRMS (ESI-TTOF) m/z $[M+H]^+$ calculated for $C_{16}H_{21}O_5$ 293.1388 found 293.1393

^{1}H NMR (300 MHz, $CDCl_3$): δ 7.35 (s, 1H), 4.74 (dd, *J* = 5.6, 2.5 Hz, 2H), 2.58-2.53 (m, 2H), 2.50 (s, 1H), 2.48–2.43 (m, 1H) 2.04–1.96 (m, 1H), 1.52 (s, 9H), 1.50 (s, 3H).

^{13}C NMR (75 MHz, $CDCl_3$): δ 199.5, 172.7, 163.7, 153.3, 133.7, 82.4, 75.6, 53.2, 44.2, 35.3, 32.0, 28.5, 28.2, 24.5;

Preparation of 3-(but-3-yn-1-yl) 1-(*tert*-butyl) (*S*)-3-methyl-6-oxocyclohex-1-ene-1,3-dicarboxylate (29*S*):

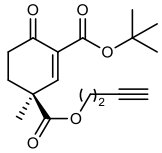

Following the **General Procedure A** using: **S1a** (400.0 mg, 2.35 mmol), **S2m** (400.0 mg, 2.59 mmol) and catalyst **S3b** (24.57 mg, 0.047 mmol) in 1,4-dioxane (2.35 mL, 1.0 M) at room temperature for 3 days. After removal of the volatile compounds under reduced pressure, purification by flash chromatography on silica gel (hexanes 0-25% ethyl acetate) gave the product as a colorless oil (394.0 mg, 55%).

ee: -84% with catalyst **S3b**

HRMS (ESI-TTOF) m/z $[M+H]^+$ calculated for $C_{17}H_{23}O_5$ 307.1545 found 307.1545

^{1}H NMR (300 MHz, $CDCl_3$): δ 7.34 (s, 1H), 4.26 (m, 2H), 2.55 (m, 2H), 2.51 (m, 1H), 2.47 (s, 1H), 2.44 (m, 1H), 1.98 (m, 2H), 1.50 (s, 9H), 1.49 (s, 3H).

^{13}C NMR (75 MHz, $CDCl_3$): δ 193.5, 173.0, 163.6, 153.7, 133.4, 82.1, 79.4, 70.2, 63.0, 44.2, 35.3, 31.9, 28.1, 24.6, 18.9;

Preparation of 1-(*tert*-butyl) 3-(pent-4-yn-1-yl) (*S*)-3-methyl-6-oxocyclohex-1-ene-1,3-dicarboxylate
(30*S*):

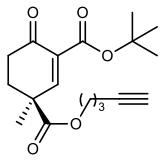

Following the **General Procedure A** using: **S1a** (370.0 mg, 2.17 mmol), **S2n** (402.0 mg, 2.39 mmol) and catalyst **S3b** (22.7 mg, 0.043 mmol) in 1,4-dioxane (2.10 mL, 1.0 M) at room temperature for 3 days. After removal of the volatile compounds under reduced pressure, purification by flash chromatography on silica gel (hexanes 0-25% ethyl acetate) gave the product as a colorless oil (354.0 mg, 51%).

ee: -81% with catalyst **S3b**

HRMS (ESI-TTOF) m/z $[M+H]^+$ calculated for $C_{18}H_{25}O_5$ 321.1701 found 321.1702

^{1}H NMR (300 MHz, $CDCl_3$): δ 7.35 (s, 1H), 4.27 (t, *J* = 6.9 Hz, 2H), 2.57-2.51 (m, 2H), 2.47-2.43 (m, 1H), 2.29 (td, *J* = 6.9 Hz, 2.3 Hz, 2H), 2.03-2.00 (m, 1H), 1.99-1.97 (m, 1H), 1.91-1.86 (m, 2H), 1.52 (s, 9H), 1.49 (s, 3H).

^{13}C NMR (75 MHz, $CDCl_3$): δ 193.6, 173.3, 163.7, 153.9, 133.4, 82.6, 82.3, 69.5, 64.3, 44.4, 35.4, 32.1, 28.2, 27.4, 24.7, 15.3;

Preparation of 1-(*tert*-butyl) 3-(hex-5-yn-1-yl) (*S*)-3-methyl-6-oxocyclohex-1-ene-1,3-dicarboxylate
(31*S*):

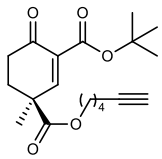

Following the **General Procedure A** using: **S1a** (510.0 mg, 3.00 mmol), **S2o** (600.6 mg, 3.30 mmol) and catalyst **S3b** (31.3 mg, 0.020 mmol) in 1,4-dioxane (3.00 mL, 1.0 M) at room temperature for 3 days. After removal of the volatile compounds under reduced pressure, purification by flash chromatography on silica gel (hexanes 0-25% ethyl acetate) gave the product as a colorless oil (359.0 mg, 36%).

ee: -86% with catalyst **S3b**

HRMS (ESI-TTOF) m/z $[M+H]^+$ calculated for $C_{19}H_{27}O_5$ 335.1858 found 335.1864

^{1}H NMR (300 MHz, $CDCl_3$): δ 7.35 (s, 1H), 4.20-4.16 (m, 2H), 2.54-2.51 (m, 2H), 2.47-2.42 (m, 1H), 2.23 (dt, *J* = 6.6, 3.3 Hz, 2H), 2.03-1.98 (m, 1H), 1.96 (s, 1H), 1.82 – 1.75 (m, 2H), 1.61-1.56 (m, 2H), 1.51 (s, 9H), 1.48 (s, 3H).

^{13}C NMR (75 MHz, $CDCl_3$): δ 193.7, 173.4, 163.7, 154.1, 133.3, 82.3, 69.1, 63.4, 44.4, 35.5, 32.1, 28.5, 28.2, 27.7, 25.0, 24.7, 18.2;

Preparation of 4-azido-*N*,*N*-dimethylaniline (S19):

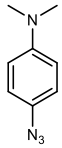

4-azido-*N*,*N*-dimethylaniline (**S19**) was synthesized according to the literature procedure.[12]

Preparation of 1-(*tert*-butyl) 3-((1-(4-(dimethylamino)phenyl)-1*H*-1,2,3-triazol-4-yl)methyl) 3-methyl-6-oxocyclohex-1-ene-1,3-dicarboxylate

(32*R*/32*S*):

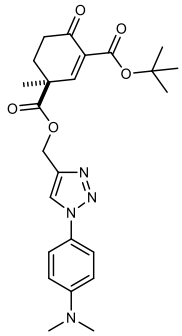

To the solution of **28*R*/28*S*** (30.0 mg, 0.103 mmol, 1 eq.) in methylene chloride (0.2 mL) was added compound **S19** (16.2 mg, 0.103 mmol, 1 eq.). To this mixture was added the solution of copper(II) sulfate pentahydrate (2.6 mg, 0.010 mmol, 0.1 eq.) and sodium ascorbate (10.2 mg, 0.051 mmol, 0.5 eq.) in water (0.2 mL) and methanol (0.1 mL). The reaction mixture was vigorously stirred at 25°C. After 3 hours the mixture was diluted with methylene chloride and water then the aqueous phase was washed with methylene chloride two times. The combined organic phases were washed with brine then dried over anhydrous Na_2SO_4, filtered, and evaporated under reduced pressure. The crude product was purified by preparative RP-HPLC using a gradient method on a Gemini® 5µm C18 110 Å column (H_2O:MeCN = 95:5 (0.1 % HCOOH) to 100% MeCN (0.1 % HCOOH)). Compound **32*R*/32*S*** was obtained as a yellow solid (36.1 mg, 77% for **32*R***, 36.5 mg, 78% for **32*S***).

HRMS (ESI-TTOF) m/z $[M+H]^+$ calculated for $C_{24}H_{31}N_4O_5$ 455.2294 found 455.2304

^{1}H NMR (500 MHz, $CDCl_3$): δ 7.89 (s, 1H), 7.52 (d, *J* = 9.0 Hz, 2H), 7.34 (s, 1H), 6.75 (d, *J* = 9.1 Hz, 2H), 5.35 (q, *J* = 12.7 Hz, 2H), 3.00 (s, 6H), 2.56 – 2.47 (m, 2H), 2.46 – 2.40 (m, 1H), 2.03 – 1.94 (m, 1H), 1.49 (s, 9H), 1.47 (s, 3H).

^{13}C NMR (125 MHz, $CDCl_3$): δ 193.5, 173.4, 163.7, 153.6, 150.9, 133.6, 126.5, 122.1, 122.0, 112.4, 82.3, 59.0, 44.3, 40.5, 35.3, 32.0, 28.2, 28.1, 24.5, 24.4;

Preparation of 6-(3-azidophenyl)-5,8-dimethyl-1,2,3,4-tetrahydroisoquinoline (S23):

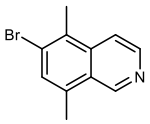

Compound **S20** was synthesized according to the literature procedures.[13]

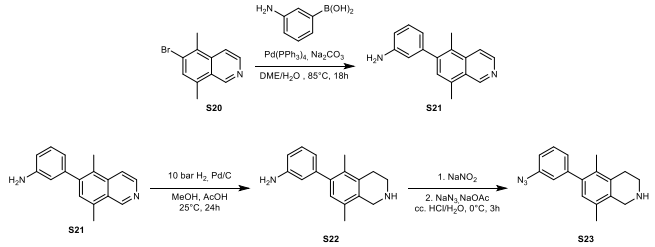

A pressure vessel was charged with compound **S20** (0.750 g, 3.19 mmol 1 eq.), (3-aminophenyl) boronic acid (0.655 g, 4.78 mmol, 1.5 eq.), Na_2CO_3 (0.676 g, 6.38 mmol, 2 eq.), $Pd(PPh_3)_4$ (0.220 g, 0.19 mmol, 0.059 eq.), 9.6 mL dimethoxyethane and 4.8 mL water and the reaction mixture was stirred at 85°C for 18 hours under a N_2 atmosphere. After completion the reaction mixture was cooled to 25°C and water and ethyl acetate was added to it. After phase separation the aqueous phase was extracted 3 times with ethyl acetate. The combined organic phase was washed with water and brine, then it was dried over anhydrous Na_2SO_4, filtered and the solvent was evaporated under reduced pressure. The crude product was purified by flash column chromatography giving compound **S21** as brownish crystals (0.680 g, 86%).

HRMS (ESI-TTOF) m/z $[M+H]^+$ calculated for $C_{17}H_{17}N_2$ 249.1391found 249.1394

^{1}H NMR (500 MHz, $CDCl_3$): δ 9.52 (s, 1H), 8.58 (d, *J* = 7.5 Hz, 1H), 7.75 – 7.72 (m, 1H), 7.40 (s, 1H), 7.21 (td, *J* = 7.7, 1.9 Hz, 1H), 6.72 – 6.67 (m, 2H), 6.65 – 6.63 (m, 1H), 2.64 (s, 3H), 2.61 (s, 3H).

^{13}C NMR (125 MHz, $CDCl_3$): δ 150.2, 146.4, 142.9, 142.6, 140.5, 135.2, 133.2, 130.9, 129.7, 129.3, 128.3, 120.2, 117.3, 116.2, 114.0, 18.4, 15.4;

A pressure vessel was charged with a solution of compound **S21** (0.400 g, 1.61 mmol, 1 eq.) in 8 mL methanol and 94 µL 98% acetic acid. The atmosphere was changed to N_2 then palladium on carbon was added (0.171 g, 0.161 mmol, 0.1 eq.) and vessel was charged with 10 bar H_2 and the reaction mixture was stirred at 25°C for 24 hours. After completion the reaction mixture was filtered on a pad of Celite then evaporated. The crude mixture was dissolved in methylene chloride then washed 2 times with a 10% NaOH solution. The organic phase was washed with water and brine, then it was dried over anhydrous Na_2SO_4, filtered and the solvent was evaporated under reduced pressure giving compound **S22** as an orange oil (0.230g, 56%).

HRMS (ESI-TTOF) m/z $[M+H]^+$ calculated for $C_{17}H_{21}N_2$ 253.1704 found 253.1708

^{1}H NMR (500 MHz, $CDCl_3$): δ 7.17 (t, *J* = 7.7 Hz, 1H), 6.96 (s, 1H), 6.67 – 6.67 (m, 2H), 6.59 (s, 1H), 4.00 (s, 2H), 3.19 (t, *J* = 6.1 Hz, 2H), 2.72 (t, *J* = 6.1 Hz, 2H), 2.22 (s, 3H), 2.06 (s, 3H).

^{13}C NMR (125 MHz, $CDCl_3$): δ 146.2, 143.5, 140.1, 133.7, 132.0, 129.4, 129.1, 129.0, 120.1, 116.4, 113.5, 46.8, 43.1, 29.8, 26.9, 19.0, 15.4;

A solution of compound **S22** (0.320 g, 1.26 mmol, 1 eq.) in 6 mL conc. HCl was cooled to 0°C, then a solution of $NaNO_2$ (0.200 g, 2.9 mmol, 2.3 eq.) in 6 mL water was added dropwise, and the reaction mixture was stirred for 2 hours at 0°C. After this, a solution of NaN_3 (0.188g, 2.9 mmol, 2.3 eq.) and NaOAc (2.62g, 3.19 mmol, 2.5 eq.) in 6 mL water was added dropwise, and the reaction mixture was stirred for a further 1 hour at 0°C. The pH was set to 7 with an aqueous $NaHCO_3$ solution, and the aqueous phase was extracted 3 times with chloroform. The combined organic phase was washed with water and brine, then it was dried over anhydrous Na_2SO_4, filtered, and the solvent was evaporated under reduced pressure, giving compound **S23** as a white solid without further purification (0.110 g, 67%).

HRMS (ESI-TTOF) m/z $[M+H]^+$ calculated for $C_{17}H_{19}N_4$ 279.1609found 279.1611

^{1}H NMR (500 MHz, $CDCl_3$): δ 7.37 (t, *J* = 7.8 Hz, 1H), 7.05 (dt, *J* = 7.7, 1.3 Hz, 1H), 6.99 (ddd, *J* = 8.0, 2.4, 1.0 Hz, 1H), 6.94 (t, *J* = 2.0 Hz, 1H), 6.93 (s, 1H), 3.98 (s, 2H), 3.18 (t, *J* = 6.0 Hz, 2H), 2.71 (t, *J* = 6.0 Hz, 2H), 2.23 (s, 3H), 2.04 (s, 3H).

^{13}C NMR (125 MHz, $CDCl_3$): δ 144.4, 139.9, 138.6, 134.9, 134.0, 133.1, 129.5, 129.3, 128.8, 126.4, 120.2, 117.4, 47.4, 43.5, 27.5, 19.0, 15.4;

Preparation of 1-(*tert*-butyl) 3-((1-(3-(5,8-dimethyl-1,2,3,4-tetrahydroisoquinolin-6-yl)phenyl)-1H-1,2,3-triazol-4-yl)methyl) (*S*)-3-methyl-6-oxocyclohex-1-ene-1,3-dicarboxylate (33*S*):

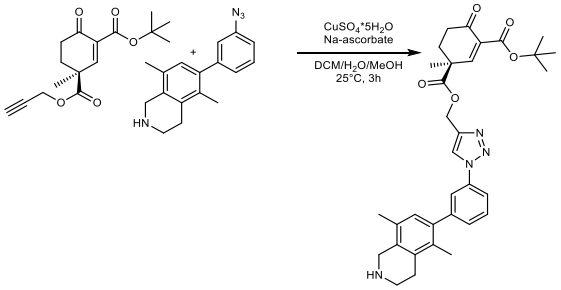

To the solution of **28*S*** (100.0 mg, 0.340 mmol, 1 eq.) in *tert* butyl alcohol (1.0 mL) was added compound **S23** (95.0 mg, 0.340 mmol, 1 eq.). To this mixture was added the solution of copper(II) sulfate pentahydrate (16.0 mg, 0.068 mmol, 0.2 eq.) and sodium ascorbate (33.0 mg, 0.170 mmol, 0.5 eq.) in water (1.0 mL). The reaction mixture was vigorously stirred at 25°C. After 3 days the mixture was diluted with methylene chloride and water then the aqueous phase was washed with methylene chloride two times. The combined organic phases were washed with brine then dried over anhydrous Na_2SO_4, filtered, and evaporated under reduced pressure. Compound **33*S*** was obtained as a green oil and was used without further purification (160.0 mg, 83%).

HRMS (ESI-TTOF) m/z $[M+H]^+$ calculated for $C_{33}H_{39}N_4O_5$ 571.2920 found 571.2925

^{1}H NMR (500 MHz, $CDCl_3$): δ 8.05 (s, 1H), 7.72 – 7.71 (m, 1H), 7.65 (t, *J* = 2.0 Hz, 1H), 7.55 (t, *J* = 7.8 Hz, 1H), 7.37 (d, *J* = 7.6 Hz, 1H), 7.34 (s, 1H), 6.98 (s, 1H), 5.38 (q, *J* = 12.8 Hz, 2H), 3.78 – 3.67 (m, 1H), 2.88 – 2.66 (m, 2H), 2.54 – 2.49 (m, 3H), 2.48 – 2.43 (m, 2H), 2.25 (s, 3H), 2.07 (s, 3H), 2.04 – 1.98 (m, 2H), 1.49 (s, 9H), 1.48 (s, 3H).

^{13}C NMR (125 MHz, $CDCl_3$) partial: δ 193.5, 173.5, 163.8, 153.4, 144.6, 143.1, 136.8, 134.3, 133.8, 131.0, 130.4, 129.6, 128.9, 122.1, 121.7, 118.9, 82.4, 58.9, 44.3, 35.3, 32.0, 29.9, 28.2, 28.1, 24.6, 22.8, 19.0, 15.5;

Preparation of 1-(*tert*-butyl) 3-(3-(4-(dimethylamino)phenyl)prop-2-yn-1-yl) 3-methyl-6-oxocyclohex-1-ene-1,3-dicarboxylate (34*R*/34*S*):

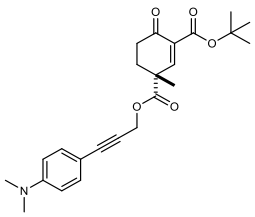

Into a flame-dried vial under a nitrogen atmosphere was added $Pd(PPh_3)_2Cl_2$ (14.4 mg, 0.020 mmol, 0.06 eq.) and CuI (7.2 mg, 0.038 mmol, 0.11 eq.). To this vial was added a solution of compound **28*R*/28*S*** (100.0 mg, 0.171 mmol, 1 eq.) and 4-iodo-*N*,*N*-dimethylaniline (84.5 mg, 0.342 mmol, 1 eq.) in anhydrous tetrahydrofuran (1.0 mL) and diisopropylamine (1.0 mL). The reaction mixture was stirred at 25°C for 1 hour and when the starting material was consumed it was filtered through a pad of Celite then evaporated. The residue was purified by flash column chromatography on silica gel using hexane: ethyl acetate = 1:1 as eluent to afford **34*R*/34*S*** as yellow oils (26.9 mg, 19% for **34*R***, 40.2 mg, 29% for **34*S***).

HRMS (ESI-TTOF) m/z $[M+H]^+$ calculated for $C_{24}H_{30}NO_5$ 412.2123 found 412.2137

^{1}H NMR (500 MHz, $CDCl_3$): δ 7.40 (s, 1H), 7.32 (d, *J* = 8.9 Hz, 2H), 6.61 (d, *J* = 8.9 Hz, 2H), 4.97 (q, *J* = 15.4 Hz, 2H), 2.98 (s, 6H), 2.63 – 2.56 (m, 1H), 2.55 – 2.46 (m, 2H), 2.03 – 1.99 (m, 1H), 1.54 (s, 3H), 1.52 (s, 9H).

^{13}C NMR (125 MHz, $CDCl_3$): δ 193.6, 172.9, 163.7, 153.7, 150.6, 133.2, 130.3, 111.8, 108.6, 88.5, 82.3, 80.2, 54.6, 44.3, 40.2, 35.4, 32.0, 28.2, 24.5;

Preparation of 1-(*tert*-butyl) 3-(3-(pyridin-4-yl)prop-2-yn-1-yl) 3-methyl-6-oxocyclohex-1-ene-1,3-dicarboxylate (35*R*/35*S*):

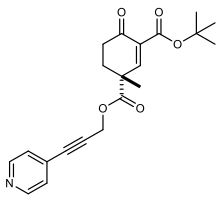

Into a flame-dried vial under a nitrogen atmosphere was added $Pd(PPh_3)_2Cl_2$ (7.2 mg, 0.010 mmol, 0.06 eq.) and CuI (3.6 mg, 0.019 mmol, 0.11 eq.). To this vial was added a solution of compound **28*R*/28*S*** (50.0 mg, 0.171 mmol, 1 eq.) and 4-iodopyridine (35.1 mg, 0.171 mmol, 1 eq.) in anhydrous tetrahydrofuran (0.375 mL) and diisopropylamine (0.375 mL). The reaction mixture was stirred at 25°C for 4 hours and when the starting material was consumed it was filtered through a pad of Celite then evaporated. The residue was purified by flash column chromatography on silica gel using hexane: ethyl acetate = 1:1 as eluent to afford **35*R*/35*S*** as yellow oils (24,9 mg, 40% for **35*R***, 39.1 mg, 62% for **35*S***).

HRMS (ESI-TTOF) m/z $[M+H]^+$ calculated for $C_{21}H_{24}NO_5$ 370.1654 found 370.1660

^{1}H NMR (500 MHz, $CDCl_3$): δ 8.60 (s, 2H), 7.37 (s, 1H), 7.30 (d, *J* = 5.0 Hz, 2H), 5.03 – 4.95 (m, 2H), 2.63 – 2.48 (m, 3H), 2.07 – 1.95 (m, 1H), 1.54 (s, 3H), 1.52 (s, 9H).

^{13}C NMR (125 MHz, $CDCl_3$): δ 210.0, 193.3, 172.6, 154.2, 153.0, 149.9, 133.8, 86.9, 84.4, 82.3, 53.5, 44.2, 35.2, 31.9, 28.1, 24.5;

Preparation of unnatural amino acids (36-38):

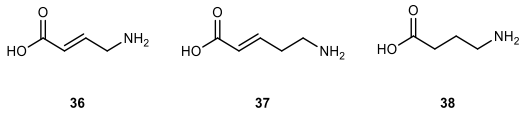

36 **37** **38**

Compounds **36**, **37**, **38** were synthesized according to literature procedures[14–18] as fluorenylmethoxycarbonyl (Fmoc) protected amino acids and unnatural peptides were chemically synthesized using solid phase peptide synthesis (on Rink Amid resin, PS3 peptide synthesizer, Protein Technologies) with Fmoc/^{t}Bu strategy and purified by RP-HPLC using a Jupiter 300 Å C18 column (Phenomenex). The quality of the peptides was verified by HPLC-MS (Shimadzu LCMS-2020).

Preparation of azido pepMNK1 (S24):

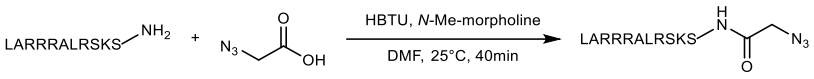

Azidoacetic acid was synthesized according to literature procedure.[19]

The peptide was chemically synthesized using solid phase peptide synthesis (on Rink Amid resin, PS3 peptide synthesizer, Protein Technologies) with Fmoc/^{t}Bu strategy and purified by RP-HPLC using a Jupiter 300 Å C18 column (Phenomenex). The quality of the peptide was verified by HPLC-MS (Shimadzu LCMS-2020).

HRMS (ESI-TTOF) m/z $[M+H]^+$ calculated for $C_{56}H_{106}N_{27}O_{15}$ 1396.8356 found 1396.8422

Preparation of 28*S*-pepMNK1_C:

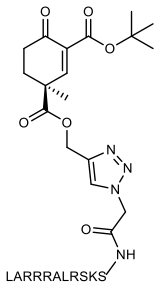

To the solution of **28*S*** (20.0 mg, 0.068 mmol, 1 eq.) in *tert*-butyl alcohol (0.15 mL) was added **S24** (96.0 mg, 0.068 mmol, 1 eq.). To this mixture was added the solution of copper(II) sulfate pentahydrate (17.0 mg, 0.068 mmol, 1 eq.) and sodium ascorbate (14.0 mg, 0.068 mmol, 1 eq.) in water (0.1 mL). The reaction mixture was vigorously stirred at 25°C. After 3 days the mixture was diluted with water then filtered using a syringe filter and the target compound was purified by a semi-preparative HPLC giving the title compound as white solid.

HRMS (ESI-TTOF) m/z $[M+H]^+$ calculated for $C_{72}H_{126}N_{27}O_{20}$ 1688.9666 found 1688.9762

Preparation of 28*S*-pepMNK1_K_CF:

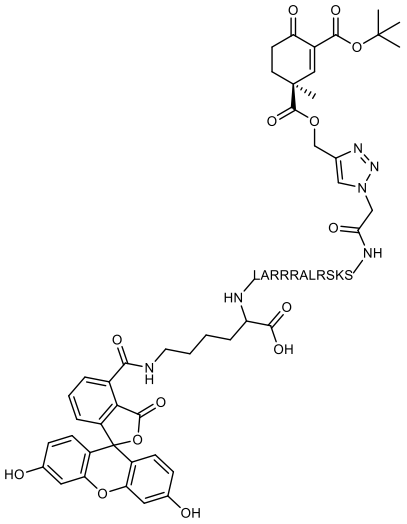

The azide group containing peptide was chemically synthesized using solid-phase peptide synthesis (on Rink Amide resin (low loading 0.2 mmol/g), PS3 peptide synthesizer, Protein Technologies) with the Fmoc/^{t}Bu strategy. The C-terminal lysine side chain protecting group, 1-(4,4-dimethyl-2,6-dioxocyclohex-1-ylidene)ethyl (Dde), was removed using 2% hydrazine in *N*,*N*-dimethylformamide. 5(6)-Carboxyfluorescein was coupled to the side chain of the lysine on the resin using a PS3 peptide synthesizer. The peptide cleavage was carried out by a TFA/H2O/Tris (95/2.5/2.5) mixture and the peptide was purified by RP-HPLC using a Jupiter 300 Å C18 column (Phenomenex). The quality of the peptide was verified by HPLC-MS (Shimadzu LCMS-2020). Then, the solution of 28S (3.6 mg, 0.012 mmol, 1 eq.) in tert-butyl alcohol (0.15 mL) was added to azido-pepMNK1_K-CF (23.0 mg, 0.012 mmol, 1 eq.). To this mixture was added the solution of copper(II) sulfate pentahydrate (3.0 mg, 0.012 mmol, 1 eq.) and sodium ascorbate (2.5 mg, 0.012 mmol, 1 eq.) in water (0.1 mL). The reaction mixture was vigorously stirred at 25°C. After 3 days, the mixture was diluted with water, then filtered using a syringe filter, and the target compound was purified by semi-preparative HPLC, yielding the title compound as a yellow solid.

Preparation of *t*ert-butyl (*E*)-2-cyano-4,4-dimethylpent-2-enoate (40):

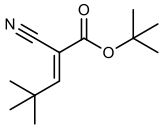

A mixture of pivaldehyde (1.22 g, 14.2 mmol), tert¬-butyl cyanoacetate (1.00 g, 7.1 mmol), acetic acid (0.406 mL, 7.1 mmol) and pyridine (0.573 mL, 7.1 mmol) was heated at reflux for 1 h. A second portion of pivaldehyde (1.22 g, 14.2 mmol) was added. The refluxing of the mixture was continued for 18 h. After cooling, the mixture was poured into 1N aqueous HCl (50 mL). The resulting mixture was extracted with EtOAc (3*50 mL). The combined organic layers were washed with 1N aqueous HCl, dried over anhydrous Na2SO4 and concentrated to give a colorless oil. The oil was purified by flash chromatography on SiO2 using hexane-EtOAc (9:1) as the eluent to give compound **40** as a colorless oil (1.00 g, 68% yield).

HRMS (ESI-TTOF) m/z $[M+H]^+$ calculated for $C_{12}H_{20}NO_2$ 210.1494 found 210.1499

^{1}H NMR (500 MHz, $CDCl_3$): δ 7.54 (s, 1H), 1.54 (s, 9H), 1.30 (s, 9H).

^{13}C NMR (125 MHz, $CDCl_3$): δ 170.5, 161.0, 114.4, 107.3, 83.5, 34.8, 28.9, 27.9;

Preparation of methyl acetyl-*L*-histidinate (S25):

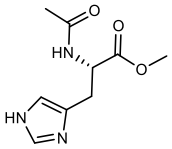

Compound **S25** was prepared according to the literature procedures.[20]

Preparation of 3-(*tert*-butyl) 1-methyl (1*R*)-1-methyl-4-oxocyclohexane-1,3-dicarboxylate (3´´*R*):

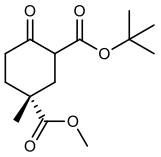

To the solution of compound **3*R*** (100.0 mg, 0.373 mmol, 1 eq.) in anhydrous pyridine (0.573 mL) was added $NaBH_4$ (14.1 mg, 0.373 mmol, 1 eq.) at 0°C. The reaction mixture was stirred at 0°C for 15 minutes. 10 mL of saturated NH_4Cl solution was added to the reaction mixture and it was stirred for 5 minutes. The aqueous phase was washed with diethyl ether three times. The combined organic phases were washed with brine two times then dried over anhydrous Na_2SO_4, filtered, and evaporated under reduced pressure. Purification by flash chromatography on silica gel (hexanes 0-25% ethyl acetate) gave compound **3´´*R*** as a colorless oil (49.0 mg, 49%).

HRMS (ESI-TTOF) m/z $[M+Na]^+$ calculated for $C_{14}H_{22}O_5Na$ 293.1364 found 293.1372

^{1}H NMR (500 MHz, $CDCl_3$): δ 12.36 (s, 1H), 3.69 (s, 3H), 2.72 (dd, *J* = 16.1, 1.4 Hz, 1H), 2.41 – 2.22 (m, 2H), 2.13 – 1.99 (m, 2H), 1.65 – 1.58 (m, 1H), 1.51 (s, 9H), 1.24 (s, 3H).

^{13}C NMR (125 MHz, CDCl3): δ 177.4, 172.4, 170.0, 97.1, 81.3, 52.1, 41.4, 32.2, 30.6, 28.4, 26.6, 24.4;

Preparation of 3-(*tert*-butyl) 1-methyl (1*S*,5*R*)-6-methylene-4-oxobicyclo[3.2.1]octane-1,3-dicarboxylate (6''*R*,*R*):

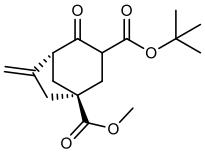

To the solution of compound **6*R*,*R*** (50.0 mg, 0.171 mmol, 1 eq.) in anhydrous pyridine (0.263 mL) was added $NaBH_4$ (6.5 mg, 0.171 mmol, 1 eq.) at 0°C. The reaction mixture was stirred at 0°C for 15 minutes. 5 mL of saturated NH_4Cl solution was added to the reaction mixture and it was stirred for 5 minutes. The aqueous phase was washed with diethyl ether three times. The combined organic phases were washed with brine two times then dried over anhydrous Na_2SO_4, filtered, and evaporated under reduced pressure. Purification by flash chromatography on silica gel (hexanes 0-25% ethyl acetate) gave compound **6''*R*,*R*** as a colorless oil (10.6 mg, 21%).

HRMS (ESI-TTOF) m/z $[M+Na]^+$ calculated for $C_{16}H_{22}O_5Na$ 317.1364 found 317.1375

^{1}H NMR (500 MHz, $CDCl_3$): δ 12.17 (s, 1H), 5.05 (t, *J* = 2.4 Hz, 1H), 4.76 (t, *J* = 2.2 Hz, 1H), 3.73 (s, 3H), 3.06 (d, *J* = 4.3 Hz, 1H), 2.79 (dt, *J* = 17.1, 2.2 Hz, 1H), 2.68 (dd, *J* = 15.9, 1.8 Hz, 1H), 2.48 – 2.43 (m, 1H), 2.35 (dd, *J* = 15.9, 1.5 Hz, 1H), 2.08 (ddd, *J* = 11.1, 4.4, 1.5 Hz, 1H), 1.92 (dd, *J* = 11.1, 2.0 Hz, 1H), 1.49 (s, 9H).

^{13}C NMR (125 MHz, CDCl3): δ 202.9, 176.4, 173.5, 150.6, 106.0, 81.4, 59.0, 52.2, 48.6, 48.4, 41.0, 36.8, 34.4, 28.4;

NMR Spectra

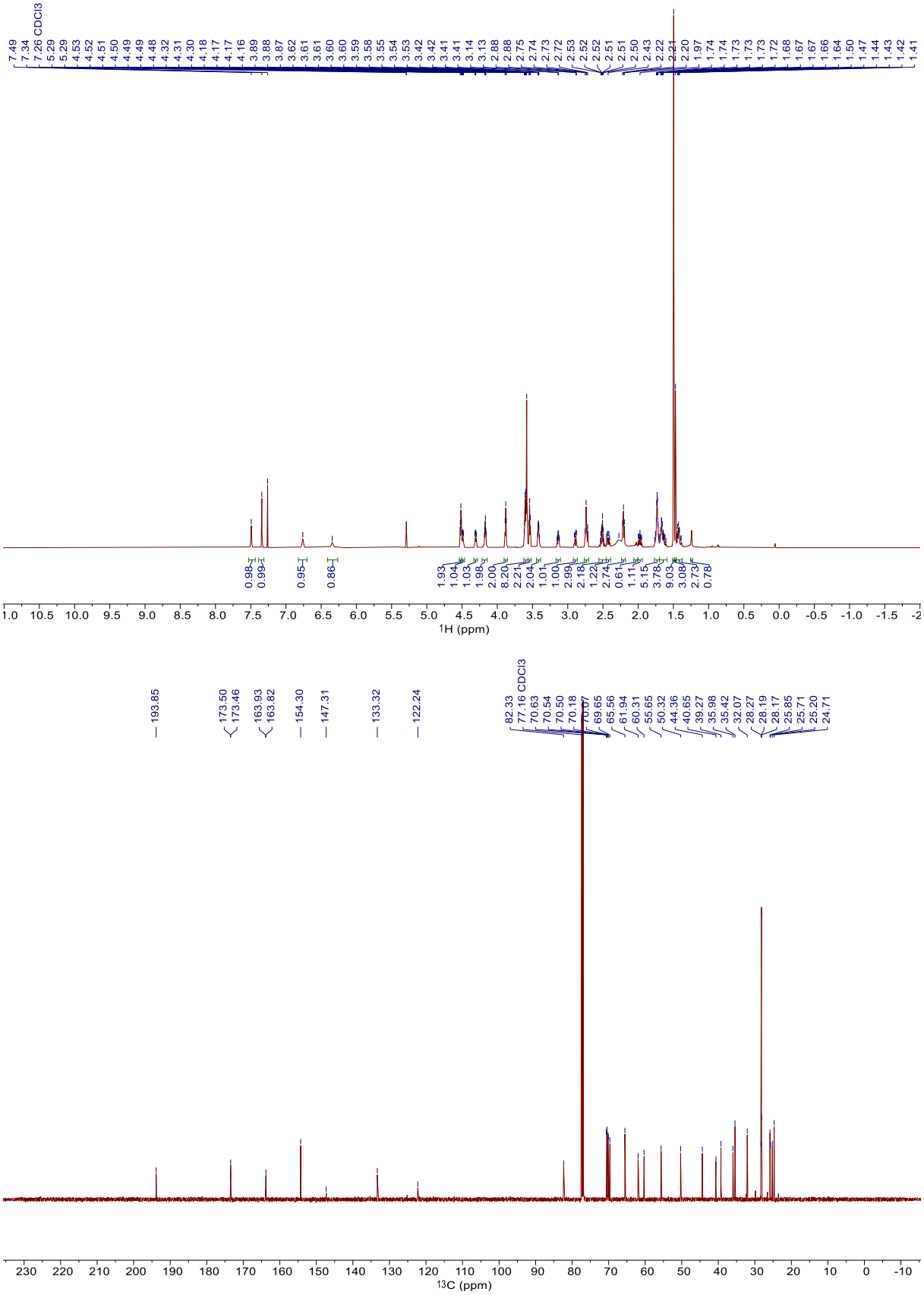

Supplementary Fig. 29. The ^{1}H-NMR (600 MHz) and ^{13}C-NMR (151 MHz) spectra of compound **2-biotin** in $CDCl_3$

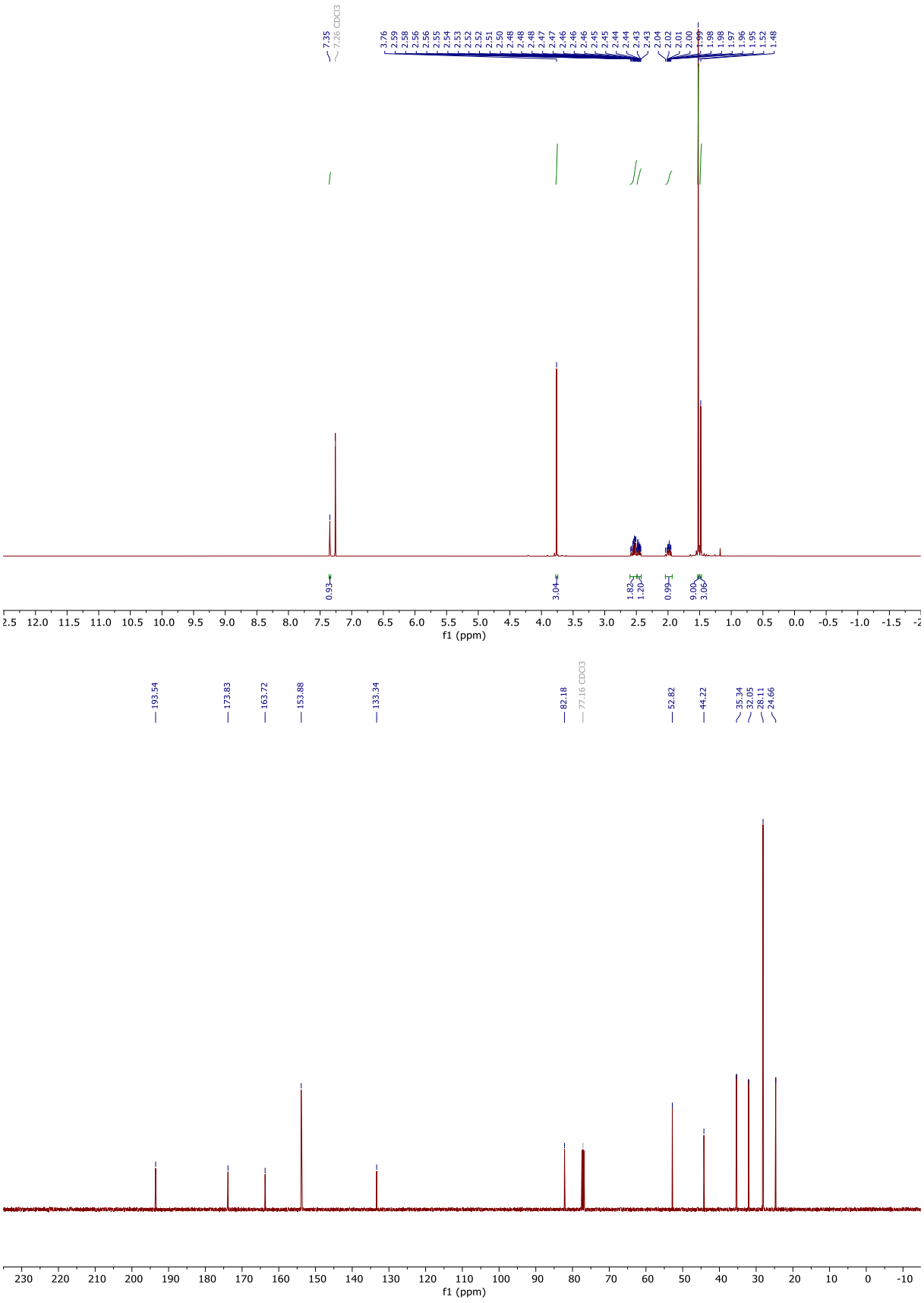

Supplementary Fig. 30. The ^{1}H-NMR (500 MHz) and ^{13}C-NMR (125 MHz) spectra of compound **3**, **3*R*/3*S*** in $CDCl_3$

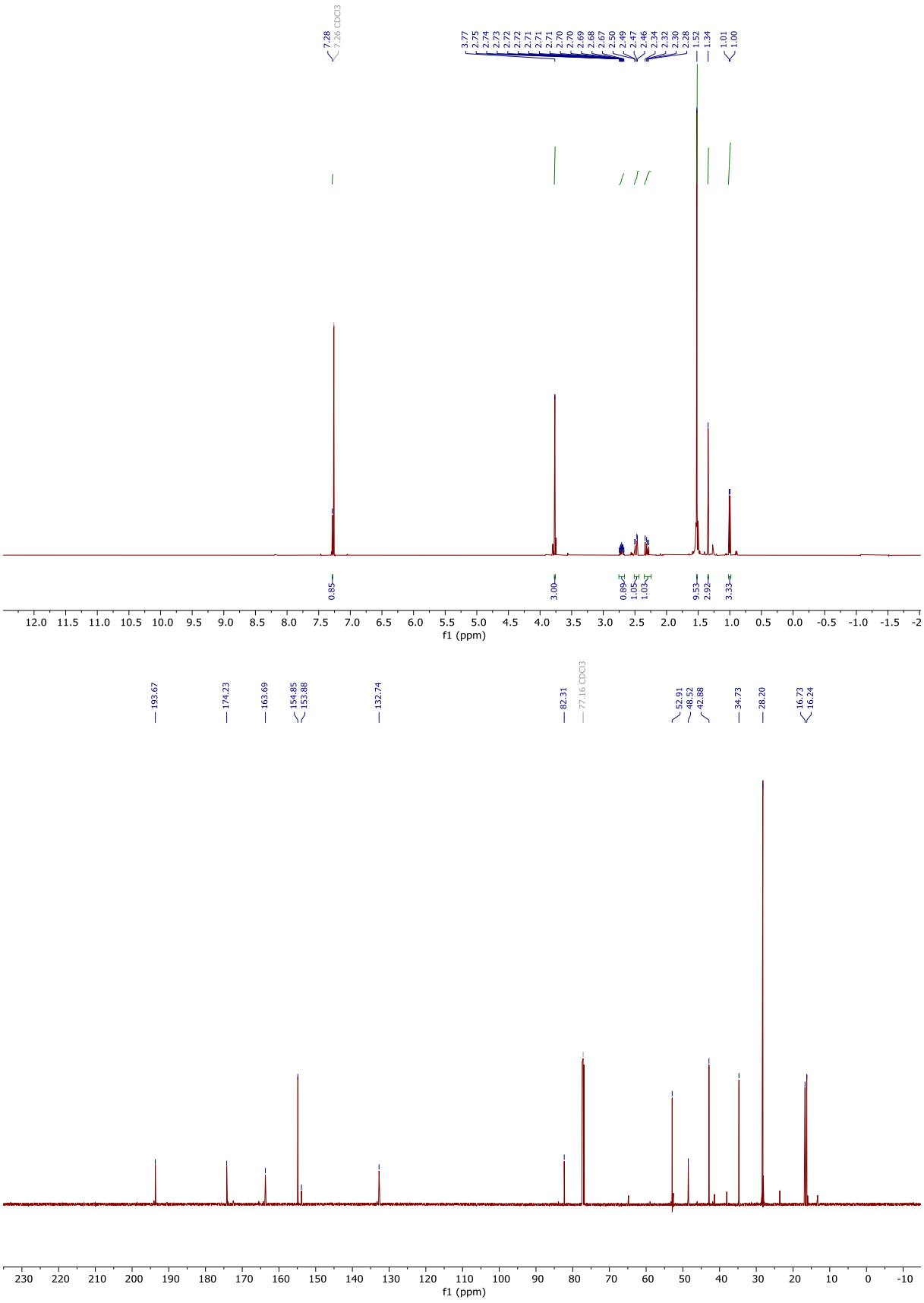

Supplementary Fig. 31. The ^{1}H-NMR (500 MHz) and ^{13}C-NMR (125 MHz) spectra of compound **3'*R*** in $CDCl_3$

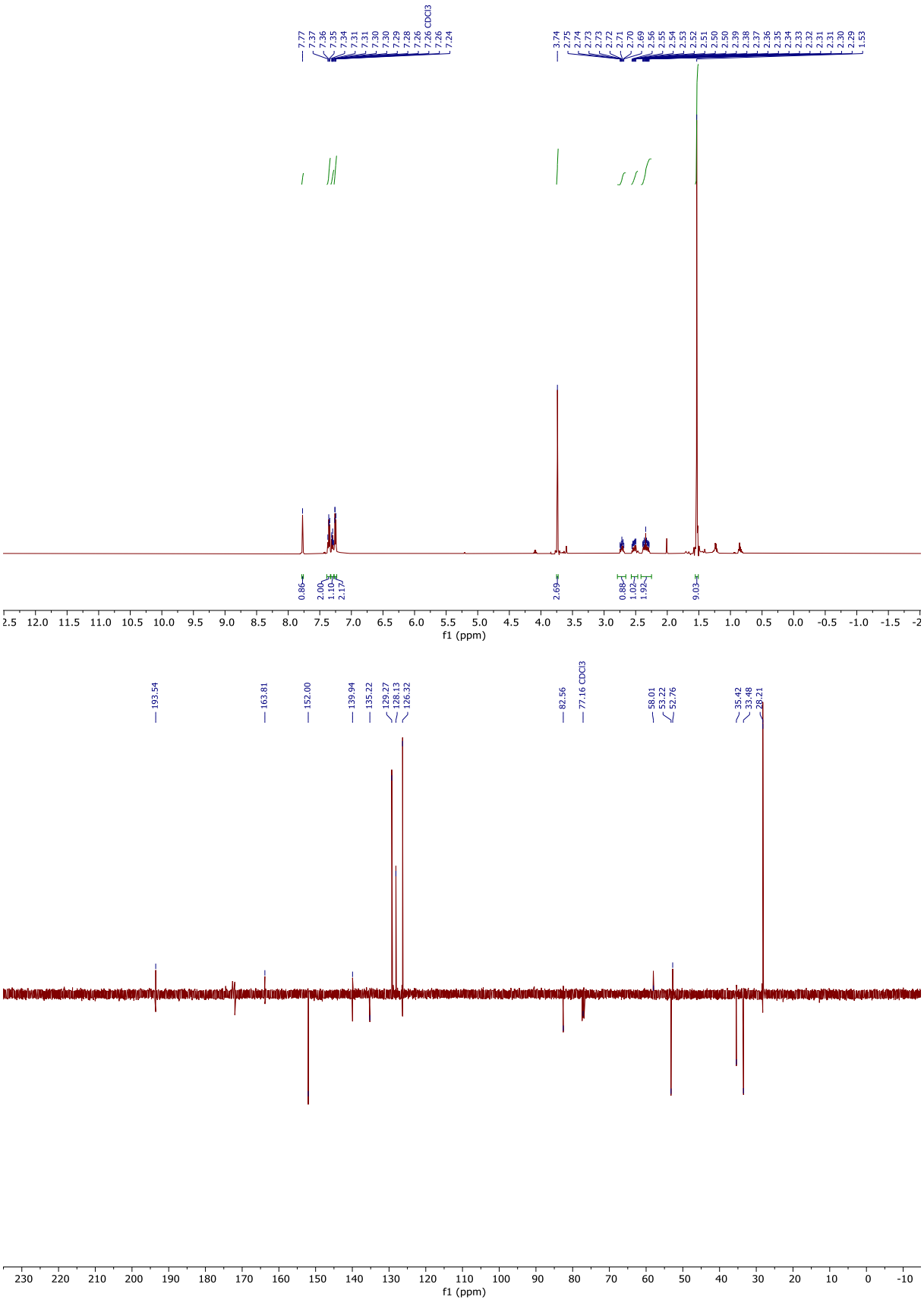

Supplementary Fig. 32. The ^{1}H-NMR (500 MHz) and APT-NMR (125 MHz) spectra of compound **5** in $CDCl_3$

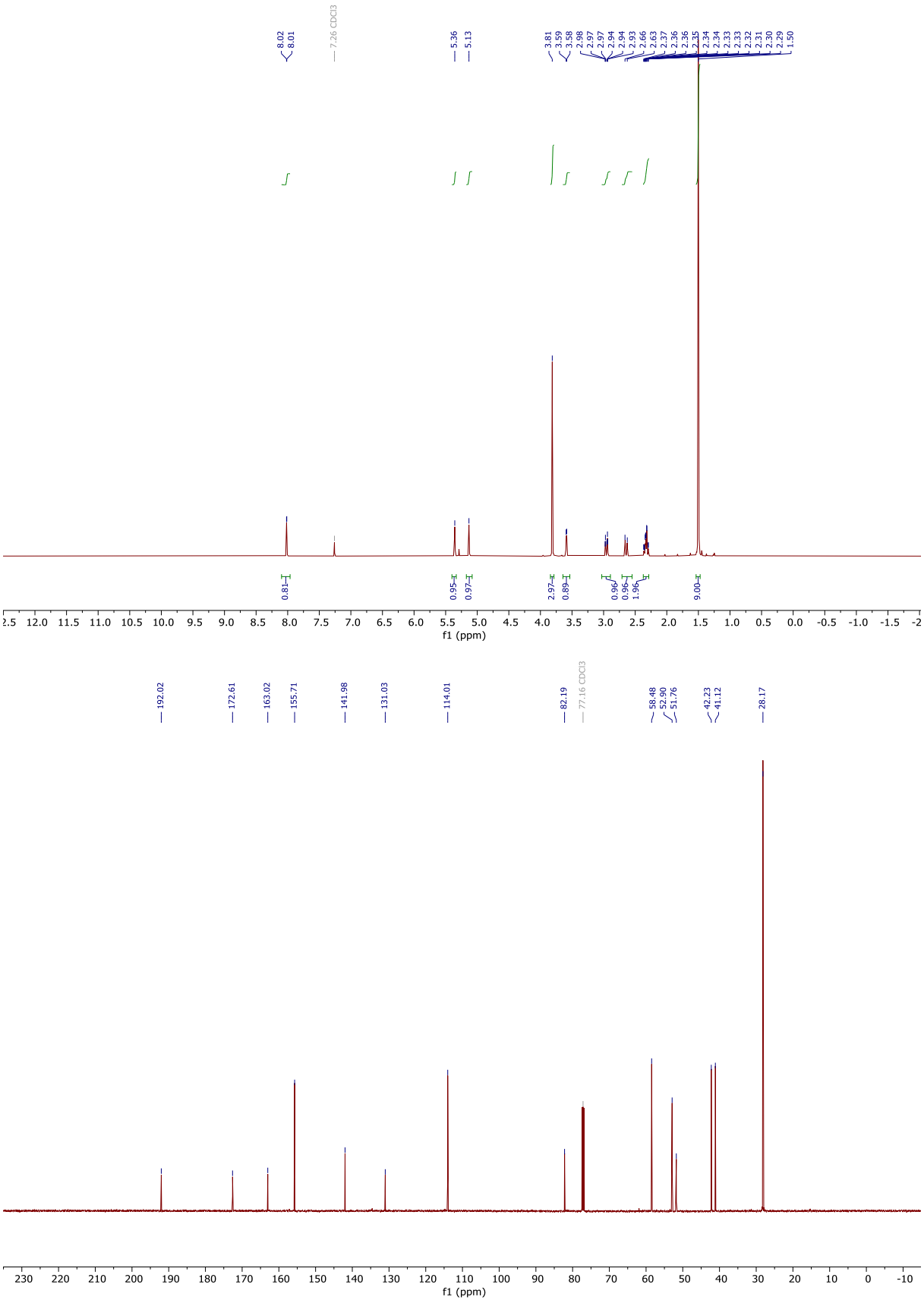

Supplementary Fig. 33. The ^{1}H-NMR (500 MHz) and ^{13}C-NMR (125 MHz) spectra of compound **6**, **6*R*,*R*/6*S*,*S*** in $CDCl_3$

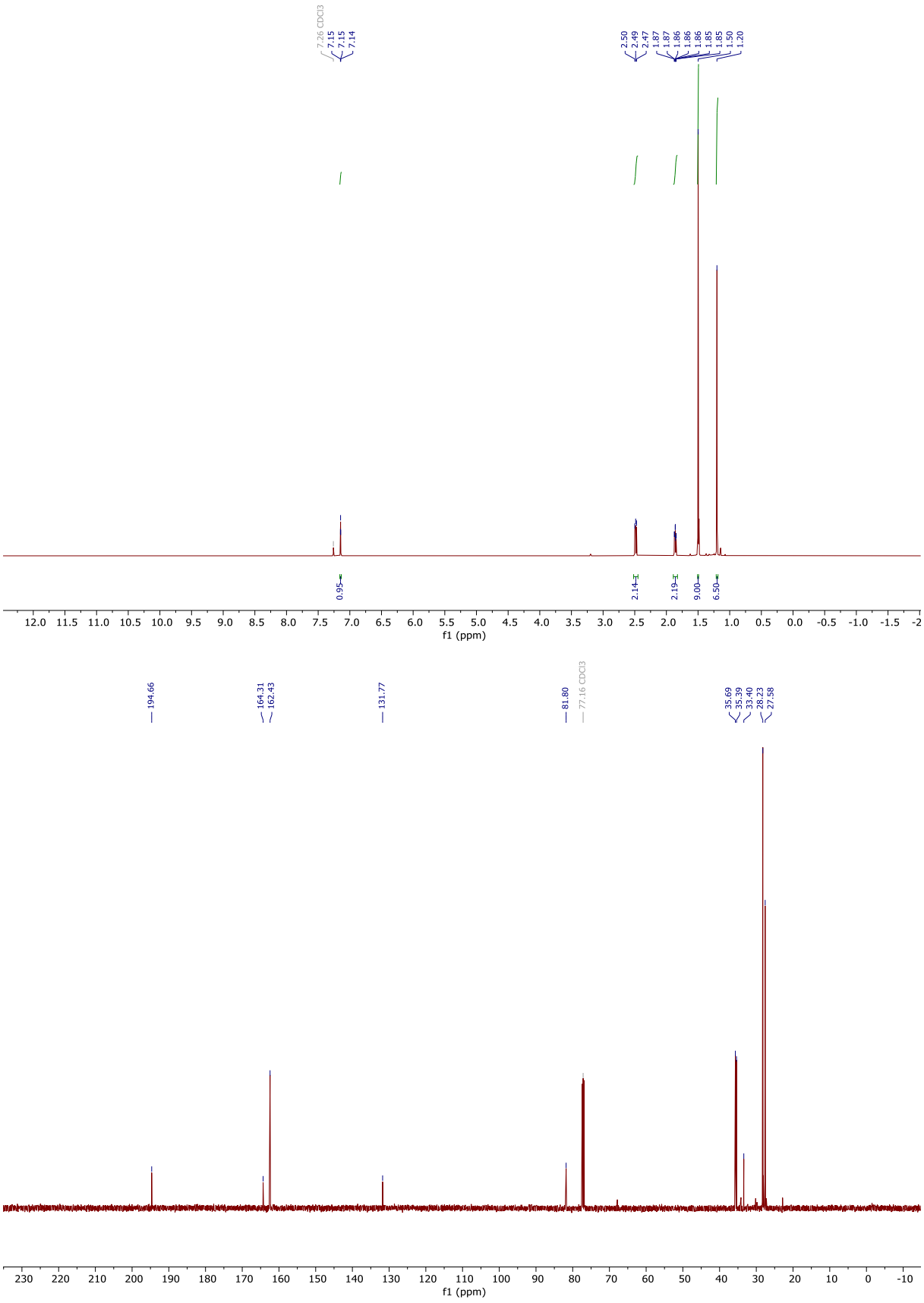

Supplementary Fig. 34. The ^{1}H-NMR (500 MHz) and ^{13}C-NMR (125 MHz) spectra of compound **7** in $CDCl_3$

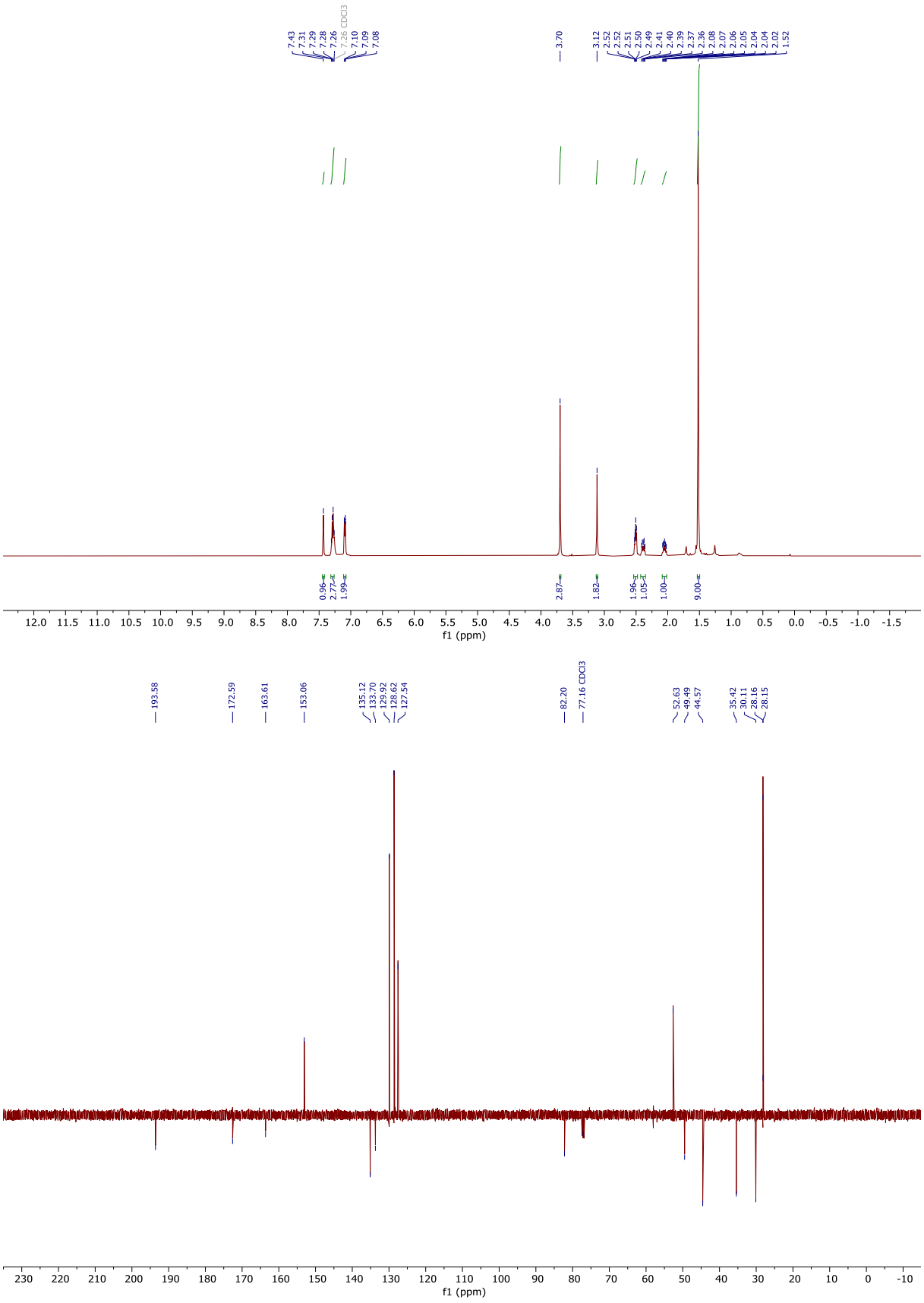

Supplementary Fig. 35. The ^{1}H-NMR (500 MHz) and APT-NMR (125 MHz) spectra of compound **8**, **8*R***/**8*S*** in $CDCl_3$

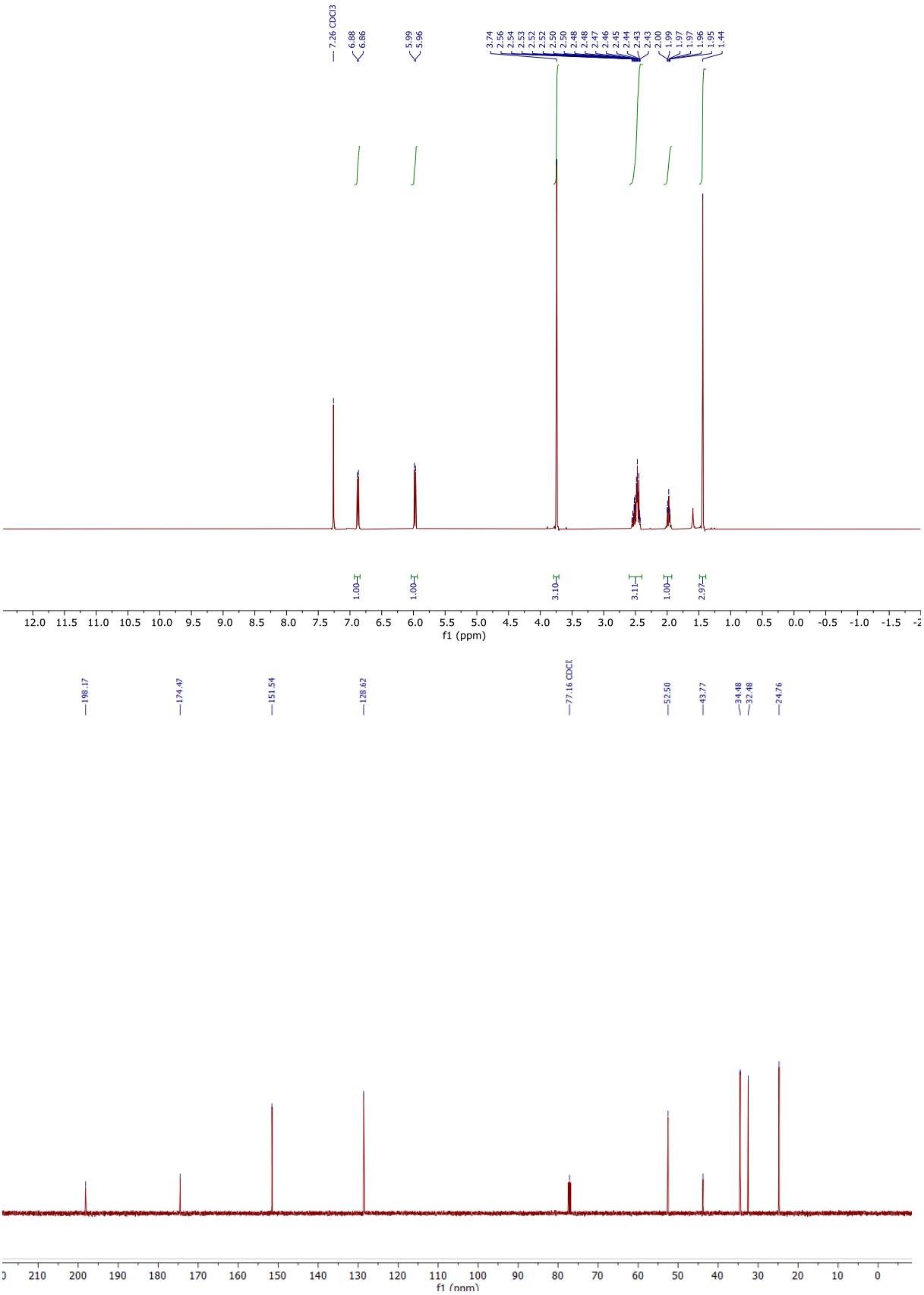

Supplementary Fig. 36. The ^{1}H-NMR (500 MHz) and ^{13}C-NMR (125 MHz) spectra of compound **9** in $CDCl_3$

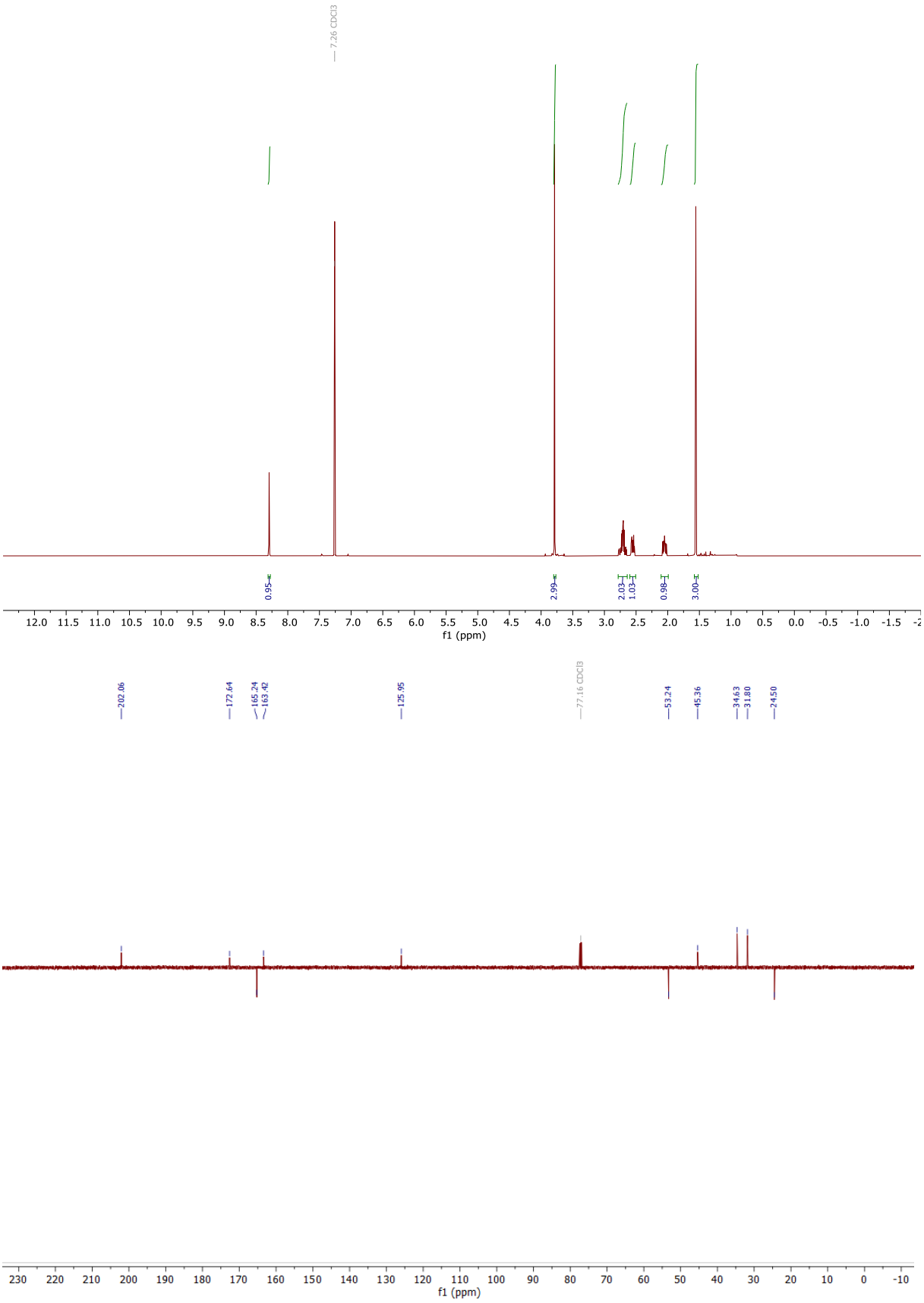

Supplementary Fig. 37. The ^{1}H-NMR (500 MHz) and APT-NMR (125 MHz) spectra of compound **10**,**10*R***/**10*S*** in $CDCl_3$

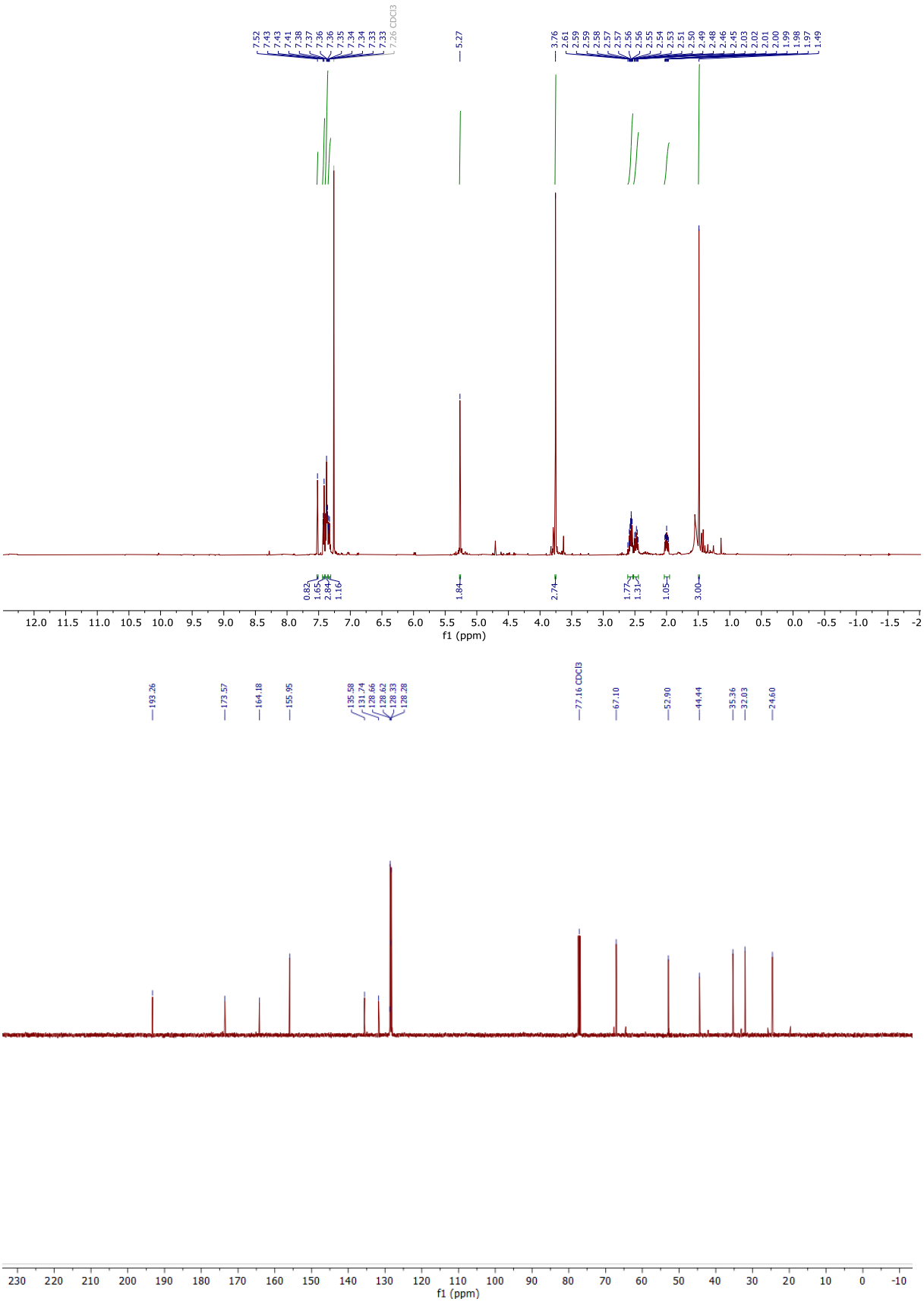

Supplementary Fig. 38. The ^{1}H-NMR (500 MHz) and ^{13}C-NMR (125 MHz) spectra of compound **12**, **12R**/**12S** in $CDCl_3$

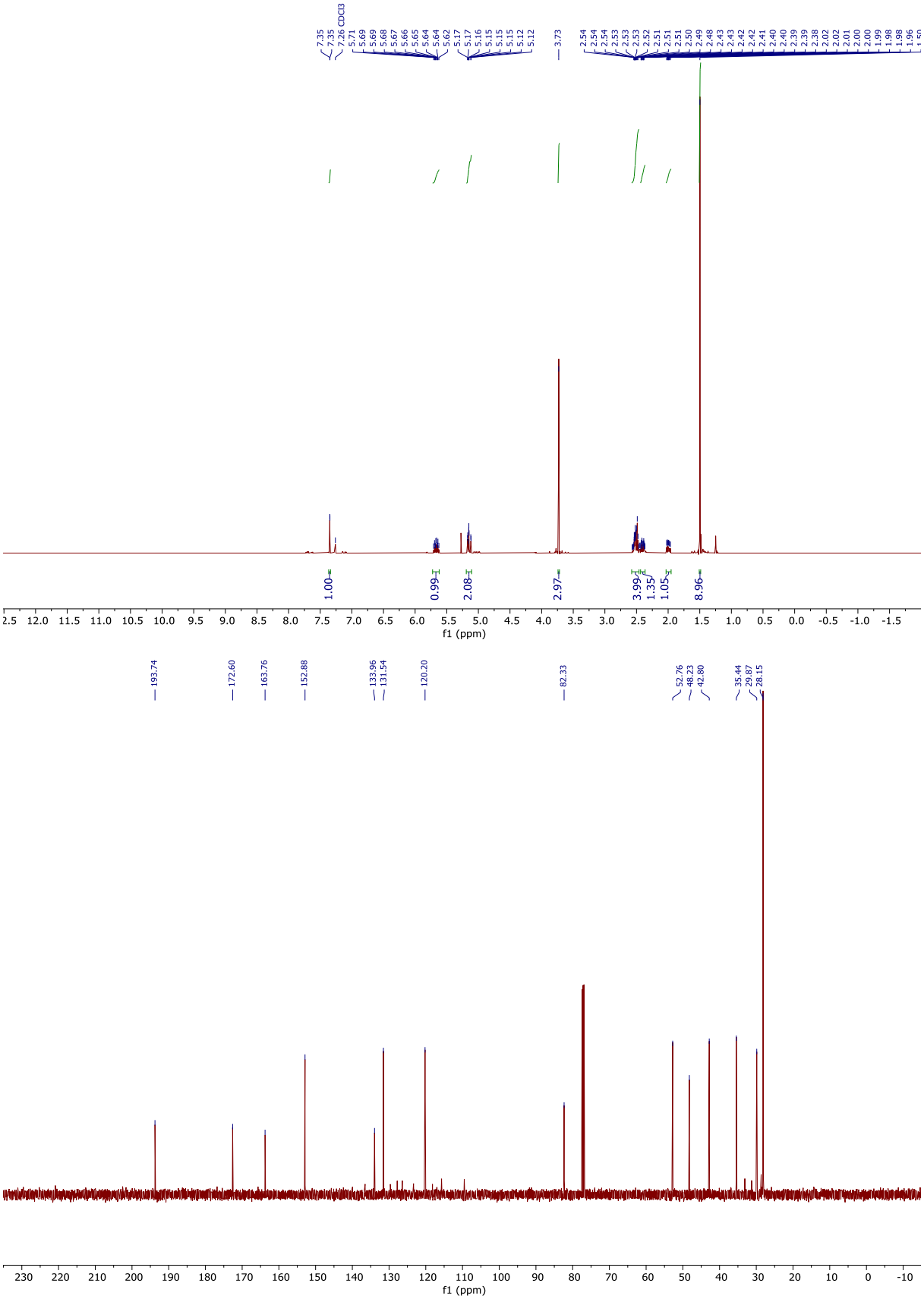

Supplementary Fig. 39. The ^{1}H-NMR (500 MHz) and ^{13}C-NMR (125 MHz) spectra of compound **13**, **13*R*/13*S*** in $CDCl_3$

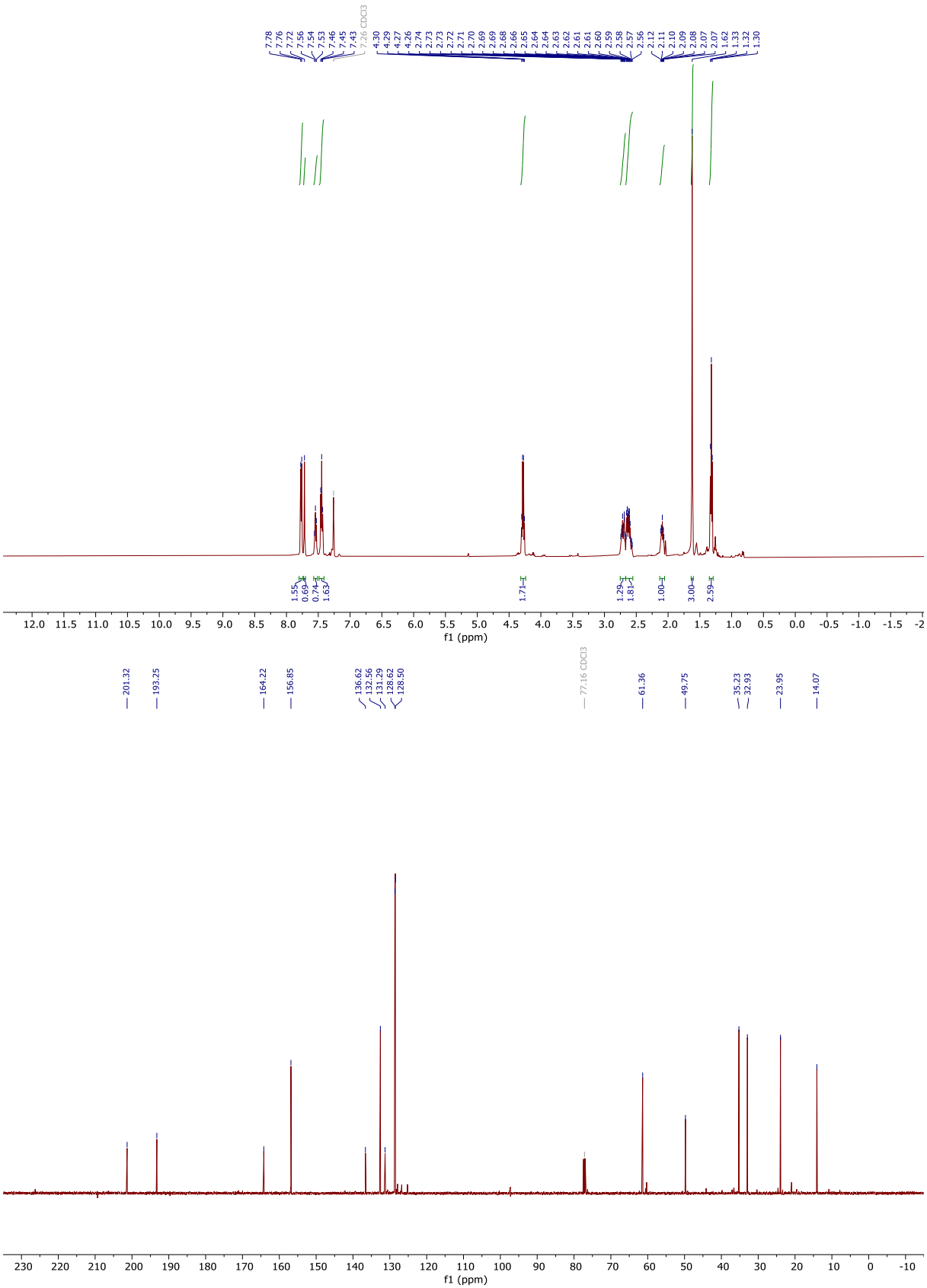

Supplementary Fig. 40. The ^{1}H-NMR (500 MHz) and ^{13}C-NMR (125 MHz) spectra of compound **14** in $CDCl_3$

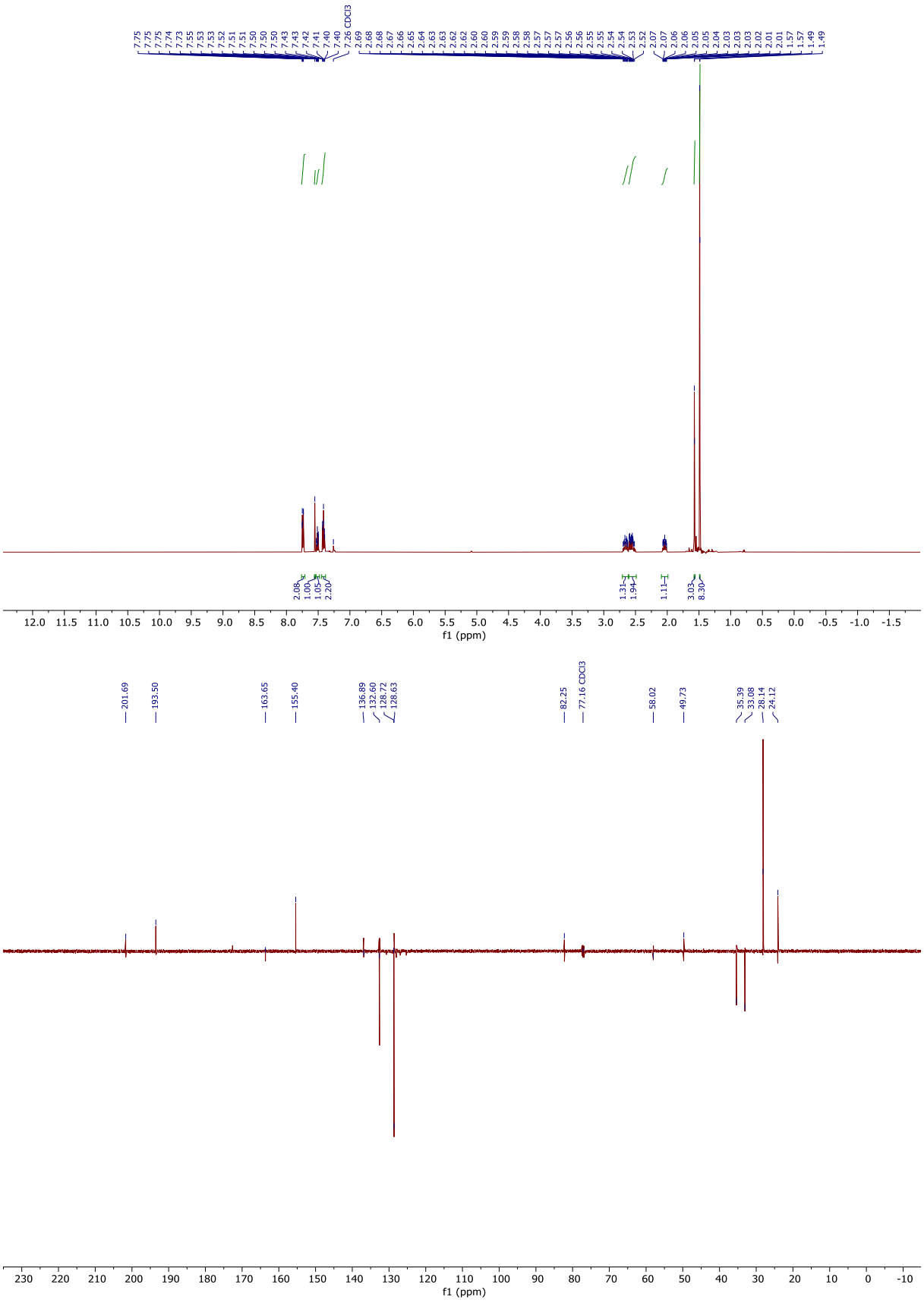

Supplementary Fig. 41. The ^{1}H-NMR (500 MHz) and APT-NMR (125 MHz) spectra of compound **15** in $CDCl_3$

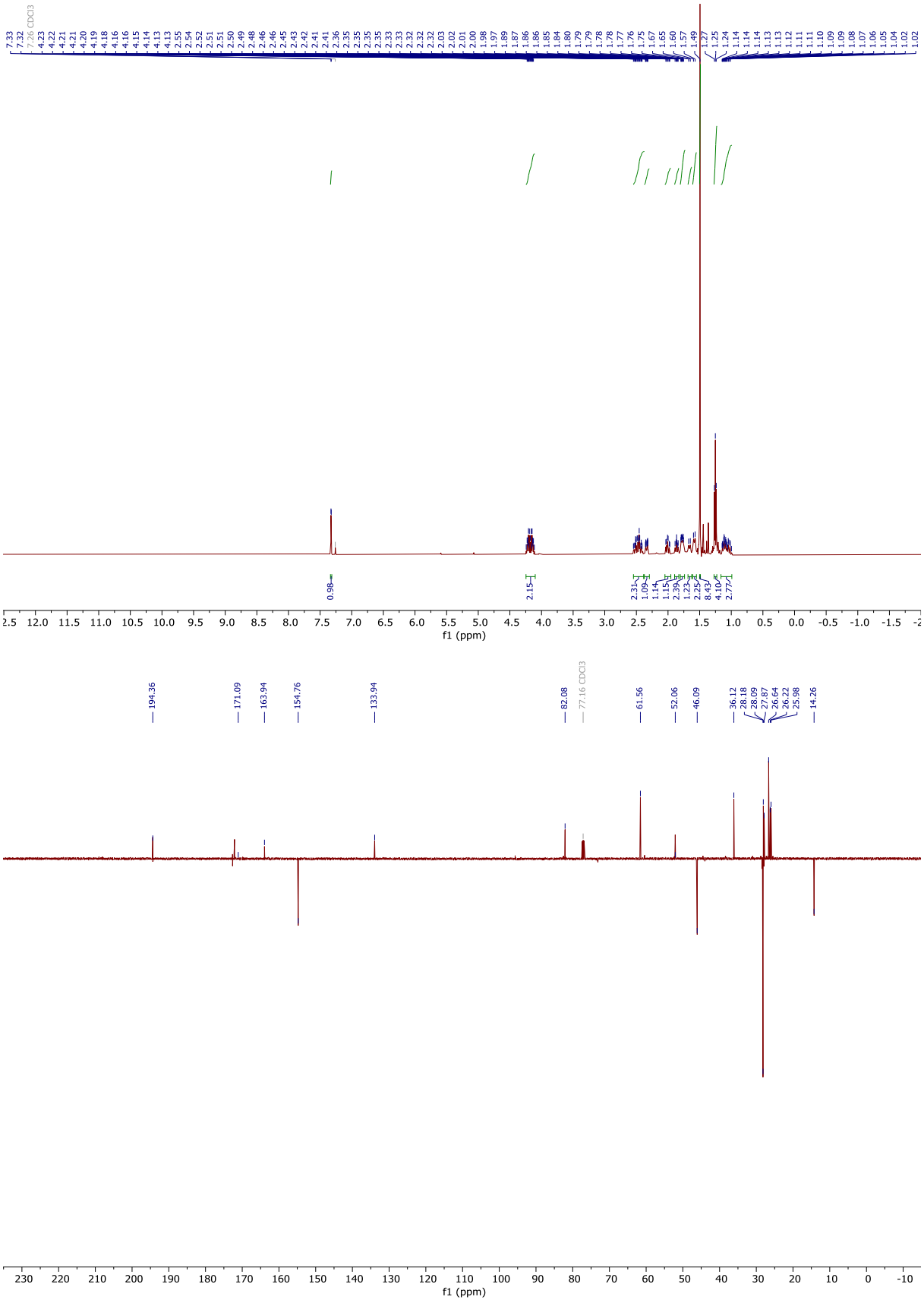

Supplementary Fig. 42. The ^{1}H-NMR (500 MHz) and APT-NMR (125 MHz) spectra of compound **16** in $CDCl_3$

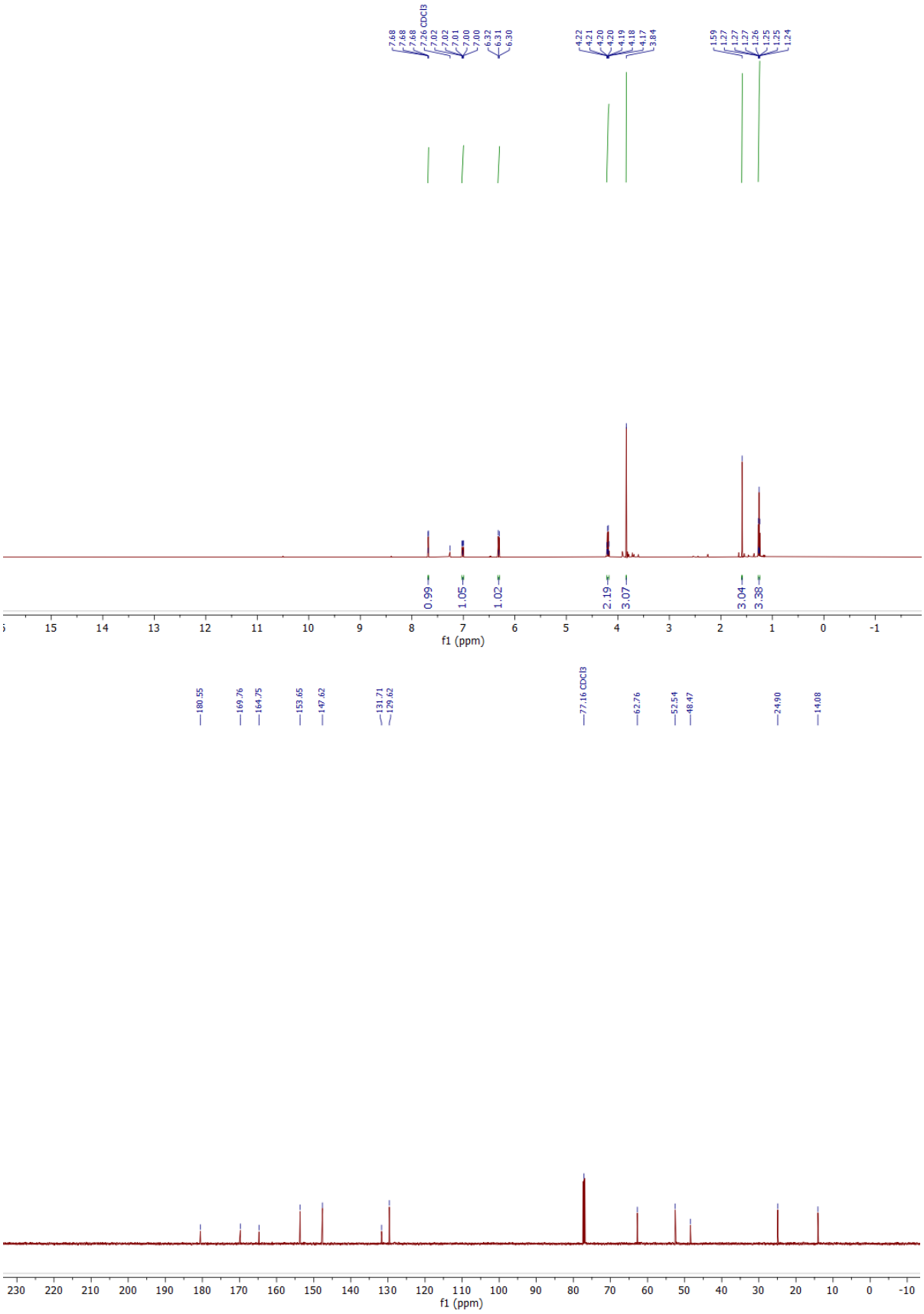

Supplementary Fig. 43. The ^{1}H-NMR (500 MHz) and ^{13}C-NMR (125 MHz) spectra of compound **17** in $CDCl_3$

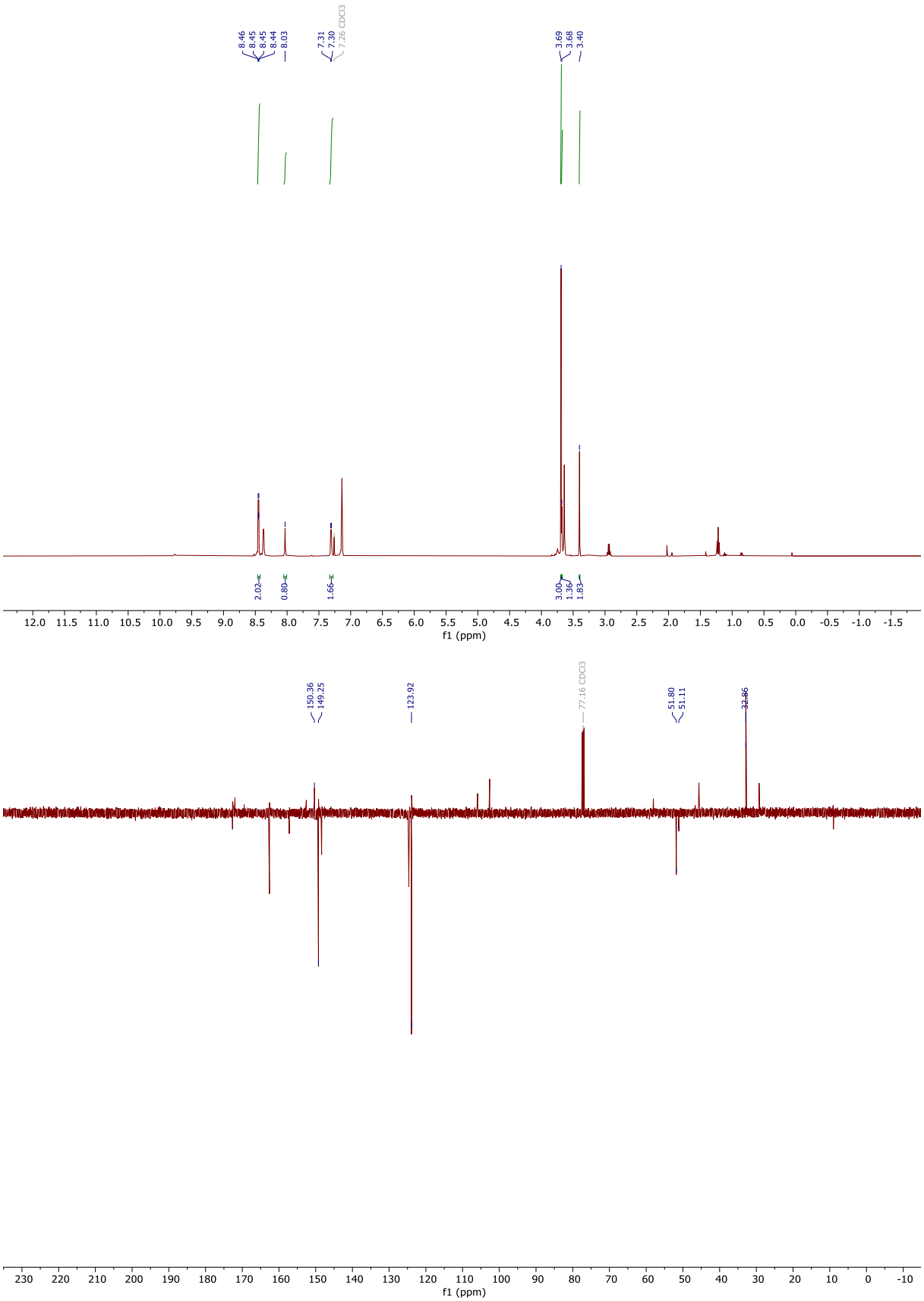

Supplementary Fig. 44. The ^{1}H-NMR (500 MHz) and APT-NMR (125 MHz) spectra of compound **S2k** in $CDCl_3$

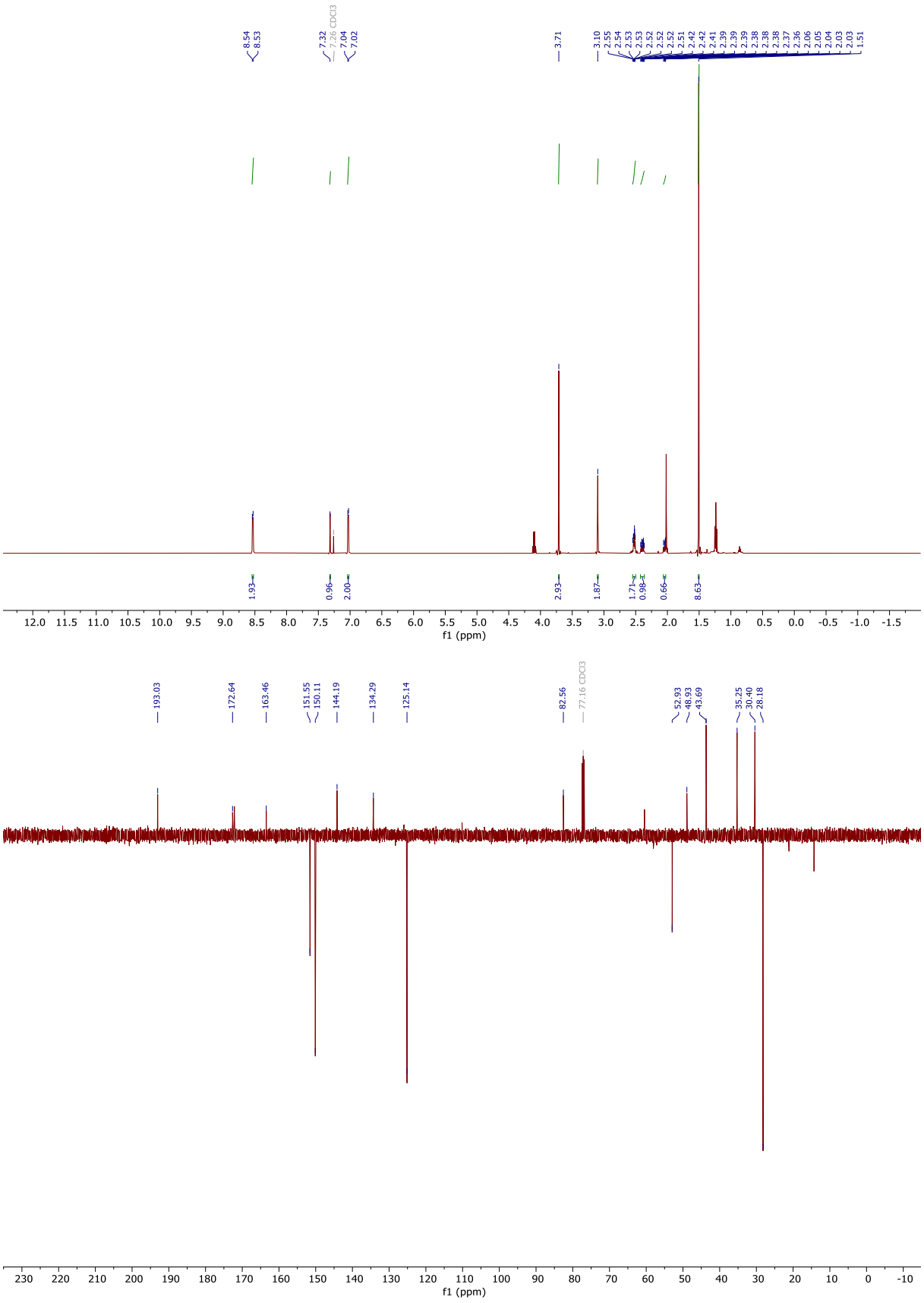

Supplementary Fig. 45. The ^{1}H-NMR (500 MHz) and APT-NMR (125 MHz) spectra of compound **S7** in $CDCl_3$

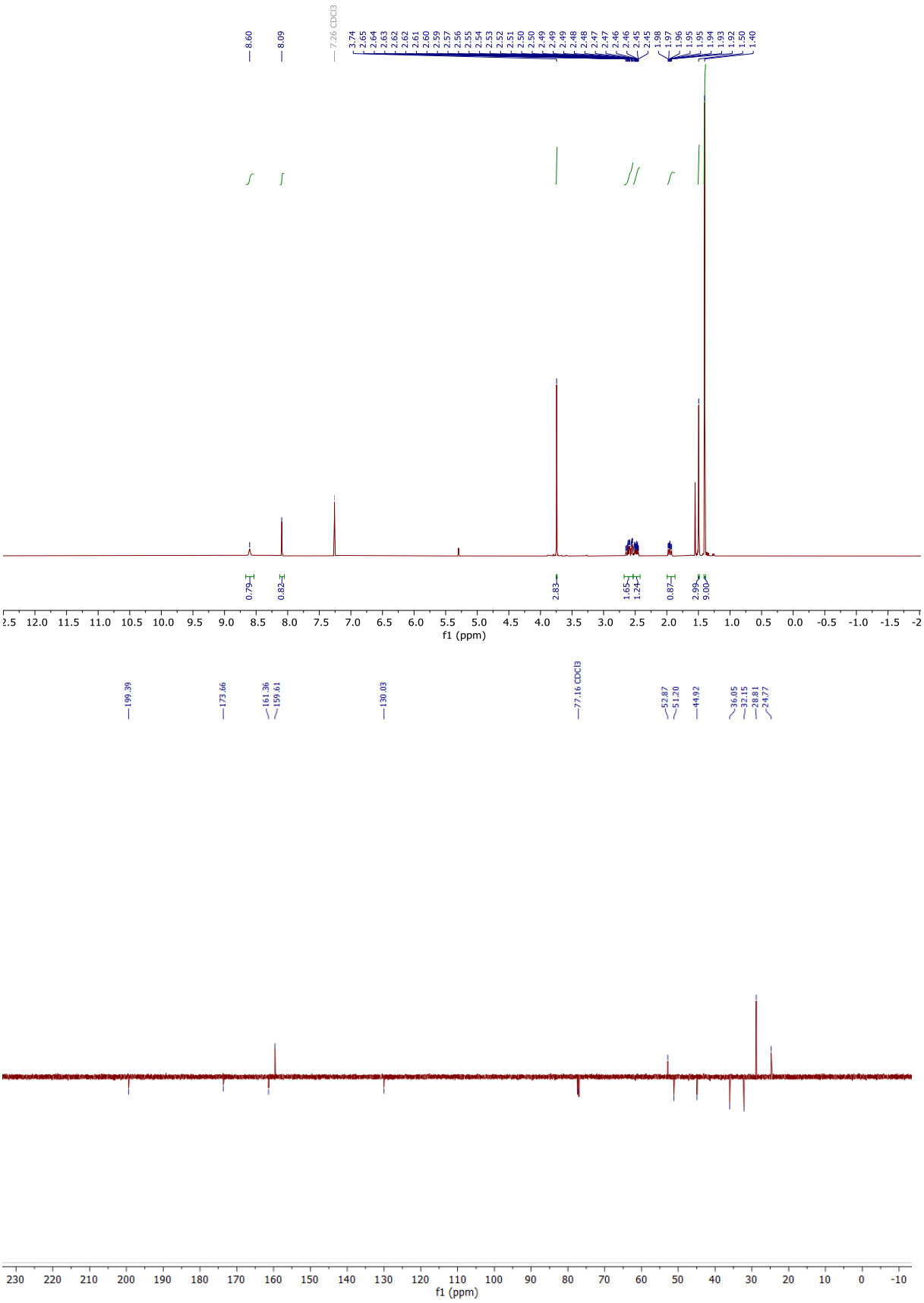

Supplementary Fig. 46. The ^{1}H-NMR (500 MHz) and APT-NMR (125 MHz) spectra of compound **18**/**18*R*** in $CDCl_3$

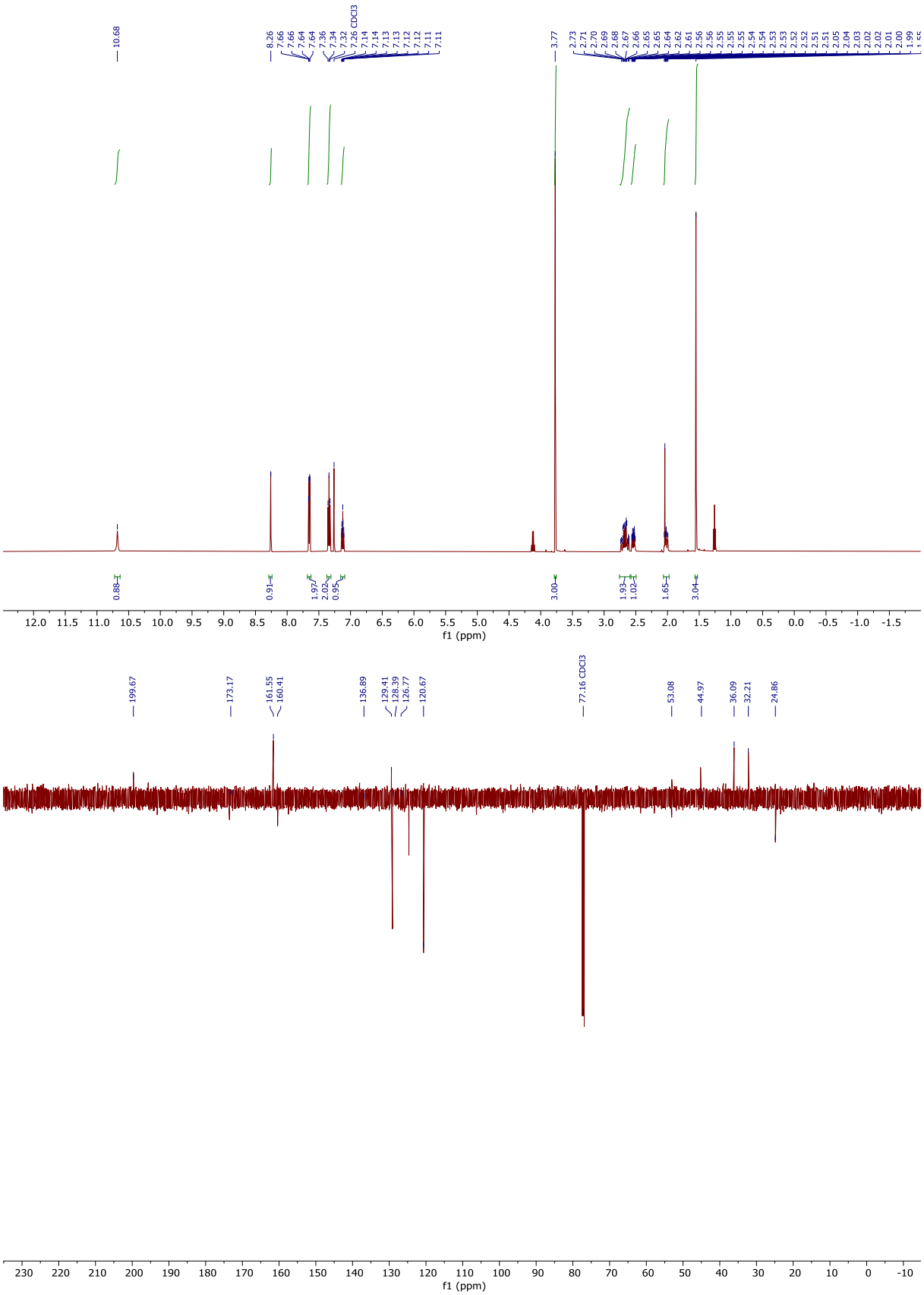

Supplementary Fig. 47. The ^{1}H-NMR (500 MHz) and APT-NMR (125 MHz) spectra of compound **19** in $CDCl_3$

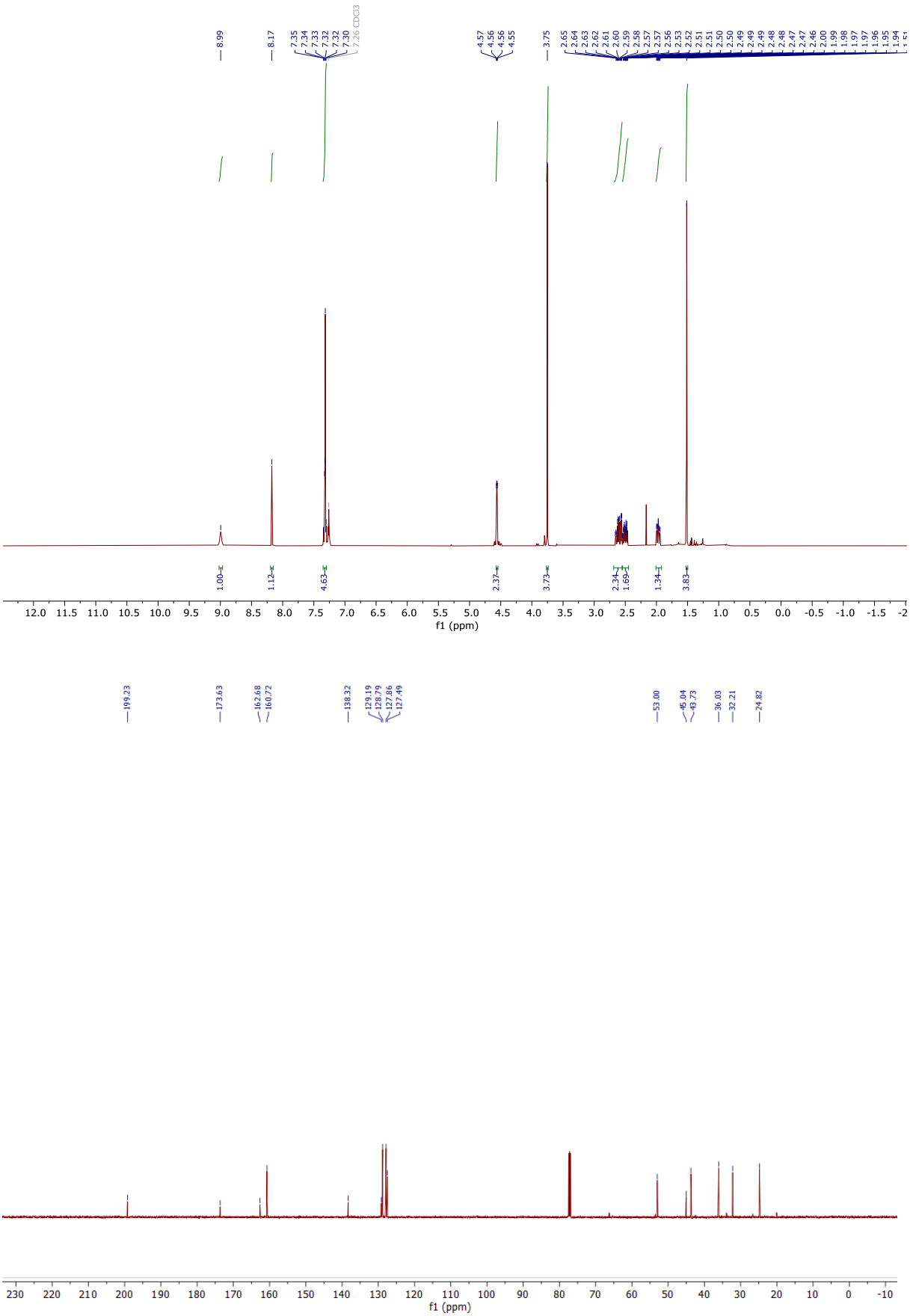

Supplementary Fig. 48. The ^{1}H-NMR (500 MHz) and ^{13}C-NMR (125 MHz) spectra of compound **20** in $CDCl_3$

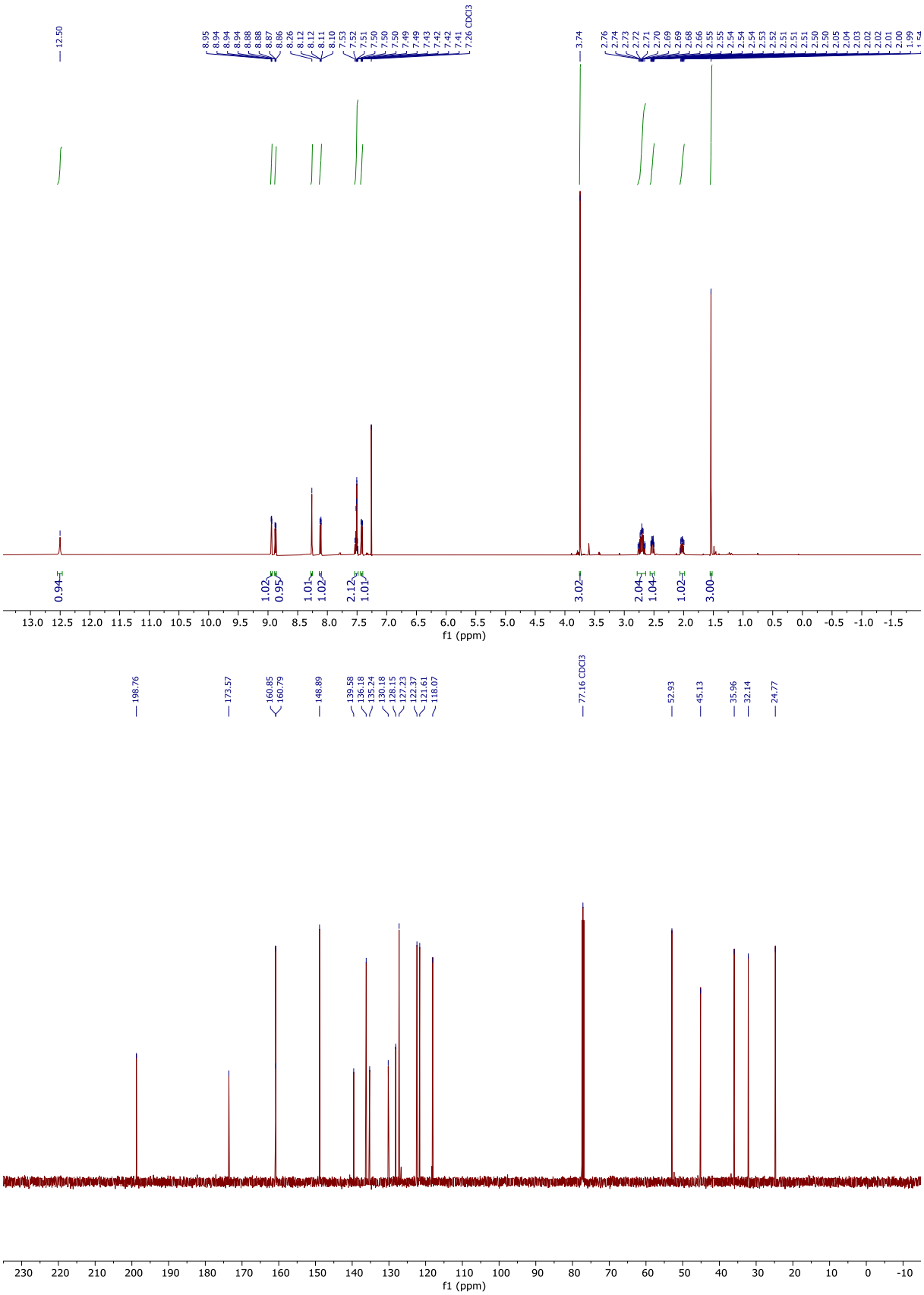

Supplementary Fig. 49. The ^{1}H-NMR (500 MHz) and ^{13}C-NMR (125 MHz) spectra of compound **21** in $CDCl_3$

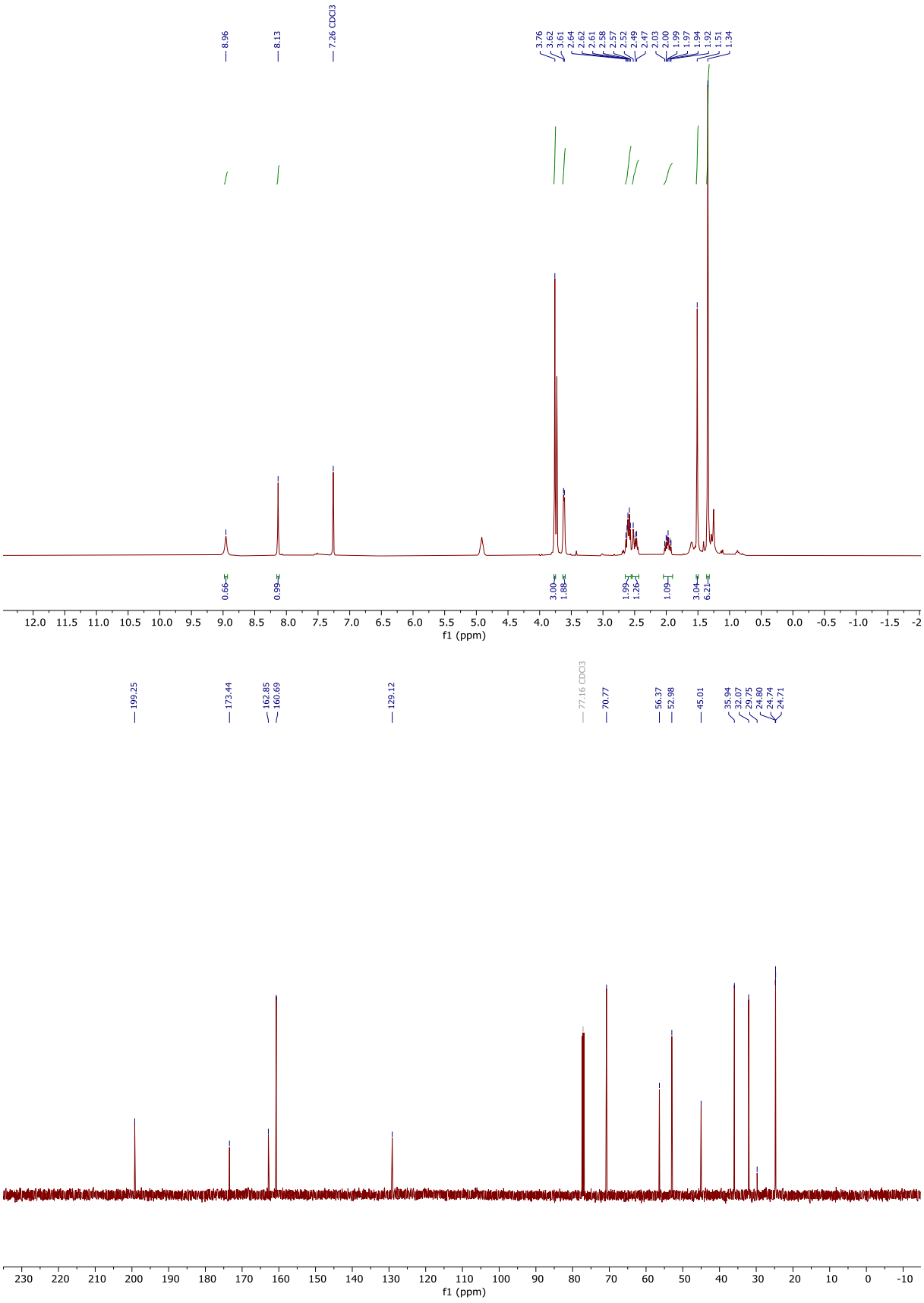

Supplementary Fig. 50. The ^{1}H-NMR (300 MHz) and ^{13}C-NMR (75 MHz) spectra of compound **22** in $CDCl_3$

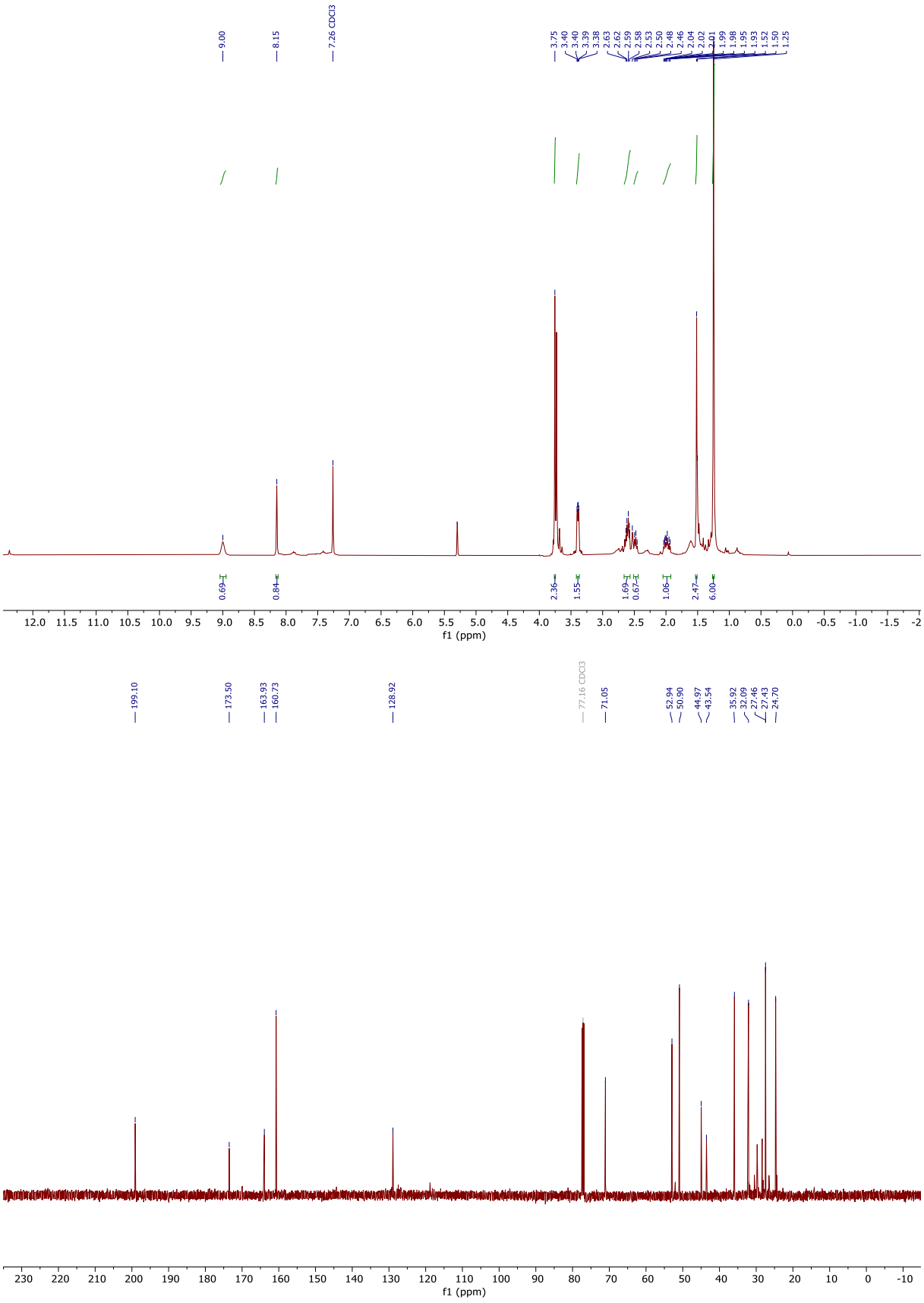

Supplementary Fig. 51. The ^{1}H-NMR (300 MHz) and ^{13}C-NMR (75 MHz) spectra of compound **23** in $CDCl_3$

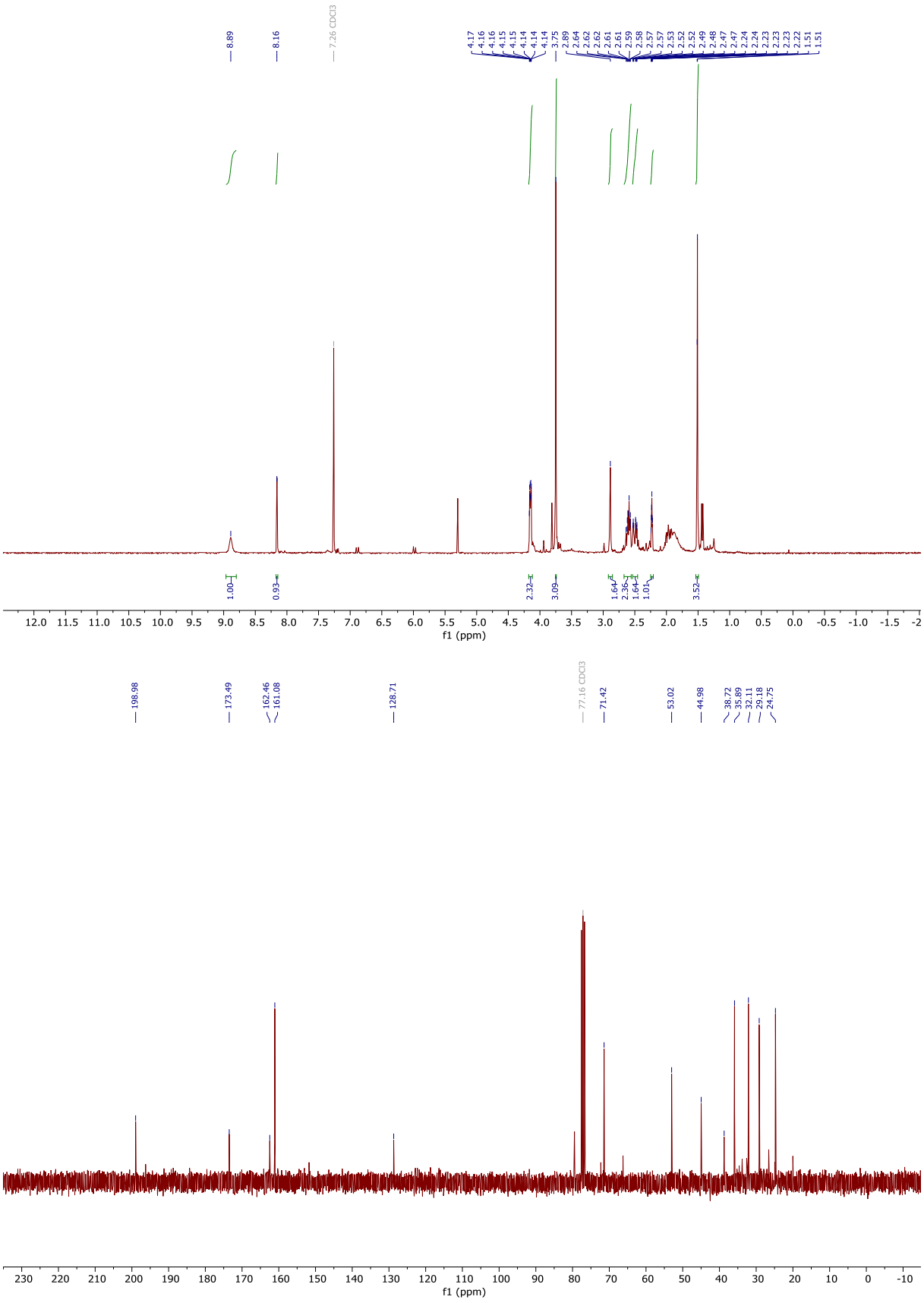

Supplementary Fig. 52. The ^{1}H-NMR (500 MHz) and ^{13}C-NMR (125 MHz) spectra of compound **S8** in $CDCl_3$

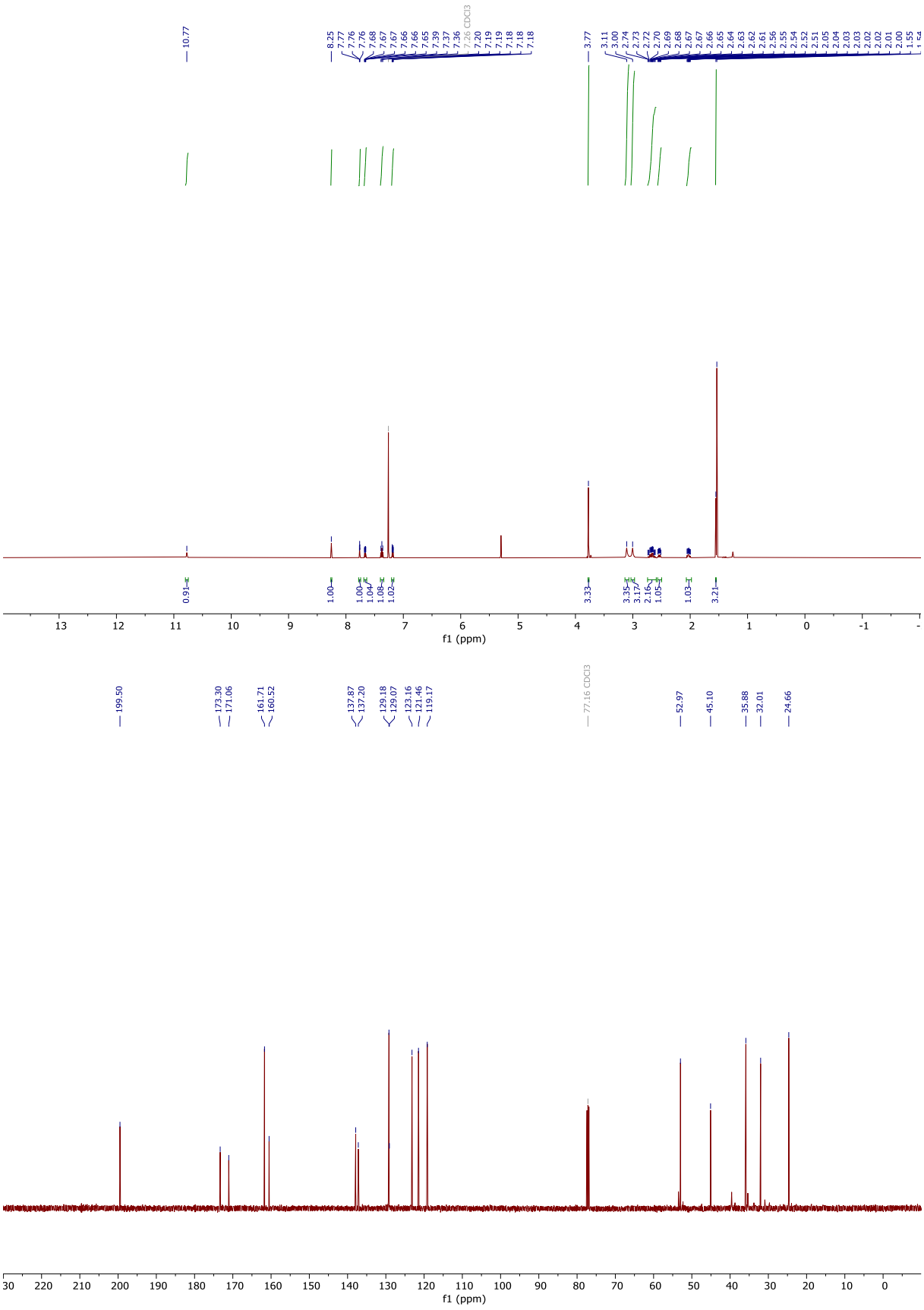

Supplementary Fig. 53. The ^{1}H-NMR (500 MHz) and ^{13}C-NMR (125 MHz) spectra of compound **19'*S*** in $CDCl_3$

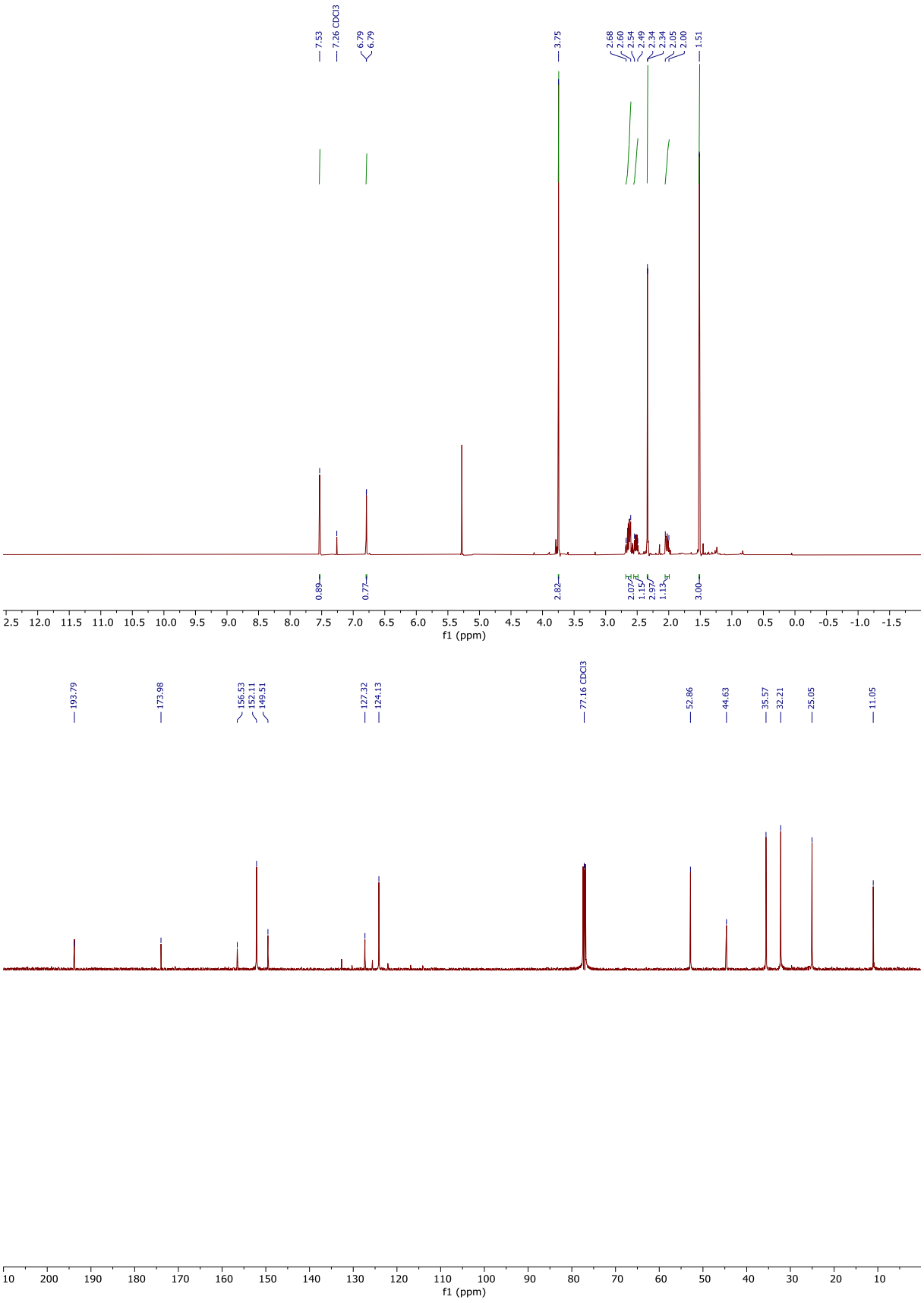

Supplementary Fig. 54. The ^{1}H-NMR (500 MHz) and ^{13}C-NMR (125 MHz) spectra of compound **24** in $CDCl_3$

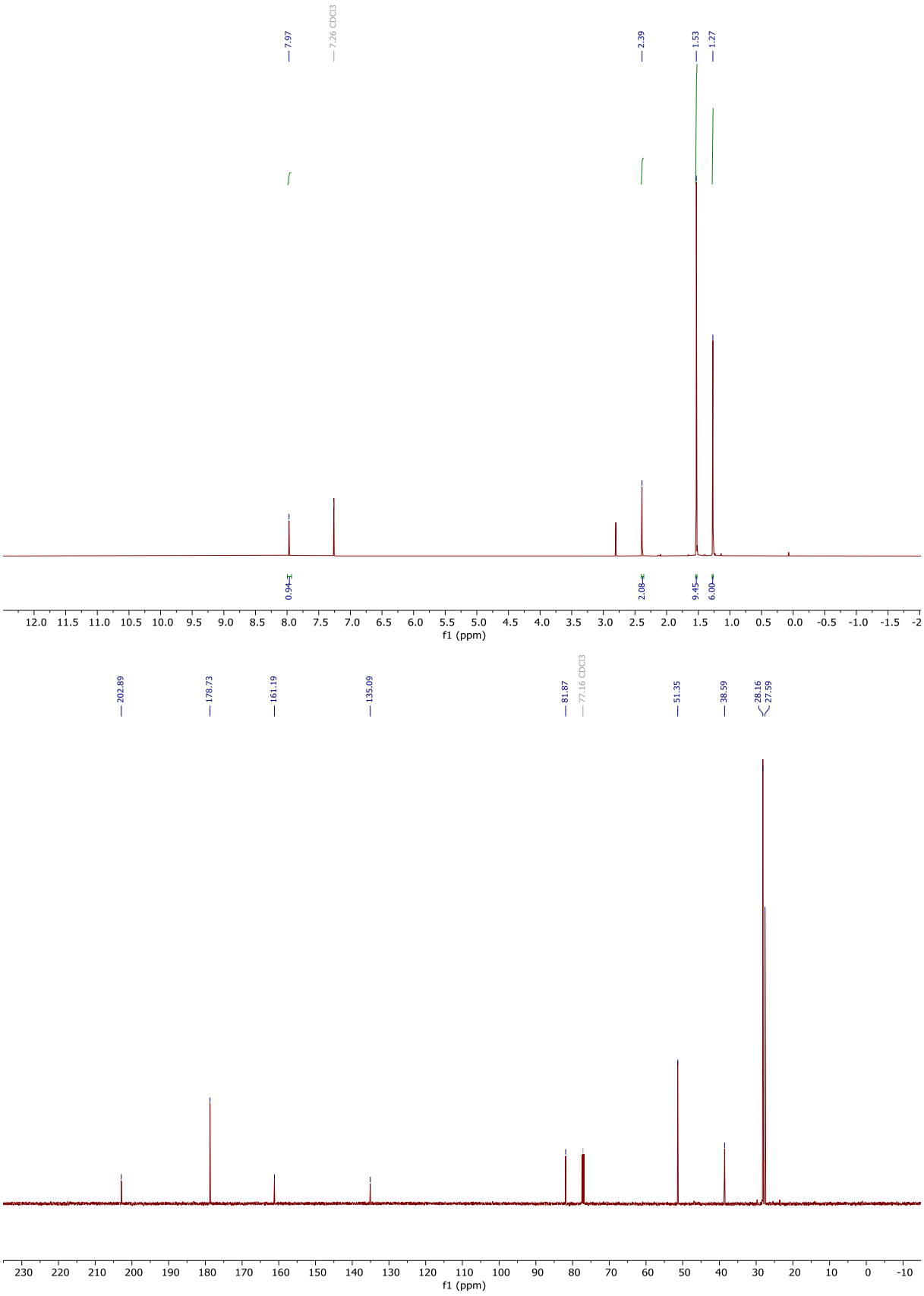

Supplementary Fig. 55. The ^{1}H-NMR (500 MHz) and ^{13}C-NMR (125 MHz) spectra of compound **26** in $CDCl_3$

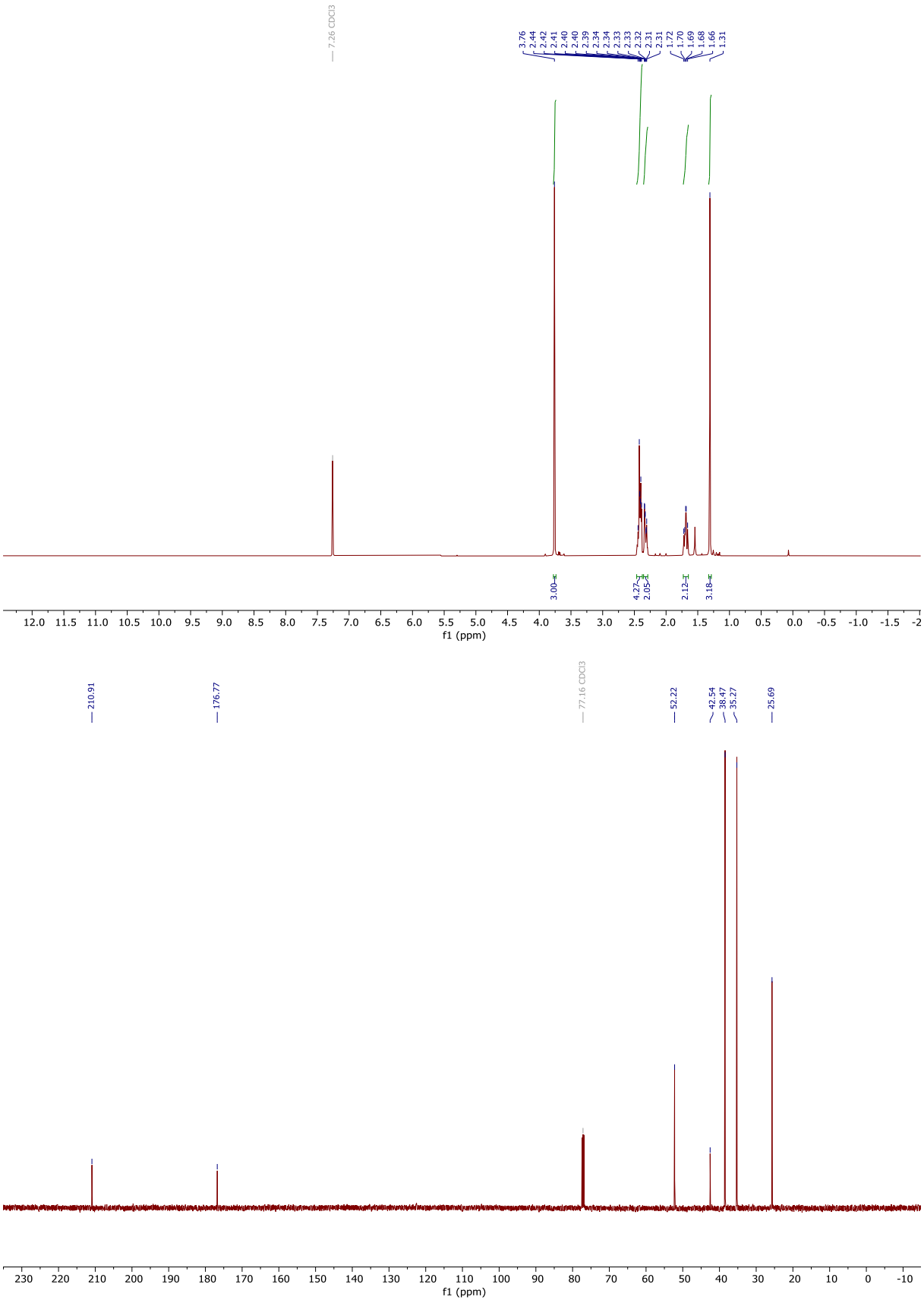

Supplementary Fig. 56. The ^{1}H-NMR (500 MHz) and ^{13}C-NMR (125 MHz) spectra of compound **S10** in $CDCl_3$

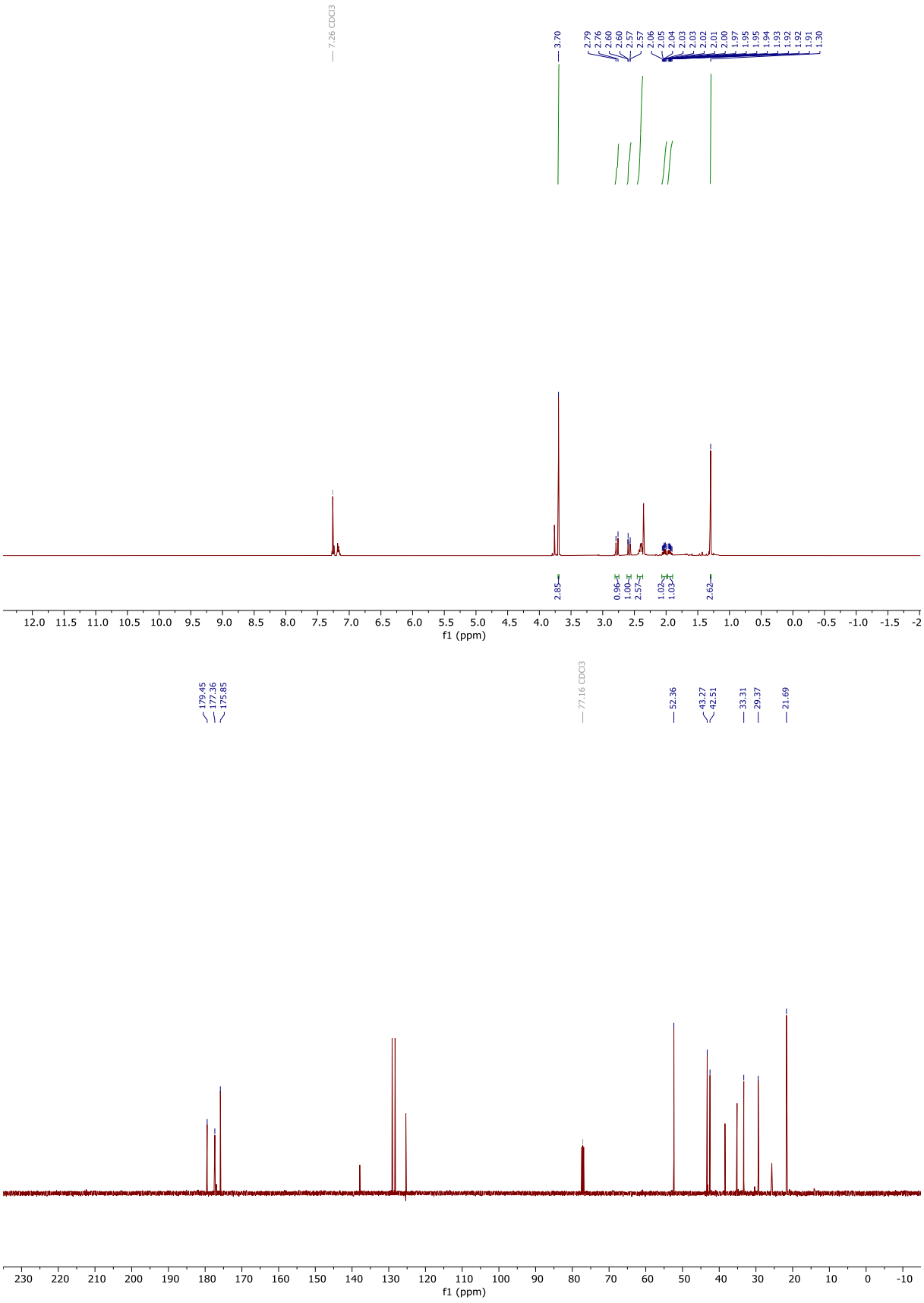

Supplementary Fig. 57. The ^{1}H-NMR (500 MHz) and ^{13}C-NMR (125 MHz) spectra of compound **S11** in $CDCl_3$

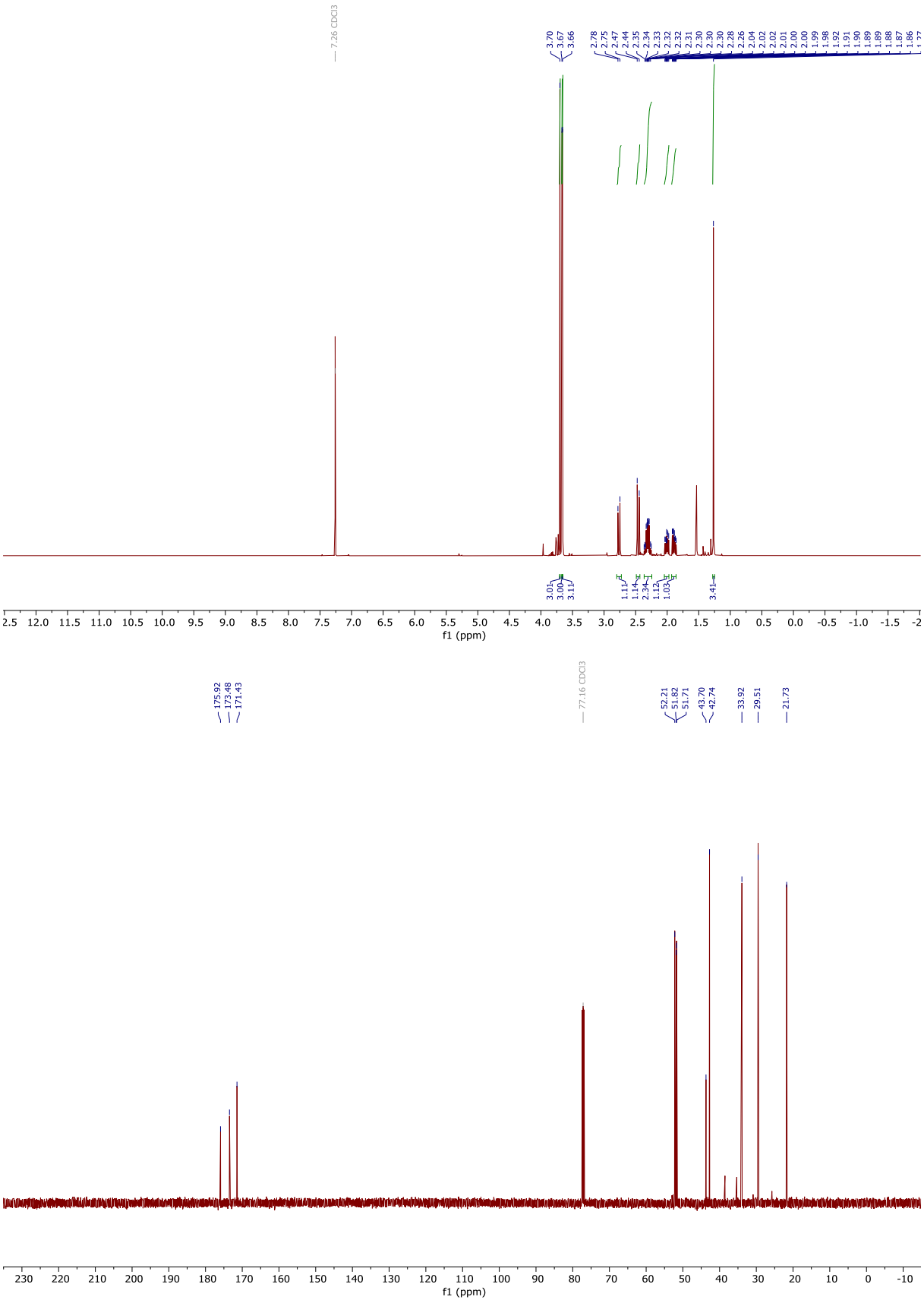

Supplementary Fig. 58. The ^{1}H-NMR (500 MHz) and ^{13}C-NMR (125 MHz) spectra of compound **S12** in $CDCl_3$

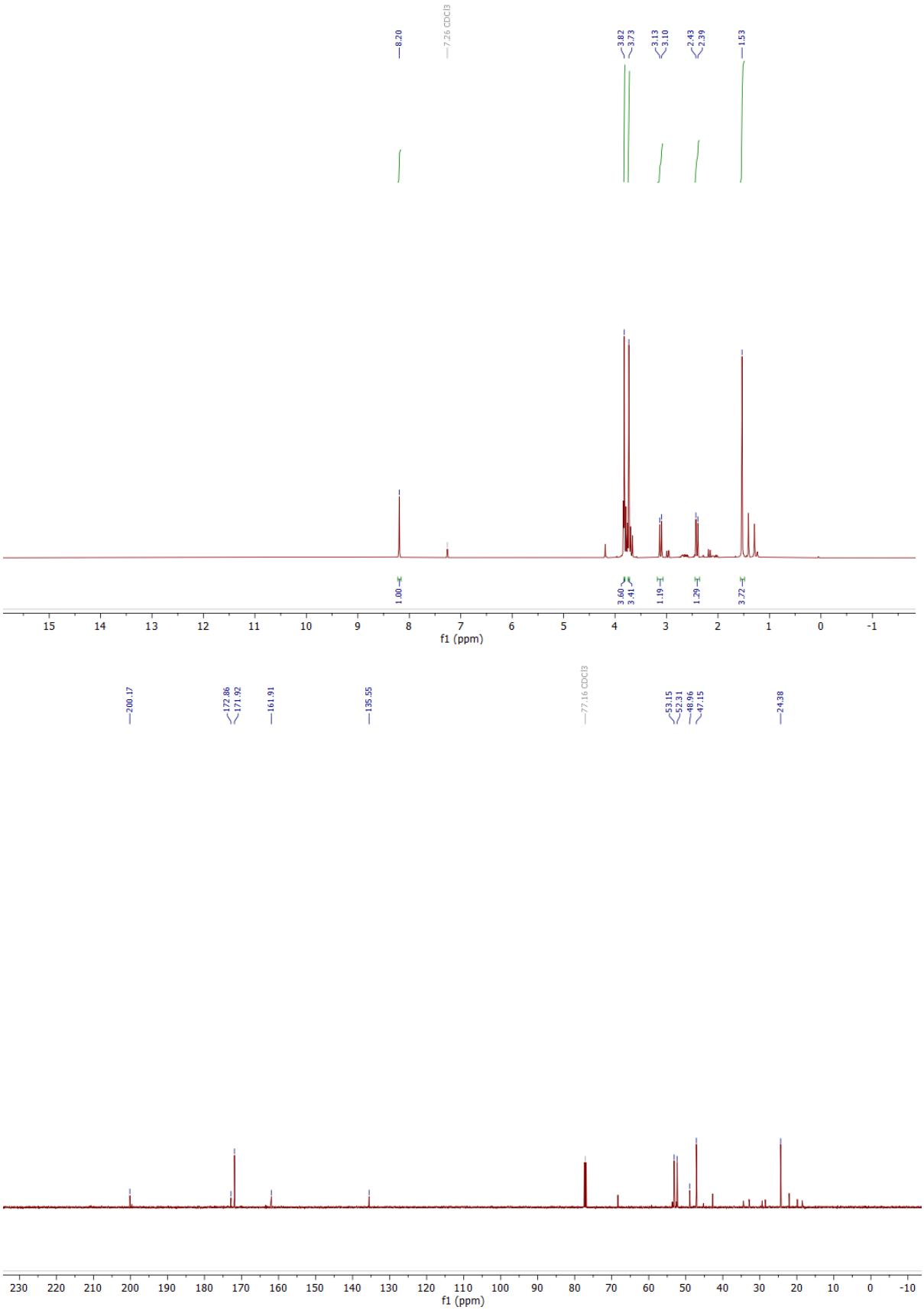

Supplementary Fig. 59. The ^{1}H-NMR (500 MHz) and ^{13}C-NMR (125 MHz) spectra of compound **S15** in $CDCl_3$

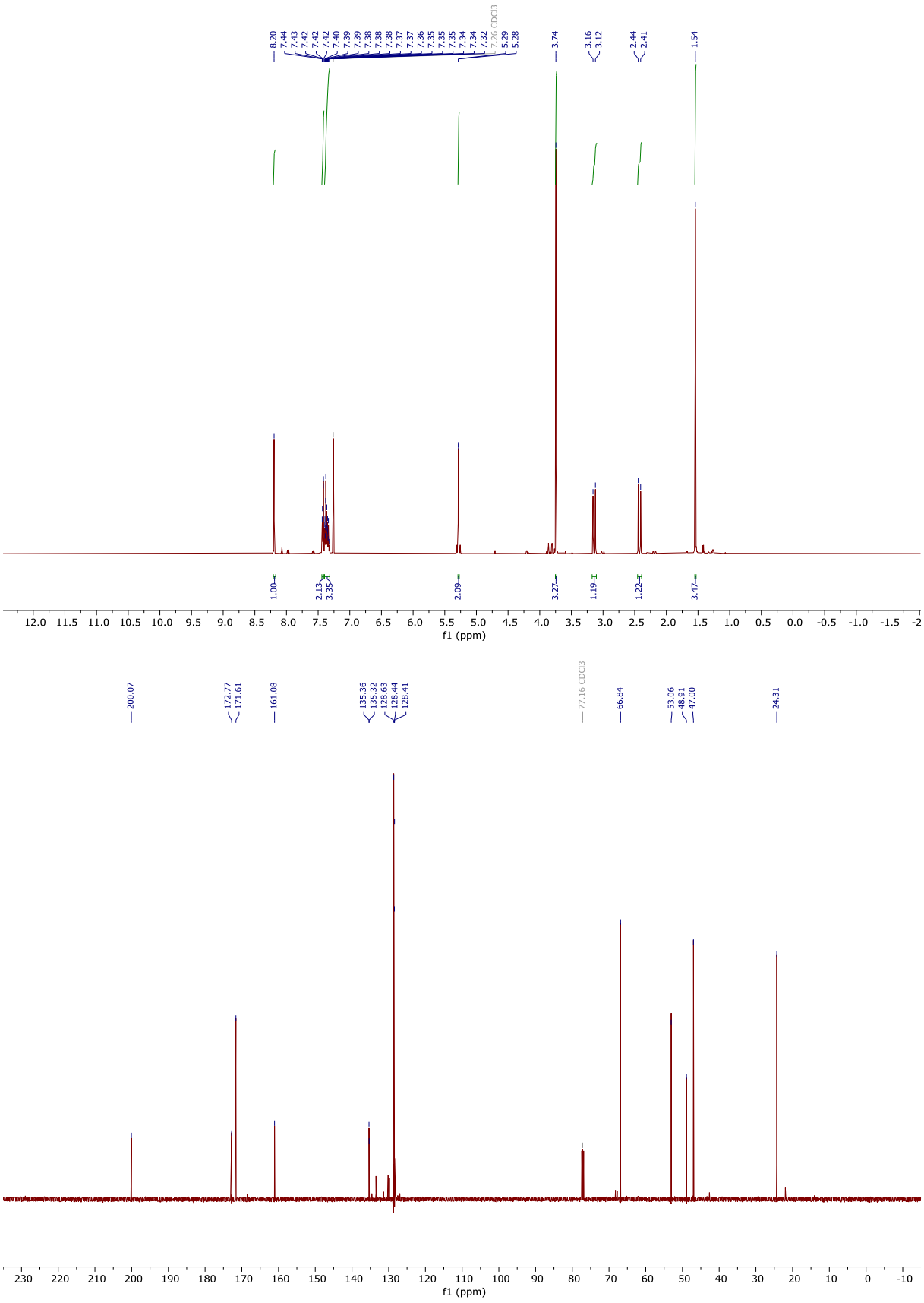

Supplementary Fig. 60. The ^{1}H-NMR (500 MHz) and ^{13}C-NMR (125 MHz) spectra of compound **27** in $CDCl_3$

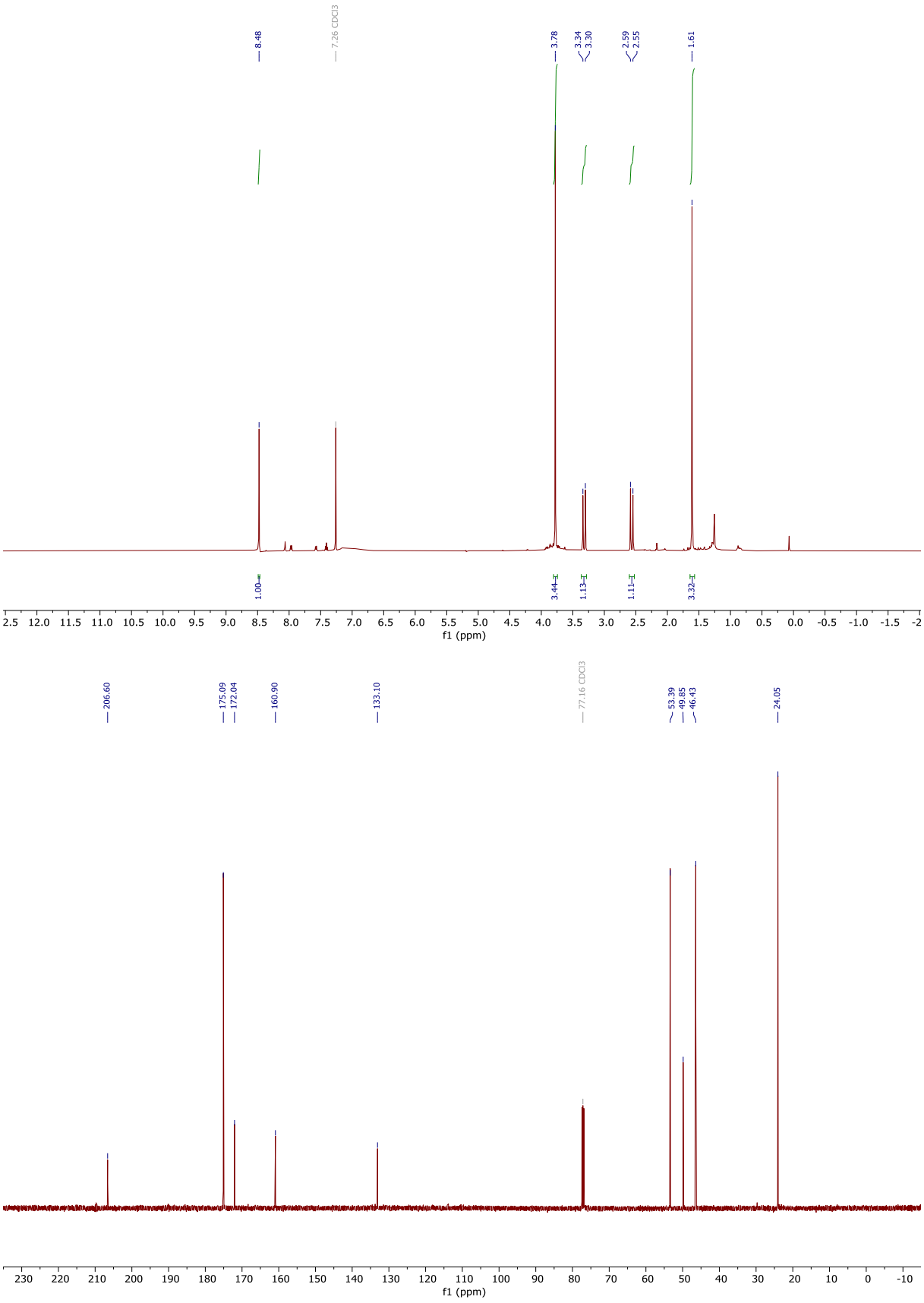

Supplementary Fig. 61. The ^{1}H-NMR (500 MHz) and ^{13}C-NMR (125 MHz) spectra of compound **S16** in $CDCl_3$

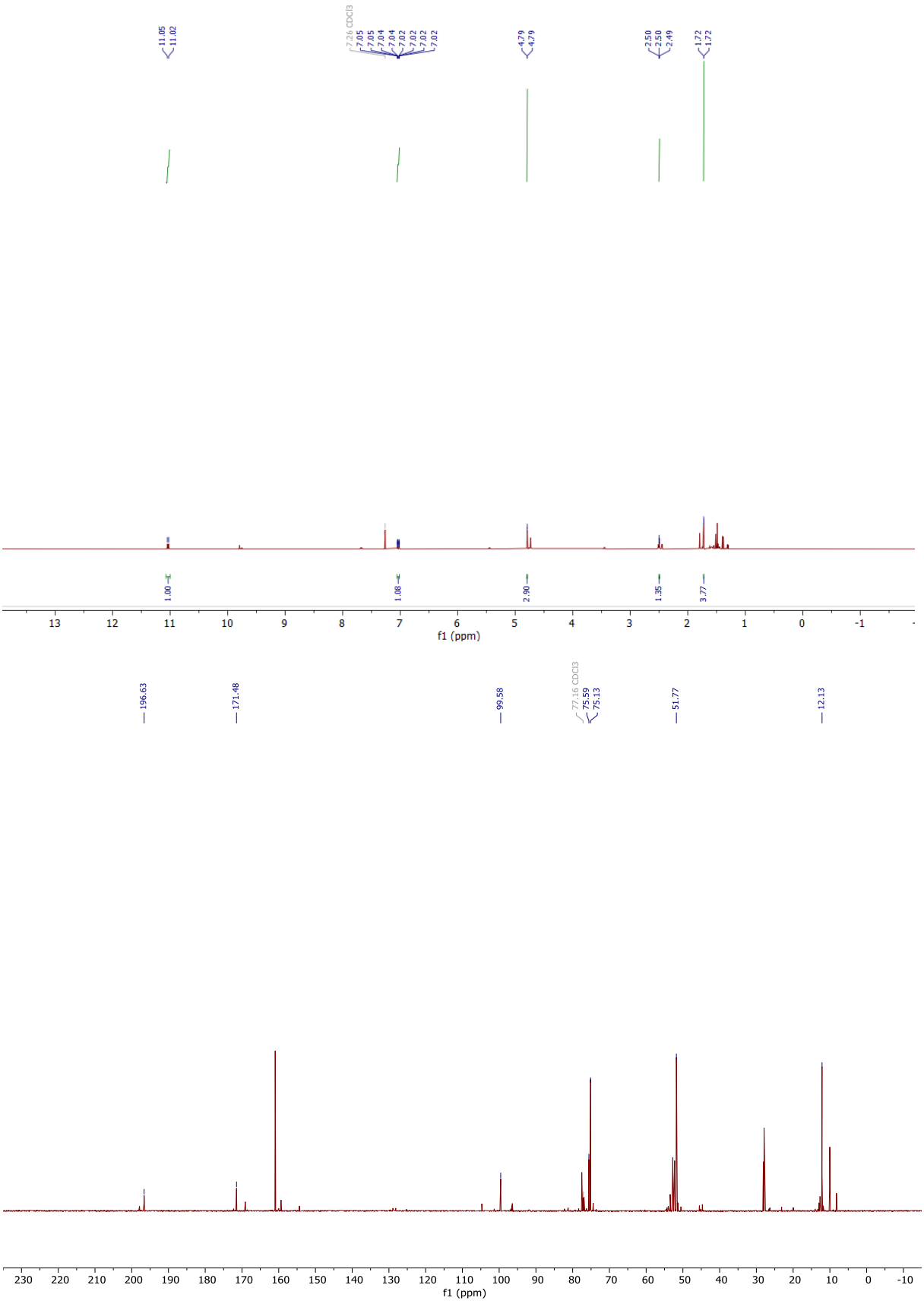

Supplementary Fig. 62. The ^{1}H-NMR (500 MHz) and ^{13}C-NMR (125 MHz) spectra of compound **S2l** in $CDCl_3$

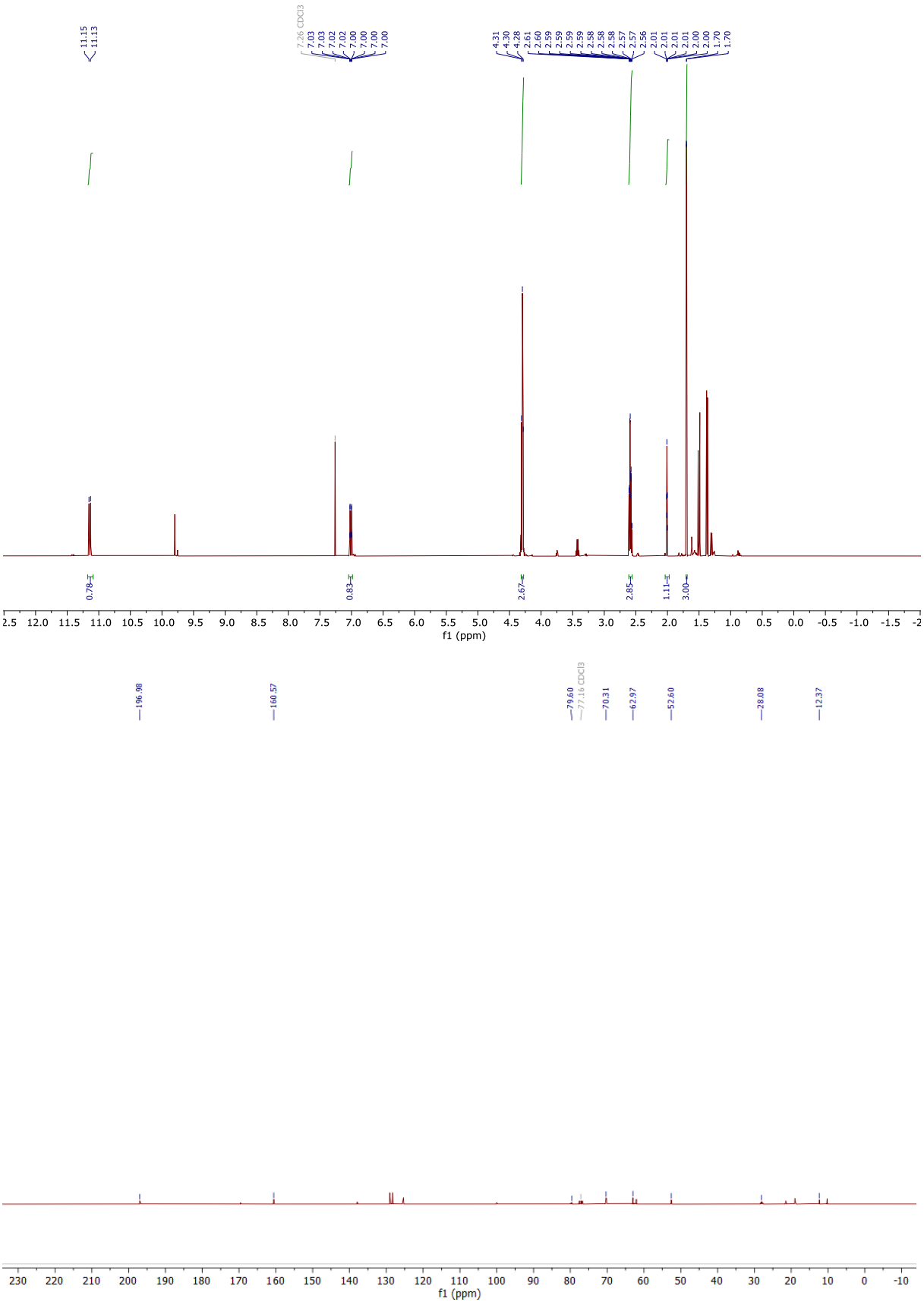

Supplementary Fig. 63. The ^{1}H-NMR (500 MHz) and ^{13}C-NMR (125 MHz) spectra of compound **S2m** in $CDCl_3$

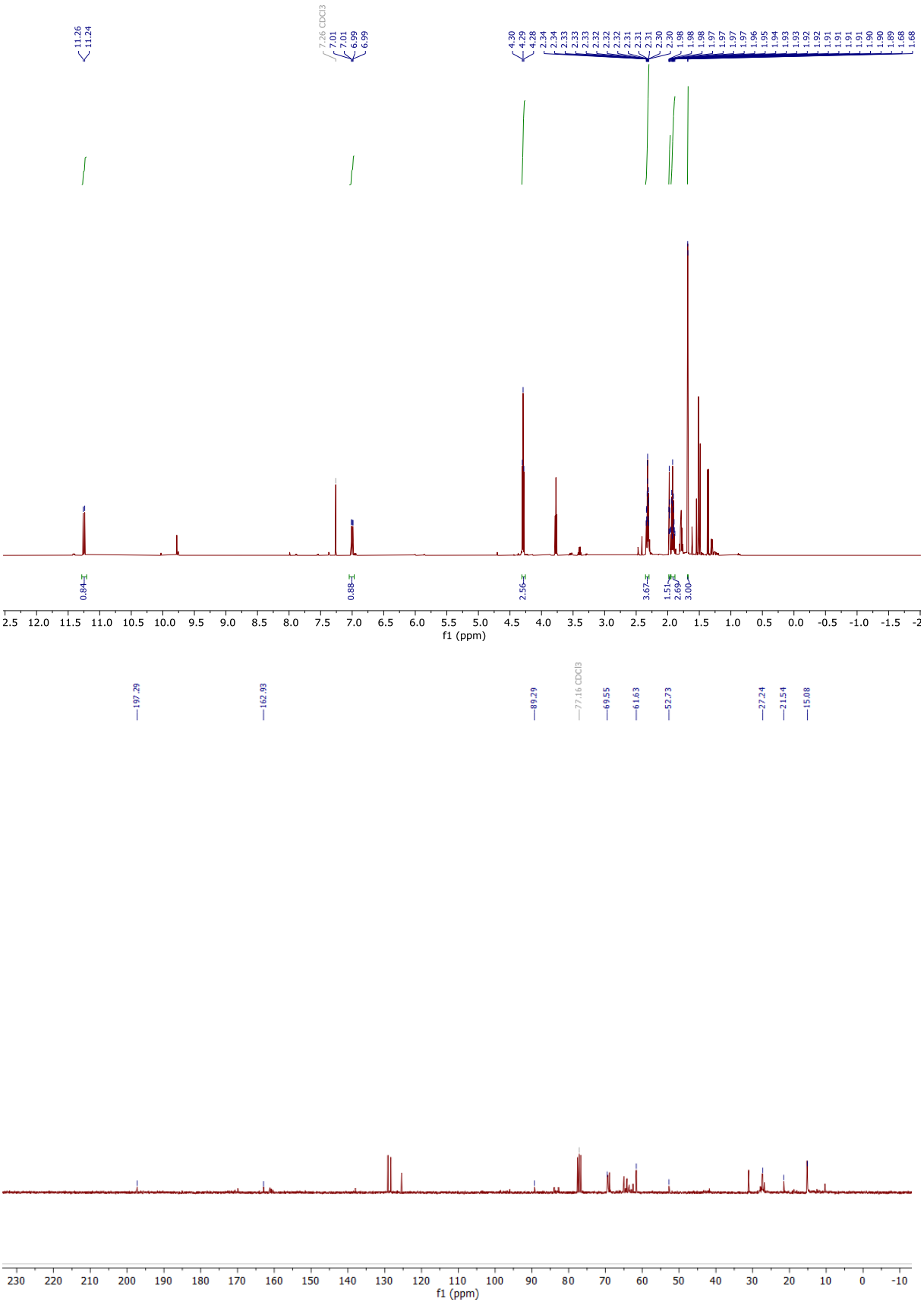

Supplementary Fig. 64. The ^{1}H-NMR (300 MHz) and ^{13}C-NMR (75 MHz) spectra of compound **S2n** in $CDCl_3$

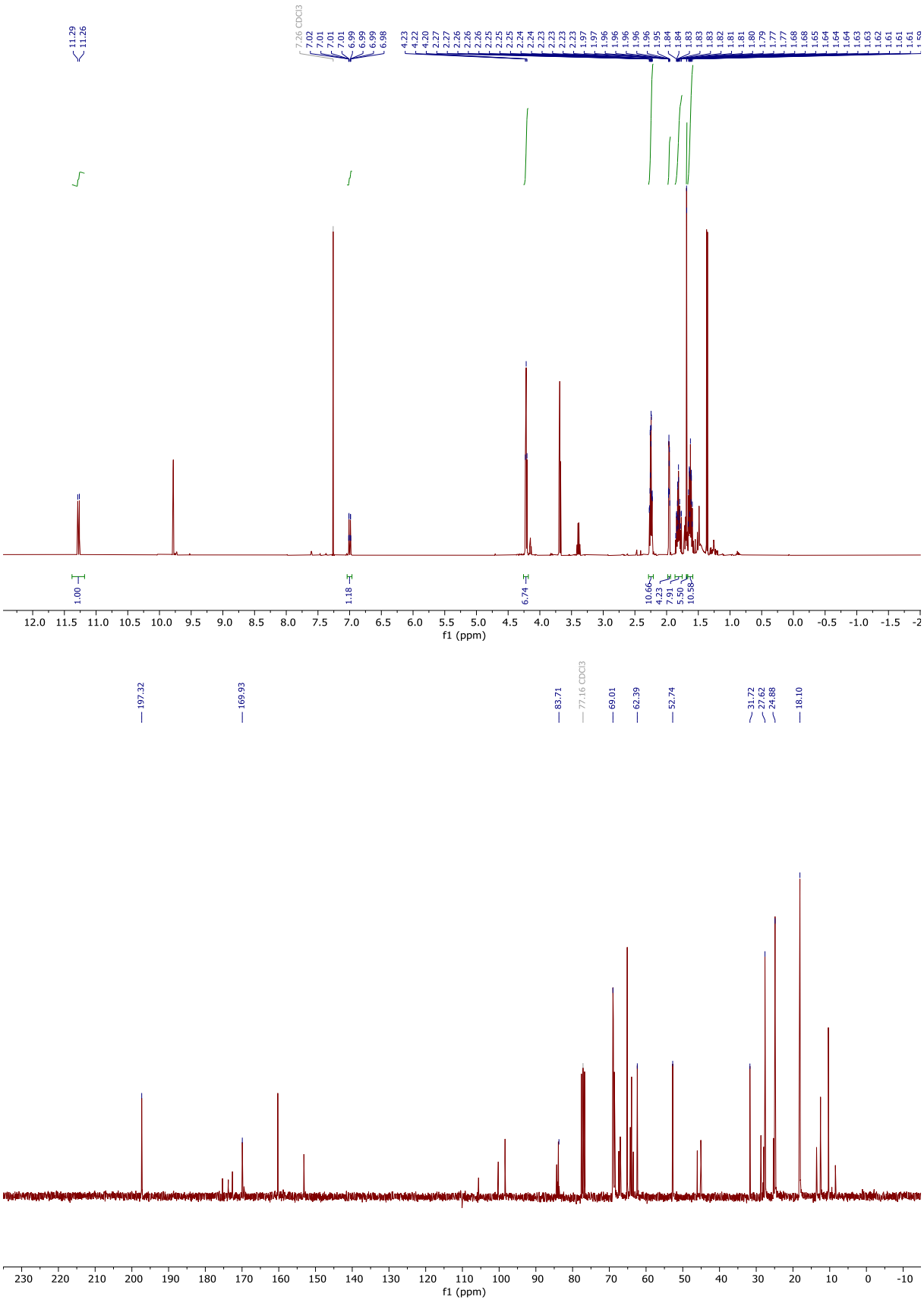

Supplementary Fig. 65. The ^{1}H-NMR (300 MHz) and ^{13}C-NMR (75 MHz) spectra of compound **S2o** in $CDCl_3$

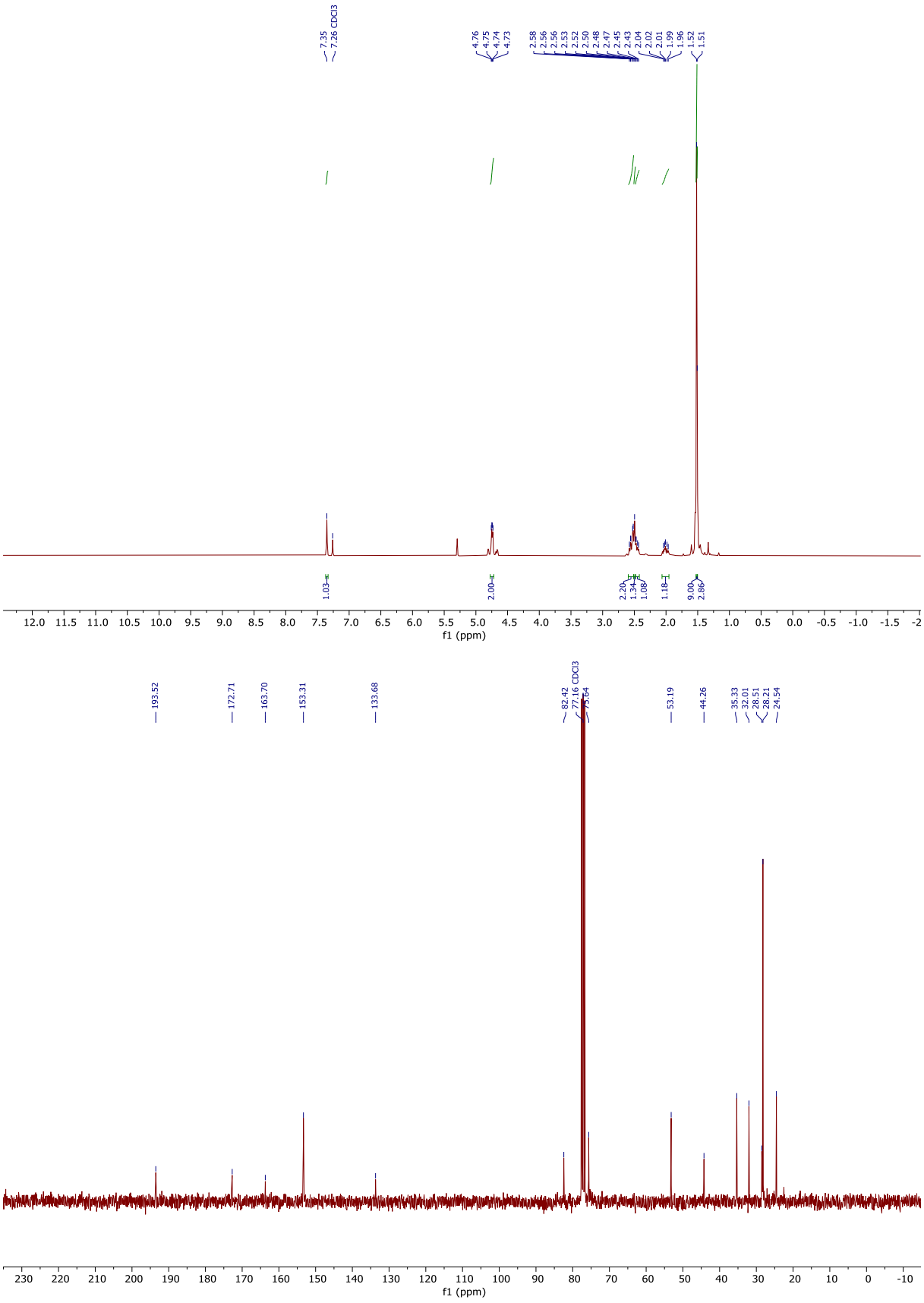

Supplementary Fig. 66. The ^{1}H-NMR (300 MHz) and ^{13}C-NMR (75 MHz) spectra of compound **28*R*/28*S*** in $CDCl_3$

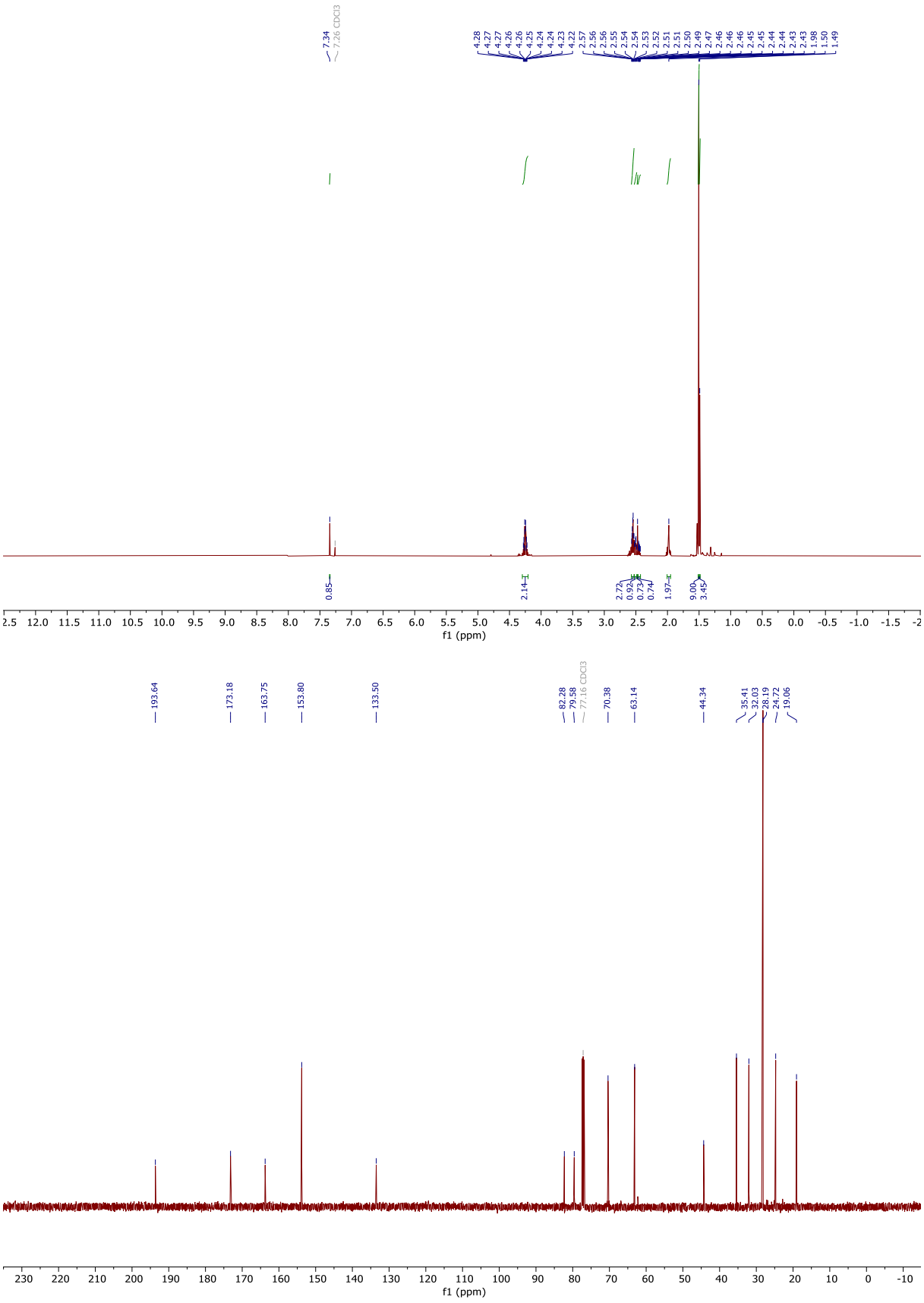

Supplementary Fig. 67. The ^{1}H-NMR (300 MHz) and ^{13}C-NMR (75 MHz) spectra of compound **29*S*** in $CDCl_3$

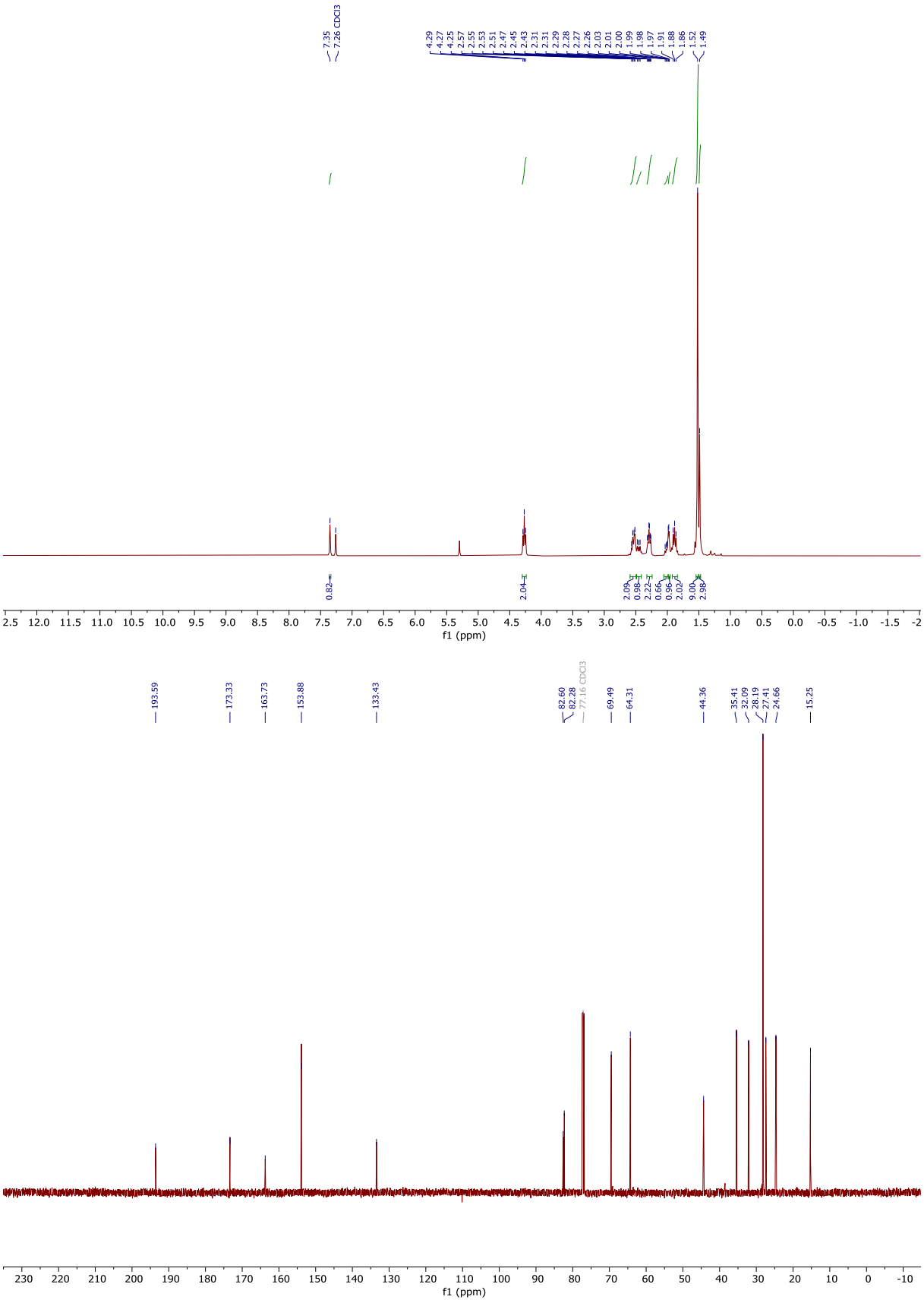

Supplementary Fig. 68. The ^{1}H-NMR (300 MHz) and ^{13}C-NMR (75 MHz) spectra of compound **30*S*** in $CDCl_3$

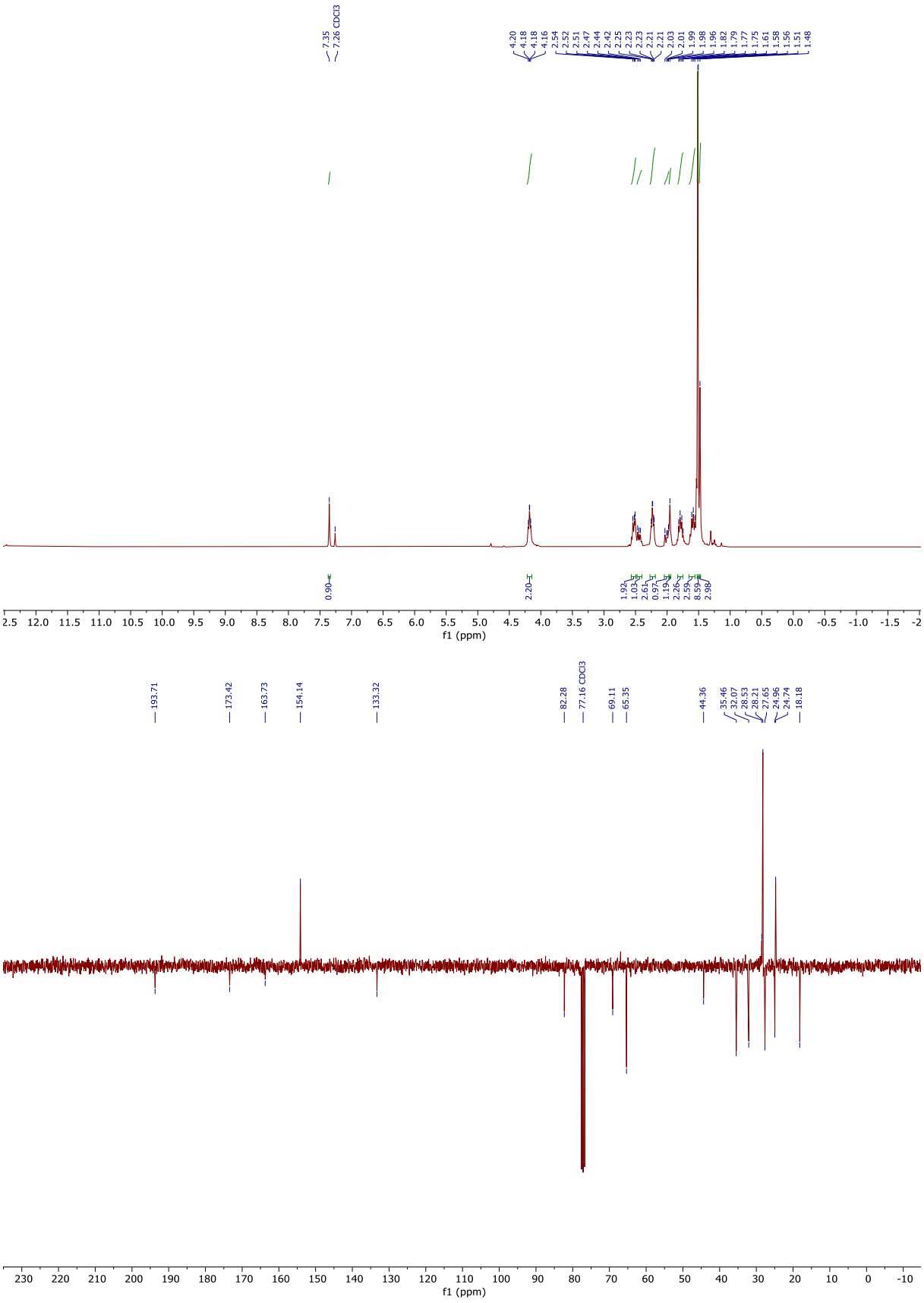

Supplementary Fig. 69. The ^{1}H-NMR (300 MHz) and APT-NMR (75 MHz) spectra of compound **31*S*** in $CDCl_3$

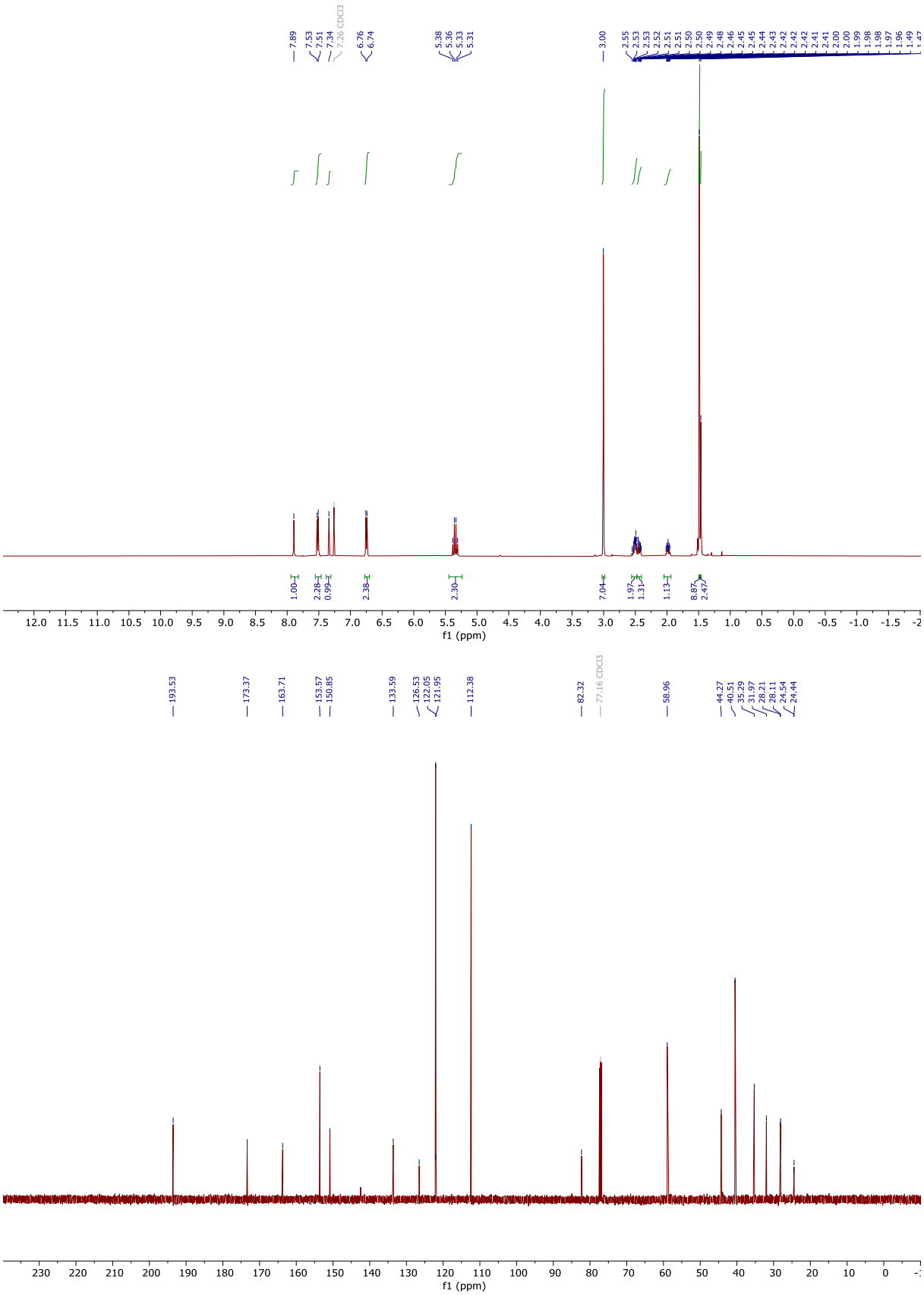

Supplementary Fig. 70. The ^{1}H-NMR (500 MHz) and ^{13}C-NMR (125 MHz) spectra of compound **32*R*/32*S*** in $CDCl_3$

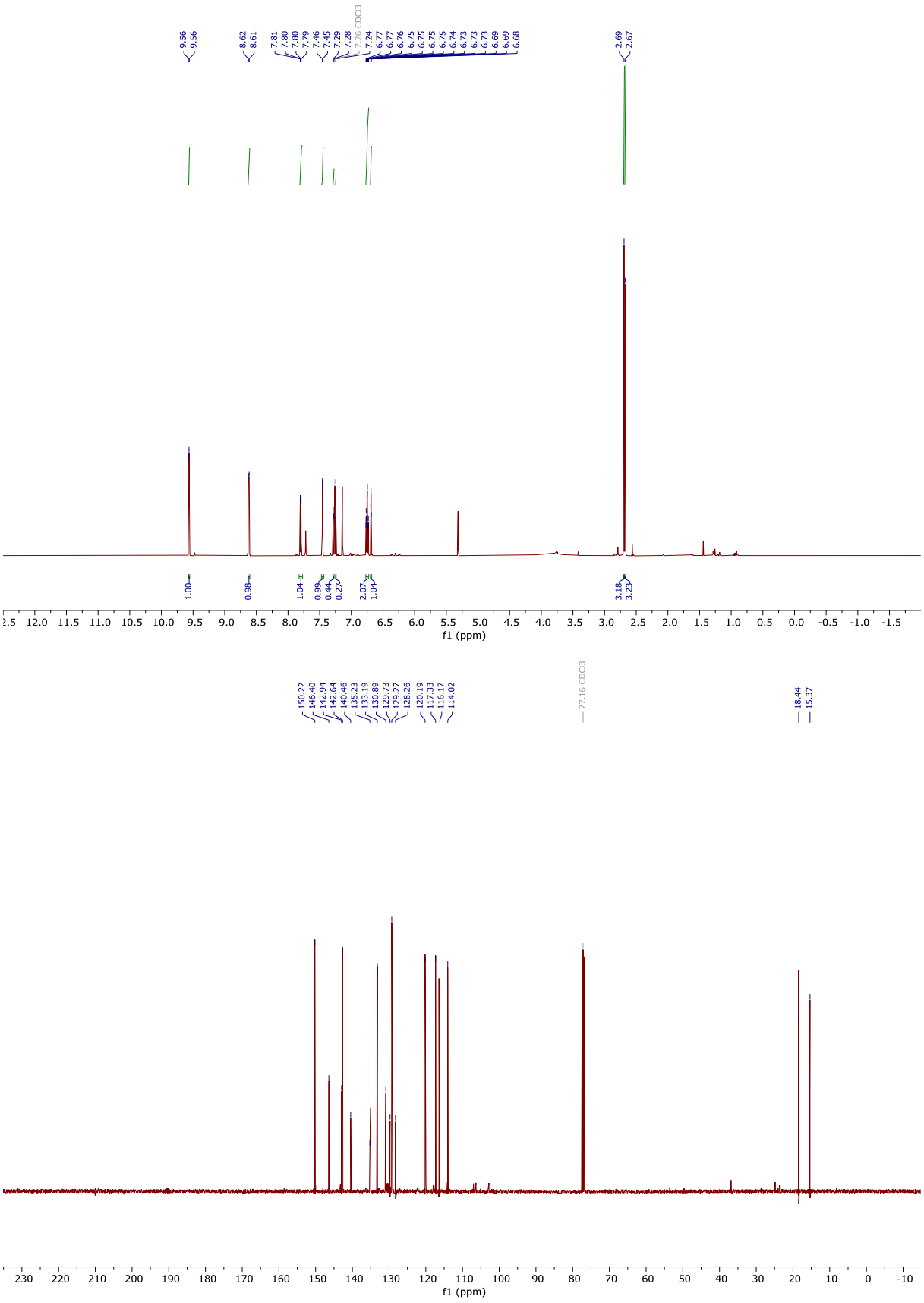

Supplementary Fig. 71. The ^{1}H-NMR (500 MHz) and ^{13}C-NMR (125 MHz) spectra of compound **S20** in $CDCl_3$

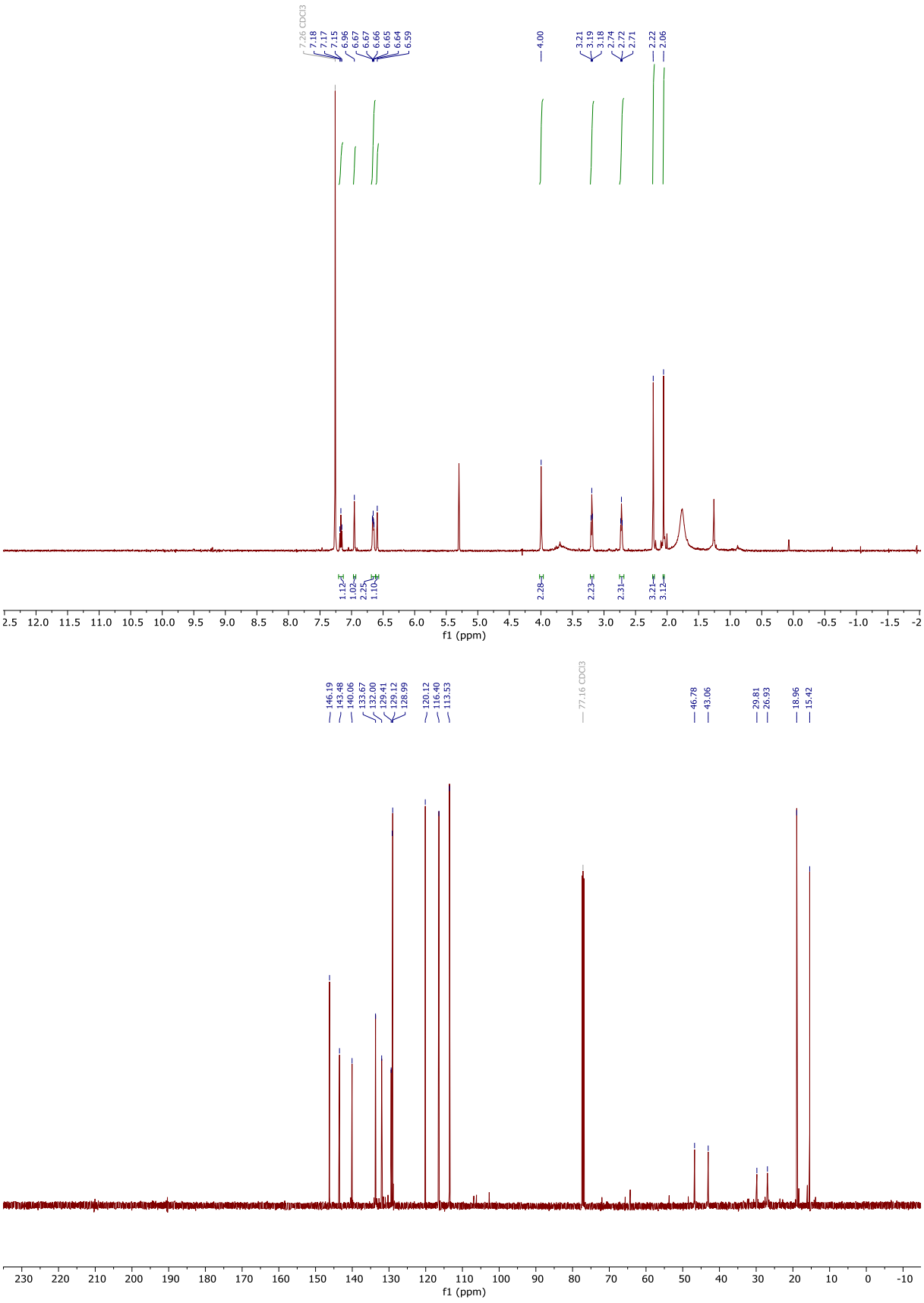

Supplementary Fig. 72. The ^{1}H-NMR (500 MHz) and ^{13}C-NMR (125 MHz) spectra of compound **S21** in $CDCl_3$

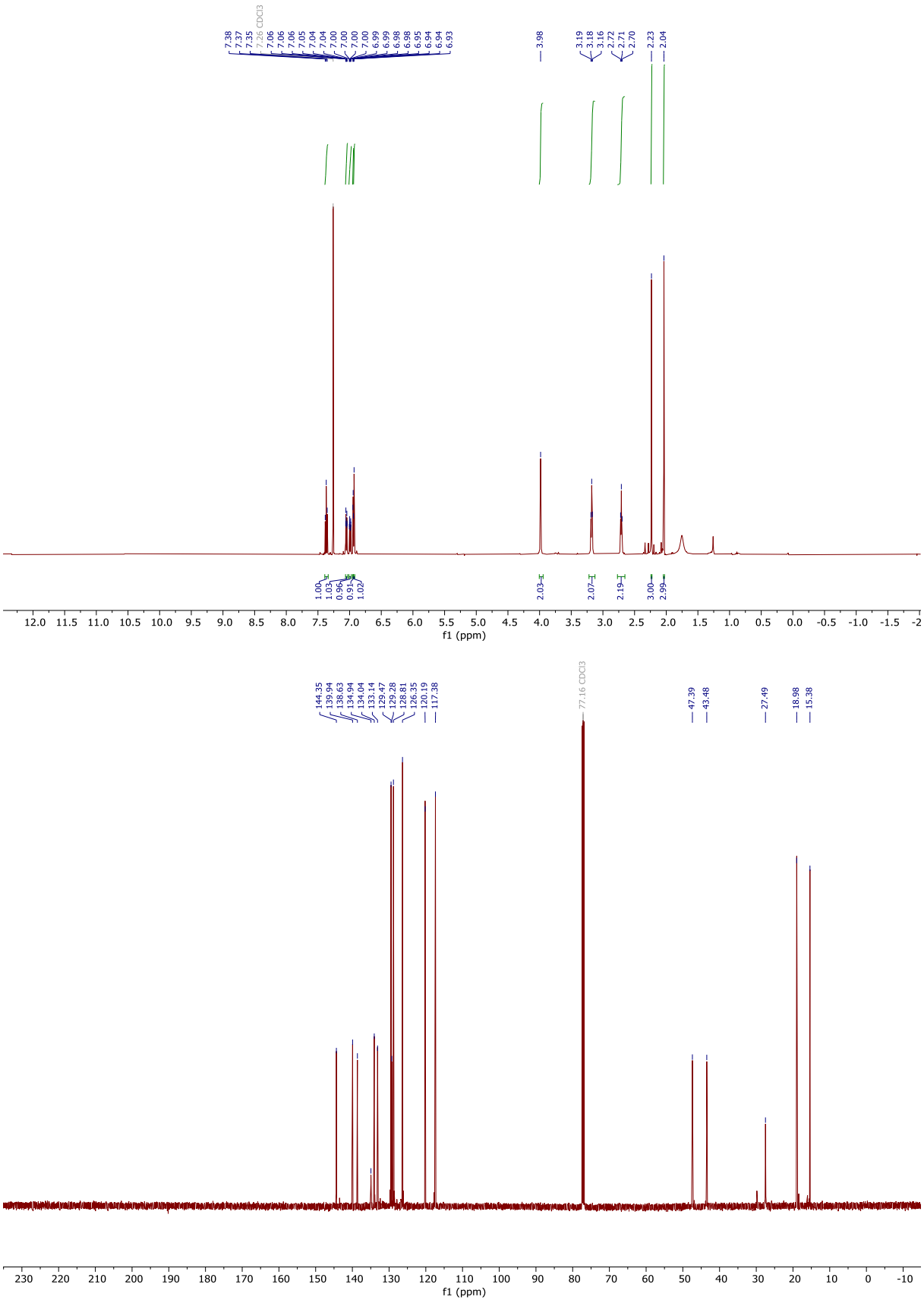

Supplementary Fig. 73. The ^{1}H-NMR (500 MHz) and ^{13}C-NMR (125 MHz) spectra of compound **S22** in $CDCl_3$

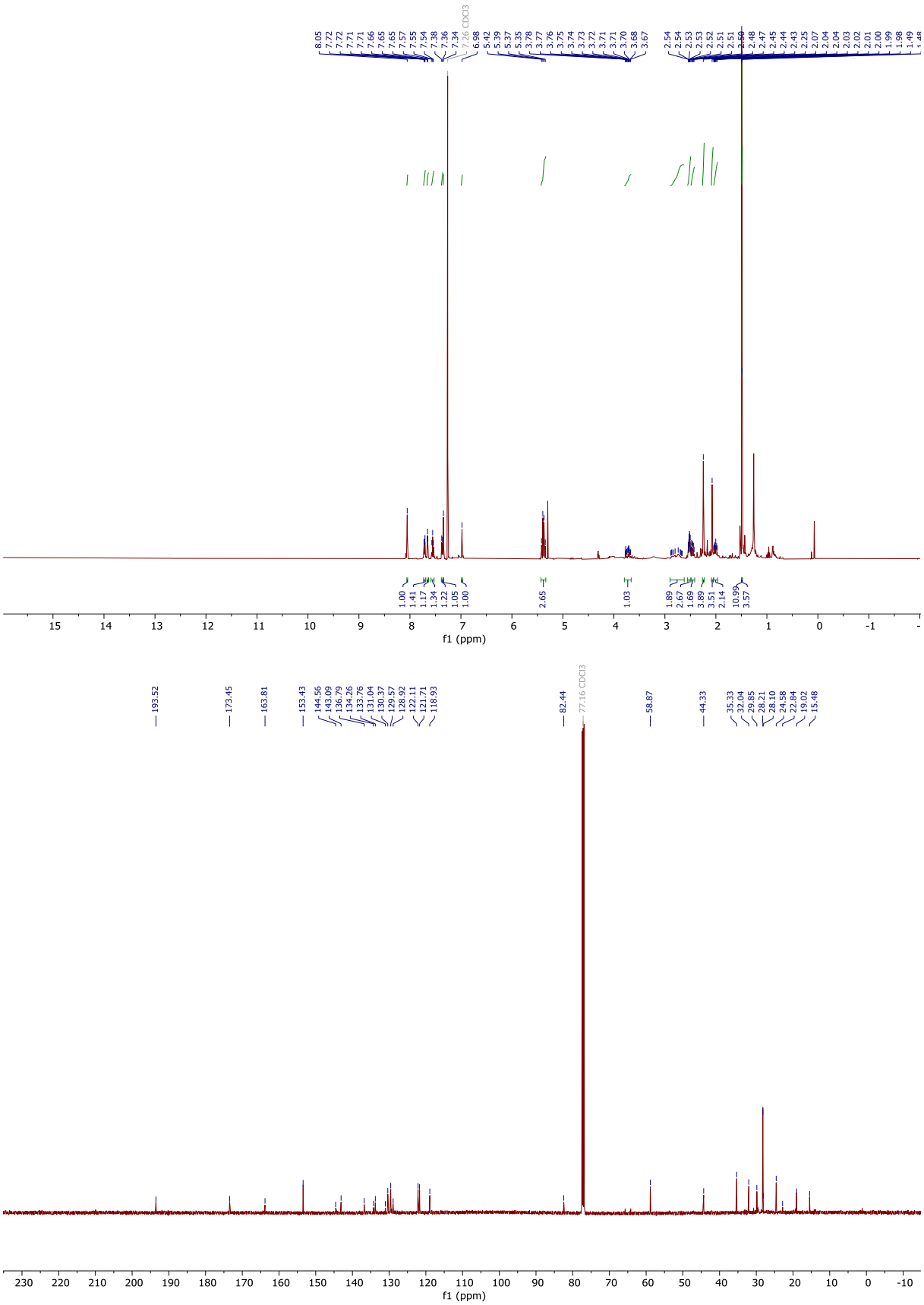

Supplementary Fig. 74. The ^{1}H-NMR (500 MHz) and ^{13}C-NMR (125 MHz) spectra of compound **33*S*** in $CDCl_3$

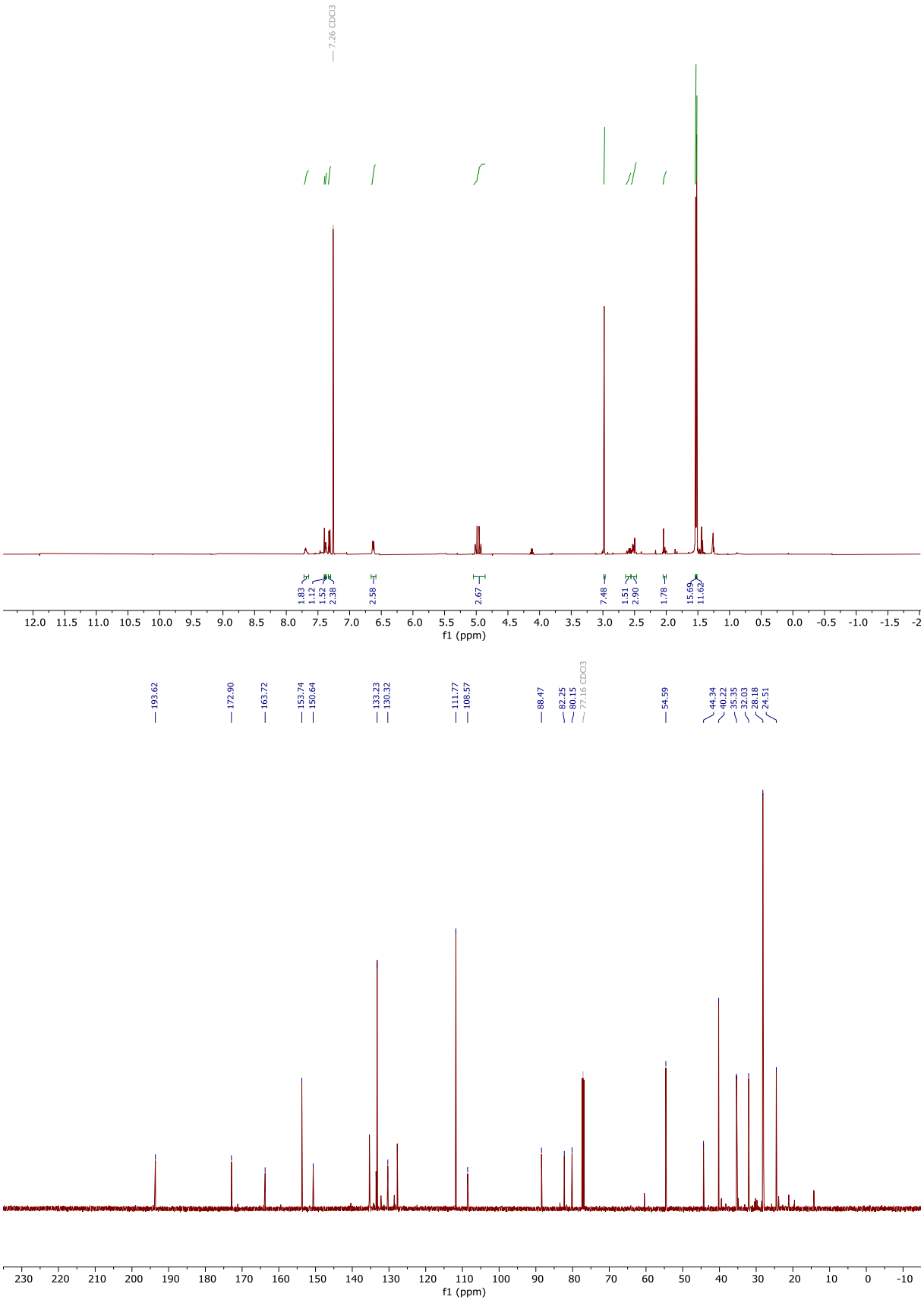

Supplementary Fig. 75. The ^{1}H-NMR (500 MHz) and ^{13}C-NMR (125 MHz) spectra of compound **34*R*/34*S*** in $CDCl_3$

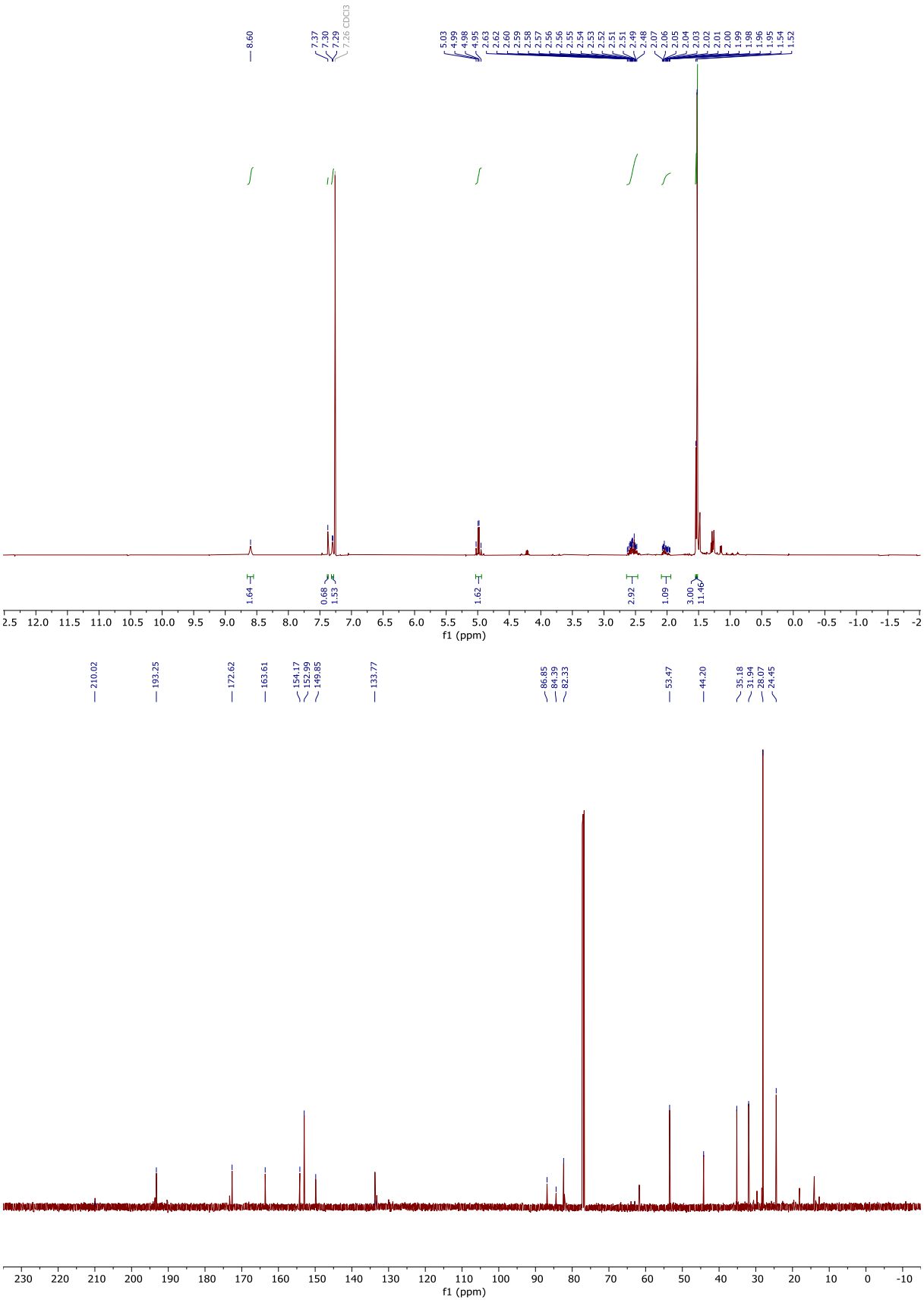

Supplementary Fig. 76. The ^{1}H-NMR (500 MHz) and ^{13}C-NMR (125 MHz) spectra of compound **35*R*/35*S*** in $CDCl_3$

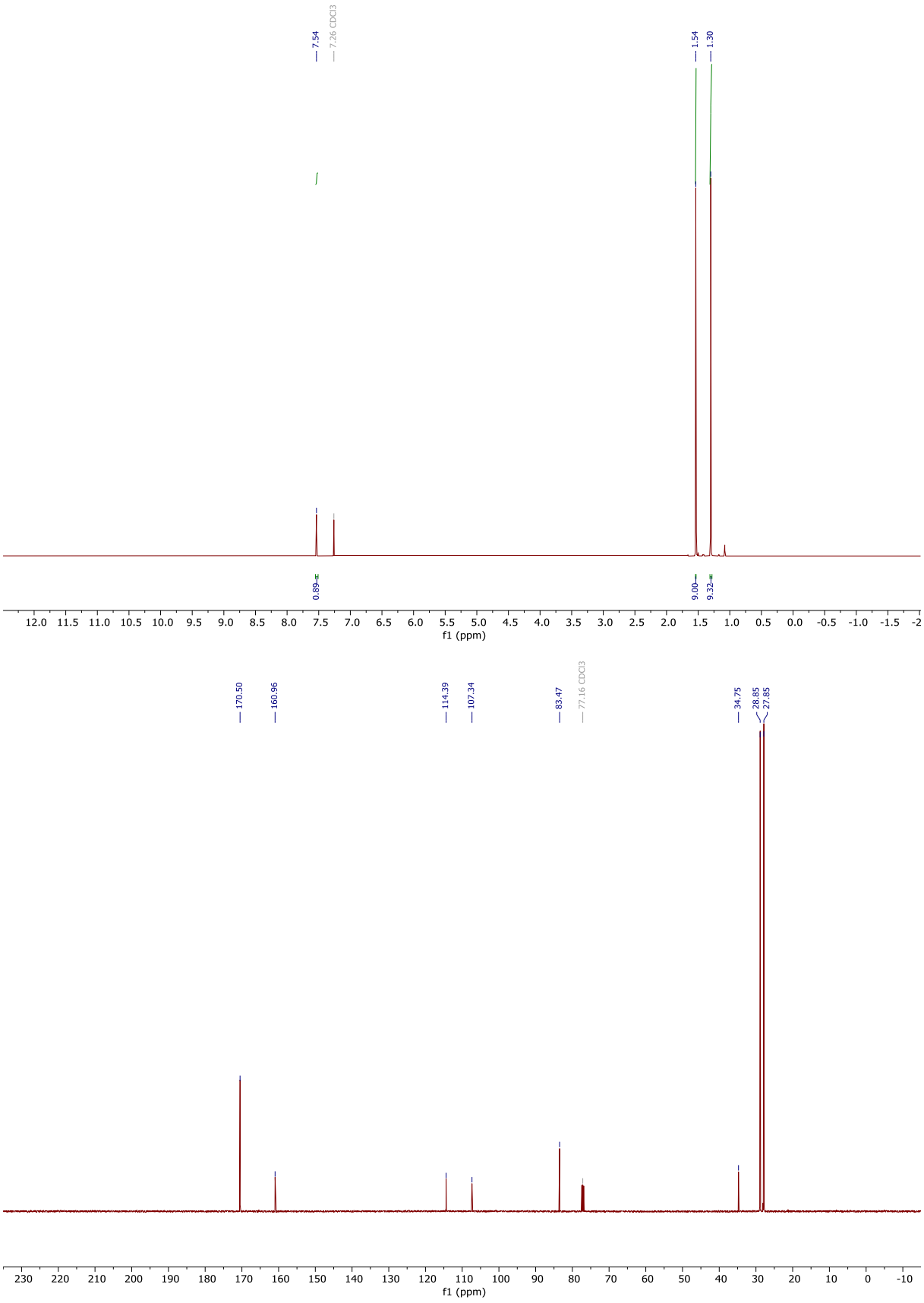

Supplementary Fig. 77. The ^{1}H-NMR (500 MHz) and ^{13}C-NMR (125 MHz) spectra of compound **40** in $CDCl_3$

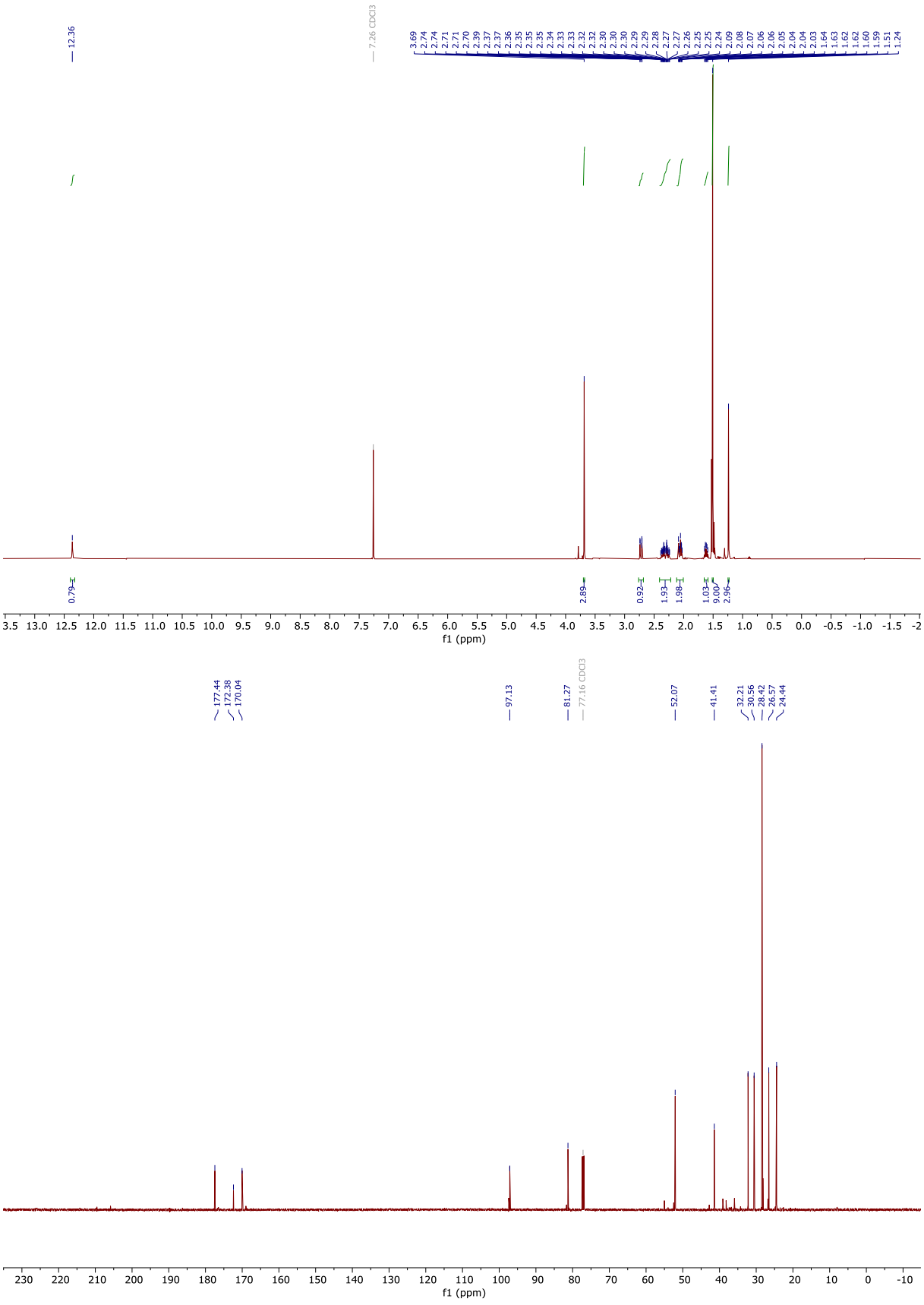

Supplementary Fig. 78. The ^{1}H-NMR (500 MHz) and ^{13}C-NMR (125 MHz) spectra of compound **3''*R*** in $CDCl_3$

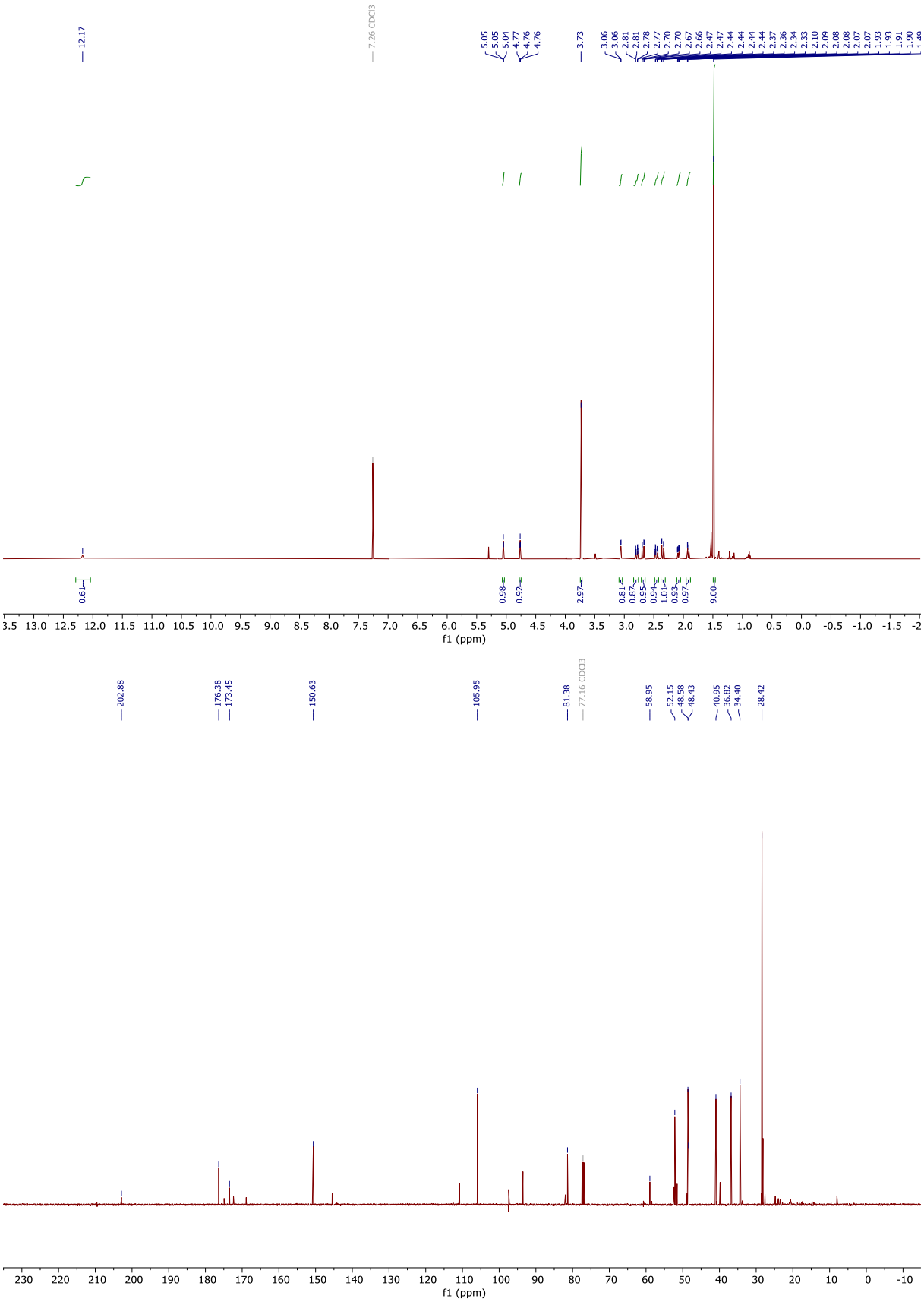

Supplementary Fig. 79. The ^{1}H-NMR (500 MHz) and ^{13}C-NMR (125 MHz) spectra of compound **6''*R*,*R*** in $CDCl_3$

High-performance liquid chromatography chromatograms

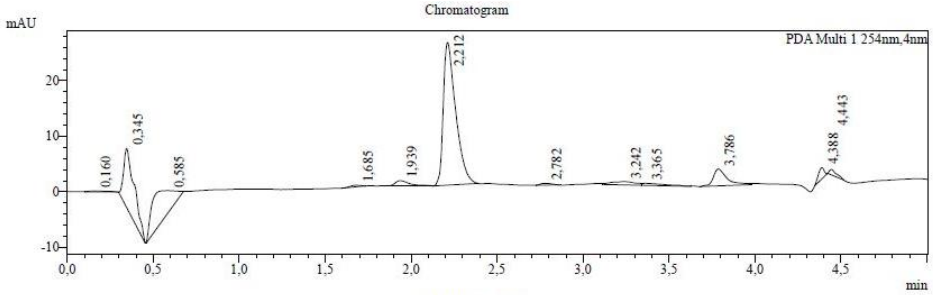

Peak Table

PDA Ch1 254nm

Peak#	Ret. Time	Area	Area%	Height	Height%	Name
1	0,160	1257	0,470	165	0,335	
2	0,345	45369	16,958	10646	21,641	
3	0,585	49464	18,489	4070	8,273	
4	1,685	1181	0,441	254	0,517	
5	1,939	5249	1,962	919	1,868	
6	2,212	128952	48,201	25726	52,298	
7	2,782	1521	0,568	318	0,646	
8	3,242	5847	2,185	620	1,260	
9	3,365	3349	1,252	377	0,766	
10	3,786	17208	6,432	3044	6,189	
11	4,388	5298	1,980	2052	4,172	
12	4,443	2837	1,061	1001	2,036	
Total		267532	100,000	49191	100,000	

Supplementary Fig. 80. The high-performance liquid chromatography chromatogram of compound **2-biotin**

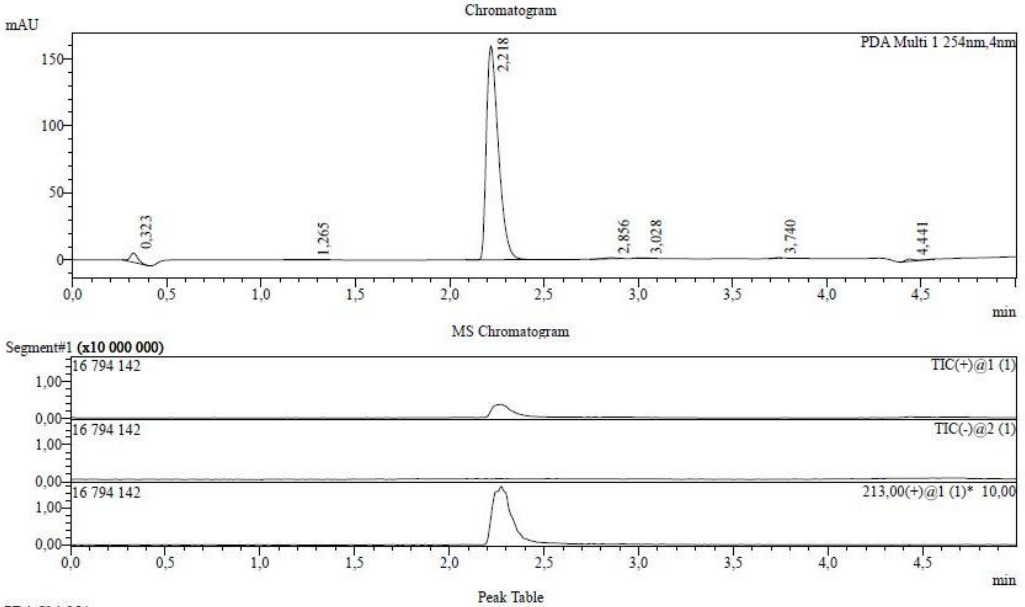

Peak Table

PDA Ch1 254nm

Peak#	Ret. Time	Area	Area%	Height	Height%	Name
1	0,323	19161	2,603	6851	4,038	
2	1,265	1199	0,163	171	0,101	
3	2,218	704557	95,706	159625	94,096	
4	2,856	4114	0,559	878	0,517	
5	3,028	471	0,064	199	0,118	
6	3,740	742	0,101	306	0,181	
7	4,441	5921	0,804	1609	0,949	
Total		736165	100,000	169640	100,000	

Supplementary Fig. 81. The high-performance liquid chromatography chromatogram of compound **3**/**3*R***/**3*S***

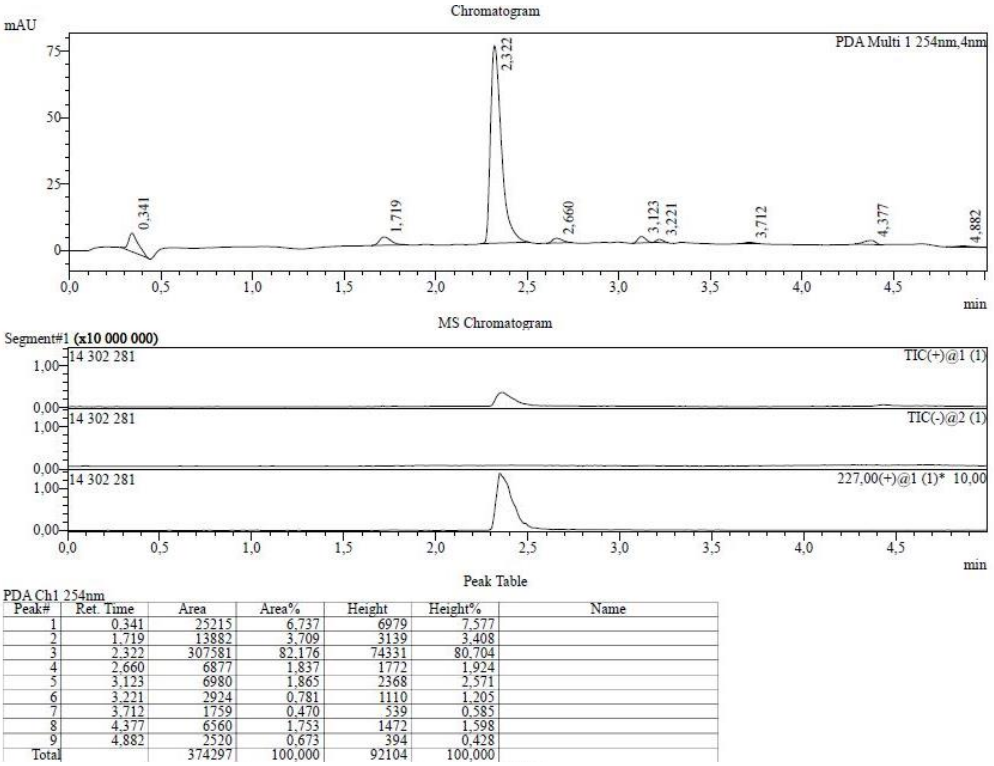

Peak Table

PDA Ch1 254nm

Peak#	Ret. Time	Area	Area%	Height	Height%	Name
1	0,341	25215	6,737	6979	7,577	
2	1,719	13882	3,709	3139	3,408	
3	2,322	307581	82,176	74331	80,704	
4	2,660	6877	1,837	1772	1,924	
5	3,123	6980	1,865	2368	2,571	
6	3,221	2924	0,781	1110	1,205	
7	3,712	1759	0,470	539	0,585	
8	4,377	6560	1,753	1472	1,598	
9	4,882	2520	0,673	394	0,428	
Total		374297	100,000	92104	100,000	

Supplementary Fig. 82. The high-performance liquid chromatography chromatogram of compound **3'*R***

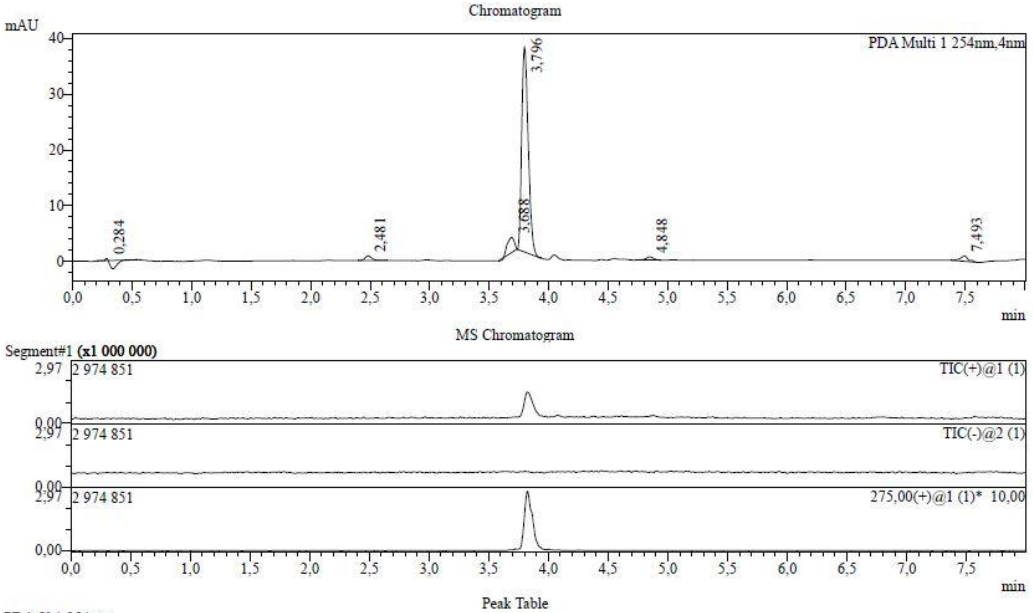

Peak Table

PDA Ch1 254nm

Peak#	Ret. Time	Area	Area%	Height	Height%	Name
1	0,284	-5266	-3,368	367	0,867	
2	2,481	3153	2,017	803	1,895	
3	3,688	11361	7,266	2719	6,417	
4	3,796	140402	89,792	36929	87,151	
5	4,848	2272	1,453	550	1,298	
6	7,493	4442	2,841	1005	2,372	
Total		156364	100,000	42373	100,000	

Supplementary Fig. 83. The high-performance liquid chromatography chromatogram of compound **5**

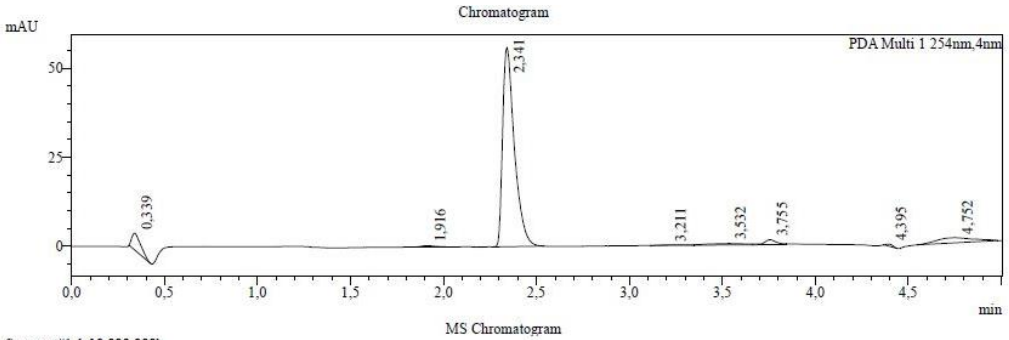

Peak Table

PDA Ch1 254nm

Peak#	Ret. Time	Area	Area%	Height	Height%	Name
1	0,339	15244	5,109	4645	7,154	
2	1,916	1725	0,578	326	0,501	
3	2,341	246595	82,638	56042	86,328	
4	3,211	1444	0,484	146	0,225	
5	3,532	5590	1,873	384	0,592	
6	3,755	6216	2,083	1377	2,121	
7	4,395	1252	0,420	564	0,869	
8	4,752	20338	6,816	1434	2,209	
Total		298404	100,000	64918	100,000	

Supplementary Fig. 84. The high-performance liquid chromatography chromatogram of compound **6, 6*R*,*R*/6*S*,*S***

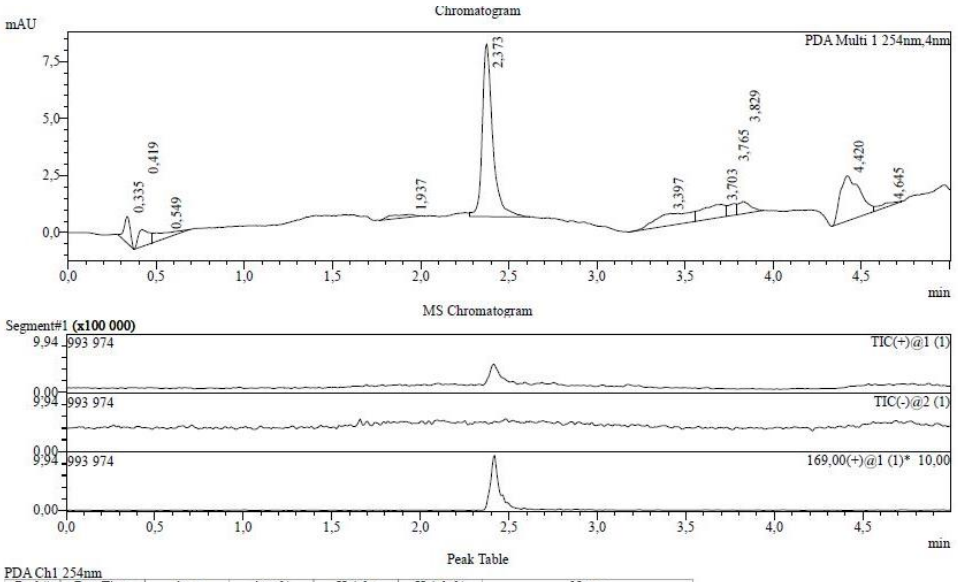

Peak Table

PDA Ch1 254nm

Peak#	Ret. Time	Area	Area%	Height	Height%	Name
1	0,335	2660	3,553	1173	8,297	
2	0,419	3201	4,276	743	5,250	
3	0,549	2512	3,356	251	1,772	
4	1,937	1364	1,822	113	0,799	
5	2,373	31294	41,807	7581	53,603	
6	3,397	7500	10,019	524	3,707	
7	3,703	5505	7,354	567	4,006	
8	3,765	1715	2,291	503	3,555	
9	3,829	2572	3,436	533	3,769	
10	4,420	15258	20,384	1974	13,960	
11	4,645	1274	1,702	181	1,282	
Total		74854	100,000	14142	100,000	

Supplementary Fig. 85. The high-performance liquid chromatography chromatogram of compound **7**

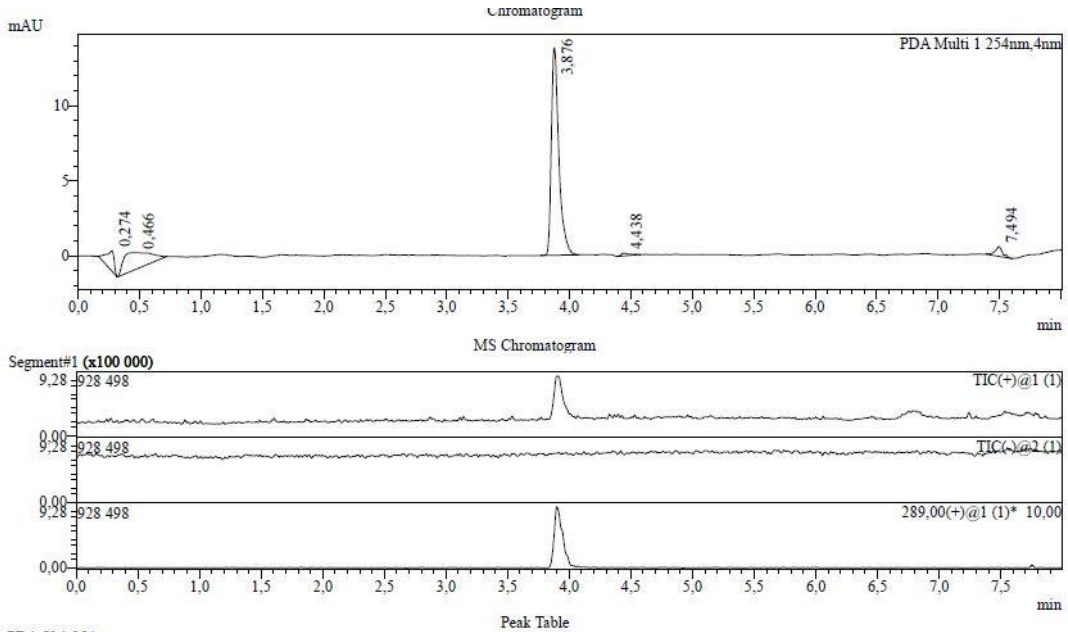

Peak Table

PDA Ch1 254nm

Peak#	Ret. Time	Area	Area%	Height	Height%	Name
1	0,274	5640	6,605	1369	7,975	
2	0,466	17422	20,401	1124	6,549	
3	3,876	58834	68,891	13843	80,654	
4	4,438	845	0,989	178	1,035	
5	7,494	2660	3,115	650	3,788	
Total		85402	100,000	17164	100,000	

Supplementary Fig. 86. The high-performance liquid chromatography chromatogram of compound **8**, **8*R*/8*S***

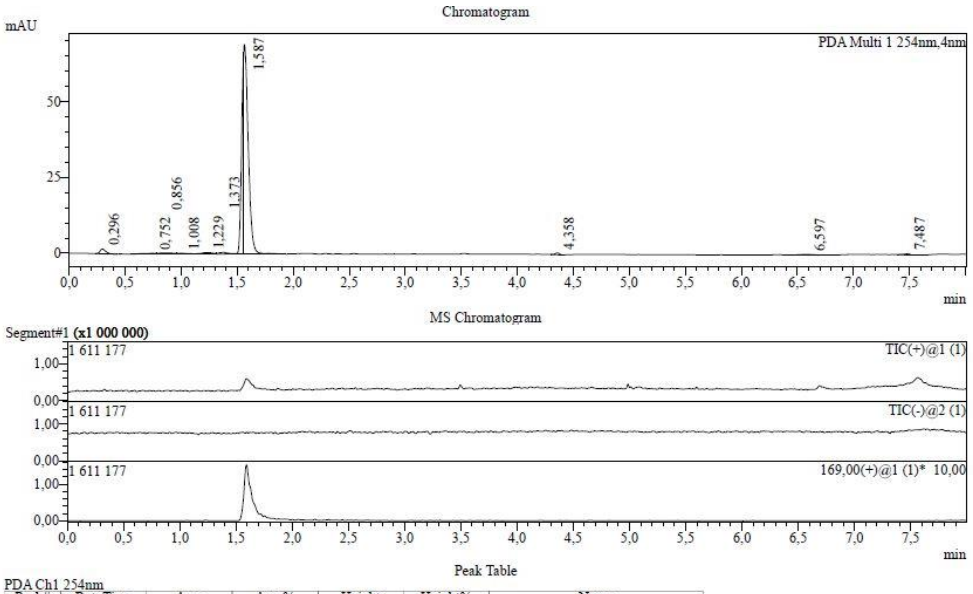

Peak Table

PDA Ch1 254nm

Peak#	Ret. Time	Area	Area%	Height	Height%	Name
1	0,296	5432	1,808	1535	2,595	
2	0,752	2504	0,833	281	0,475	
3	0,856	3629	1,208	399	0,674	
4	1,008	1874	0,623	292	0,494	
5	1,229	3533	1,176	456	0,771	
6	1,373	98299	32,708	530	0,896	
7	1,587	181214	60,298	54491	92,113	RT:1,587
8	4,358	1550	0,516	612	1,035	
9	6,597	1004	0,334	124	0,209	
10	7,487	1492	0,497	436	0,738	
Total		300531	100,000	59156	100,000	

Supplementary Fig. 87. The high-performance liquid chromatography chromatogram of compound **9**

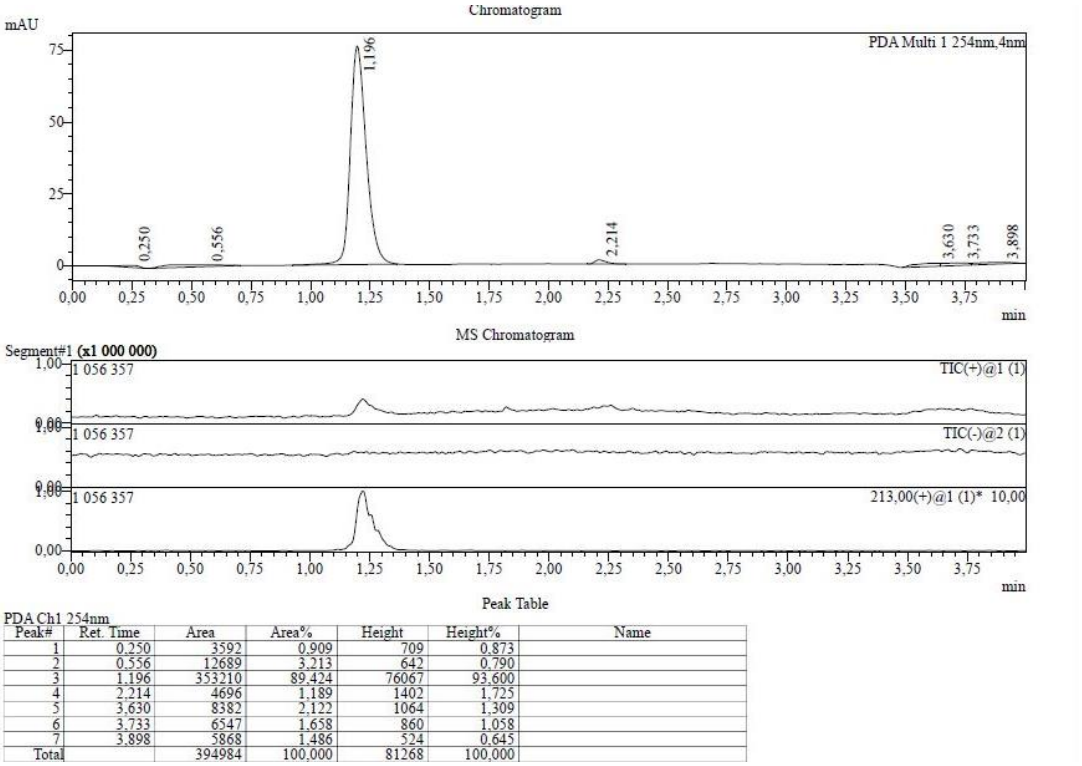

Peak Table

PDA Ch1 254nm

Peak#	Ret. Time	Area	Area%	Height	Height%	Name
1	0,250	3592	0,909	709	0,873	
2	0,556	12689	3,213	642	0,790	
3	1,196	353210	89,424	76067	93,600	
4	2,214	4696	1,189	1402	1,725	
5	3,630	8382	2,122	1064	1,309	
6	3,733	6547	1,658	860	1,058	
7	3,898	5868	1,486	524	0,645	
Total		394984	100,000	81268	100,000	

Supplementary Fig. 88. The high-performance liquid chromatography chromatogram of compound **10**, **10*R*/10*S***

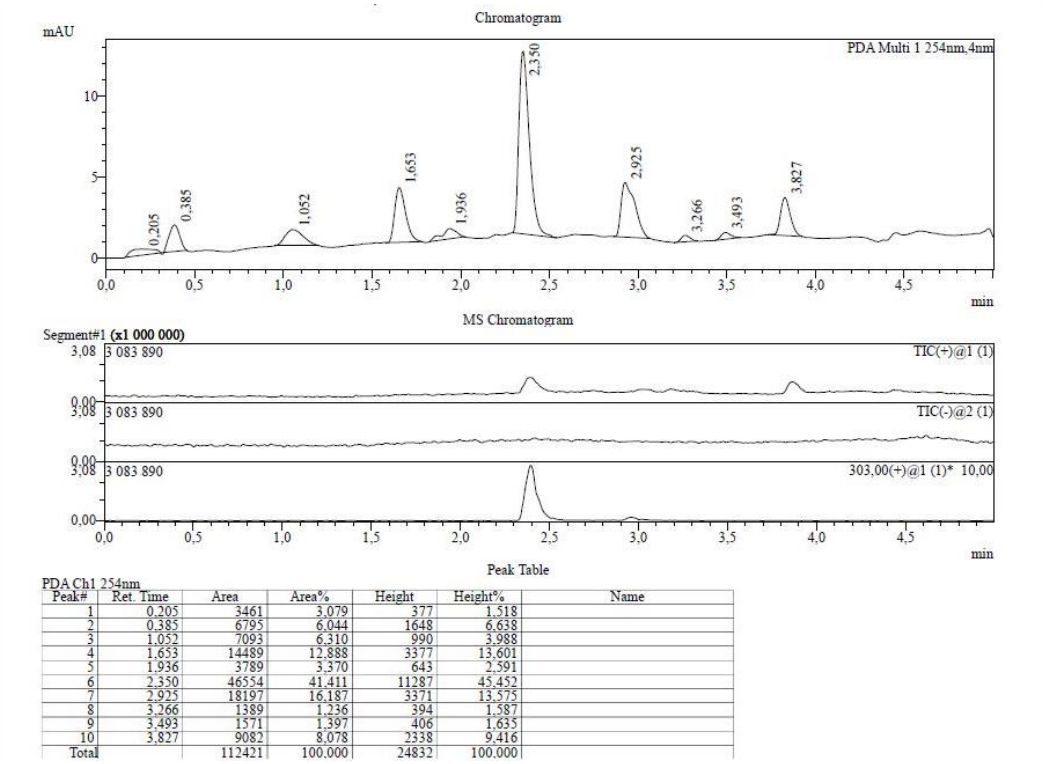

Peak Table

PDA Ch1 254nm

Peak#	Ret. Time	Area	Area%	Height	Height%	Name
1	0,205	3461	3,079	377	1,518	
2	0,385	6795	6,044	1648	6,638	
3	1,052	7093	6,310	990	3,988	
4	1,653	14489	12,888	3377	13,601	
5	1,936	3789	3,370	643	2,591	
6	2,350	46554	41,411	11287	45,452	
7	2,925	18197	16,187	3371	13,575	
8	3,266	1389	1,236	394	1,587	
9	3,493	1571	1,397	406	1,635	
10	3,827	9082	8,078	2338	9,416	
Total		112421	100,000	24832	100,000	

Supplementary Fig. 89. The high-performance liquid chromatography chromatogram of compound **12**, **12*R*/12*S***

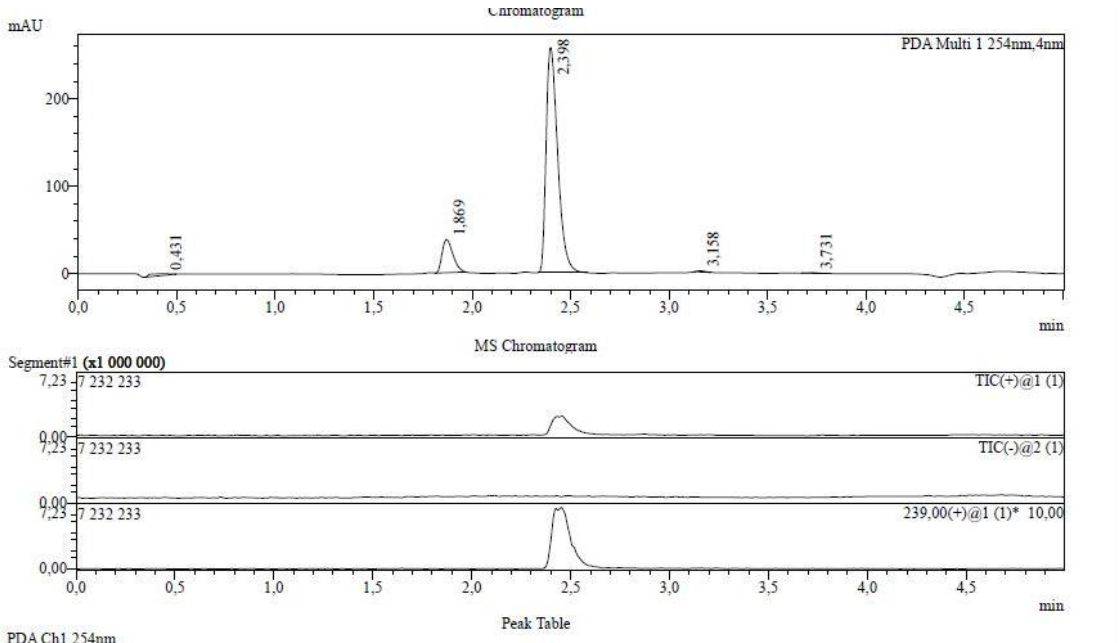

Peak Table

PDA Ch1 254nm

Peak#	Ret. Time	Area	Area%	Height	Height%	Name
1	0,431	16675	1,368	1972	0,660	
2	1,869	144523	11,858	37725	12,624	
3	2,398	1052522	86,362	257319	86,107	
4	3,158	3486	0,286	1378	0,461	
5	3,731	1531	0,126	443	0,148	
Total		1218737	100,000	298837	100,000	

Supplementary Fig. 90. The high-performance liquid chromatography chromatogram of compound **13, 13*R*/13*S***

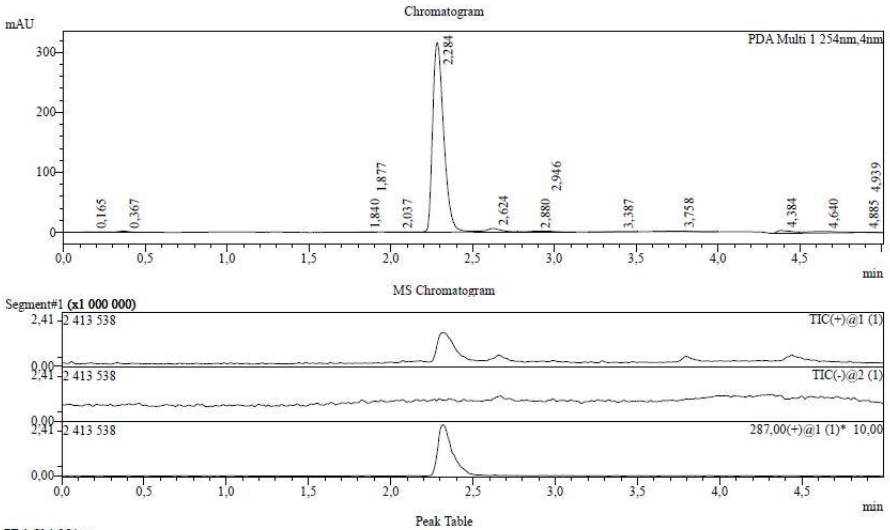

Peak Table

PDA Ch1 254nm

Peak#	Ret. Time	Area	Area%	Height	Height%	Name
1	0,165	5032	0,305	554	0,164	
2	0,367	9038	0,547	1732	0,512	
3	1,840	1583	0,096	364	0,108	
4	1,877	1415	0,086	412	0,122	
5	2,037	2254	0,136	348	0,103	
6	2,284	1489484	90,192	316842	93,619	
7	2,624	43389	2,627	6079	1,796	
8	2,880	7873	0,477	1293	0,382	
9	2,946	8643	0,523	1318	0,389	
10	3,387	2257	0,137	208	0,061	
11	3,758	6508	0,394	729	0,215	
12	4,384	30537	1,849	4909	1,451	
13	4,640	39038	2,364	2610	0,771	
14	4,885	2665	0,161	616	0,182	
15	4,939	1762	0,107	423	0,125	
Total		1651467	100,000	338439	100,000	

Supplementary Fig. 91. The high-performance liquid chromatography chromatogram of compound **14**

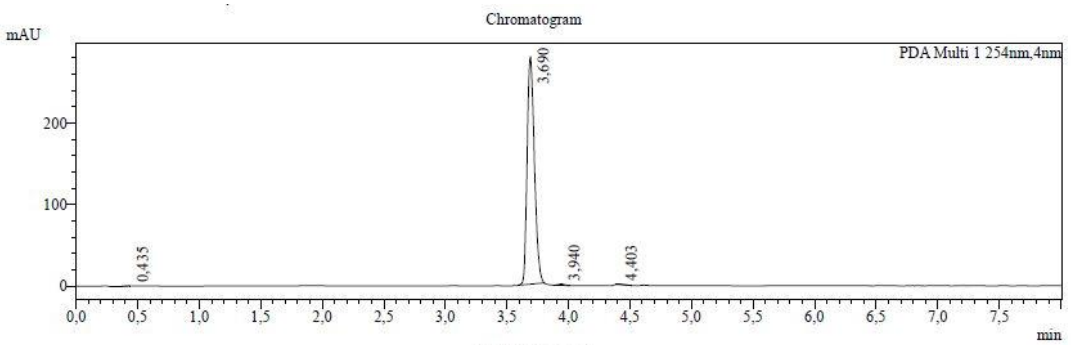

Peak Table

PDA Ch1 254nm

Peak#	Ret. Time	Area	Area%	Height	Height%	Name
1	0,435	985	0,085	14	0,005	
2	3,690	1143525	99,172	279407	99,172	
3	3,940	5668	0,492	1607	0,570	
4	4,403	2892	0,251	711	0,252	
Total		1153071	100,000	281739	100,000	

Supplementary Fig. 92. The high-performance liquid chromatography chromatogram of compound **15**

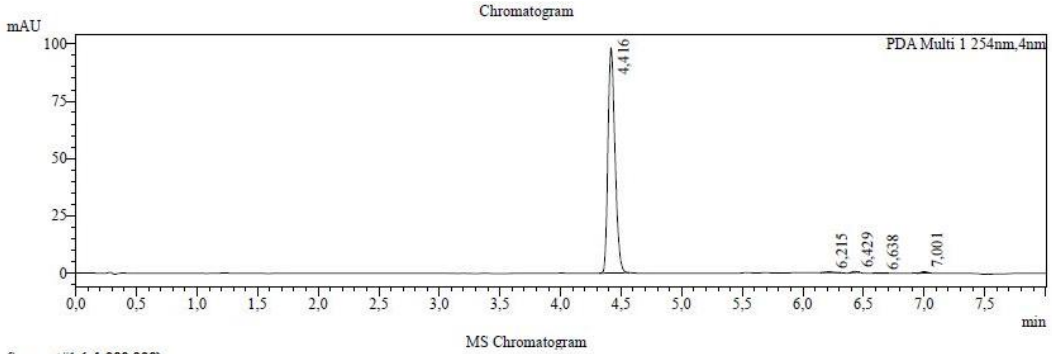

Peak Table

PDA Ch1 254nm

Peak#	Ret. Time	Area	Area%	Height	Height%	Name
1	4,416	396425	98,619	98333	98,378	
2	6,215	1433	0,356	310	0,310	
3	6,429	1608	0,400	558	0,558	
4	6,638	468	0,116	130	0,130	
5	7,001	2041	0,508	623	0,624	
Total		401975	100,000	99954	100,000	

Supplementary Fig. 93. The high-performance liquid chromatography chromatogram of compound **16**

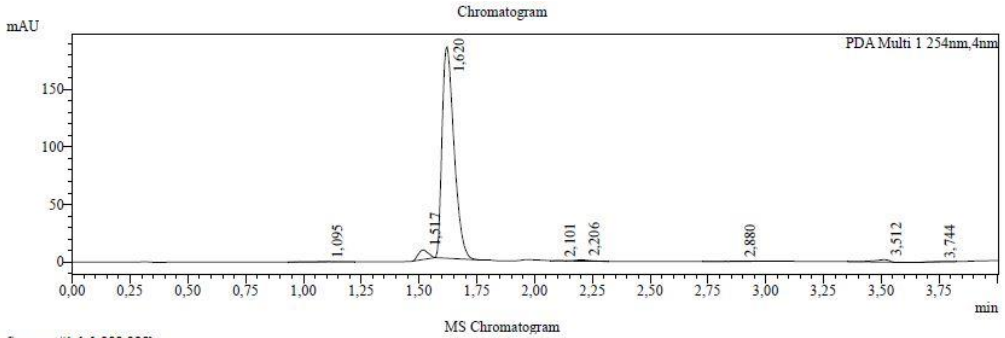

Peak Table

PDA Ch1 254nm

Peak#	Ret. Time	Area	Area%	Height	Height%	Name
1	1,095	2312	0,327	246	0,125	
2	1,517	25338	3,582	8108	4,138	
3	1,620	662542	93,659	183890	93,857	
4	2,101	492	0,070	188	0,096	
5	2,206	4006	0,566	983	0,502	
6	2,880	1339	0,189	179	0,091	
7	3,512	9351	1,322	2037	1,040	
8	3,744	2015	0,285	295	0,150	
Total		707395	100,000	195926	100,000	

Supplementary Fig. 94. The high-performance liquid chromatography chromatogram of compound **17**

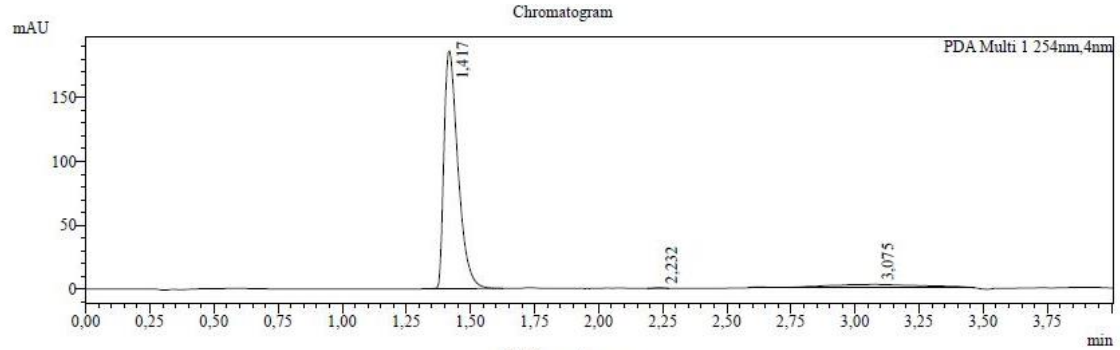

Peak Table

PDA Ch1 254nm

Peak#	Ret. Time	Area	Area%	Height	Height%	Name
1	1,417	708607	90,993	186693	98,401	
2	2,232	1134	0,146	402	0,212	
3	3,075	69009	8,862	2632	1,387	
Total		778750	100,000	189727	100,000	

Supplementary Fig. 95. The high-performance liquid chromatography chromatogram of compound **S7**

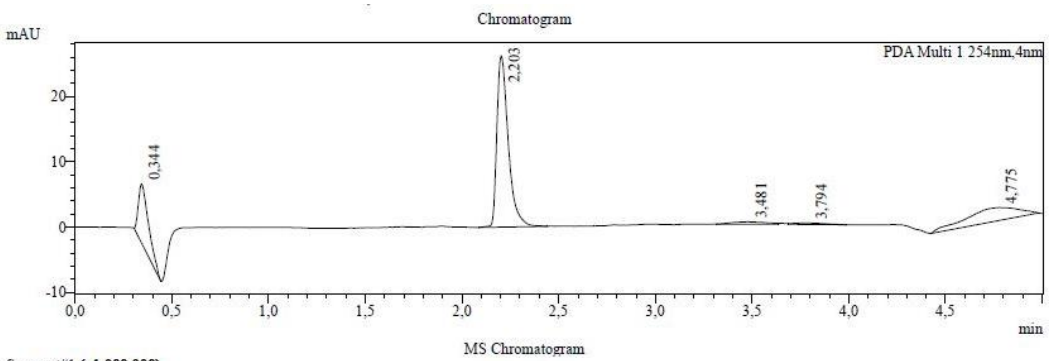

Peak Table

PDA Ch1 254nm

Peak#	Ret. Time	Area	Area%	Height	Height%	Name
1	0,344	32406	17,346	9071	23,926	
2	2,203	107333	57,452	26265	69,276	
3	3,481	4369	2,339	358	0,944	
4	3,794	2646	1,416	250	0,659	
5	4,775	40067	21,447	1970	5,196	
Total		186820	100,000	37914	100,000	

Supplementary Fig. 96. The high-performance liquid chromatography chromatogram of compound **18**/**18*R***

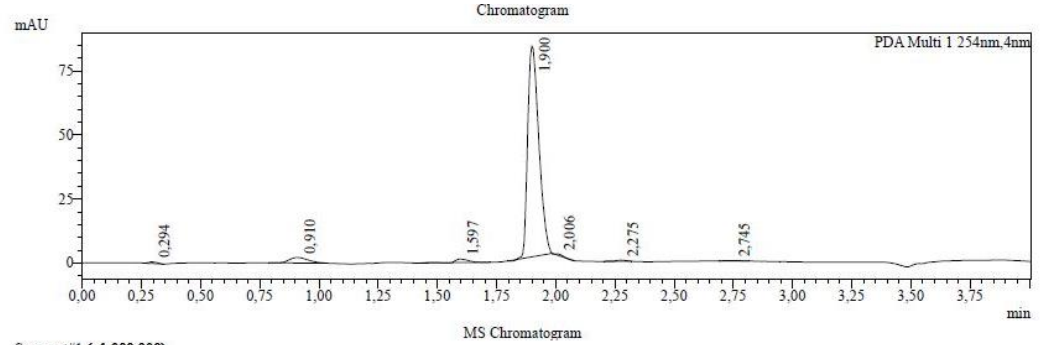

Peak Table

PDA Ch1 254nm

Peak#	Ret. Time	Area	Area%	Height	Height%	Name
1	0,294	1381	0,474	604	0,688	
2	0,910	11790	4,046	2134	2,433	
3	1,597	5450	1,871	1403	1,600	
4	1,900	270060	92,689	82498	94,074	
5	2,006	222	0,076	457	0,521	
6	2,275	1579	0,542	412	0,469	
7	2,745	878	0,301	188	0,214	
Total		291360	100,000	87695	100,000	

Supplementary Fig. 97. The high-performance liquid chromatography chromatogram of compound **19**

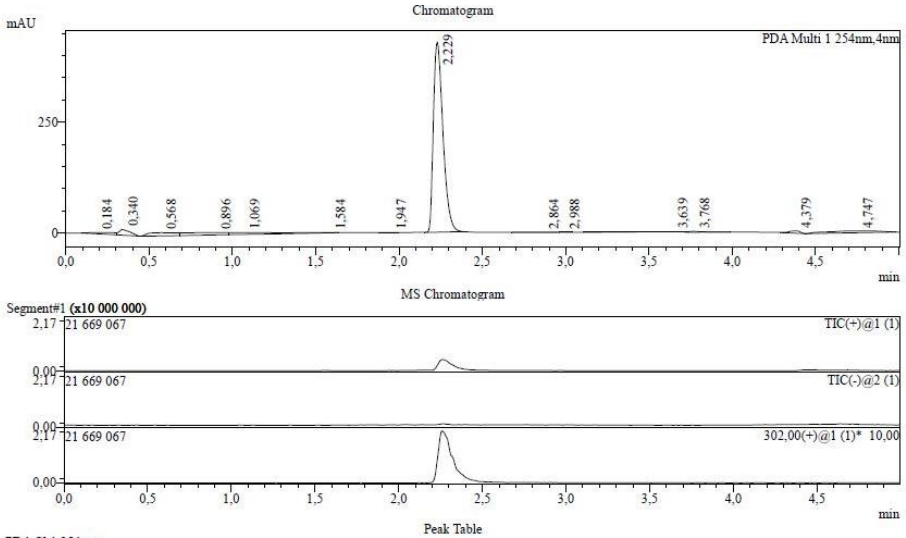

Peak#	Ret. Time	Area	Area%	Height	Height%	Name
1	0,184	34699	1,557	2572	0,541	
2	0,340	59459	2,668	12863	2,707	
3	0,568	86081	3,863	7201	1,515	
4	0,896	98123	4,404	5188	1,092	
5	1,069	64481	2,894	4130	0,869	
6	1,584	24655	1,106	436	0,092	
7	1,947	335	0,015	72	0,015	
8	2,229	1707098	76,612	429599	90,406	
9	2,864	2218	0,100	228	0,048	
10	2,988	960	0,043	251	0,053	
11	3,639	23357	1,048	1143	0,240	
12	3,768	10465	0,470	1853	0,390	
13	4,379	22587	1,014	5287	1,113	
14	4,747	93734	4,207	4368	0,919	
Total		2228249	100,000	475191	100,000	

Supplementary Fig. 98. The high-performance liquid chromatography chromatogram of compound **20**

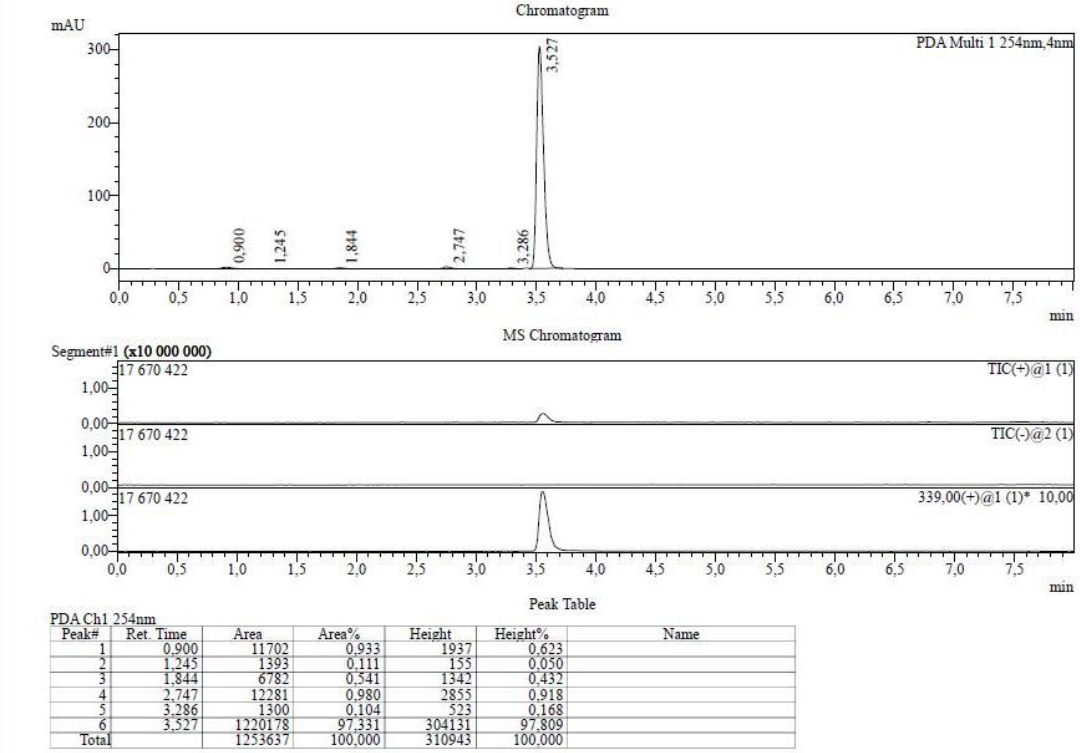

Peak#	Ret. Time	Area	Area%	Height	Height%	Name
1	0,900	11702	0,933	1937	0,623	
2	1,245	1393	0,111	155	0,050	
3	1,844	6782	0,541	1342	0,432	
4	2,747	12281	0,980	2855	0,918	
5	3,286	1300	0,104	523	0,168	
6	3,527	1220178	97,331	304131	97,809	
Total		1253637	100,000	310943	100,000	

Supplementary Fig. 99. The high-performance liquid chromatography chromatogram of compound **21**

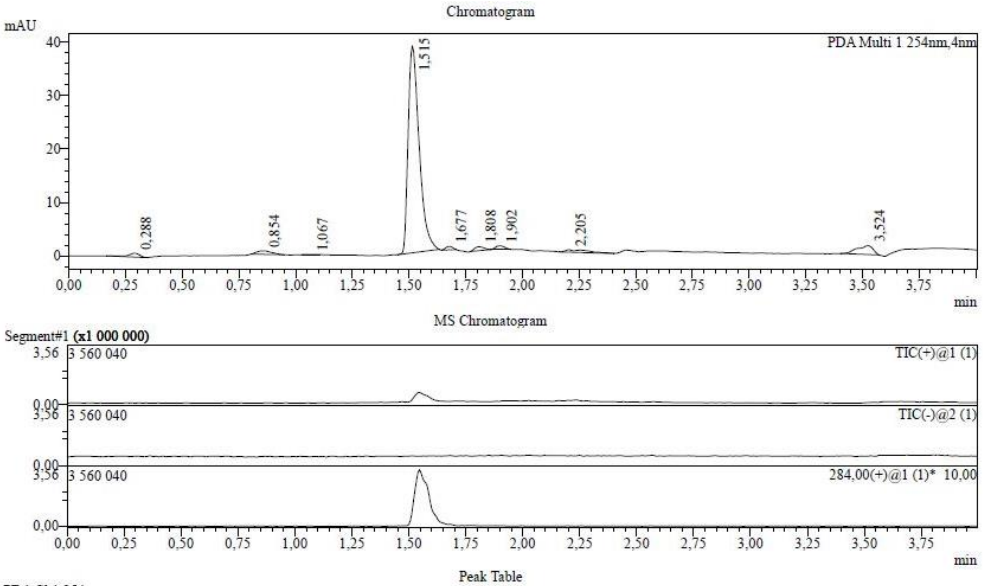

Peak Table

PDA Ch1 254nm

Peak#	Ret. Time	Area	Area%	Height	Height%	Name
1	0,288	2473	1,616	740	1,670	
2	0,854	2870	1,875	621	1,402	
3	1,067	89	0,058	34	0,076	
4	1,515	131212	85,705	38769	87,558	
5	1,677	1352	0,883	630	1,422	
6	1,808	2228	1,455	751	1,697	
7	1,902	1745	1,140	648	1,464	
8	2,205	3167	2,068	434	0,981	
9	3,524	7961	5,200	1651	3,729	
Total		153097	100,000	44278	100,000	

Supplementary Fig. 100. The high-performance liquid chromatography chromatogram of compound **22**

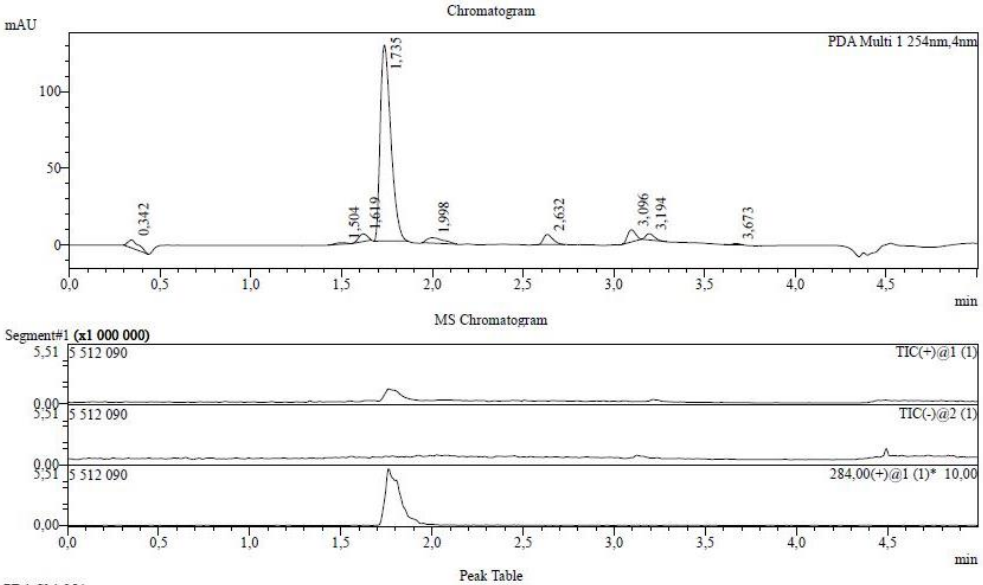

Peak Table

PDA Ch1 254nm

Peak#	Ret. Time	Area	Area%	Height	Height%	Name
1	0,342	22234	3,434	5390	3,332	
2	1,504	4326	0,668	1008	0,623	
3	1,619	16595	2,563	4953	3,062	
4	1,735	518314	80,057	127636	78,903	
5	1,998	22519	3,478	3512	2,171	
6	2,632	23515	3,632	6511	4,025	
7	3,096	24615	3,802	7776	4,807	
8	3,194	13352	2,062	4115	2,544	
9	3,673	1963	0,303	861	0,532	
Total		647434	100,000	161762	100,000	

Supplementary Fig. 101. The high-performance liquid chromatography chromatogram of compound **23**

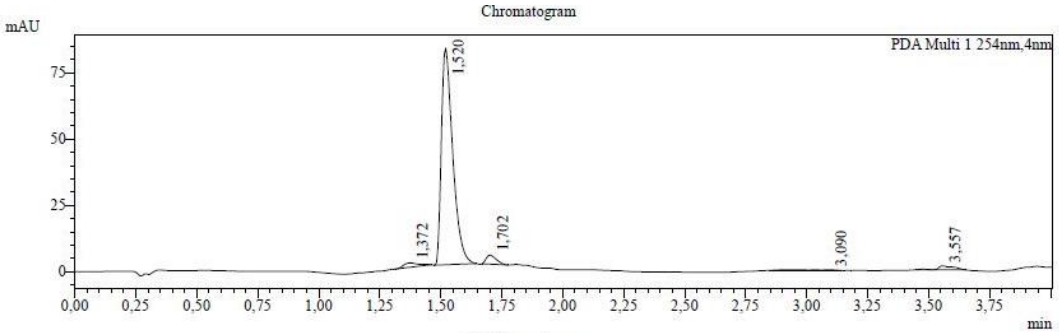

Peak Table

PDA Ch1 254nm

Peak#	Ret. Time	Area	Area%	Height	Height%	Name
1	1.372	7375	2.526	1693	1.909	
2	1.520	264927	90.733	81785	92.248	
3	1.702	9754	3.340	3391	3.825	
4	3.090	3139	1.075	299	0.338	
5	3.557	6791	2.326	1490	1.681	
Total		291986	100.000	88658	100.000	

Supplementary Fig. 102. The high-performance liquid chromatography chromatogram of compound **S8**

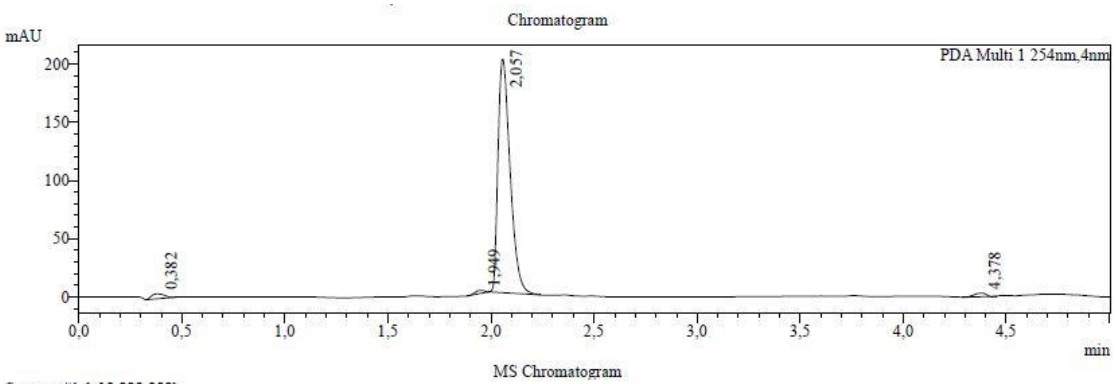

Peak Table

PDA Ch1 254nm

Peak#	Ret. Time	Area	Area%	Height	Height%	Name
1	0.382	18758	2.186	4218	2.001	
2	1.949	9096	1.060	2761	1.310	
3	2.057	818773	95.422	200741	95.240	
4	4.378	11429	1.332	3054	1.449	
Total		858056	100.000	210774	100.000	

Supplementary Fig. 103. The high-performance liquid chromatography chromatogram of compound **19'*S***

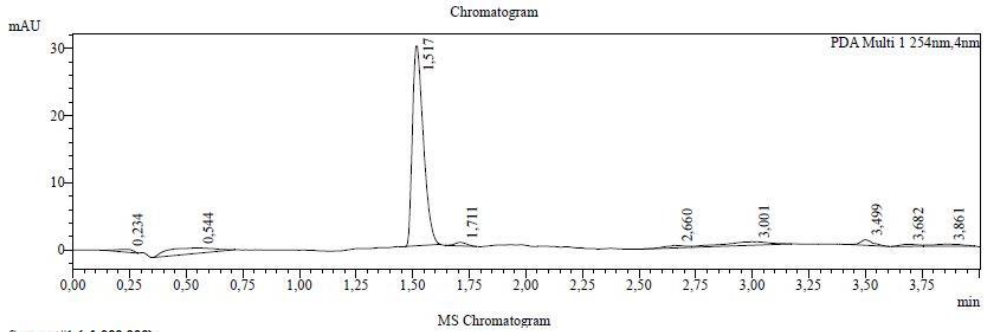

Peak Table

PDA Ch1 254nm

Peak#	Ret. Time	Area	Area%	Height	Height%	Name
1	0,234	1992	1,467	412	1,219	
2	0,544	13271	9,776	822	2,434	
3	1,517	100353	73,923	29689	87,916	
4	1,711	1911	1,407	536	1,587	
5	2,660	2536	1,868	376	1,113	
6	3,001	8041	5,923	521	1,543	
7	3,499	3038	2,238	802	2,376	
8	3,682	1716	1,264	305	0,902	
9	3,861	2895	2,133	307	0,910	
Total		135752	100,000	33770	100,000	

Supplementary Fig. 104. The high-performance liquid chromatography chromatogram of compound **24**

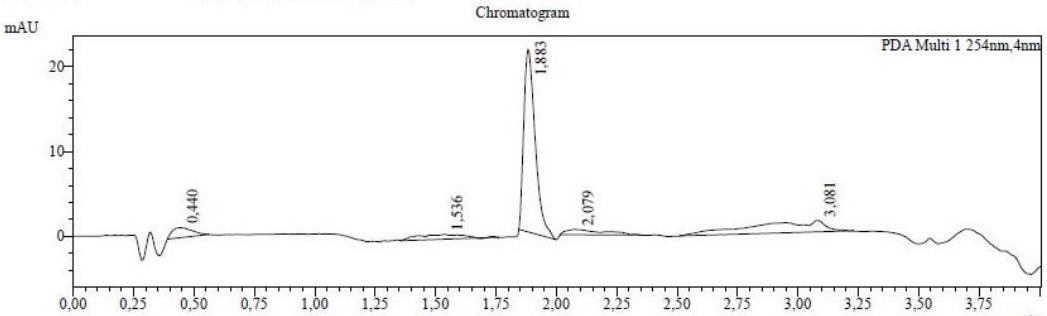

Peak Table

PDA Ch1 254nm

Peak#	Ret. Time	Area	Area%	Height	Height%	Name
1	0,440	6957	5,742	1184	4,671	
2	1,536	7450	6,149	573	2,261	
3	1,883	70496	58,181	21593	85,185	
4	2,079	6904	5,698	634	2,501	
5	3,081	29360	24,231	1364	5,382	
Total		121167	100,000	25349	100,000	

Supplementary Fig. 105. The high-performance liquid chromatography chromatogram of compound **26**

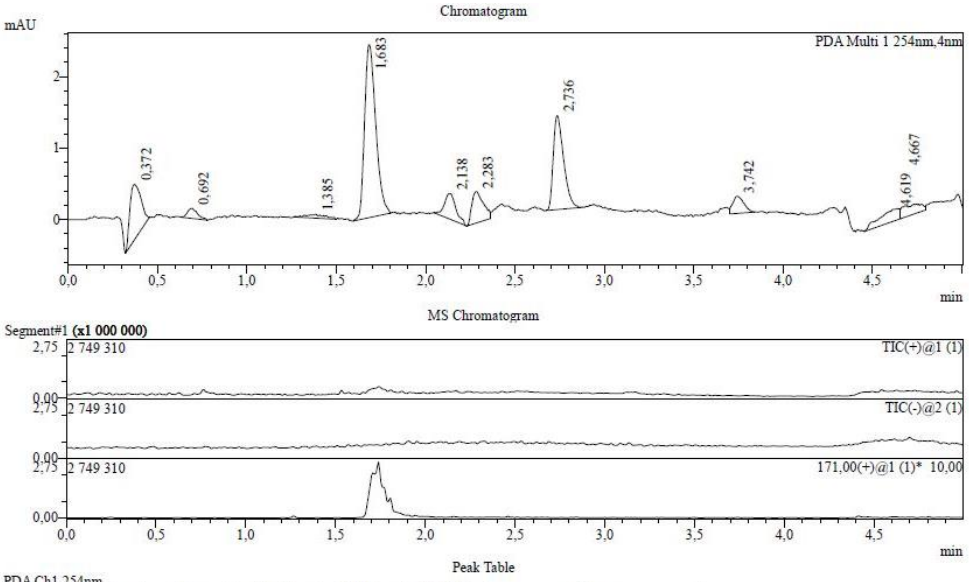

Peak Table

PDA Ch1 254nm

Peak#	Ret. Time	Area	Area%	Height	Height%	Name
1	0,372	3370	12,399	774	12,735	
2	0,692	542	1,992	143	2,360	
3	1,385	384	1,412	55	0,903	
4	1,683	10509	38,660	2421	39,853	
5	2,138	1568	5,767	361	5,936	
6	2,283	1991	7,324	440	7,250	
7	2,736	5317	19,560	1317	21,680	
8	3,742	1025	3,770	242	3,982	
9	4,619	1452	5,342	163	2,685	
10	4,667	1026	3,773	159	2,615	
Total		27182	100,000	6074	100,000	

Supplementary Fig. 106. The high-performance liquid chromatography chromatogram of compound **S10**

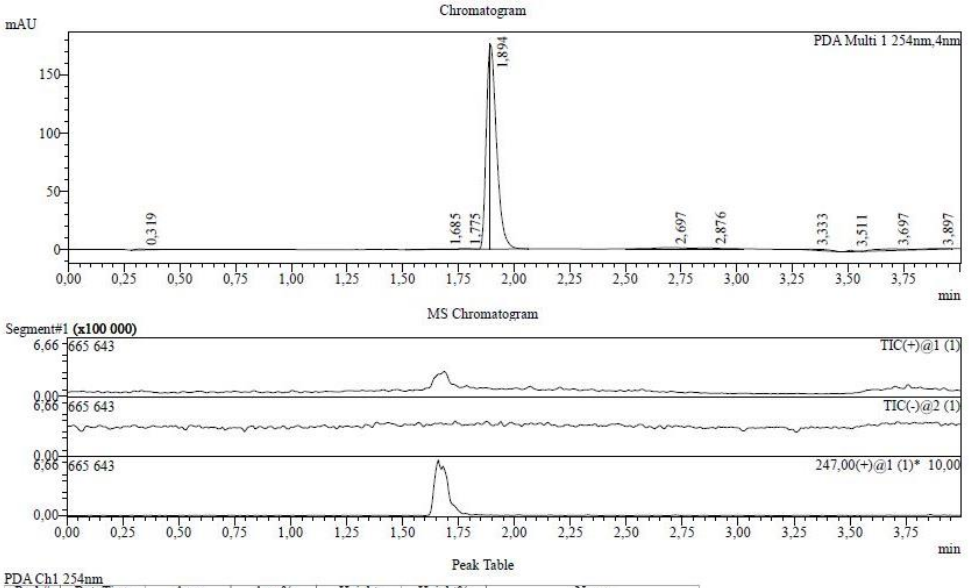

Peak Table

PDA Ch1 254nm

Peak#	Ret. Time	Area	Area%	Height	Height%	Name
1	0,319	2708	0,433	809	0,439	
2	1,685	3184	0,509	355	0,192	
3	1,775	246099	39,362	675	0,366	
4	1,894	321070	51,353	176343	95,608	
5	2,697	12899	2,063	1265	0,686	
6	2,876	9286	1,485	965	0,523	
7	3,333	7327	1,172	764	0,414	
8	3,511	2645	0,423	1204	0,653	
9	3,697	14643	2,342	1361	0,738	
10	3,897	5364	0,858	703	0,381	
Total		625224	100,000	184444	100,000	

Supplementary Fig. 107. The high-performance liquid chromatography chromatogram of compound **S12**

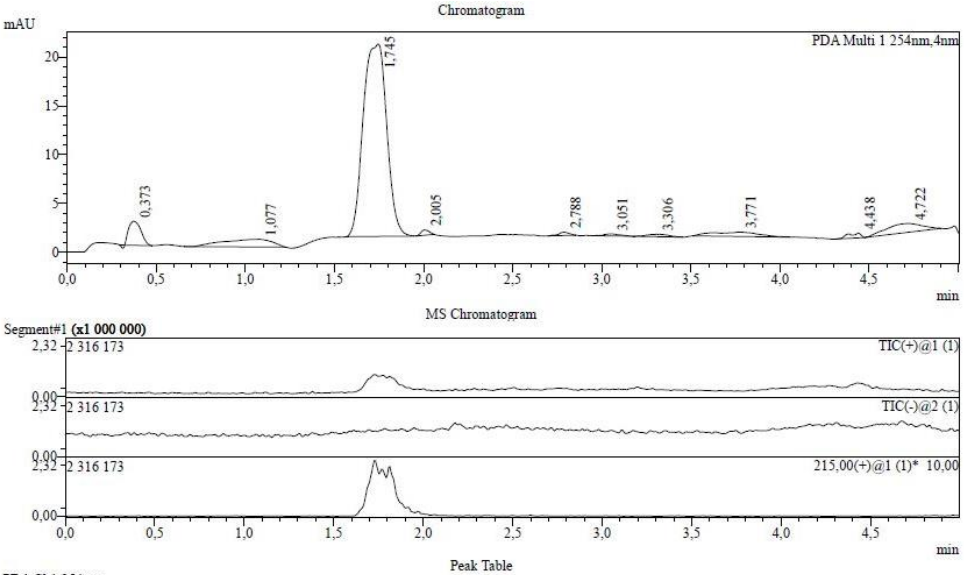

Peak Table

PDA Ch1 254nm

Peak#	Ret. Time	Area	Area%	Height	Height%	Name
1	0,373	11635	4,885	2468	9,413	
2	1,077	15367	6,451	793	3,023	
3	1,745	181003	75,989	19764	75,386	
4	2,005	1764	0,741	559	2,131	
5	2,788	1372	0,576	339	1,294	
6	3,051	1235	0,518	208	0,793	
7	3,306	2057	0,864	255	0,973	
8	3,771	7995	3,356	449	1,713	
9	4,438	2486	1,043	488	1,860	
10	4,722	13283	5,577	895	3,413	
Total		238196	100,000	26217	100,000	

Supplementary Fig. 108. The high-performance liquid chromatography chromatogram of compound **S13**

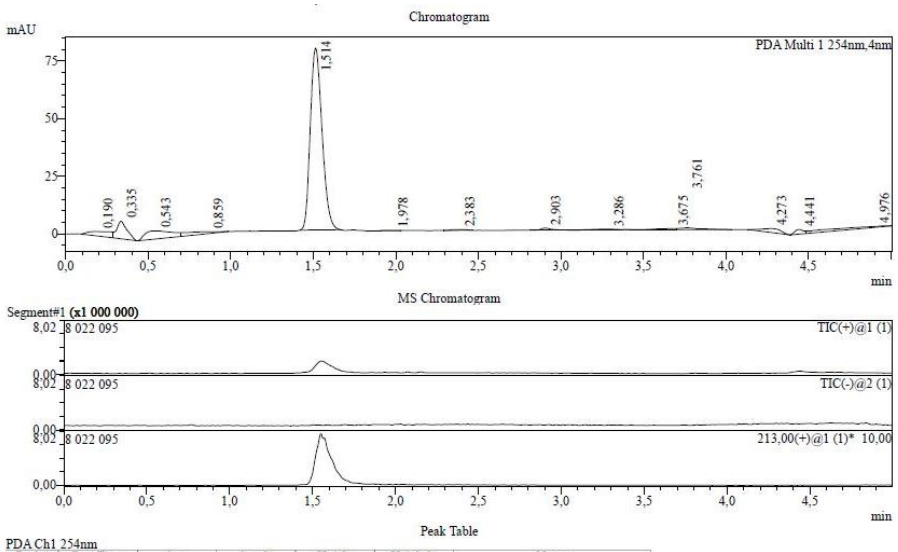

Peak Table

PDA Ch1 254nm

Peak#	Ret. Time	Area	Area%	Height	Height%	Name
1	0,190	19900	3,537	1891	1,893	
2	0,335	32437	5,766	7678	7,686	
3	0,543	40076	7,124	3538	3,542	
4	0,859	15309	2,721	840	0,840	
5	1,514	390264	69,375	78893	78,976	
6	1,978	1489	0,265	251	0,252	
7	2,383	2416	0,429	385	0,386	
8	2,903	3681	0,654	892	0,892	
9	3,286	3871	0,688	340	0,340	
10	3,675	4462	0,793	500	0,501	
11	3,761	6348	1,128	812	0,813	
12	4,273	13902	2,471	1694	1,695	
13	4,441	7489	1,331	2015	2,017	
14	4,976	20895	3,714	166	0,166	
Total		562539	100,000	99895	100,000	

Supplementary Fig. 109. The high-performance liquid chromatography chromatogram of compound **S15**

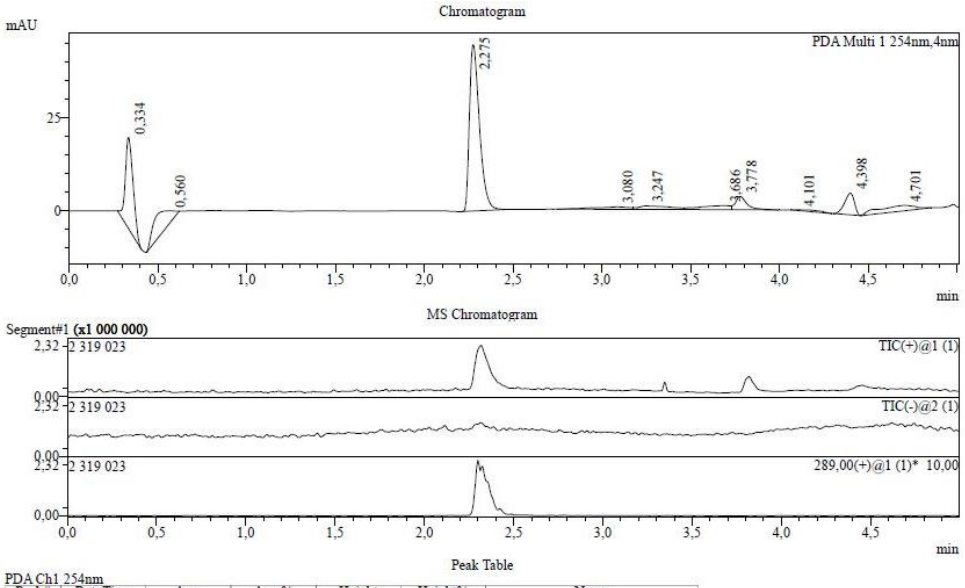

Peak Table

PDA Ch1 254nm

Peak#	Ret. Time	Area	Area%	Height	Height%	Name
1	0,334	73392	18,811	24464	28,332	
2	0,560	41958	10,754	3586	4,153	
3	2,275	175805	45,060	44609	51,663	
4	3,080	9234	2,367	633	0,733	
5	3,247	11826	3,031	947	1,096	
6	3,686	12985	3,328	1085	1,257	
7	3,778	15995	4,100	3559	4,121	
8	4,101	3489	0,894	208	0,241	
9	4,398	22284	5,712	5812	6,731	
10	4,701	23184	5,942	1444	1,672	
Total		390154	100,000	86347	100,000	

Supplementary Fig. 110. The high-performance liquid chromatography chromatogram of compound **27**

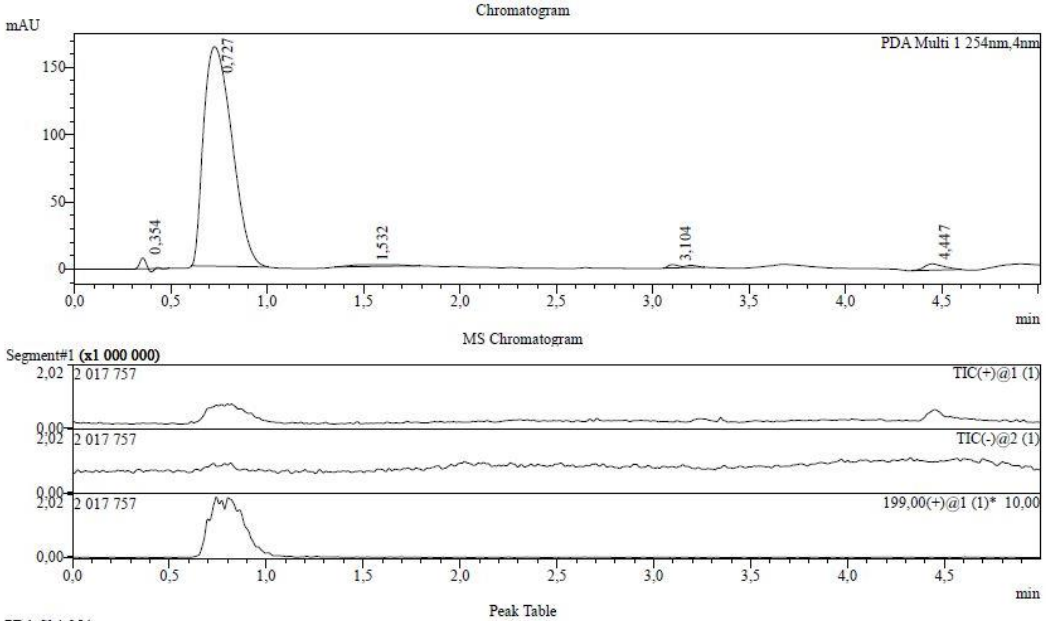

Peak Table

PDA Ch1 254nm

Peak#	Ret. Time	Area	Area%	Height	Height%	Name
1	0,354	13672	0,778	8008	4,454	
2	0,727	1672894	95,149	163358	90,855	
3	1,532	23645	1,345	1438	0,800	
4	3,104	15956	0,908	2445	1,360	
5	4,447	32023	1,821	4552	2,532	
Total		1758191	100,000	179801	100,000	

Supplementary Fig. 111. The high-performance liquid chromatography chromatogram of compound **S16**

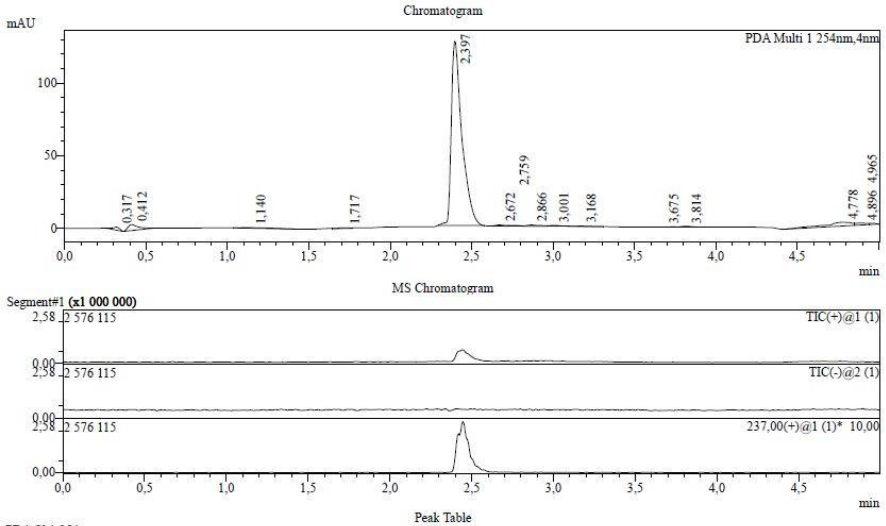

Peak Table

PDA Ch1 254nm

Peak#	Ret. Time	Area	Area%	Height	Height%	Name
1	0,317	5374	0,804	2005	1,411	
2	0,412	19066	2,853	4117	2,896	
3	1,140	5846	0,875	342	0,241	
4	1,717	2287	0,342	445	0,313	
5	2,397	575670	86,145	126796	89,185	
6	2,672	2755	0,412	693	0,488	
7	2,759	2007	0,300	513	0,361	
8	2,866	4661	0,698	827	0,582	
9	3,001	3458	0,517	647	0,455	
10	3,168	2121	0,317	344	0,242	
11	3,675	1095	0,164	128	0,090	
12	3,814	2329	0,349	618	0,435	
13	4,778	32675	4,890	2631	1,851	
14	4,896	7174	1,074	1333	0,938	
15	4,965	1735	0,260	732	0,515	
Total		668253	100,000	142172	100,000	

Supplementary Fig. 112. The high-performance liquid chromatography chromatogram of compound **28*R*/28*S***

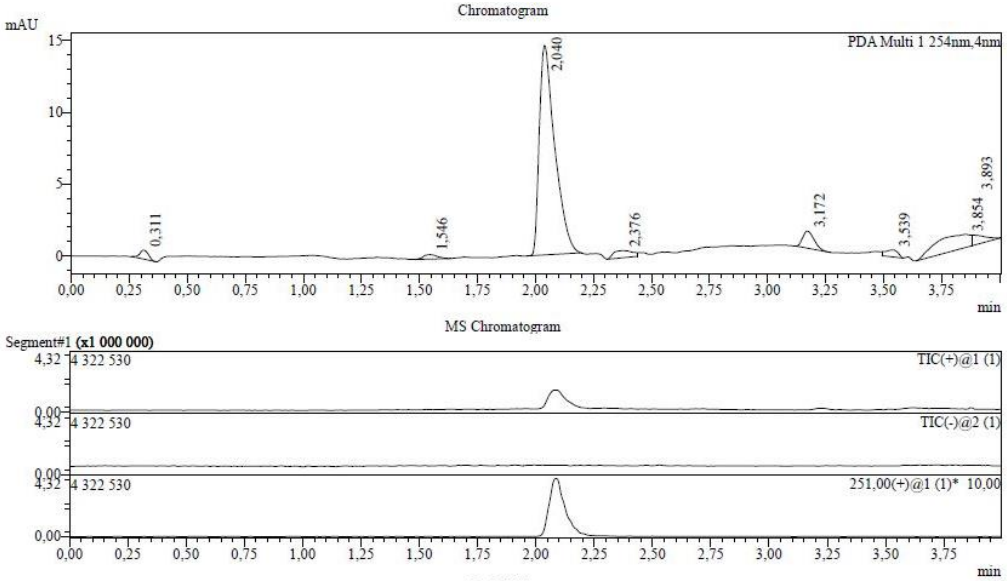

Peak Table

PDA Ch1 254nm

Peak#	Ret. Time	Area	Area%	Height	Height%	Name
1	0,311	1556	1,667	629	3,260	
2	1,546	1337	1,433	313	1,620	
3	2,040	67795	72,648	14594	75,626	
4	2,376	2890	3,097	505	2,615	
5	3,172	4027	4,315	1184	6,136	
6	3,539	1737	1,861	481	2,493	
7	3,854	11499	12,322	912	4,725	
8	3,893	2480	2,657	680	3,525	
Total		93320	100,000	19297	100,000	

Supplementary Fig. 113. The high-performance liquid chromatography chromatogram of compound **29*S***

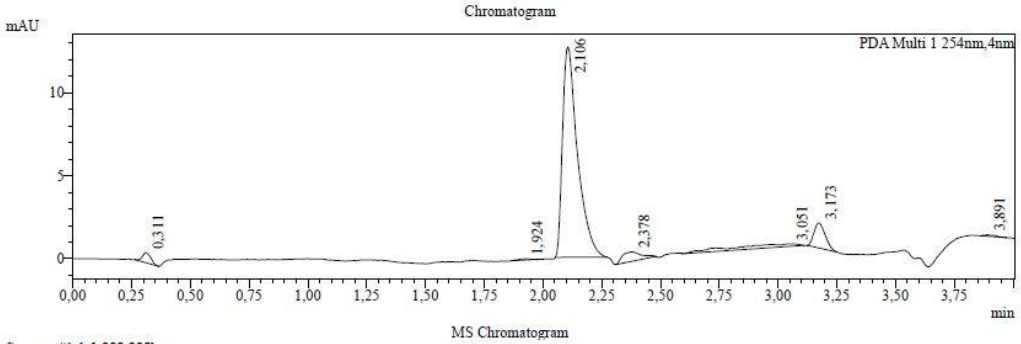

Peak Table

PDA Ch1 254nm

Peak#	Ret. Time	Area	Area%	Height	Height%	Name
1	0,311	1477	2,087	614	3,912	
2	1,924	279	0,395	74	0,472	
3	2,106	56256	79,494	12680	80,843	
4	2,378	3328	4,703	572	3,645	
5	3,051	4202	5,937	151	0,962	
6	3,173	4975	7,030	1514	9,652	
7	3,891	251	0,354	81	0,514	
Total		70767	100,000	15685	100,000	

Supplementary Fig. 114. The high-performance liquid chromatography chromatogram of compound **30*S***

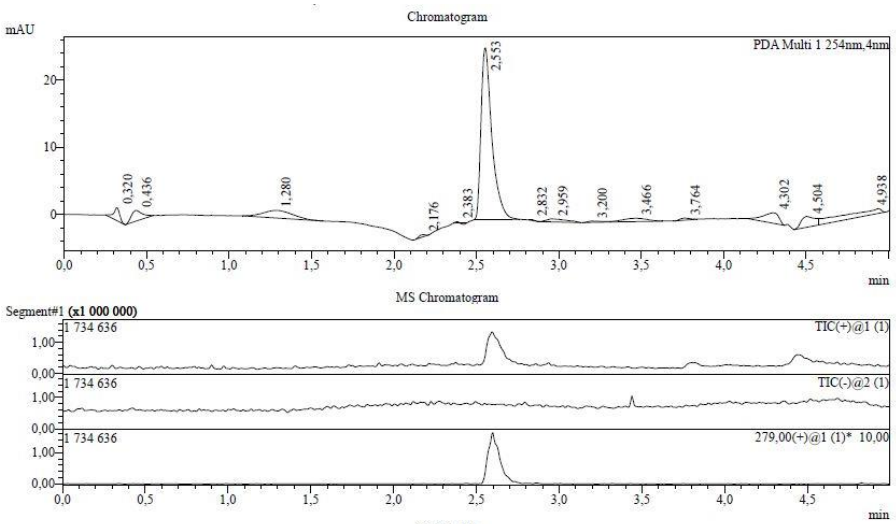

Peak Table

PDA Ch1 254nm

Peak#	Ret. Time	Area	Area%	Height	Height%	Name
1	0,320	4823	2,507	1951	5,407	
2	0,436	7567	3,933	1592	4,412	
3	1,280	14362	7,465	1130	3,130	
4	2,176	971	0,505	319	0,884	
5	2,383	-115	-0,060	183	0,507	
6	2,553	117129	60,881	25516	70,702	
7	2,832	151	0,078	96	0,265	
8	2,959	3741	1,944	441	1,223	
9	3,200	1181	0,614	205	0,569	
10	3,466	5141	2,672	506	1,402	
11	3,764	1194	0,620	297	0,824	
12	4,302	10273	5,340	1560	4,323	
13	4,504	9495	4,935	1584	4,390	
14	4,938	16477	8,565	708	1,962	
Total		192389	100,000	36089	100,000	

Supplementary Fig. 115. The high-performance liquid chromatography chromatogram of compound **31*S***

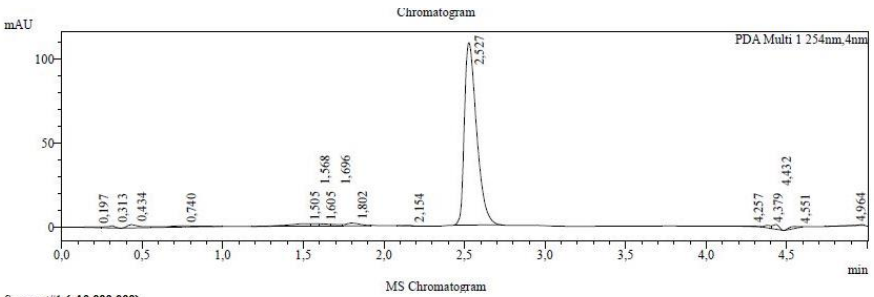

Peak Table

PDA Ch1 254nm

Peak#	Ret. Time	Area	Area%	Height	Height%	Name
1	0,197	2449	0,370	375	0,297	
2	0,313	4334	0,655	1253	0,993	
3	0,434	10824	1,635	1930	1,530	
4	0,740	11774	1,779	770	0,610	
5	1,505	14375	2,172	1458	1,155	
6	1,568	4353	0,658	1408	1,115	
7	1,605	4672	0,706	1240	0,982	
8	1,696	4041	0,611	970	0,769	
9	1,802	10219	1,544	1733	1,373	
10	2,154	1505	0,227	391	0,310	
11	2,527	573548	86,662	108652	86,092	
12	4,257	1718	0,260	290	0,230	
13	4,379	4145	0,626	1489	1,180	
14	4,432	6935	1,048	2795	2,215	
15	4,551	5267	0,796	1055	0,836	
16	4,964	1665	0,252	395	0,313	
Total		661823	100,000	126204	100,000	

Supplementary Fig. 116. The high-performance liquid chromatography chromatogram of compound **32*R*/32*S***

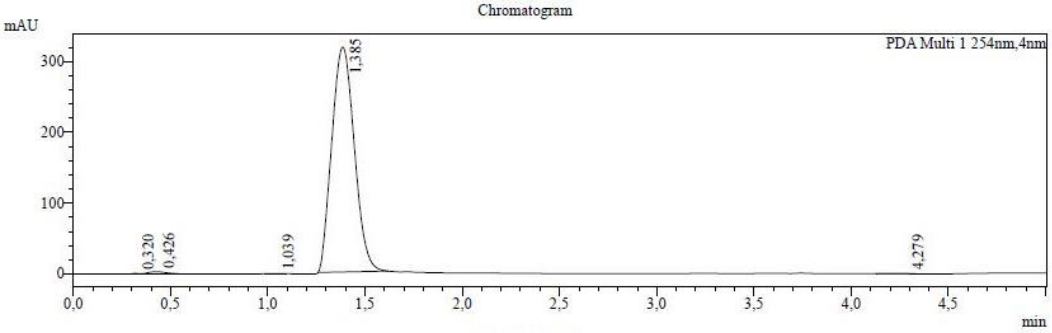

Peak Table

PDA Ch1 254nm

Peak#	Ret. Time	Area	Area%	Height	Height%	Name
1	0,320	1627	0,063	689	0,214	
2	0,426	19758	0,765	3185	0,989	
3	1,039	578	0,022	144	0,045	
4	1,385	2556924	99,018	317696	98,601	
5	4,279	3400	0,132	488	0,151	
Total		2582286	100,000	322203	100,000	

Supplementary Fig. 117. The high-performance liquid chromatography chromatogram of compound **S20**

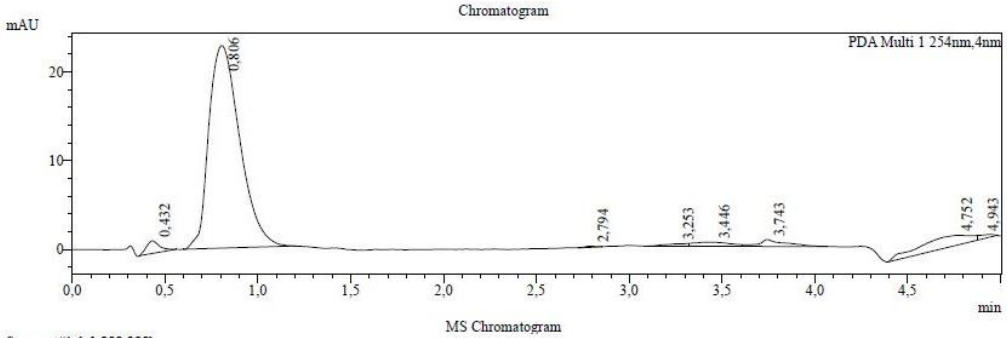

Peak Table

PDA Ch1 254nm

Peak#	Ret. Time	Area	Area%	Height	Height%	Name
1	0,432	7195	2,274	1421	5,202	
2	0,806	264873	83,710	22830	83,597	
3	2,794	527	0,166	131	0,478	
4	3,253	2494	0,788	271	0,992	
5	3,446	6323	1,998	460	1,683	
6	3,743	7775	2,457	766	2,806	
7	4,752	25205	7,966	1148	4,205	
8	4,943	2025	0,640	283	1,037	
Total		316416	100,000	27309	100,000	

Supplementary Fig. 118. The high-performance liquid chromatography chromatogram of compound **S21**

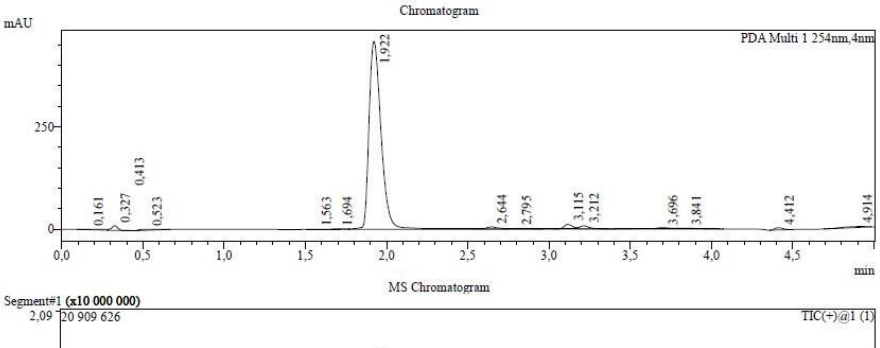

Peak Table

PDA Ch1 254nm

Peak#	Ret. Time	Area	Area%	Height	Height%	Name
1	0,161	13615	0,503	1045	0,204	
2	0,327	27676	1,023	10871	2,121	
3	0,413	1733	0,064	913	0,178	
4	0,523	20175	0,746	2433	0,475	
5	1,563	1451	0,054	309	0,060	
6	1,694	11889	0,440	1674	0,327	
7	1,922	2442940	90,326	459136	89,575	
8	2,644	22945	0,848	4474	0,873	
9	2,795	6389	0,236	837	0,163	
10	3,115	39416	1,457	11010	2,148	
11	3,212	32362	1,197	7282	1,421	
12	3,696	25377	0,938	3245	0,633	
13	3,841	15004	0,555	1634	0,319	
14	4,412	18721	0,692	5452	1,064	
15	4,914	24886	0,920	2259	0,441	
Total		2704578	100,000	512574	100,000	

Supplementary Fig. 119. The high-performance liquid chromatography chromatogram of compound **S22**

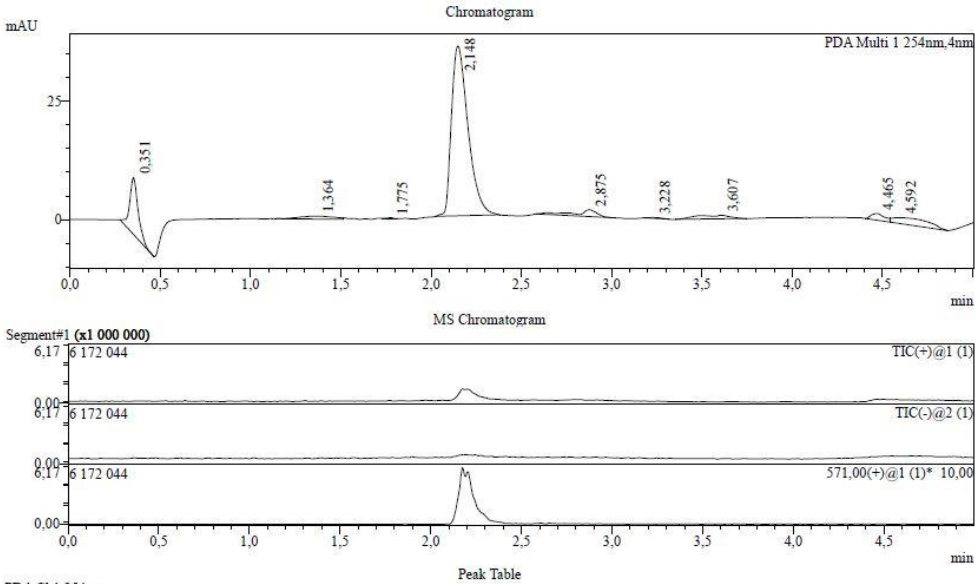

Peak Table

PDA Ch1 254nm

Peak#	Ret. Time	Area	Area%	Height	Height%	Name
1	0,351	38193	11,677	12038	22,365	
2	1,364	8171	2,498	620	1,153	
3	1,775	986	0,301	269	0,500	
4	2,148	229227	70,085	35913	66,719	
5	2,875	12445	3,805	1440	2,675	
6	3,228	860	0,263	178	0,331	
7	3,607	10045	3,071	758	1,408	
8	4,465	7565	2,313	1384	2,570	
9	4,592	19578	5,986	1226	2,278	
Total		327070	100,000	53827	100,000	

Supplementary Fig. 120. The high-performance liquid chromatography chromatogram of compound **33*S***

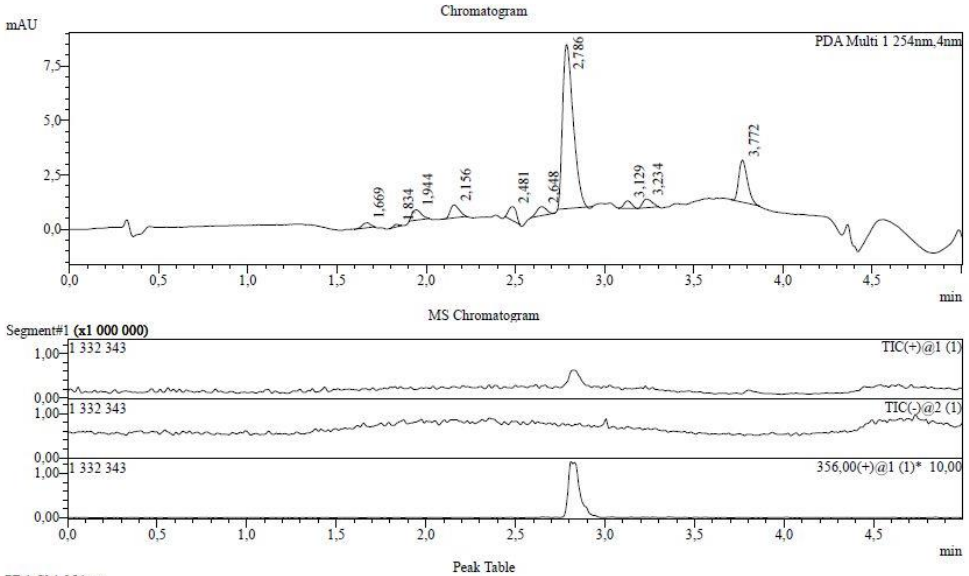

Peak Table

PDA Ch1 254nm

Peak#	Ret. Time	Area	Area%	Height	Height%	Name
1	1,669	740	1,532	225	1,778	
2	1,834	270	0,558	115	0,911	
3	1,944	1728	3,577	478	3,773	
4	2,156	2045	4,234	592	4,678	
5	2,481	1826	3,781	628	4,959	
6	2,648	1581	3,272	411	3,243	
7	2,786	31119	64,423	7526	59,434	
8	3,129	1018	2,107	352	2,777	
9	3,234	1453	3,007	399	3,148	
10	3,772	6525	13,509	1937	15,298	
Total		48305	100,000	12663	100,000	

Supplementary Fig. 121. The high-performance liquid chromatography chromatogram of compound **34*R*/34*S***

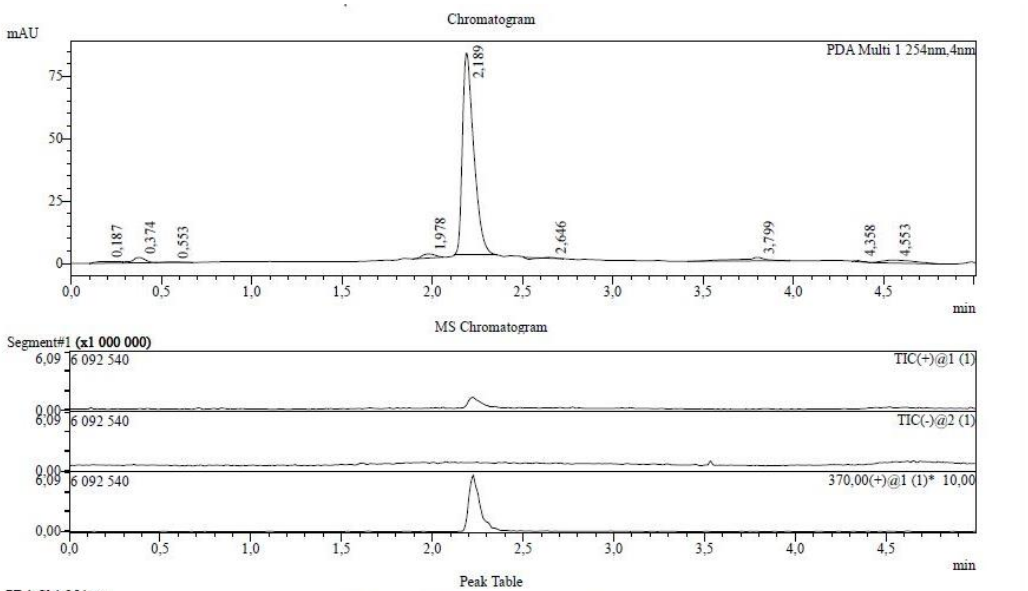

Peak Table

PDA Ch1 254nm

Peak#	Ret. Time	Area	Area%	Height	Height%	Name
1	0.187	5995	1.459	668	0.751	
2	0.374	10707	2.606	2163	2.431	
3	0.553	1703	0.414	240	0.270	
4	1.978	7880	1.918	1611	1.811	
5	2.189	354566	86.300	80864	90.898	
6	2.646	-1052	-0.256	371	0.417	
7	3.799	14315	3.484	1395	1.568	
8	4.358	1186	0.289	479	0.539	
9	4.553	15553	3.786	1170	1.316	
Total		410851	100.000	88962	100.000	

Supplementary Fig. 122. The high-performance liquid chromatography chromatogram of compound **35*R*/35*S***

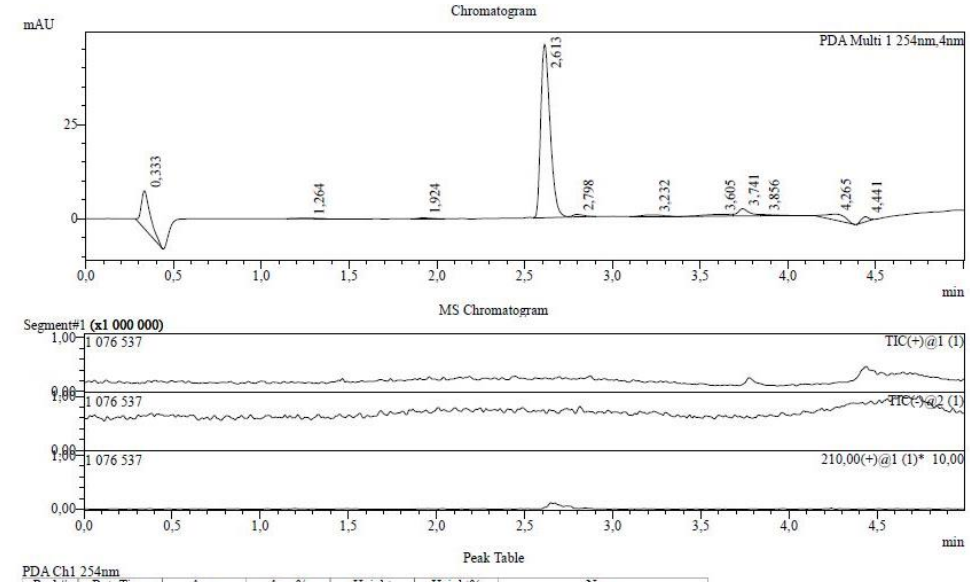

Peak Table

PDA Ch1 254nm

Peak#	Ret. Time	Area	Area%	Height	Height%	Name
1	0.333	35391	14.284	10018	15.852	
2	1.264	1581	0.638	172	0.272	
3	1.924	1517	0.612	289	0.458	
4	2.613	170658	68.879	46158	73.036	
5	2.798	2806	1.133	649	1.027	
6	3.232	3554	1.434	372	0.589	
7	3.605	5299	2.139	448	0.710	
8	3.741	8915	3.598	1880	2.975	
9	3.856	1611	0.650	334	0.529	
10	4.265	12272	4.953	1541	2.438	
11	4.441	4164	1.681	1337	2.116	
Total		247767	100.000	63199	100.000	

Supplementary Fig. 123. The high-performance liquid chromatography chromatogram of compound **40**

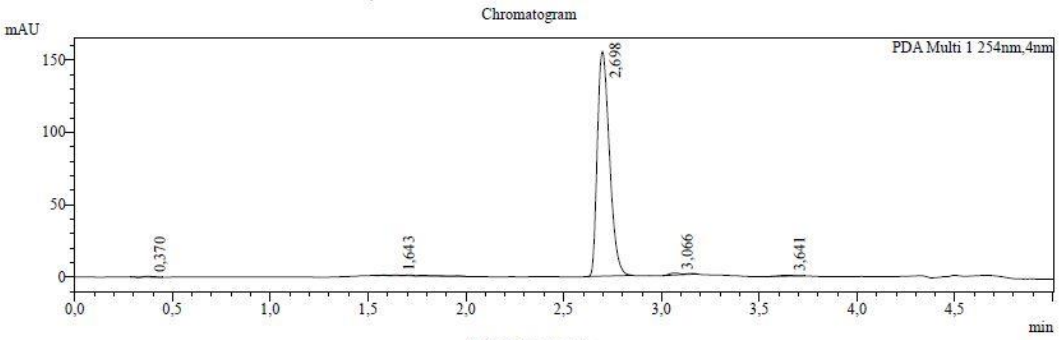

Peak Table

PDA Ch1 254nm

Peak#	Ret. Time	Area	Area%	Height	Height%	Name
1	0,370	1791	0,259	694	0,437	
2	1,643	7960	1,152	477	0,300	
3	2,698	670528	97,043	155536	98,002	
4	3,066	6934	1,004	1413	0,890	
5	3,641	3749	0,543	587	0,370	
Total		690962	100,000	158706	100,000	

Supplementary Fig. 124. The high-performance liquid chromatography chromatogram of compound **3''*R***

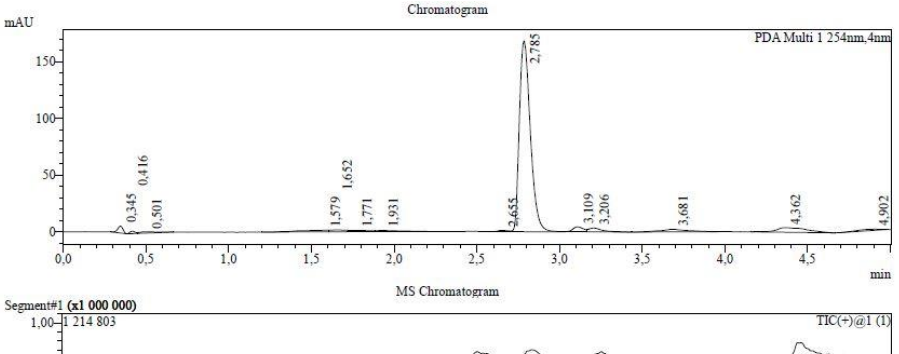

Peak Table

PDA Ch1 254nm

Peak#	Ret. Time	Area	Area%	Height	Height%	Name
1	0,345	13485	1,373	6118	3,077	
2	0,416	5035	0,513	2181	1,097	
3	0,501	9115	0,928	1220	0,614	
4	1,579	18305	1,863	1369	0,688	
5	1,652	11460	1,167	1530	0,769	
6	1,771	8606	0,876	1156	0,581	
7	1,931	9867	1,004	1040	0,523	
8	2,655	4278	0,435	1023	0,514	
9	2,785	774097	78,802	168164	84,565	
10	3,109	19184	1,953	4440	2,233	
11	3,206	19076	1,942	3344	1,682	
12	3,681	27546	2,804	2255	1,134	
13	4,362	50103	5,100	3979	2,001	
14	4,902	12176	1,240	1038	0,522	
Total		982334	100,000	198858	100,000	

Supplementary Fig. 125. The high-performance liquid chromatography chromatogram of compound **6''*R*,*R***

SUPPLEMENTARY REFERENCES

1. Póti, Á. L. et al. Phosphorylation-Assisted Luciferase Complementation Assay Designed to Monitor Kinase Activity and Kinase-Domain-Mediated Protein-Protein Binding. Int. J. Mol. Sci. **24**, (2023).

2. Berkes, B. *et al.* Expedient and Diastereodivergent Assembly of Terpenoid Decalin Subunits having Quaternary Stereocenters through Organocatalytic Robinson Annulation of Nazarov Reagent. *Chemistry – A European Journal* **22**, 18101–18106 (2016).

3. Varga, S. *et al.* Total Syntheses of (−)-Minovincine and (−)-Aspidofractinine through a Sequence of Cascade Reactions. *Angewandte Chemie International Edition* **59**, 13547–13551 (2020).

4. Flaugh, M. E., Crowell, T. A. & Farlow, D. S. Acid-Catalyzed Annelation of α-Alkyl Aldehydes and α,β-Unsaturated Ketones. A One-Pot Synthesis of 4,4-Dimethyl-2-cyclohexen-l-one. *Journal of Organic Chemistry* **45**, 5399–5400 (1980).

5. Deny, L. J. *et al.* Bis-Michael Acceptors as Novel Probes to Study the Keap1/Nrf2/ARE Pathway. *J Med Chem* **59**, 9431–9442 (2016).

6. Brown, T. H. *et al.* Isocytosine H2-receptor histamine antagonists II. Synthesis and evaluation of biological activity at histamine H1- and H2-receptors of 5-(heterocyclyl)methylisocytosines. *Eur J Med Chem* **24**, 65–72 (1989).

7. Zhang, J. *et al.* A hydrogen bonding motif for forming extended assemblies. *Chemical Communications* **46**, 1062 (2010).

8. GARY, G. *et al.* Compounds and compositions for treating conditions associated with nlrp activity. **WO2017184624A1**, (2019).

9. Schultz, A. G. & Sundararaman, P. Stereochemical Control in Cyclofunctionalization of Olefinic Alcohols and Olefinic Phenols with Benzeneselenenyl Chloride. *Journal of Organic Chemistry* **49**, 2455–2462 (1984).

10. Peelen, T. J., Chi, Y., English, E. P. & Gellman, S. H. Synthesis of 4,4-disubstituted 2-aminocyclopentanecarboxylic acid derivatives and their incorporation into 12-helical β-peptides. *Org Lett* **6**, 4411–4414 (2004).

11. Meyer, C., Piva, O. & Pete, J. P. [2+2] Photocycloadditions and Photorearrangements of 2-Alkenylcarboxamido-2-cycloalken-1-ones. *Tetrahedron* **56**, 4479–4489 (2000).

12. El-Mansy, M. F., Kang, J. Y., Lingampally, R. & Carter, R. G. Proline Sulfonamide-Catalyzed, Domino Process for Asymmetric Synthesis of Amino- and Hydroxy-Substituted Bicyclo[2.2.2]octanes. *European J Org Chem* **2016**, 150–157 (2016).

13. Schulz, A., Thomas, M. & Villinger, A. Tetrazastannoles *versus* distannadiazanes – a question of the tin(<scp>ii</scp>) source. *Dalton Transactions* **48**, 125–132 (2019).

14. Horváth, D., Domonyi, F., Palkó, R., Lomoschitz, A. & Soós, T. Regioexhaustive Functionalization of the Carbocyclic Core of Isoquinoline: Concise Synthesis of Oxoaporphine Core and Ellipticine. *Synthesis (Stuttg)* **50**, 2181–2190 (2018).

15. Maynard, S. J., Almeida, A. M., Yoshimi, Y. & Gellman, S. H. New charge-bearing amino acid residues that promote β-sheet secondary structure. *J Am Chem Soc* **136**, 16683–16688 (2014).

16. Bendiabdellah, Y. *et al.* One-Pot Synthesis of Fused-Tetracyclic Scaffolds Employing a Lewis Acid Promoted Domino Reaction of Naphthoquinones. *Synthesis (Stuttg)* 2321–2333 (2011) doi:10.1055/S-0030-1260073.

17. Elemes, Y. & Foote, C. S. Stepwise Mechanisms in the Ene Reaction of α,β-Unsaturated Esters with N-Phenyl-1,2,4-triazoline-3,5-dione and Singlet Oxygen. Intermolecular Primary and Secondary Hydrogen Isotope Effects. *J Am Chem Soc* **114**, 6044–6050 (1992).

18. Alan Aitken, R., Armstrong, J. M., Drysdale, M. J., Ross, F. C. & Ryan, B. M. Flash vacuum pyrolysis of stabilised phosphorus ylides. Part 15.1 Generation of alkoxycarbonyl(sulfenyl)carbenes and their intramolecular insertion to give alkenyl sulfides. *J Chem Soc Perkin 1* 593–604 (1999) doi:10.1039/A808813F.

19. Mandal, P. K., Ren, Z., Chen, X., Xiong, C. & McMurray, J. S. Structure-affinity relationships of glutamine mimics incorporated into phosphopeptides targeted to the SH2 domain of signal transducer and activator of transcription 3. *J Med Chem* **52**, 6126–6141 (2009).

20. Schmitz, J., Li, T., Bartz, U. & Gütschow, M. Cathepsin B Inhibitors: Combining Dipeptide Nitriles with an Occluding Loop Recognition Element by Click Chemistry. *ACS Med Chem Lett* **7**, 211–216 (2016).

21. Schädel, N. *et al.* Synthesis of Imidazole and Histidine-Derived Cross-Linkers as Analogues of GOLD and Desmosine. *Synthesis (Stuttg)* **53**, 2260–2268 (2021).